Aqueous Arnebia Euchroma (Royle) I. M. Johnst Extract Promotes Cutaneous Wound Healing

Dissertation
with the aim of achieving a doctoral degree
at the Faculty of Mathematics, Informatics
and Natural Sciences
Department of Biology
of Universität Hamburg

submitted by
Janine Radtke

Hamburg 2017

Day of oral defense: July 20th, 2017

The following evaluators recommend the admission of the dissertation:

Prof. Johanna M. Brandner

Prof. Thorsten Burmester

Date of the approval for publication: July 20th, 2017

Contents

1. Summary

As long as skin trauma occurs frequently during lifetime, the demand for new effective wound healing therapies will rise. In the case of deregulated wound closure, caused by metabolic or vascular diseases and infections, impaired and chronic wounds arise, which evoke huge costs for the health care systems worldwide. One source of new wound healing concepts, which reinforce endogenous wound healing mechanisms, is based on long-term use therapies from the phytotherapeutic repertoire of Traditional Chinese Medicine (TCM).

Hypothesis-driven literary research was performed and *Astragalus propinquus* Schischkin, *Rehmannia glutinosa* (Gaertn.) DC., *Coptis chinensis* Franch and *Arnebia euchroma* (Royle) I. M. Johnst were investigated due to their wound healing promoting capacities in an *ex vivo* porcine wound healing model (WHM). Here, defined acute wounds were created and their epidermal regeneration was evaluated after 48 h. During this investigation, the application of aqueous *Arnebia euchroma* extract (ARE) showed the most prominent acceleration on early re-epithelialization of the investigated herbal extracts. Its wound application significantly improved epidermal regeneration to 161.8 ± 16.4 % in comparison to the controls in porcine WHMs. Additional positive impact on the subgroups of intrinsic good and bad healing donor specimens in porcine and human WHMs indicates the usage of this extract on impaired healing wounds. Following, the regenerating impact of an aqueous and an ethanolic ARE were analyzed to evaluate the complex wound healing capacities of this plant. The ethanolic ARE showed no wound healing promotion during this early event of re-epithelialization.

The observed improved re-epithelialization cannot be explained by improved *in vitro* wound healing of primary epidermal keratinocytes or dermal fibroblast. Here, the wound recovery of both cell types was dose-dependently decreased by the AREs treatment. Further investigations on cultured keratinocytes treated with the aqueous ARE revealed reduced cell-matrix adherence which can be beneficial for migration that is needed during wound recovery. Both AREs showed positive influence on early barrier formation. Furthermore, the aqueous extract increased the viability and dramatically enhanced the cellular energy level of primary cultured fibroblast. This was accompanied with influenced protein levels of extracellular matrix (ECM)

molecules. Particular, the amount of fibronectin protein showed a three-fold increased trend by the treatment. The enhanced ECM formation provides a network, which enables accelerated migration of cells and therefore epidermal recovery. Additional, anti-oxidative and chromatographic investigations revealed the radical scavenging capacity of the aqueous ARE which benefits wound healing.
These investigations firstly demonstrate wound healing promotion capacity of aqueous *A. euchroma*. The positive influence on re-epithelialization supports its use on early wounds in patients with deregulated epidermal regeneration. This thesis provides an approach for the usage of aqueous ARE as a new therapeutic wound healing concept. Further studies are required to elucidate the detailed mechanisms behind the extracts´ wound healing promotion. The main active compounds have to be revealed. These will enable proper application of the aqueous ARE and optimize its therapeutic approach.

Zusammenfassung

Solange Hautverletzungen regelmäßig auftreten, wird die Nachfrage nach neuen effektiven Wundheilungstherapien weiter steigen. Gestörte Wundheilung wird durch metabolische oder vaskuläre Erkrankungen verursacht und führt zu wundheilungsverzögerten und chronischen Wunden. Deren Behandlung verursacht hohe Kosten für die Gesundheitssysteme weltweit. Eine Quelle für neue Behandlungskonzepte stellen die Überlieferungen von phytotherapeutischen Ansätzen der Traditionellen Chinesischen Medizin dar. Hier werden endogene Wundheilungsprozesse durch die komplexe Wirkung individueller Pflanzenkombinationen unterstützt.
Aufgrund hypothesengestützter Bewertung von Originalliteratur wurden *Astragalus propinquus* Schischkin, *Rehmannia glutinosa* (Gaertn.) DC., *Coptis chinensis* Franch and *Arnebia euchroma* (Royle) I. M. Johnst als Kandidatenpflanzen identifiziert. Diese wurden in einem porcinen *ex vivo* Wundheilungsmodell hinsichtlich ihrer wundheilungsfördernden Eigenschaften untersucht. Akute Wunden wurden standardisiert erzeugt und die epidermale Regeneration unter Behandlung mit den verschiedenen Kräuterextrakten nach 48 h bewertet. Während dieser Untersuchungen zeigte der wässrige Extrakt von *Arnebia euchroma* (ARE) die am stärksten beschleunigte Re-epithelialisierung im Vergleich der untersuchten Extrakte. Durch die Applikation auf die Wunde wurde die mittlere regenerierte Epidermis signifikant auf 161.8 ± 16.4 % im Vergleich zu den Kontrollen gesteigert. Die Unterteilung in Untergruppen von intrinsisch gut oder vermindert heilenden Hautproben zeigte positiven Einfluss durch die Behandlung. Dies wurde vor allem in Hinblick auf die Unterstützung schlecht heilender Wunden deutlich. Die Wundheilungsförderung konnte auch auf humanen

Proben bestätigt werden. Im Weiteren wurde die Regenerationsförderung des wässrigen Extraktes mit einem Ethanolischen vergleichend durchgeführt, um die komplexe Wundheilungs förderung der *A. euchroma* Wurzel beurteilen zu können. Hierbei zeigte der ethanolische Extrakt keine wundheilungsfördernde Re-epithelialisierung.
Die beobachtete verbesserte Wundheilung *ex vivo* kann nicht durch den verbesserten Wundverschluss primärer Keratinozyten oder Fibroblasten *in vitro* erklärt werden. Der Wundverschluss in beiden Mono-Kulturen war durch die Behandlungen mit den Extrakten dosis-abhängig vermindert. Weitere Untersuchungen an kultivierten Keratinozyten, die mit dem wässrigen Extrakt behandelt wurden, zeigten verminderte Zell-Matrix-Adhärenz. Diese kann durchaus die Migration und damit Re-epithelialisierung der Epidermiszellen im Gewebe positiv beeinflussen. Beide Extrakte zeigten zudem positiven Einfluss auf die Ausbildung einer frühen epidermalen Barriere. Darüber hinaus erhöhte der wässrige Extrakt die Zellviabilität und das Energielevel von kultivierten Fibroblasten und beeinflusste das Proteinlevel von Vertretern der Extrazellulären Matrix. Im Besonderen wurde eine dreifach erhöhte Menge an Fibronectin detektiert, wobei dieser starke Trend keine Signifikanz zeigte. Eine gesteigerte Bildung der Extrazellulären Matrix ermöglicht ein Netzwerk, das die Migration verschiedener Zelltypen in die Wunde unterstützt und damit auch die Reepithelialisierung fördert. Darüber hinaus konnten anti-oxidative und chromatographische Untersuchungen belegen, dass der wässrige Extrakt Verbindungen enthält, die Radikalfangeigenschaften besitzen. Diese können die *ex vivo* beobachtete Wundheilung fördern.
Diese Untersuchungen beschreiben erstmalig die Wundheilungsförderung eines wässrigen Extraktes von *A. euchroma*. Der positive Einfluss auf die Reepitelialisierung unterstützt dessen Verwendung zur Behandlung frischer Wunden bei Patienten mit verminderter epidermaler Regeneration. Diese Dissertation stellt einen Ansatz für die klinische Anwendung des wässrigen Extraktes als neues therapeutisches Wundheilungskonzept dar. Weiterführende Analysen sind notwendig, um den detaillierten Wirkmechanismus, der der geförderten Wundheilung zugrunde liegt, zu beleuchten. Dabei sollten die Hauptwirkkomponenten bestimmt werden. Dieses Herangehen wird helfen die klinische Verwendung des wässrigen Extraktes zu optimieren.

2. Introduction

Skin injuries caused by cuts, trauma, accidents, falls and burns that occur in life, can cause permanent damage. Wound regeneration is a dynamic, highly regulated and energy-dependent process. It includes the interplay of epidermal and dermal cells, the extracellular matrix (ECM) molecules accompanied by immune cells, and various chemical mediators (Eming *et al.*, 2007). Essential wound healing mechanisms are detoxification and phagocytosis, cell migration (including cellular attachment and detachment), cell proliferation and the rebuilding of the restored tissue with an intact barrier (Singer *et al.*, 1999). An aging population, rising metabolic disorders, increased obesity and pathogen infections enhances the occurrence of impairment during convalescence (Natarajan *et al.*, 2000; Dreifke *et al.*, 2015; Dunnill *et al.*, 2017). The potential for serious infections, which follows disabilities and hospitalization, tend to elevate the risk of chronic wounds.

The development of new treatment strategies with a focus on impaired wound healing is still necessary. Current approaches with several wound dressings - including chemical mediators, split-thickness or epithelial autografts, as well as cell transplantations - are used in the clinic (Singer *et al.*, 1999; Dreifke *et al.*, 2015). These therapeutic agents, which are slightly expensive, could prove to be ineffective and possibly have adverse effects. Therefore, phytotherapeutics, as non-expensive and widely accessible treatments, are getting more and more in focus of current wound healing research (Budovsky *et al.*, 2015). Complementary medicines are mainly based on herbal treatments with long-term experiences, but evidence-based research studies which explain the underlying mechanisms are often missing (Effert *et al.*, 2007). Herbal extracts contain many chemical molecules that may operate as a multi-component treatment of different wound healing associated pathways and mechanism at the same time.

This project focuses the wound healing capacities of *A. euchroma*, which is a therapeutic herb used in Traditional TCM. The root of *A. euchroma* is used to treat poorly healing wounds. The underlying mechanism for improvement of the healing process and the affected cell types were investigated.

2.1. Composition and Function of the Skin

The skin, as the biggest organ of the human body, plays an important role as a border, which protects the corpus from the outer environment (Reinke *et al.*, 2012). Important functions of the integument are the regulation of the osmotic and thermobalance and sensory perception of exterior influences. The skin is built by the outer epidermis with underlying dermis and subcutis (Fig. 2.1, A), which include different specialized cell types. Glands and hair follicles are special functional appendages, which are located in the dermal sheet discharging to the surface of the epidermis (Bäsler *et al.*, 2016). Embedded blood and lymphatic vessels enable an accurate skin nutrition and gas supply. This is important to establish healthy homeostasis which can become imbalanced through disease or injury. Additionally, this complex organ is supplemented by a defined network of primary afferent and autonomic nerves. They are important for skin sensory, modulation of the immune response, inflammation, as well as the healing of wounds (Roosterman *et al.*, 2006).

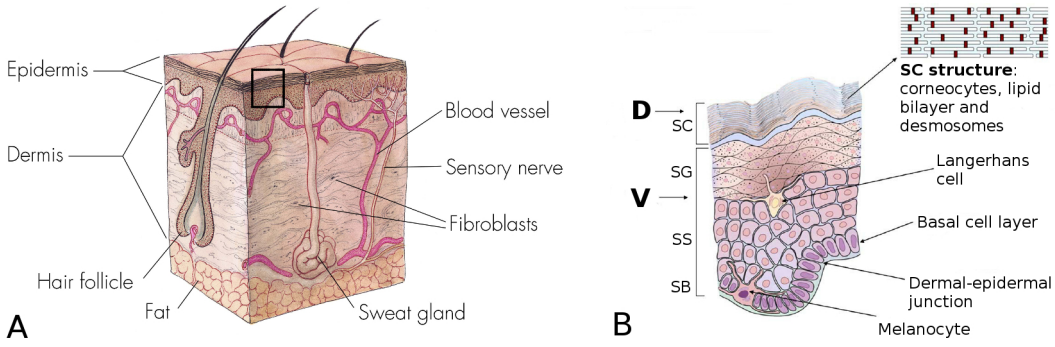

Figure 2.1.: Schematic drawing of the skin with an enlarged cross-section of the epidermis. (A) Overview of skin layers cross section: epidermis, dermis and subcutaneous fat tissue (subcutis); the rectangle marks the (B) enlarged epidermal layer. (B) Overview of the epidermal (V) vital layers from the lower *stratum basale* (SB) to *stratum spinosum* (SS) and *stratum granulosum* (SG). The *stratum corneum* (SC; D = dead) with dead corneocytes complete the epidermal layer to the outside [modified from (A) National Institutes of General Medical Science and (B) (Visscher *et al.*, 2009).

The epidermis is a constantly renewing stratified squamous epithelium built by four layers: (1) the *stratum basale* on the basal membrane connects epidermis and dermis. Apical follow (2) *stratum spinosum*, (3) *stratum granulosum* and (4) *stratum corneum* (Fritsch, 2004; Visscher *et al.*, 2009; Fig. 2.1, B). The epidermis has basal excrescences in the dermis which are named rete ridges, the dermal areas in between are called dermal papillae (Fritsch, 2004). This interlocked structure offers the epidermal-dermal adhesion and enables further skin elongation. The dominating cell type of the epidermis is the keratinocyte which interacts further with rarer cell types.
The epidermal layers can be identified by their different composition of cytokeratins

(CK), keratin-containing filaments, and junction molecules that are important for the layers function. Keratinocytes of the basal membrane have a proliferating undifferentiated character and express *exempli gratia* (*e.g.*) CK 5, CK 14 and CK 15 (Usui *et al.*, 2008). The cells pass through the epidermal layers with rising differentiation, which is indicated by the expression of CK 10, CK 1 and CK 2 (Fritsch, 2004; Usui *et al.*, 2008; Eckert & Rorke, 1989). During this process, the keratinocytes change their shape and the keratin production increases as well as lipid release till they reach the outer layer. Here, in the *stratum corneum*, the epidermis contains compact, dead, flattened corneocytes with cornified envelopes which replace the normal cell membranes. These corneocytes, together with the intermediate lipids, function as a physical barrier (Brandner *et al.*, 2015).

Melanocytes are present in the *stratum basale* of the epidermis. These cells produce melanin (Fritsch, 2004). This skin coloring pigment promotes free radical and light scavenging protection induced by external influences as *e.g.* UV light. Neuroendocrine Merkel cells function as mechanoreceptors (Fritsch, 2004). Suprabasal Langerhans cells, other dendritic cells, and leukocytes are present cell types belonging to the immune system (Fritsch, 2004).

The skin has different components that function as barriers: the natural microbiome, the physical barrier of the *stratum corneum*, the tight junction barrier in the *stratum granulosum*, the barrier provided by the innate and adaptive immune system, and the chemical response of the homed cells (Brandner *et al.*, 2002; Bäsler *et al.*, 2016). The barrier function mainly enables skin homeostasis, prevents loss of soluble factors to the outer environment, and protects the body from pathogens and other harmful risks from the outside (Brandner *et al.*, 2015). Between epithelial cells, cell-cell connections as *e.g.* desmosomes are present which enable a dynamic but tight cellular attachment (Brandner *et al.*, 2015). Various hemi-/desmosomes connect the *stratum basale* with the basal membrane and the keratinocytes of the *stratum spinosum*. Within the *stratum granulosum*, a further intercellular connection type built of tight junctions is prominent. These cell-cell connections intensify the existing physical barrier of the *stratum corneum*, enable a dense tissue connection and a selective electron, ion and molecular, cell-cell and intercellular transport through the epidermis (Fritsch, 2004; Bäsler *et al.*, 2016).

The underlying dermis consists mainly of connective tissue where fibroblasts are the dominant cell type. This layer is responsible for the rigidity and flexibility of the skin and contains the providing vessels and nerves (Fritsch, 2004). It mainly consists of structural fibers as collagens, fibrin, fibronectin and elastin which are produced as ECM molecules by mostly fibroblasts (Chester & Brown, 2016). The dermis can be divided in the upper *stratum papillare*, which contains looser collagen filaments. They

are connected to the epidermal basal membrane and the lower *stratum reticulare*, which comprises a tighter collagen network (Fritsch, 2004). Collagen represents 80 % of the dry dermis weight in adults. These central proteins enable the structure and strength of the dermal sheet (Booth *et al.*, 1980). Here, around 80 % are collagen type I and 10 % collagen type III which have fiber characters. Collagen fibers contain three alpha peptides chains which are arranged as triple helices (Fritsch, 2004). Fibroblasts synthesize collagen peptide chains in a multistage process with complex post-translational modifications. An exception is *e.g.* collagen IV, which is also expressed by keratinocytes. Collagen type IV forms networks instead of fiber structures. This collagen IV net, combined with laminin 1 and others, forms basal membrane structures between dermis and epidermis (Fritsch, 2004). The cellular density of the dermis is multiples lower compared to the epidermis. In contrast to the epidermis, the dermis is rich in blood and lymphatic vessels that provide the cellular supply (Singer *et al.*, 1999). The additional embedded nerves enable sensory signal transduction and take part in the neuroimmune endocrine system of the skin (Roosterman *et al.*, 2006). Mast cells are secretory effector cells which can be found in the ECM. They have an essential role in the normal dermal function and during the restoration of skin trauma, angiogenesis and inflammation (Fritsch, 2004). The process that enables the regeneration in trauma cases is called wound healing, and it occurs continuously during a lifetime.

2.2. Wound Healing

An injury to an integer skin can occur by physical, thermal, or chemical causes. It is restored by complex regulated dynamic processes: different cytokines and growth factors released from the wound side in combination with chemical mediators and molecules of the ECM affect epithelial and mesenchymatic cells to close the injury in an appropriate amount of time (J. Li *et al.*, 2007; Singer *et al.*, 1999; Velnar *et al.*, 2009). According to Velnar *et al.* a wound that achieves a restored anatomical appearance within a certain time, which shows an intact barrier and normal skin function, is defined as a healed wound (Velnar *et al.*, 2009; Budovsky *et al.*, 2015). In general, the restoration of an injury can be divided into three phases that occur, in part, contemporaneously: (A) hemostasis and inflammation, (B) re-epithelialization and granulation, and (C) the remodeling phase (Fig. 2.2, A - C; Gurtner *et al.*, 2008; Singer *et al.*, 1999).

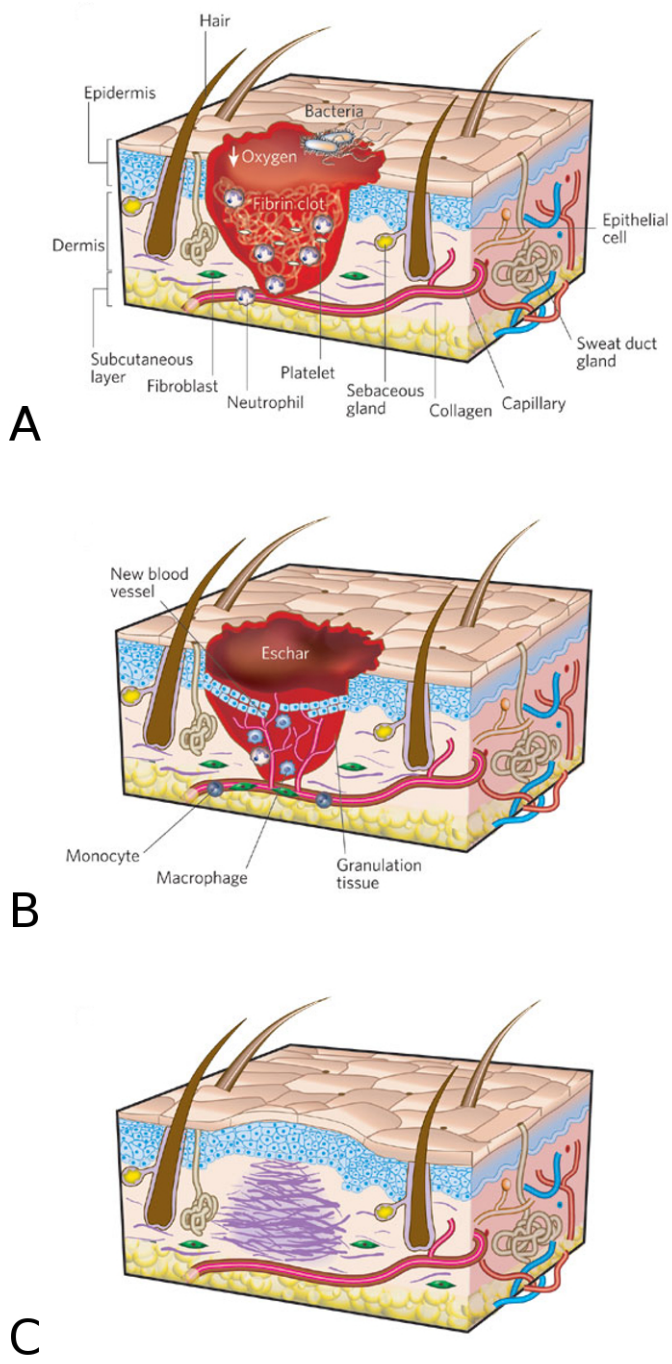

Figure 2.2.: The three wound healing phases: (A) hemostasis/inflammation, (B) re-epithelialization/ granulation and (C) tissue remodeling. (A) Inflammation starts directly after wounding and can last up to 48 h past injury when a fibrin clot enabled hemostasis. (B) Granulation tissue formation and re-epithelialization begins within 24 h of the injury and can last up to one year. It is dominated by fibroblasts migration and proliferation as well as neovascularization. Epidermal keratinocytes (blue) migrate from the wound edges and re-epithelialize the wounded area. (C) The tissue remodeling consists mainly of ECM re-arrangement and wound contraction of the improvised collagen matrix. The resulting re-epithelialized wound misses hair follicles and glands (modified from Gurtner *et al.*, 2008).

2.2.1. Hemostasis and Inflammation Phase

During the inflammatory stage, vascular processes and hemostasis enable a stop to the bleeding. Immediately after wounding, hemostasis is initiated (J. Li *et al.*, 2007; Reinke & Sorg, 2012; Fig. 2.2, A). Here, thrombocytes aggregate by contact to collagens and fibronectin of the vascular ECM. A provisory clot, consisting of mainly fibrin and further fibronectin, thrombospondins and vitronectin, is cross-linked to preventing blood loss (Reinke & Sorg, 2012; J. Li *et al.*, 2007; Chester & Brown, 2016).

Platelets release *e.g.* adenosine diphosphate, serotonin and adhesion-related molecules as fibronectin, fibrinogen, von Willebrand factor/factor VIII and thrombospondin that support blood aggregation with former mediator secretion (J. Li *et al.*, 2007). Leukocytes and thrombocytes release chemical signal molecules *e.g.* tumor necrosis factor alpha (TNF-α) and interleukins (Il) which promote inflammation. Secreted vascular endothelial growth factor (VEGF), hypoxia-induced factor 1 alpha, fibroblast growth factor (FGF) 2 and transforming growth factor beta (TGF-β) induce blood vessel constriction with the following extension. This enables the invasion of inflammatory cells as monocytes, neutrophils and other lymphocytes (J. Li *et al.*, 2007; Velnar *et al.*, 2009; Werner & Grose, 2003). The intrinsic coagulation cascade is mediated by the enzyme Hageman factor XII. This enzyme metabolizes prothrombin to thrombin which converts fibrinogen to insoluble fibrin (J. Li *et al.*, 2007). The tissue factor lipoprotein is the initiator of the extrinsic coagulation that is secreted by endothelial cells of the injured tissue and by activated monocytes (J. Li *et al.*, 2007). The resulting fibrin clot accumulates several chemotactic molecules and growth factors as *e.g.* epidermal growth factor (EGF), TNF-α, FGF 2 and insulin-like growth factor (IGF) 1. These molecules enable migration and invasion of further immune active leucocytes, fibroblasts, keratinocytes and endothelial cells (J. Li *et al.*, 2007; Reinke & Sorg, 2012).
The inflammatory phase helps to clean the wound area. Here, leucocytes and macrophages are recruited by different cytokines into the wound bed to start their wound cleaning (J. Li *et al.*, 2007). They release proteinases, remove dead tissue and disarm pathogens to prevent infections (Simpson & Ross, 1972; J. Li *et al.*, 2007; Eming *et al.*, 2007; Velnar *et al.*, 2009). Neutrophil granulocytes are attracted by *e.g.* degraded fibrin products, TGF-β, platelet-derived growth factor (PDGF), proteases and interleukins which are secreted by mast cells and others (Noli & Miolo, 2001).
Monocytes that are attracted by *e.g.* degradation products of thrombin, collagens and fibronectin differentiate to macrophages (Kunkel *et al.*, 1991; Sherry *et al.*, 1988; Singer *et al.*, 1999). Further, they secrete inflammatory molecules: reactive oxygen species (ROS), enzymes and growth factors like PDGF, VEGF, FGF, TGF-α and TGF-β. These increase the inflammation and induce the granulation phase by attracting fi-

broblasts, keratinocytes and endothelial cells (Fallanga, 1993; DiPietro & Polverini, 1993). ROS especially act as secondary messengers to many wound healing associated mechanisms by promoting cell migration, angiogenesis and supporting host defense (Dunnil *et al.*, 2017). The balance between moderate and high ROS level is fundamental to the outcome of the wound healing. Excessive ROS may cause cellular damage whereas balanced levels positively stimulate the wound repair mechanism. During the early inflammation neutrophils are the dominant cell type, whereas finally, more monocytes are present in the wound bed (J. Li *et al.*, 2007). Phagocytosis of both cell types is mediated by proteins of the immune complement system (J. Li *et al.*, 2007). Macrophages cleanse the wound bed and digest pathogens and tissue deposits. They control the inflammation by degrading the remaining neutrophils after proper wound cleaning (J. Li *et al.*, 2007). Hypoxic macrophages, in comparison to normal ones, produce angiogenic growth factors. These factors establish a migration gradient for endothelial cells, which induce new blood vessel creation. The secretion of stimulatory molecules and growth factors within the inflammatory phase is essential for proper wound regeneration and initiates the re-epithelialization phase (Reinke & Sorg, 2012). Additionally, the cutaneous neuronal innervations enable neuromediator interactions. Present high-affinity receptors and regulatory proteases influence the tissue inflammation processes and the general integrity of the skin (Roosterman *et al.*, 2006).

2.2.2. Re-epithelialization and Granulation Phase

During the inflammation stage, the granulation and re-epithelialization phase is initiated within hours after injury (Fig. 2.2, B). Macrophages and wound area associated cells release chemical mediators such as TGF-α and -β, EGF, FGF, interferon gamma, PDGF and fibronectin that attract fibroblasts and other effectors to migrate into the wound and start proliferation (Fallanga, 1993; Singer *et al.*, 1999; Gailit *et al.*, 1996; Reinke *et al.*, 2012). Fibroblasts begin to proliferate at the wound margins after injury, which is further promoted by an acidic oxygen level (J. Li *et al.*, 2007). They are attracted by growth factors, and produce and release provisory ECM molecules below the fibrin clot (Gailit *et al.*, 1996; Singer *et al.*, 1999; Velnar *et al.*, 2009).
Beside chemical attraction, the dermal and epidermal reconstruction is enabled by the improvisationally built ECM. This ECM mainly contains fibrin, fibronectin, proteoglycans, glycosaminoglycans, hyaluronic acid and collagen type III and provides the framework and contact guidance for migrating cells (Gailit *et al.*, 1996; Roberts & Sporn, 1987; Ross *et al.*, 1985; J. Li *et al.*, 2007; Reinke *et al.*, 2012). The expression of these involved proteins is increased during ECM generation. Integrins, as ubiquitously expressed cell membrane receptors, are used by all migrating cells to attach to fibronectin

and collagens (Grove, 1982; Gailit *et al.*, 1996; Senger *et al.*, 1997; J. Li *et al.*, 2007). The built granulation tissue consists of remaining macrophages, endothelial cells and mainly fibroblasts. Fibroblasts secrete molecules of the ECM, which provide a reservoir of cytokines, growth factors and collagen fibrils that enable wound contraction (J. Li *et al.*, 2007; Reinke & Sorg, 2012). Meanwhile, fibroblasts differentiate to several subpopulations such as myofibroblasts and cells with a profibrotic phenotype. Myofibroblasts can contract the wound sides with actin filament bundles which is mediated by *e.g.* TGF-β, epinephrine, placental growth factor, angiotensin and vasopressin (Werner & Grose, 2003; Sethi *et al.*, 2002; Velnar *et al.*, 2009). Here, cytoplasmatic actin from myofibroblasts pseudopodia is binding to collagen bound fibronectin from the ECM. The wound contraction is realized by stretching the fibers to the cell (Sethi *et al.*, 2002). Moreover, the profibrotic phenotype of fibroblasts enables enhanced protein synthesis (Clark, 1993).

The re-epithelialization and granulation phase is further dominated by keratinocytes epithelial recovery of the wound area. Keratinocytes from the wound margin and epidermal stem cells from hair follicles start the re-epithelialization of the injured area within the first hours following the trauma (Velnar *et al.*, 2009). Between 24 and 72 h after injury, keratinocytes from the wound margin, behind the migratory keratinocytes, increases proliferation (Usui *et al.*, 2008). The migrating cells use the provisory matrix to adhere and migrate, mediated by *e.g.* keratinocytes growth factor (KGF), EGF, nerve growth factor and IGF-1 (Sun *et al.*, 1991 as cited in J. Li *et al.*, 2007; Werner & Grose, 2003). The migratory process of keratinocytes and fibroblasts is conducted as a balanced cellular adherence and detachment. It is enabled by different enzymes as collagenases, elastases and matrix metalloproteinases (MMPs). These proteases break cell-cell and cell-matrix connections to adhesion molecules as integrins and laminins to achieve cellular movement (J. Li *et al.*, 2007; Reinke & Sorg, 2012). Epithelial cells of the wound margins enhance proliferation due to increased TGF-α, EGF and KGF levels, which also elevate cellular migration (J. Li *et al.*, 2007; Reinke & Sorg, 2012). The keratinocytes of the leading edge flatten their cell shape, form lamellipodia and rearrange intercellular tono and actin filaments. They migrate while reducing proliferation (Usui *et al.*, 2008). This helps to save energy for cellular movement processes over the provisional matrix (Reinke & Sorg, 2012; J. Li *et al.*, 2007). Migrating keratinocytes stop by contact inhibition when both wound tongues meet in the center of the wounded area. The present cells start to adhere to each other and rebuild intercellular connections as desmosomes (J. Li *et al.*, 2007). Migrating keratinocytes were shown to express CK 10, CK 2 and laminin 5 which indicates an early differentiated phenotype (Usui *et al.*, 2008). Two days after acute injury, keratinocytes of the regenerating epidermis increase CK 6 and CK 16 expression. The cellular

differentiation enables the restoration of the basal membrane between epidermis and dermis, of a selective permeable tight junction barrier and of the stratified epidermal layers (J. Li *et al.*, 2007; Brandner *et al.*, 2015). It is regulated by a rising calcium gradient, which influences keratinocytes differentiation *in vivo* and *in vitro* (Bikle & Tu, 2012). Keratinocytes occur, depending on the epidermal layer, with undifferentiated characters or with different differentiated phenotypes. Undifferentiated cells are mainly present in the basal layer of uninjured tissue but may occur widespread in non-stratified tissue as it is present in the regenerating epidermis. They are able to proliferate under low calcium concentrations (Bikle & Tu, 2012). Keratinocytes proliferation is increased in the center of the wound whereas cellular differentiation and basal membrane regeneration is enhanced at the wound margins (Laplante *et al.*, 2001; J. Li *et al.*, 2007). Restoration of the basal membrane is an essential process to enable the functional integrity of the skin. It occurs days after injury (J. Li *et al.*, 2007). Collagen type IV, as the main component of the basal lamina, builds two-dimensional networks with laminin 1 and others. Therefore, it is directly associated with the integrity of the basal membrane (Saarialho-Kere *et al.*, 1993). Protein expression of collagen IV increases during the basal membrane reconstruction. Collagen IV is additionally an important component of the provisional ECM. Together with other structural compounds, it provides a network for all migrating cells which can enter the wound area mediated by integrin receptors (Grove, 1982; J. Li *et al.*, 2007).
In addition, new blood capillaries are sprouting out of existing vessels to enable oxygen and nutrition provision of the new tissue. This neovascularization is supported by angiogenesis factors as low oxygen content in combination with elevated lactic acid, PDGF, basal FGF, angiopoietins, TGF-β and hydroxypropionic acid. Here, proliferating endothelial cells migrate into the wound area and start new vessel formation (Singer *et al.*, 1999; J. Li *et al.*, 2007; Reinke & Sorg, 2012). The main promoter is VEGF which is increasingly expressed by nearly all cell types during wound healing process. It initiates endothelial migration and sprouting, and induces B-cell lymphoma 2 expression that is involved in anti-apoptotic pathways (Gerber *et al.*, 1998; J. Li *et al.*, 2007). Angiogenesis is highly dependent on ECM structure and organization. Endothelial cells migrate with the assistance of this network binding straitening to adhesion molecules such as integrins (J. Li *et al.*, 2007; Reinke & Sorg, 2012). The new blood vessels, on the other hand, recruit more immune cells and provide further cytokines. Smooth muscle cells assist the endothelial cells in achieving higher capillary wall stability, which enables differentiation to new vein and arteries (Reinke & Sorg, 2012).

2.2.3. Remodeling Phase

The remodeling of the improvised ECM and restoration of the wound area is completing the wound healing process (Fig. 2.2, C). The granulation tissue consists of the generated improvisational, fibronectin and collagen type III rich ECM, which is infused by many blood vessels (Welch *et al.*, 1990). The rebuilt scar tissue is dominated by collagen type I and fewer capillaries which enable consistency and flexibility of the regenerated tissue (J. Li *et al.*, 2007; Reinke & Sorg, 2012). The increased collagen type I expression is mediated by fibroblast growth factors as TGF-β and FGF (Visse & Nagase, 2003; Haukipuro *et al.*, 1991). The collagen type III degradation mediated by MMPs is control inhibited by tissue inhibitor of metalloproteinases (TIMPs). MMPs and TIMPs exist in equilibrium in healthy skin. The regenerated tissue has less cell density and flexibility, and can achieve up to 70 % of its original strength within one year of the injury (Gurtner *et al.*, 2008; Abercrombie *et al.*, 1956). Functional structures, such as hair follicles and glands, cannot be regenerated and are therefore lost due to the injury. These appendages are not present in scar tissue just like rete ridges (Robson *et al.*, 2001). Therefore, regenerated tissue is less elastic than unwounded tissue and has reduced sensory capability.
Many cell types and regulatory molecules are involved in wound regeneration. They finally have to be removed from the wound area by degradation, apoptosis and necrosis. This constitutes a delicately regulated equilibrium of molecular synthesis and degradation (Reinke & Sorg, 2012; Velnar *et al.*, 2009).

2.2.4. Wound Healing Complications

The complex, time and energy required for the wound healing process can be interrupted by different alterations. These can either enlarge the defect or elongate the rehabilitation time (Abercrombie *et al.*, 1956; Natarajan *et al.*, 2000; Velnar *et al.*, 2009). One pathophysiologic event in slow or impaired healing wounds is a deficient blood supply. A decreased blood and oxygen supplies induce reduced energy levels in the wound bed which further disturbs the proper healing process (Im & Hoopes, 1970). This impaired wound healing can be caused by metabolic diseases such as diabetes or vein dysfunctions. Furthermore, bacteria are omnipresent. The type and amount of microorganisms, their virulence, together with the local blood supply and the individual patient's constitution, determine wound infection development or normal healing (Velnar *et al.*, 2009). Incomplete wound cleaning of pathogens and necrotic tissue or other foreign particles increases inflammation. This phase may last for weeks and cause chronic inflammation resulting in worse wound healing outcomes due to im-

paired granulation formation and cell migration. In the case of prolonged inflammation erythema, edema, heat and local pain may occur (Velnar *et al.*, 2009; Reinke & Sorg, 2012). Moreover, chronic wounds often have elevated amounts of oxygen radicals, which are, in healthy skin, involved in tissue balance and in proper wound healing (Dunnil, 2015). However, increased ROS causes oxidative stress. This may result in elevated inflammation by increased secretion of pro-inflammatory cytokines (Dunnil *et al.*, 2017). Increased ROS level generates the damage of DNA molecules, lipids, ECM proteins accompanied by cell death induction and therefore prolongate wound healing (R. Thakur *et al.*, 2011; Moseley *et al.*, 2004). Furthermore, the balance between growth factors, MMPs and TIMPs, and degradation signals can be disturbed and tissue hypoxia, necrosis and infections occur (Velnar *et al.*, 2009). Disrupted equilibrium of MMPs and TIMPs can cause improperly delayed wound healing (Visse & Nagase, 2003; Li *et al.*, 2007; Lobmann *et al.*, 2002). These alterations lead to effector cell wound healing associated capability loss as *e.g.* appropriate migration, proliferation and adhesion. This may result in impaired wounds, unaesthetic scars or functional loss of the tissue (Welch *et al.*, 1990; Velnar , 2009). Furthermore, chronic wounds often miss the well-controlled sequence of the described healing phases. They show contemporaneous phases at different wound sites (J. Li *et al.*, 2007).
Wound healing can be impaired due to vascular and metabolic diseases, allergies, aging, treatment intolerances and adverse effects. Current research is focusing on the identification of effective regeneration promoting reagents, which support multiple steps during the wound healing phases.

2.3. Usage of Herbal Treatments from Traditional Chinese Medicine

TCM therapies are based on theories, beliefs, and experiences, which are thousands of years old. Trial and error passed on knowledge about plants, minerals and animal products through the generations (Ho & Ong, 2015). This complementary medicine is still an important part in the health care of rural and urban Asia (Efferth *et al.*, 2007). Different from classical western medicine, TCM focuses on the holistic human health consisting of body, mind and environment. Here, complex sources of discomforts are treated with individual therapies (Ho & Ong, 2015). Phytotherapeutics are used as a patient´s individual herbal combination. Herbal treatment, as well as acupuncture, tuina massages, movement and breathing exercises by qigong and specific nourishment, are important therapeutic approaches of TCM.
Promotion of epidermal regeneration in the shortest possible time with minimal scar-

ring, less pain and without discomfort is the aim of wound care (R. Thakur *et al.*, 2011). Phytotherapeutic strategies, using herbal compound complexities, are widespread in human healthcare. However, the wound healing effects of the herbal compositions are often not completely evidence-based investigated (Soni & Singhai, 2012; Budovsky *et al.*, 2015). Herbal mechanism studies are more complex in comparison to single compound investigations. Each analysis is another part, which enables a better overview of the complete underlying mode of action.

Plants show multifunctional wound healing promotion including moisturizing effects, anti-inflammatory, anti-bacterial, anti-oxidative as well as cell proliferation and migration-enhancing capacities (R. Thakur *et al.*, 2011; Budovsky *et al.*, 2015). Radical scavenging by herbal secondary metabolites is an especially important wound healing promotion process (Soni & Singhai, 2012). During wound regeneration, generated ROS and harmful lipid peroxidation can be prevented by increased anti-oxidant level. Anti-oxidants further protected from DNA damage and defended fibroblasts' viability and collagen fibril strength (Soni & Singhai, 2012). Herbal ingredients can influence additive or synergistically the expression and regulation of genes and proteins (especially of collagens and ECM molecules). These effects promoted cell migration, adhesion and proliferation (Budovsky *et al.*, 2015).

Phytochemical bioactive molecules, as some alkaloids, promoted wound healing by enhancing fibroblasts autocrine TGF-β 1 and EGF activity (Dong *et al.*, 2005), and supported angiogenesis (Morimoto *et al.*, 2008). Some representatives of flavonoids were well studied for their astringent, anti-oxidative and anti-microbial activities (Tsuchiya *et al.*, 1990). They were described to enhance re-epithelization by promoting cell viability (Suntar, 2010) and increasing fibroblasts proliferation and viability (Muhammed *et al.*, 2013; Soni & Singhai, 2012; Budovsky *et al.*, 2015). A couple of terpene/essential oils were observed to improve wound healing by increasing fibroblast proliferation (Ozturk *et al.*, 2006) and migration (Kuonen *et al.*, 2013). They suppressed pro-inflammatory cytokine expression (Park *et al.*, 2003), promoted angiogenic gene and growth factors expression as well as the ECM rearrangement (Coldren *et al.*, 2003). Further, some saponin/glycosides were shown to inhibit inflammation, increase fibroblasts viability, and fibroblasts (Czemplik *et al.*, 2012) as well as keratinocytes migration and general collagen fiber production *in situ* (Y. S. Kim *et al.*, 2011). All these representatives improved wound recovery.

This study was focused on traditionally used (i) *Astragalus propinquus* Schischkin (*A. propinquus*), (ii) *Rehmannia glutinosa* (Gaertn.) DC. (*R. glutinosa*), (iii) *Coptis chinensis* Franch (*C. chinensis*) and (iv) *A. euchroma*. These medicinal herbs were selected by hypothesis-driven literature search accompanied by published scientific investigations.

2.3.1. *Astragalus Propinquus* Schischkin.

Radix of *A. propinquus* (synonym: *A. membranaceus*; family: *Fabaceae*) is named Huangqi in TCM. The aqueous extract is ethnopharmacologically used to treat chronic ulcers and fistula. It is traditionally described to promote the release of blood accumulation, improve microcirculation and angiogenesis (Chinese Pharmacopoeia Comission, 2010; Hempen & Fischer, 2006; Greten, 2009). The widespread herb is used in most formulations for anti-diabetic therapies because it helps in lowering blood glucose level (J. Li *et al.*, 2004; WHO, 1999), stimulates the immune system and shows anti-bacterial properties (Hoo *et al.*, 2010). The root appears yellow/ocher-colored with a cavernous phenotype (Greten, 2009) (Fig. 2.3).

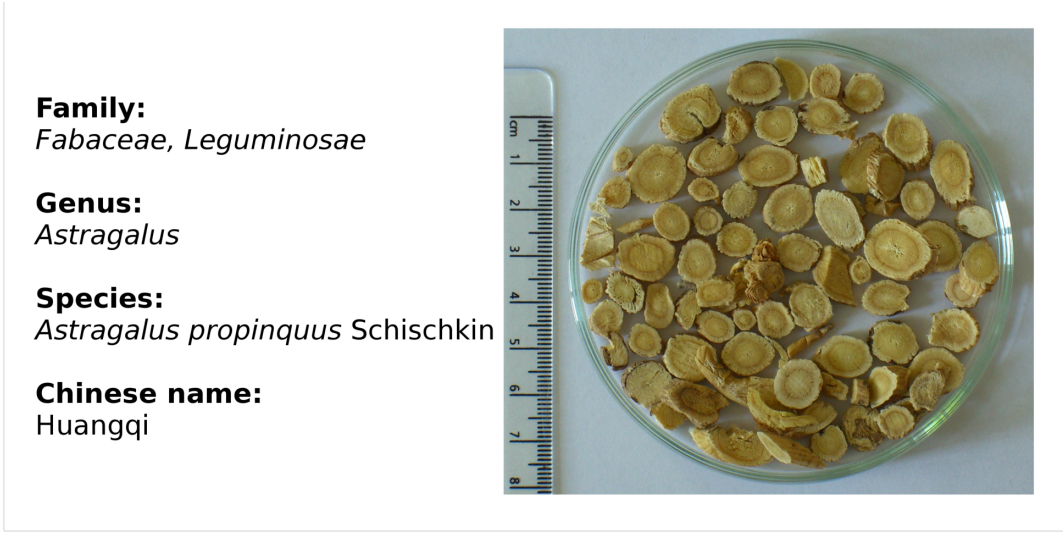

Figure 2.3.: Dried and cut *A. propinquus* radix material with belonging taxonomy

Two aqueous herbal formulations containing 30 % or 27 % *A. propinquus* (and other herbs) increased the cellular viability of primary diabetic fibroblast and CRL-7522 fibroblast cell line *in vitro* (T. Lau *et al.*, 2007).
Furthermore, a single aqueous extract of *A. propinquus* showed anti-inflammatory capacity in human macrophages (THP-1), mouse macrophages (RAW-Blue, Hoo *et al.*, 2010; RAW 264.7, K.-M. Lau *et al.*, 2012) and a human skin fibroblasts cell line (Hs27, Q. Zhang *et al.*, 2011) *in vitro*. It further promoted the viability of diabetic fibroblast (T. Lau *et al.*, 2009) and proliferation of normal human fibroblasts (T. Lau *et al.*, 2007; K.-M. Lau *et al.*, 2012). The proliferation of human primary keratinocytes was enhanced by a primary aqueous soxhlet extract (final 80 % ethanolic) treatment (Ren *et al.*, 2012). Angiogenesis promotion capability was observed *in vitro* in human umbilical vein endothelial cells (HUVEC) treated with a 50 % ethanolic extract (ethanol in water; Huh *et al.*, 2011) and human endothelial cells (HMEC1) cultured in the presence of an aqueous *A. propinquus* extract (K.-M. Lau *et al.*, 2012).

A. propinquus contains mainly flavonoids, saponins and polysaccharides (Auyeung *et al.*, 2016; WHO, 1999). Single components have been identified and analyzed in several studies due to their wound healing capacities. Formononetin, a flavonoid, enhanced blood microcirculation, expression of early growth response factors 1 protein that resulted in improved wound closure and increased proliferation in endothelial HUVEC (Huh *et al.*, 2011). The results indicated promotion of wound healing and endothelial repair through the regulation of the extracellular signal-regulated kinase and mitogen-activated protein kinase (MAPK) pathways. This chemical component further enhanced the capillary network in cultured explanted skeletal muscle stained with anti-von Willebrand factor (Huh *et al.*, 2011). These angiogenesis-related findings, observed in *in vitro* cell culture and in explanted muscles, increased the assumption that formonectin and *A. propinquus* positively influence vascularization. This is an important mechanism during wound regeneration. Astragaloside IV, a further main component from *A. propinquus*, improved wound healing in a diabetic mouse model. Here, re-epithelialization was increased and collagen deposition enhanced. ECM-related genes, such as collagen type IIIa and fibronectin, were enhanced expressed. Increased number of endothelial cells together with increased VEGF and von Willebrand factor expression pointed again to improved angiogenesis associated with wound healing (Luo *et al.*, 2016). Additionally, astragaloside IV showed photo-aging protection effects on UV-irradiated fibroblasts as result of a decreased activation of MMPs and the MAPK pathway (Yang *et al.*, 2011). It prevented inflammatory related gene expression by inhibiting nuclear factor kappa-light-chain-enhancer of activated B-cells (NFχB) *in vivo* in mice (Zhang & Frei, 2015) and *in vitro* in primary fibroblast (Yang *et al.*, 2011).

2.3.2. *Rehmannia Glutinosa* (Gaertn.) DC.

R. glutinosa (TCM: Shengdihung; family: *Plantaginaceae*) is another herb used to treat different kinds of wounds and skin diseases. It is described to stop bleeding, lower infections and cure exanthemas and ulcers (Greten, 2009). The dried radix of *R. glutinosa* has a shape of big black bulbs (Fig. 2.4). It has anti-mycotic, anti-bacterial, immune suppressive as well as liver protective properties (R.-X. Zhang *et al.*, 2008; Greten, 2009; WHO, 2007). This common herb is widely used in Asia (WHO, 2007).
The aqueous extract is used in many herbal therapies for diabetes because of its hypoglycemic effects. They were observed as *e.g.* enhanced insulin production and reduced glycogen amounts in the liver (W. L. Li *et al.*, 2004; Xie & Du, 2011). *R. glutinosa* was described for its broad pharmacological activities on immune, blood, endocrine, nervous as well as cardiovascular system (R.-X. Zhang *et al.*, 2008). Acute wounds in rats re-epithelialized faster just as the diabetic ulcer on the rat's feet treated with the

aqueous extract (T. W. Lau *et al.* 2008 & 2009). Lau and coworkers demonstrated improved blood vessel regeneration and reduced inflammation in a diabetic foot ulcer model and in an inflammation model in rats (T. W. Lau *et al.*, 2009). *In vitro*, fibroblast viability was significantly enhanced by an combined extract therapy, containing 14 or 17 % *R. glutinosa*, as well as by the single extract in the CRL-7522 cell line (T. Lau *et al.*, 2007). Aqueous *R. glutinosa* extract further increased the viability of fibroblasts derived from diabetic patients (T. Lau *et al.*, 2007 & 2009).

Family:
Plantaginaceae

Genus:
Rehmannia

Species:
Rehmannia glutinosa (Gaertn.) DC.

Chinese name:
Shengdihuang

Figure 2.4.: Dried *R. glutinosa* radix material with belonging taxonomy

R. glutinosa mainly contains amino acids, saccharides, flavonoids, inorganic ions and iridoids (R.-X. Zhang *et al.*, 2008; WHO, 2007). 2,5-dihydroxyacetophenone, one of the main compounds of *R. glutinosa*, showed anti-inflammatory impact in mouse macrophages. This effect was measured by decreased nitrogen monoxide level, increased expression of pro-inflammatory cytokines, such as TNF-α and Il-6, and reduced activation of NFκB and MAPK related pathways (Han *et al.*, 2012).

2.3.3. Combined Treatment of *A. Propinquus* and *R. Glutinosa*

Traditionally, *A. propinquus* and *R. glutinosa* are used as an aqueous herbal combination with other herbs or as a two herb formulation (ratio 2:1). A clinical trial demonstrated that 35 of 40 patients with diabetic foot ulcers were protected from amputation by oral treatment with an aqueous extract combination of *A. propinquus* and *R. glutinosa* amongst other herbs. The small case number did not allow further statistical evaluation (Wong *et al.*, 2001). Furthermore, the application of the herbal combination significantly reduced wound size in a diabetic mouse model (Tam *et al.*, 2011). Here, tissue regeneration and fibroblast proliferation were increased. Moreover,

angiogenesis relevant processes, such as blood vessel formation and cell migration of endothelial HUVEC, were enhanced (Tam *et al.*, 2011; T. W. Lau *et al.*, 2008; K.-M. Lau *et al.*, 2012). Lau *et al.* demonstrated viability improvement *in vitro* in primary human fibroblasts by the combined treatment in comparison to the single herbal extracts (T. Lau *et al.*, 2007). This effect was present in cultured fibroblasts of diabetic donors as well. Additionally, gene expression associated with angiogenesis and wound healing related pathways, such as inflammation, proliferation and ECM formation, was increased in Hs27 fibroblast cell line due to the treatment with the herbal extract combination (Tam *et al.*, 2011; Q. Zhang *et al.*, 2011). An aqueous combined decoction (concentrated and alcohol added to final 80 % ethanol) improved wound re-epithelialization by significantly enhancing the viability and proliferation of human primary keratinocytes *in vitro* (Ren *et al.*, 2012).

2.3.4. *Coptis Chinensis* Franch.

The herb *C. chinensis* (TCM: Huanglian; family: *Ranunculaceae*) is traditionally used in various aqueous herbal combinations to treat inflammatory diseases. This is caused by its anti-oxidative (Jung *et al.*, 2009; Friedemann *et al.*, 2014), anti-inflammatory (J. M. Kim *et al.*, 2010), disinfecting, detoxifying, anti-bacterial and anti-mycotic capacities (K. C. Huang, 1999; Kong *et al.*, 2009; Remppis *et al.*, 2010). It was shown that *C. chinensis* has strong anti-helicobacter pylori activity, which reassured the anti-inflammatory and anti-bacterial impact (Ma *et al.*, 2010). *C. chinensis* was further used to treat ulcers (Hempen & Fischer, 2006). The rhizome appears as yellow root filaments widespread in China (Fig. 2.5; WHO, 1999). *C. chinensis* extract was described for its anti-diabetic properties (Zheng, 2004). Orally given it decreased the blood glucose level of normal mice (W. L. Li *et al.*, 2004). An aqueous herbal formulation, containing this herb amongst others, showed anti-inflammatory effects in HaCaT keratinocytes and mouse macrophages. These findings supported its usage for inflammatory skin diseases (Jin *et al.*, 2015). The applied aqueous extract of *C. chinensis* reduced radiation-induced tissue damage by reduction of oxidative stress in rats (X.-J. Wang *et al.*, 2013). *C. chinensis* further supported hemostasis and granulation tissue formation, which is important for the treatment of impaired wounds (Hempen & Fischer, 2006).

The main components of *C. chinensis* are berberine, coptisine, berberastine, jatrorrhizine and palmitine (WHO, 1999; Friedemann *et al.*, 2014). Berberine from *C. chinensis* was described for its various pharmacological activities such as immunosuppression (Xu *et al.*, 2005), anti-viral, anti-microbial, anti-inflammatory (Remppis *et al.*, 2010), anti-cancer and cholesterol lowering effects (Feng *et al.*, 2010). Feng and

Family:
Ranunculaceae

Genus:
Coptis

Species:
Coptis chinensis Franch.

Chinese name:
Huanglian

Figure 2.5.: Dried and cut *C. chinensis* root material with belonging taxonomy

coworkers further demonstrated its hepatotoxic protection impact in a tetrachloride induced liver injury rat model.

2.3.5. *Arnebia Euchroma* (Royle) I. M. Johnst.

A. euchroma is pharmacologically named Zicao in TCM (family: *Boraginaceae*). Zicao is used for the therapy of exanthema, eczema, skin infections, burn wounds, chronic skin ulcer and gastrointestinal obstructions (Chinese Pharmacopoeia Commission, 2010; Greten, 2009). Zicao comprises the genera Lithospermum, *Onosma* and Arnebia which all belong to the same family. These genera can be easily mixed because of their macroscopic and pharmacological similarities (Chinese Pharmacopoeia Commission, 2010). Plants of these genera grow in several alpine regions of Asia and northern Africa (Nasiri *et al.*, 2016). The radix of Zicao is traditionally boiled in oil, for external, and in water for oral therapy (Chinese Pharmacopoeia Commission, 2010). All three species are known for the presence of hydrophobic pyrrolizidine alkaloids (PAs) (Röder & Rengel-Mayer, 1993; Röder, 1995; Kretschmer, 2011; Fu *et al.*, 2002). Some of these compounds could cause hepatic damage and in high and long-term doses, cancer development. Therefore the oral uptake is recommended to be reduced or avoided. Arnebia genus had the least amount of detected total PAs compared to other species used as Zicao (Röder & Rengel-Mayer, 1993; Röder 1995 & 2000). Therefore, this research was focused on *A. euchroma*. The literature review concerning the wound healing capacities of Zicao was performed with all traditionally used genera.
A. euchroma has a dark purplish-red/purplish-brown (Chinese Pharmacopoeia Commission, 2010) radix which appears arid and shrunken (Fig. 2.6). Scientific publications reported the usage of different solvents for extraction with varying treatment effects.

A. euchroma extract (ARE) of different solvents showed anti-inflammatory and antimicrobial activity (Nasiri *et al.*, 2015, ointment; Kaith *et al.*, 1996, soxhlet extract with one petrol ether after another chloroform and ethanol and an aqueous decoction; H.-M. Li *et al.*, 2011, ethanolic successively petrol ether and butanol). Oral administration of the successively extracted petrol ether, chloroform and ethanolic soxhlet ARE as well as an aqueous decoction decreased ear edema size in the rat (Kaith *et al.*, 1996). Edema reduction in human was less effective when treated with oil ARE than with the petrolatum positive control (Aliasl *et al.*, 2014). General wound healing promotion of applied oil ARE was confirmed by a clinical study (X.-W. Pei *et al.*, 2005) and in a rabbit model (X.-W. Pei *et al.*, 2006). Here, re-epithelialization of acute wounds was increased together with enhanced fibroblast cell number, blood vessel and collagen fiber amount. Aliasl *et al.* demonstrated decreased erythema, reduced crusting, better wound appearance and enhanced epithelial confluence in carbon dioxide laser induced burn wounds treated with an oil ARE in rats (Aliasl *et al.*, 2014). Burn wounds treated with an ethanolic ARE showed enhanced epithelialization, promoted fibroblasts proliferation together with decreased inflammation in a rat model (S. Ashkani-Esfahani *et al.*, 2012, 1:1, v/v, ethanol in water; Nasiri *et al.*, 2015, ointment) and reduced healing period in the clinic (Nasiri *et al.*, 2016, ointment). Additionally, a diethyl ether extract significantly accelerated the healing of burn wounds in rats, accompanied by higher amounts of fibroblasts and collagen fibers, and reduced inflammatory cells (Pirbalouti *et al.,* 2009).

Wound healing promotion was further demonstrated in diabetic mice with an ether extract of *Lithospermum erythrorhizon* Siebold & Zucc. (*L. erythrorhizon*) resulting in reduced inflammatory phase and supported granulation stage (Fujita *et al.*, 2003). A 95 % ethanolic *L. erythrorhizon* extract treatment improved proliferation of human embryonic fibroblast cell line up to 25 % (Hsiao *et al.*, 2012). Moreover, reduced ROS production was measured together with increased protein expression related to antioxidant and anti-apoptotic mechanisms. These findings indicated the extracts mediated tissue protection against hyper-inflammation. Additionally, Hasio and coworkers described improved cell mobility and increased collagen secretion, which helped to close the injury (Hsiao *et al.*, 2012). An aqueous extract of *L. erythrorhizon* did not affect the proliferation of primary human keratinocytes and fibroblasts but enhanced *in vitro* wound recovery in lower doses 24 h after wounding in both cell types (H. Kim *et al.*, 2011). Photoprotection by treatment with an ether extract of *L. erythrorhizon* was demonstrated in cultured human keratinocytes (Ishida & Sakaguchi, 2007). Yoo *et al.* showed reduced oxidative stress in a methanolic *L. erythrorhizon* extract pre-treated human keratinocyte cell line and fibroblasts, which was induced by hydrogen peroxide or UV irradiation (Yoo *et al.*, 2014). This effect occurred together with enhanced

viability *in vitro*. Moreover, an orally given, 70 % ethanolic extract of *L. erythrorhizon* significantly increased the *stratum corneum* hydration and the amount of total ceramides. It further affected the clinical severity positively in patients with atopic dermatitis (Cho *et al.*, 2008) and in an atopic dermatitis mouse model (Lee *et al.*, 2009). Chang *et al.* demonstrated a time and dose-dependent skin moisturizing effect of a 95 % ethanolic *L. erythrorhizon* extract in addition to a reduced trans-epidermal water loss of healthy human skin (M.-J. Chang *et al.*, 2008). Increased fibroblast viability was detected by treatment with an n-hexane-dichloromethane extract of an *Onosma* species (Ozgen *et al.*, 2006).

Family:
Boraginaceae

Genus:
Arnebia

Species:
Arnebia euchroma (Royle)
I.M.Johnst.

Chinese name:
Zicao

Figure 2.6.: Dried and cut *A. euchroma* root material with belonging taxonomy

Main components of *A. euchroma* are naphthoquinones such as the chiral molecules alkannin and shikonin together with their derivatives. Naphthoquinones are mainly used as coloring pigments in food and textile industry, cosmetics and healthcare (Papageorgiou *et al.*, 1999). Alkannin and shikonin are both described for their anti-fungal (Sasaki *et al.*, 2000), anti-microbial (Chen *et al.*, 2003; Haghbeen *et al.*, 2011), anti-HIV (Chen *et al.*, 2003), radical scavenging (Assimopoulou & Papageorgiou, 2005) and anti-inflammatory capabilities (Haghbeen *et al.*, 2011). They showed cytotoxic and potentially anti-tumorigenic capacities in different tumor identities (Gaddipati *et al.*, 2000; Z.-S. Huang *et al.*, 2004, Hou *et al.*, 2006; Xiong *et al.*, 2009; I.-C. Chang *et al.*, 2010; Papageorgiou *et al.*, 1999 & 2008). The anti-cancer effect of shikonin was demonstrated in a clinical trial by significantly reduced tumor growth in late-stage lung cancer patients without further therapeutic options (X. P. Guo *et al.*, 1991). In addition, naphthoquinones are used for wound therapy because of their re-epithelization, angiogenesis and granulation tissue formation promotion (Papageorgiou *et al.*, 1999; Ozaki *et al.*, 1998). Alkannin and shikonin showed comparable wound healing capacities on granulation tissue formation in a wound model in rats. Here, fibroblast

proliferation was increased together with accelerated collagen fiber formation (Ozaki *et al.*, 1998). The observed improvement in wound healing capacity of both molecules was additionally documented in acute wounds in dogs (Karayannopoulou *et al.*, 2011). The effect was described by improved angiogenesis, increased epithelial thickness and collagen fiber content of the resulting granulation tissue. Moreover, shikonin reduced ear edema in mice and paw swelling in rat models (W. J Wang *et al.*, 1994; Andujar *et al.*, 2010). This anti-inflammatory impact was supplemented by the finding that shikonin inhibited NFκB induction in RAW264.7 mouse macrophages (Andujar *et al.*, 2010). Papageorgiou applied in the eighties for a patent on different naphthoquinone derivatives containing wound healing formulations (Papageorgiou, 1981). Further clinical trials confirmed the positive impact of shikonin and enabled the pharmacological development of naphthoquinone containing trauma formulations as HELIXDERM® and HISTOPLASTIN RED® (Papageorgiou *et al.,* 2008). Described intoxications of naphthoquinone derivatives are caused by increased ROS generation (Papageorgiou *et al.*, 1999; Klaus *et al.*, 2010).

Arnebin-1, a further compound of *A. euchroma*, improved wound healing in acute and impaired punch wounds in rats. Here, re-epithelialization, angiogenesis and granulation tissue formation together with collagen and fibronectin synthesis were increased (Sidhu *et al.*, 1999).

The diverse described, positive wound healing associated impacts of *A. euchroma* root advise the usage of the complex molecular capacities of the radix extract instead of single molecules as naphthoquinone derivatives. This enlarges possible wound healing promotion impacts. Compared to single compound drugs, diverse secondary metabolites of herbal extracts may act synergistic or additive, wherefore the actual compound dose could be reduced, which further decrease potential intoxication.

2.4. Aim of the Study

Delayed and impaired wound healing is still a rising health care problem worldwide because chronic wounds often fail to respond to available treatments (Blakytny & Jude, 2006; Budovsky *et al.*, 2015). Therefore, the request for new effective and complex acting wound healing therapeutics is still present. The scientific interest in medicinal herbs and their ingredient compounds expanded during the last years. The interplay of traditionally used botanicals and modern medicinal knowledge could result in more effective wound healing strategies with reduced adverse effects. TCM provides a broad source of herbs for wound healing treatment. However, herbal therapeutics consist of a broad mixture of secondary metabolites and possible effective compounds; therefore,

it is complicated to discover active molecules out of herbal combinations as they are traditionally used. Empirical studies were mainly performed with single compounds or single herbal extracts, which partly fail to explain the actual ethnopharmacological effectiveness.

The aims of this study were:

(i) The proof of the traditional described Chinese herbal extracts wound healing capacities in a porcine *ex vivo* WHM and the discovery of the herbal extract with the most promising re-epithelialization promoting impact.

(ii) The extract characterization due to the chemical composition of the candidate herb by thin layer chromatography (TLC), ultra high-performance liquid chromatography - high-resolution mass spectrometry (UHPLC-HRMS) as well as UHPLC - evaporative light scattering detector (ELSD) and determination of its anti-oxidative capacities.

(iii) The investigation of the regeneration underlying mechanism and identification of the affected cell types by studying the extracts impact *in situ* and in cultured primary human skin cells *in vitro*. Here, wound healing associated mechanism including cell viability, proliferation, migration, adhesion, apoptosis induction as well as the formation of an improvisational ECM and a barrier were addressed.

(iv) The determination of the most effective wound recovery by different extract application time points and application methods to enable optimal therapeutic extract usage for cutaneous wound healing strategies.

3. Material and Methods

Material

In this section, experimental equipment and chemicals are listed with manufacturers specifications.

3.1. Technical Equipment

The technical materials and equipment were provided by the cell culture lab of the Department of Dermatology and Venerology of the University Clinic Hamburg-Eppendorf (short: DermaLab) as well as of the laboratory of the HanseMerkur Center for Traditional Chinese Medicine at the UKE (short: HMZ for TCM) or collaborating laboratories (Tab. 3.1).

Table 3.1.: The technical equipment, including manufacturer information, is listed in alphabetical order below (company based in Germany, DE, if not mentioned differently).

Equipment description	**Manufacturer**
Cell counter, Countess	Thermo Fisher Scientific (Schwerte)
Cell culture dishes (2, 5 and 10 cm), Falcon®	VWR (Darmstadt)
Cell culture plates 1) 12; 24; 48; 96 well, Falcon® 2) 96 well, CellStar®, Greiner bio-one 3) 96 well, white, luminescent Nunc™ MicroWell	 1) VWR 2) Roth (Karlsruhe) 3) Thermo Fisher Scientific
Cell culture flasks, T25, T75, T125; Falcon®	VWR
Cell freezing container, Mr. Frosty™	Thermo Fisher Scientific

Equipment description	**Manufacturer**
Cell scraper	Sarstedt Ag & Co. (Nümbrecht)
Centrifuge 1) Laborfuge 400e 2) Biofuge fresco 3) Cooling centrifuge, Multifuge 1 S-R 4) Universal 320 / 320 R 5) Bachofer Vacuum Concentrator	 1 - 3) Heraeus Instruments (Hanau) 4) Hettich Lab Technology (Tuttlingen) 5) Bachofer GmbH (Reutlingen)
Centrifuge tubes 0.5; 1.5; 2; 5 ml	Eppendorf (Hamburg)
Centrifuge tubes 15; 50 ml 1) CELLSTAR®, PP, sterile 2) Falcon®	 1) Roth 2) VWR
Coloring cradle	Roth
Column for chromatography 1) Acquity UPLC® BEH C18 2) Filter, UHPLC, SPE C18	 1) Milford (Massachusetts, US) 2) Finisterre (Teknokroma®, US)
Cotton buds, small head (autoclaved)	Karl Beese GmbH & Co. KG (Barsbüttel)
Cryomatrix, embedding media (frozen sections)	Leica (Nussloch, DE)
Cryostat, CM 3050	Leica
Cryostat blades, 819	Leica
Cryotubes, 1 ml	Greiner bio-one (Frickenhausen)
Developing Chamber, 814019, TLC	Macherey-Nagel (Düren)
Developer (western blot film), Curix 60	Agfa (Berlin)
Digital camera 1) C 4742-95 (IF microscope) 2) EC 3 (light microscope) 3) Casio Exilim EX-Z750	 1) Hamamatsu (Hamamatsu, JP) 2) Leica 3) Casio (Norderstedt)
Dispenser, Sensi-Disc	Becton Dickinson (Heidelberg)
Electronic accurate balance 1) BI 3100 2) Kern ABS, 0.1 mg - 200 g 3) ISO 9001	 1) Sartorius (Hannover) 2) Th. Geyer Hamburg GmbH (Hamburg) 3) Sartorius (Hannover)

Equipment description	**Manufacturer**
ELS-Detector, Sedex 85, LT-ELSD	Sedere (Alfortville)
Equipment for SDS-Gel preparation, Mini-Protean® Tetra Handcast Systems	Bio-Rad (München)
Folded filter 1) Rotilabo®-Faltenfilter, Typ 600P, cellulose, 240 mm 2) Whatman, 185 mm	 1) Roth 2) GE Healthcare Life Science (Little Chatfont, UK)
Glass cuvette	Roth
Glass flask, Duran® Laboratory glass flask GL45 100, 250 and 500 ml	Roth
Forceps	AESCULAP AG (Tutlingen)
Heating block, Dri-Block DB-3	Techne (Cambridge, UK)
Impedance measurement device, cellZscope®	nanoAnalytics GmbH (Munster)
Incubator 1) BDD 6220 2) B 5060 3) B 5090 E 4) T6030	 1 - 4) Heraeus Instruments (Hanau)
Lamination shrink wrap unit, Folio, FS3602	Severin (Sundern)
Liquid nitrogen tank	Taylor-Warten (Indianapolis, US)
Micro Pipette with ring mark 1) Ringcaps®, 5/10 µl 2) Capillary pipettes Duran®, 10/20 µl	 1) Hirschmann Laborgeräte (Eberstadt) 2) Roth
Microscopes 1) Axioplan 2 (Fluorescence) 2) DMIL (light, inverse) 3) DMLS (straight light)	 1) Zeiss (Göttingen) 2 - 3) Leica
Microscopic slides, SuperFrost/Plus	Assistant, Glaswarenfabrik Karl Hecht KG (Sondheim)

Equipment description	**Manufacturer**
Mill, herbal grinding 1) Alaska KM1310S 2) Severin KM3872	 1) Real Markt (Hamburg) 2) Severin (Sundern)
Nitrocellulose membrane, 0.45 µm	Biorad
Notebook, Latitude E5500	Dell (Round Rock, US)
Parafilm®	Roth
ph meter 1) 766 Calimatic 2) pH211 microprocessor pH Meter	 1) Knick (Berlin) 2) Hanna Instruments (Vöhringen)
Pipette Research® (0.5 -10 µl, 2 - 20 µl, 10 - 100 µl, 10 - 200 µl, 100 - 1000 µl, 5000 µl)	Eppendorf
Pipette assistance 1) Macro 2) Pipetus 3) micropipetter 1 - 200 µL, TLC	 1) Brand (Wertheim) 2) Hirschmann Laborgeräte (Eberstadt) 3) Roth
Plate reader 1) Ultraspec 2000 2) Magellan Sunrise 3) Thermo Multiskan SPECTRUM microplate 4) Mithras LB 940	 1) Pharmacia Biotech (Freiburg) 2) Tecan (Crailsheim) 3) Thermo Fischer Scientific 4) Berthold (Bad Wildbad)
Power supply 1) Standard Power Pack P 25 2) Stage Controller	 1) Biometra (Göttingen) 2) Lavision Biotec (Bielefeld)
Reaction tubes 1, 1.5, 2 and 5 ml	Eppendorf
Reaction tubes 10 and 50 ml 1) Falcon® 2) Greiner bio-one, CELLSTAR®	 1) VWR 2) Roth
Rotation evaporator, Totavapor-R rotary-evaporator	Büchli (Essen)
Rotation shaker 1) tiny turner 2) Roto-Shake Genie®	 1) CTI (Idstein) 2) Scientific Industries (Bohemia, US)

Equipment description	**Manufacturer**
Round flask, Rotilabo®-Rundkolben, Enghals	Roth
Scalpel	AESCULAP AG
Scalpel blades, FEATHER #10, #11	pfm Medical AG (Cologne)
Scissor	HSB, Karl Hammacher GmbH (Solingen)
SDS-Gelelectrophoresis chamber, Mini-Protean®-Tetra-System	Bio-Rad (München)
Security cell culture bench, Hera Safe 12	Heraeus Instruments
Semidry-Blot-System, Trans-Blot®TurboTM	Bio-Rad
Shaker 1) horizontal, KS250 2) Silent Rocker 3) stedim Certomat BS-1 4) Roto-Shake Genie 5) AIP 4 plate shaker	 1) IKA Labortechnik (Staufen) 2) CTI 3) Sartorius 4) Scientific Industries (Bohemia, US) 5) Diagnostics Pasteur (Paris, FR)
Spectrometer, NanoDrop 2000c	Thermo Scientific (Waltham, Massachusetts, US)
Sterile filter unit, duapore PVDF membrane, Millex-HV, 0.45 µm	Merck
Thermo magnetic agitator 1) MR 3001 2) IKA MAG®RH and RCT, IKA® Labortechnik	 1) Heidolph (Schwabach) 2) Janke&Kunkel (Staufen)
TLC plate pre-coated ADAMANT UV254, 0.25 mm silica gel 60 with fluorescent indicator, 20 cm	Macherey-Nagel (Düren)
TLC spray equipment	Roth
TLC vaporizer equipment	Roth
Trans well, Costar Transwell # 3640,	Corning Incorporated, Corning
polyester filter 1.2 cm2, 0.4 µm	(New York, US)

Equipment description	**Manufacturer**
Ultrapure water facility 1) Astacus LS TI 2) PURELAB flex, Mod. PF2XXXXM1	 1) Membrapure GmbH (Bodennheim) 2) ELGA, Veolia Water Solutions&Technologies (Celle)
UHPLC system 1) Thermo Dionex Ultimate 3000 with heated electrospray ionization (HESI-II) source and Mass spectrometer, orbitrap Q-Exactive Plus 2) Acquity UPLC system	 1) Thermo Scientific (Waltham, MA, US) 2) Waters (Milford, MA, US)
Ultrasonic bath	Bandelin Sonorex (Berlin)
UV-light lamp, Typ NU-4	HeroLab GmbH Laborgeräte (Wiesloch)
Vacuum pump 1) Vacusip, cell culture 2) membrane vacuum pump ALCATEL, speed vacuum centrifuge 3) membrane vacuum pump Type N022AN.18, rotation evaporator	 1) Integra Biosciences (Biebertal) 2) Ehrhardt Vacuumtechnik (Henstedt-Ulzburg) 3) KNF Neuberger (Freiburg)
Vortexer 1) REAXtop 2) VF2 3) Vortex-Genie 2	 1) Heidolph (Schwabach) 2) IKA® Werke (Staufen im Breisgau) 3) Scientific Industries (Bohemia, US)
X-ray pipe, RS 225	Gulmay incorporated (Suwanee, GA, US)

3.2. Chemicals and Kits

All chemicals were provided by the DermaLab, HMZ for TCM or collaborating laboratories (Tab. 3.2). The used kits were mentioned in Tab. 3.3.

Table 3.2.: Used chemicals including manufacturer information (company based in Germany, DE, if not mentioned differently).

Substance description	**Manufacturer**
Acetic acid 1) DermaLab 2) HMZ for TCM	 1) Riedel-de Haen (Seelze) 2) Roth
Aceton	Th. Geyer Hamburg GmbH
Acetonitrile, ULC/MS grade	Biosolve Chimie SARL (Dieuze, FR)
Acrylamid	Serva (Heidelberg)
Ammoniumpersulfat (APS)	Serva
Adenosin 5'-triphosphate disodium salt hydrate (ATP)	Sigma-Aldrich (Taufkirchen)
Antimon(III)chloride reagent	Sigma-Aldrich
Aqua	Braun Melsungen AG (Melsungen)
Aqua bidestillata (*A. bidest.*) 1) HMZ for TCM 2) Collaboration lab., ULC/MS grade	 1) Roth 2) Biosolve Chimie SARL
Aqua, DEPC-treated	Eppendorf
Bacitracin	Sigma-Aldrich
β-Mercaptoethanol	Fluka (Taufkirchen)
Bisacrylamid	Serva
Bradford solution	PanReac AppliChem (Darmstadt)
Bromine phenolic blue	Sigma-Aldrich
Bovines Serum Albumin (BSA)	Roche (Mannheim)
Calciumchlorid	Serva
Calciumchloriddihydrate	Merck
Chlorophorm	Roth
Coomassie Brilliant Blue G250	Fluka
Cryo embedding solution	Thermo Fisher Scientific
DAPI (4',6-diamidino-2-phenylindol)	Roche
DermaLife® K	Lifeline Cell Tech (Frederick, US)
Dulbecco's Modified Eagle Medium (DMEM) Glucose medium	Biochrom AG (Berlin)
Diethylamin	Roth

Substance description	**Manufacturer**
Dimethylsulfoxid (DMSO)	Merck
Dragendorff-Munier-Spraying Solution	Roth
2,2-diphenyl-1-picrylhydrazyl (DPPH)	Sigma-Aldrich
Ethylendiamintetra acetat (EDTA) 1) Versen (cell culture - tested) 2) tissue culture	 1) Biochrom AG 2) Merck
Eosin G	Chroma-Gesellschaft (Münster)
Ethanol (pure) 1) DermaLab 2) HMZ for TCM	 1) Merck 2) Roth
Ethanol (methylated spirit)	Walter CMP GmbH (Hamburg)
Ethyl acetate	Roth
Eukitt	Kindler GmbH (Freiburg)
Fluoromount G	Southern Biotech (Eching)
Fetal bovine serum (FBS) 1) WHM 2) cell culture, ´GOLD´, Origin Australia	 1) Biochrom AG 2) PAA (Pasching, AT)
Formic acid 1) HMZ for TCM 2) Collaboration lab., ULC/MS grade	 1) Merck 2) Biosolve Chimie SARL
Glycerin	Roth
Glycin	Roth
Hämalaun solution according to Mayers	Merck
Haematoxylin according to Mayer, ready to use solution	Medite (Burgsdorf)
Hydrochloric acid (HCl)	Riedel-de Haen
Hydrochortison	Sigma-Aldrich
Igepal	Sigma-Aldrich
Insulin	Sigma-Aldrich
Isopentan	Sigma-Aldrich
Isopropanol	Merck

Substance description	**Manufacturer**
Lamination equipment, Severin Folio	Severin (Sundern)
Leupeptin	Sigma-Aldrich
Liquid nitrogen	TMG GmbH (Krefeld)
L-Glutamin	Biochrom AG (Berlin, DE)
Low-fat milk powder	Roth
Methanol 1) DermaLab 2) HMZ for TCM	 1) Mallinckrodt Baker (Deventer, NL) 2) Merck
MTT reagent [(3-(4,5-dimethylthiazol-2-yl)-2,5-diphenyltetrazolium bromide; thiazolyl blue)]	Sigma-Aldrich
Molybdato anhydrous phosphoric acid	Merck
N-acetyl-L-cystein (NAC)	Sigma-Aldrich
Naturstoffreagenz A	Roth
Normal goat serum (NGS)	Dianova (Hamburg)
Phosphate-buffered saline (PBS), Dulbecos, sterile with and w/o Mg^{2+}, Ca^{2+}	Biochrom AG
Penicillin	Grünenthal GmbH (Aachen)
Penicillin/Streptomycin	Biochrom AG
Petroleum gasoline	Sigma Aldrich
Phosphatase Inhibitory Mix, 100x	Cell Signaling Technology (Denver, US)
Phosphoric acid	Riedel-de Haen
Phenylmethylsulfonylfluorid (PMSF)	Sigma-Aldrich
Ponceau S	Sigma-Aldrich
Potassium chloride	Merck
di-Potassiumhydrogenphosphat-dihydrat	Merck
Potassiumhydroxid	Honeywell Riedel-de Haën (Seelze)
Spectra Multicolor Broad Range Ladder, Fermentas	Thermo Fisher Scientific
RPMI 1640 medium	Biochrom AG

Substance description	Manufacturer
Saline solution, isotone	Baxter Deutschland GmbH (Unterschleißheim)
Shikonin, #517-89-5, HPLC > 98 %	Shyuanye (Hangzhou, CHN)
Sodium chloride	Mallinckrodt Baker
Sodium chloride solution, 0.9 %	B. Braun Melsungen
Sodium deoxycholat	Sigma-Aldrich
Sodium dodecyl sulfate (SDS)	Bio-Rad
Staurosporine, Streptomyces sp., in solution, 100 µg, #569396	Calbiochem, Millipore (Darmstadt)
Sterilium®	Hartmann (Heidenheim an der Brenz)
Streptomycin	Grünenthal GmbH (Aachen)
Tetramethylethylendiamin (TEMED)	Fluka
Toluol	Roth
Triodothyronin	Sigma-Aldrich
Tris, Trizma Base	Sigma-Aldrich
Triton X-100	Sigma-Aldrich
Trolox	Sigma-Aldrich
Trypan blue	Invitrogen (Karlsruhe)
Trypsin; 2.5 %	Biochrom AG
Trypsin / EDTA; 0.05 %/0.02 %	Biochrom AG
Tween® 20	Sigma-Aldrich
Water, DEPC conditioned	Eppendorf
Water, steril	B. Braun Melsungen
Xylol	Mallinckrodt Baker

Table 3.3.: Kits and manufacturer details (company based in Germany, DE, if not mentioned differently).

Kit	Application	Manufacturer
Cell Proliferation ELISA, bromodeoxyuridine (BrdU)	Cell proliferation determination	Roche
CellTiter-Glo® Luminescent Cell Viability Assay	ATP measurement	Promega (Madison, Wi, US)
MyTaq™ DNA Polymerase	DNA amplification; mycoplasma detection	Bioline GmbH (Luckenwalde)
SuperSignal® West Pico Chemiluminescent Substrate	Chemoluminescent substrat, western blot	Thermo Fisher Scientific

3.3. Herbal Material

The dried herbal material of *Astragalus propinquus* Schischkin., certificate number Ch.B. 110401H004, *Rehmannia glutinosa* (Gaertn.) DC., certificate number Ch.B. 1105-01H034, and *Coptis chinensis* Franch., certificate number Ch.B. 081201 H053 were provided by HerbaSinica Hilsdorf GmbH (including test certificates for identity, clearance, heavy metals and pesticide analyses). *Arnebia euchroma* (Royle) I. M. Johnst. was obtained by Chinaturel Import Export B.V. (Chinaturel; source I), Rats Apotheke Stralsund (Rats Apotheke; source II) and Mehler (source III, certificate number Ch.B. 02280931). The herbal identity of all *A. euchroma* sources was proven by Phytochem® laboratory (Referenzsubstanzen GbRmbH, Ichenhausen, DE).
All plant names were verified with the *www.plantlist.org* working list of plants on December, 9th in 2016.

3.4. Buffer and Reaction Solutions

All buffers and solvents were filled up with *A. dest.* if not mentioned differently and the pH was adjusted with 1 M HCl (Tab. 3.4). Chemical solutions represented analytic purity and were stored at ambient temperature (A. T.; if not noted differently).

Table 3.4.: Buffer and solutions with their chemical ingredients [final concentration].

Buffer/Solution	**Composition**
PBS, pH 7.3 - 7.5, 10 x	160 g Sodium chloride 4 g Potassium chloride 23.2 g Sodium hydrogen phosphate 4 g Potassium hydrogen phosphate to final volume (ad) 2,000 ml
RIPA lysis buffer, 4 °C	0.61 g Tris 0.88 g Sodium chloride 0.5 g Sodium de-oxychelat 0.1 g SDS 1.5 ml Igepal ad 100 ml

Buffer/Solution	**Composition**
Proteases inhibitory Mix, 100 x, 4 °C	10 mg Leupeptin 10 mg Bacitracin 0.1 ml Pepstatin A 0.1 ml PMSF ad 1 ml (-20 °C)
Acrylamid solution, 4 °C	30 g Acrylamid [30 %] 0.8 g Bisacrylamid [0.8 %] ad 100 ml
Separation gel buffer, pH 8.8	90.83 g Tris [1.5 M] 2 SDS [0.4 %] ad 500 ml
Accumulation gel buffer, pH 6.8	12 ml Tris [120 mM] 20 g Glycerin [20 %] 20 ml β-Mercaptoethanol [20 %] 10 g SDS [10 %] spattle tip bromine phenolic blue
Blot buffer, 4 °C	80 ml Methanol [20 %] 57.6 g Glycin [192 mM] 12.1 g Tris [25 mM] 0.8 g SDS [0.02 %] ad 4,000 ml
Coomassie Brilliant Blue	400 ml Methanol [40 %] 50 ml Acetic acid [5 %] spattle tip Coomassie Brilliant Blue ad 1,000 ml
Discoloration solution	400 ml Methanol [40 %] 50 ml Acetic acid [5 %] ad 1,000 ml
Tris-buffered saline with Tween (TBS-T), 10 x, pH 7.4; working solution 1:10 in *A. dest.*	12.2 g Tris 87.66 g Sodium chloride 5 g Tween ad 1,000 ml
Low-fat milk block, 4 °C	12.5 g Low-fat milk powder [5 %] ad 250 ml with TBS-T filtered through folded filter

3.5. Tissue and Cell Culture Media

All reagents were stored at 4 °C if not mentioned differently (Tab. 3.5).

Table 3.5.: Overview of the used cell culture reagents.

Reagent	**Composition**
Culture medium for *ex vivo* WHMs	96.6 ml DMEM 2 ml FBS 1 ml Penicillin/Streptomycin 0.4 ml Hydrocortisone
Keratinocytes culture medium	99 ml DermaLife® Basal Medium, final LifeFactor supplements concentration: 6 mM L-Glutamine 0.4 % Extract PTM 1 µM Epinephrine 5 ng/ml rh TGF-α 100 ng/ml Hydrocortisone-Hemisuccinate 5 µg/ml Apo-Transferrin 0.06 mM Calcium chloride 1 ml Penicillin/Streptomycin
Keratinocytes trypsin	94 ml PBS 4 ml Trypsin (-20 °C) 2 ml EDTA
Fibroblast culture medium	89 ml RPMI 10 ml FBS 1 ml Penicillin/Streptomycin
Cell culture freezing medium	7 ml specific cell culture medium 2 ml FBS 1 ml DMSO

3.6. Antibodies

The used antibodies and their individual dilution for western blotting (WB) or immunofluorescence staining (IF) were listed below (Tab. 3.6 & Tab. 3.7). Primary and secondary antibodies for IF were diluted in PBS. Antibody isotypes were used as negative controls for IF in analog concentrations to the used primary antibodies diluted in PBS (guinea pig IgG, Santa Cruz Biotechnology, Heidelberg, DE; rabbit Ig-fraction, Dako, Hamburg, DE; mouse IgG1, R&D Systems, Wiesbaden, DE).

Table 3.6.: Primary antibodies used for western blot (WB) and immunofluorescence (IF) staining (species, dilution and manufacturer) on porcine cryosections or protein analyses of human primary fibroblast.

Primary antibody	**Species**	**Dilution**	**Company**
CK 10, GP-K10	guinea pig	IF, 1:200	Progen (Heidelberg, DE)
CK 14, RCK107	mouse	IF, 1:500	Progen
anti-MIB 1, clone Ki67	mouse	IF, 1:50	Dako
α-tubulin, clone DM1A	mouse	WB, 1:2,000	Calbiochem, Merck Millipore
anti-collagen type I #234167	rabbit	WB, 1:1,000	Merck Millipore
caspase 3, #9662	rabbit	WB, 1:600	Cell Signaling Technology (Danvers, MA, US)
cleaved caspase 3, #9664	rabbit	WB, 1:600	Cell Signaling Technology
collagen type IV, #SAB4500369	rabbit	WB, 1:500	Sigma-Aldrich
fibronectin/anastellin, #NBP1-91258	rabbit	WB, 1:500	Novusbio (Wiesbaden Nordenstadt, DE)

Primary WB antibodies were diluted in 5 % low-fat milk block (Tab. 3.6), except the anti-collagen type I antibody, which was diluted in 0.5 % low-fat milk block. Secondary WB antibodies were diluted in analogous solvent compared to their belonging primary antibody.

Table 3.7.: Schema for western blot (WB) and immunofluorescence (IF) used secondary antibodies with additional information concerning the manufacturer, species and dilution.

Secondary antibody	Species	Dilution	Company
Dylight 488-cojugated AffinityPure Donkey anti-mouse IgG (H+L)	mouse	IF, 1:600	Jackson Immuno Research (Suffolk, UK)
Goat anti-mouse Alexa-Flour 594 F(ab)$_2$	mouse	IF, 1,250	Invitrogen, Thermo Fisher Scientific
Goat anti-rabbit Alexa-Flour 594 F(ab)$_2$	rabbit	IF, 1,250	Invitrogen, Thermo Fisher Scientific
Goat anti-guinea pig Alexa-Flour 488 (H+L)	guniea pig	IF, 1:600	Invitrogen, Thermo Fisher Scientific
Goat anti-mouse MRP	mouse	WB, 1:5,000	Dako
Goat anti-guinea pig MRP	guinea pig	WB, 1:5,000	Dako
Goat anti-rabbit MRP	rabbit	WB, 1:5,000	Dako

3.7. Tissue and Cell Origins

Porcine Tissue

The wound healing capacity of different herbal extracts was evaluated on porcine *ex vivo* WHMs (patent DE10317400; Brandner *et al.*, 2004). The animal tissue was provided from a local slaughterhouse and derived directly after consumption slaughter from six-month-old, healthy, domesticated pigs (*Sus scrofa domestica*; cross-breed Yorkshire/Deutsches Edelschwein).

Human Tissue

The human tissue, used for the *ex vivo* WHMs, was provided by patients that underwent esthetical surgery in different clinics in Hamburg (DE; based on the statement of the ethics committee WF-28/12). The samples of three men and six women (thoracic, mean age ± SD: 50.3 ± 15.4 years) were used anonymously. The experiments were conducted according to the principles expressed in the Declaration of Helsinki.

Primary Human Skin Cells

The preparation of primary human keratinocytes and fibroblasts was carried out by using infant foreskin specimens that were provided by the children's surgery ward of the UKE (Hamburg, DE; age $\leq$ five years). The operations were conducted for clinical reasons and the tissue usage for experimental investigations was authorized by the ethics committee (WF-061/12).

3.8. Software

In this section the used software is listed (Tab. 3.8).

Table 3.8.: Schematically overview on the used software with functional description and manufacturer information.

Software name	**Function description**	**Manufacturer**
CellZscope 2.22.2	Measurement of the transepidermal resistance of cultured cells	NanoAnalytics GmbH
Excel 2003/2007	Calculations	Microsoft (Redmond, Washington, US)
Fiji (ImageJ)	Picture adaption (IF), evaluation (WB)	open source
Gimp	Figure adaption	open source
LAS EZ 2.1.0	Camera (EC 3) picture regulation	Leica
LyX release 2.1.4	Document processor	open source
MagellanTM 6	Photometrically extension measurement	Tecan
OpenLab 3.0.9	Picture regulation fluorescent microscope	PerkinElmer Cellular Techn. GmbH (Hamburg, DE)
Prism	Statistic and graph preparation	GraphPad (La Jolla, California, US)
SPSS 21	Statistics software	IBM (Armonk, North Castle, New York, US)
Tscratch	Analysis of scratch assay pictures	CSElab ETH (Zurich, CHE)
Word 2003/2007	Text generation	Microsoft

Methods

The following experiments were conducted in accordance with the safety instructions (protective clothing, sterile work space *etc.*) as well as with the appropriate ethics.

3.9. Hypothesis-driven Literature Search for Traditionally Used Wound Healing Promoting Chinese Herbs

The ethnopharmacology primary TCM literature was screened for medicinal herbs (Friedemann *et al.*, 2015), which are traditionally used for the treatment of skin injuries and especially impaired wounds like ulcers. Used search terms were: skin, wound, wound healing, ulcer, diabetes, impaired and chronic wounds. The resulting plant genera of the hypothesis-driven literature research (Shizhen, 2003; Chinese Chinese Pharmacopoeia Commission, 2010) were supplemented by the consolidated knowledge of TCM practitioners, who reassured the current herbal usage and relevance. They provided additional information about the therapeutic dose, application method, treatment duration and possible health risks. These data were complemented with information from scientific databases (such as *www.ncbi.nlm.nih.gov/pubmed* amongst others). Additionally, besides the above mentioned, used search terms were: the scientific plant name, traditional names, family, genus and synonymously used genera. The available scientific literature was evaluated with a focus on treatment caused improved re-epithelialization during wound healing.

3.10. Herbal Extracts Preparation

3.10.1. Herbal Extract by Decoction

The herbal extracts were prepared by using a standard operation protocol to enable similar extract compositions. The dried root material was ground with a mill (Alaska) into a fine powder. 100 ml *A. dest.* were added to 10 g of ground material in a 500 ml flask (Duran) and the mixture was boiled for 40 min at 100 °C while stirring. After boiling, the extract was centrifuged 5 min at 4960 rpm (Hettich Lab Technology; A. T.). The supernatant was collected and the ground material was boiled again with 100 µl *A. dest.* and a further centrifugation step as described before. The supernatants were combined and filtered through a folded filter (Type 600P, Roth) into a round flask and

concentrated by rotary evaporation (Büchli; 60 °C, 200 mbar). The complete drying was carried out by vacuum centrifugation (Bachofer). The resulted extracts were stored at -20 °C, protected from light and used within the next six months after extraction. The extraction yields were determined and with respect to the extraction number completed by SEM: The radix of *A. propinquus* was extracted with an average yield of 7.9 ± 0.09 % dried extract, or 0.79 g per 10 g ground herbal raw material. *R. glutinosa* radix extraction resulted in a production of 21.7 % extract. The simultaneous extraction of *A. propinquus* and *R. glutinosa* was conducted with the separately ground, raw herbal material. The powdered materials were further mixed in the ratio 2:1 (6.66 g *A. propinquus* and 3.33 g *R. glutinosa*) before the decoction process was started. The extraction yielded in an average mean of 13.4 ± 0.02 % dried extract. The extraction yield of rhizoma *C. chinensis* was 15.3 %. *A. euchroma* extraction resulted in a mean of 4.2 ± 0.03 % (source I), 4.4 ± 0.14 % (source II) and 3.2 % (source III) extract. The extracts were resolved in PBS for WHM analyses (sec. 3.12) or in the appropriate medium for cell culture experiments (sec. 3.14). Stock solutions were filtered through a syringe filter (Millipore; PVDF 0.45 µm) and further diluted in the appropriate solvent.

3.10.2. Preparation of an Ethanolic Extract

A two-step ultrasonic extraction was used to obtain an ethanolic extract of *A. euchroma*. Here, 96 % ethanol was mixed with the ground herbal material in 50 ml reaction tubes (Falcon) and extracted twice 30 min in an ultrasonic bath (Bandelin Sonorex; ratio 1:10 g/ml). Again, the resulting solutions were centrifuged, combined, filtered afterwards and dried as described for the aqueous extracts (60 °C, 400 mbar). The mean yield was 2.5 ± 0.09 % for the ethanolic *A. euchroma* extraction. The ethanolic ARE was resolved in DMSO and further diluted in PBS for WHM analyses or in the appropriate medium for cell culture experiments. Again, the stock solution was filtered through a syringe filter and further diluted in the appropriate solvent.

3.10.3. Preparation of a Methanolic Extract

Methanol is a standard solvent used for TLC fingerprint analyses (sec. 3.11.1 - 3.2.3.1.5). The ground herb was extracted in a reaction tube (50 ml, Falcon) with methanol by using an ultrasonic bath (Bandelin Sonorex; ratio 1:10 g/ml) for 15 min, A. T. From this suspension, 1 ml was transferred to a 1.5 ml reaction tube (Eppendorf) and centrifuged for 2 min (6,000 - 10,000 rpm). The supernatant was converted into a new tube and directly used for the analyses. Afterwards, the methanolic extract was stored at 4 °C, protected from light.

3.11. Biochemical Methods

3.11.1. Thin Layer Chromatography Studies to Prove the Herbal Identities and to Determine the Main Active Herbal Compound Groups

TLC enables the chromatographic separation of secondary metabolites concerning their interacting behavior with a polar silica plate (under use of different working- and derivatization solutions). It is possible to determine single ingredients when a commercial standard is used within the same experiment as a reference. This method was used to initially clarify the herbal identity compared to commercial reference extracts and to compare fingerprint patterns of raw material from different distribution origins. The analyses were performed according to the standard operation procedure instructions of the Phytochem® laboratory.
All investigated herbal raw materials were analyzed due to the occurrence of compound groups such as alkaloids, flavonoids, saponins, essential oils and anthracenes. Some representatives of these mentioned chemical groups were described for their wound healing promoting capacities (Budovsky *et al.*, 2015).

Following, the TLC results for *A. euchroma* were shown, which represents the herb with the most prominent promotion of epidermal regeneration in *ex vivo* WHMs (4.2.5).

Sample Separation

Experiments were carried out on a polar silica gel matrix plate as stationary phase (Macherey-Nagel). Different separation solvents were used as mobile phases (Tab. 3.9) depending on the analyzed chemical group. The TLC chamber (Macherey-Nagel) was filled with the mobile phase (up to 1 cm) and the saturation of the chamber room was assured by equilibration over 30 min before the separation was started. Meanwhile, 20 µl of the methanolic extracts (sec. 3.10.3) were applied on the TLC plate (exactly 1 cm from the bottom; start front marked by pencil) by using a micropipette (Roth). Blown air was used to help in drying the application point from the methanol solvent. An additional drying period ensured the complete evaporation of remaining solvent. Afterwards, the plate was put into the TLC chamber. Here, the mobile phase was separating the applied sample ingredients. The experiment was finished, when the solvent front reached nearly the top of the plate. Hence, the plate was removed and the solvent front was marked.

Table 3.9.: Schematic overview of the used separation solvents concerning the investigated elementary groups and their used ratio.

Separation mixture for	Separation solvent composition	Ratio
Flavonoids	ethyl acetate : formic acid : ethyl acetate : *A. dest.*	100 : 11 : 11 : 27
Alkaloids	toluol : ethyl acetate : diethylamine	70 : 20 : 10
Essential Oils	toluol : ethyl acetate	93 : 7
Anthracenes	ethyl acetate : methanol : *A. dest.*	100 : 17 : 13
Saponins	chloroform : methanol : *A. dest.*	64 : 50 :10

Development and Evaluation of the Thin Layer Chromatography Plate

After the separation, the plate was completely dried. The first photos were taken under visible light and UV light conditions (254 and 365 nm; Casio Exilim camera). Following, derivatization was performed with freshly prepared chemical mixtures (Tab. 3.10) depending on the analyzed chemical group), which were sprayed on the TLC plate (Roth). To evaluate the TLC and compare samples the two fronts (start and end) were measured and the retention factor (R_f) was calculated for each detected spot.

R_f = distance (test substance) [mm] / distance (solvent front) [mm]

The different herbal extracts were compared with the fingerprint of commercial reference substances (Phytochem®). Additionally, the results were analyzed under different light conditions and photo documented (daylight, UV light).

Table 3.10.: Used derivatization reagents (chemicals, evaluation and comment).

Derivatization for	Separation solvent Mix	Evaluation	Comment
Flavonoids	1 % Methanolic di-phenyl boric acid-2-aminoethylester solution (Naturstoffreagenz A)	254 and 365 nm	Coloring duration $>$ 15 min
Alkaloids	Dragendorff reagent	Visible light	Sodium nitrite intensify coloring
Essential oils	20 % Ethanolic molybdate phosphoric acid solution	Visible light	100 °C for 5 min
Anthracenes	5 % Potassium hydroxide in ethanol	254 and 365 nm	100 °C for 5 min
Saponins	5 % Antimony(III)chloride in chloroform	254 and 365 nm	100 °C under surveillance

3.11.1.1. Representative Identification of Methanolic *A. euchroma* Extracts from Different Distribution Sources

TLC investigations were performed to proof the identity of all tested herbal species and were representatively shown for *A. euchroma* below. Methanolic extracts of the herbal dried roots from different sources were prepared (I: Chinaturel; II: Rats Apotheke; III: Mehler). The separation and derivatization which was used for alkaloids did not show a signal for all tested *A. euchroma* extract sources (Fig. 3.1).

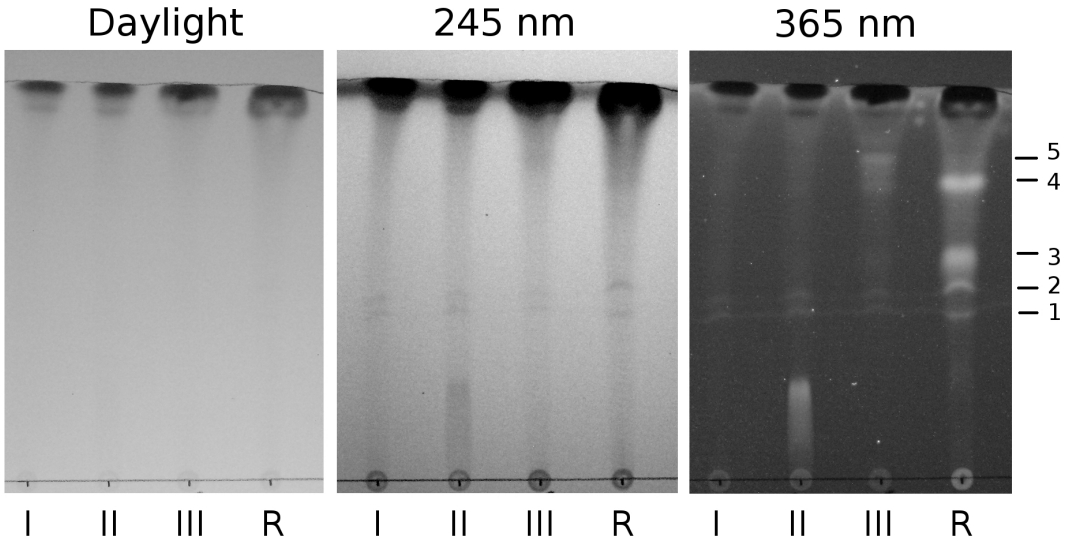

Figure 3.1.: TLC specified for the separation and detection of saponins with methanolic AREs of different herbal raw material origins (I - III) in comparison to a commercial reference ARE (R).The same membrane was visualized and evaluated under daylight, and UV light with 254 or 365 nm. All samples were identified as originated from *A. euchroma* and confirmed, despite varying signal intensities, by fingerprint pattern of the main bands in position, color and intensity (I = Chinaturel, II = Rats Apotheke, III = Mehler); The retention factor was determined as the relationship of the covered distance of the test substance to the covered distance of the solvent front. The following retention factors were calculated for the detected signals: (1) = 0.417 ± 0.001, (2) = 0.473 ± 0.007, (3) = 0.577, (4) = 0.77 and (5) = 0.818.

We got only weak signals for anthracenes. The most prominent detected subgroups were flavonoids, essential oils and saponins. Saponin bands are representatively shown in Fig. 3.1, where bands one (Rf = 0.417 ± 0.001) and two (Rf = 0.473 ± 0.007) were observed in all three extracts compared with a reference extract of *A. euchroma* (R). Lines three and four (Rf = 0.577 and 0.77) were more intensive in the reference than in the tested extracts. Moreover, there was an undefined big lube band in the beginning of the running lane of extract (II) and an additional fifth band in the methanolic extract of source (III; Rf = 0.818; UV 365 nm), that was not detectable in the extracts of other origins.

According to Phytochem® Referenzsubstanzen GbRmbH, who additionally and independently compared all three herbal material sources, the plants were identified as

A. euchroma species by fingerprint TLC. The TLC analyses and commercial HPLC (data not shown) confirmed the identity in the main peaks of all tested herbal specimens and therefore the identity proof of the herbal material.

3.11.1.2. Fingerprint Pattern Generation of the Herbal Source of *A. Euchroma* Which Showed Significant Wound Healing Improvement

Additionally, the generation of a fingerprint pattern of the wound healing promoting *A. euchroma* raw material was conducted to enable comparison with future herbal sources (Fig. 3.2).

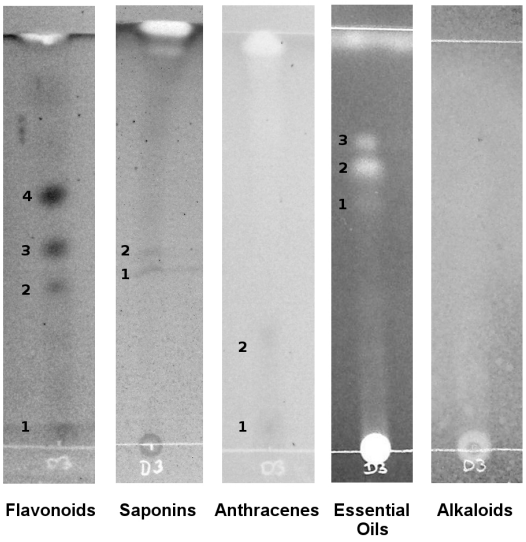

Figure 3.2.: Chromatographic fingerprint of a methanolic ARE (D3) from the herbal raw material which improved re-epithelialization in the *ex vivo* WHMs (source I). The pictures show the extracts TLC fingerprint when used with mobile phase specific for flavonoids. The retention (Rf) factor was determined as the relationship of the covered distance of the test substance to the covered distance of the solvent front. The following Rf were calculated for the detected signals: [Rf(1) = 0.04, Rf(2) = 0.39, Rf(3) = 0.49, Rf(4) = 0.61], saponins [Rf(1) = 0.42, Rf(2) = 0.48], anthracenes [Rf(1) = 0.05, Rf(2) = 0.3], essential oils [Rf(1) = 0.58, Rf(2) = 0.67, Rf(3) = 0.73] and no signals for alkaloids.

Plants may differ concerning their secondary metabolite composition depending on their habitat and the present soil and so forth. The herbal material, whose fingerprint matches this one, is expected to show similar wound healing promotion. Methanolic ARE was used to generate a TLC fingerprint profile of the main herbal ingredient compounds of wound healing promoting *A. euchroma* raw material. Signals (Fig. 3.2) belonging to anthracenes [Rf(1) = 0.05, Rf(2) = 0.3], essential oils [Rf(1) = 0.58, Rf(2) = 0.67, Rf(3) = 0.73], saponins [Rf(1) = 0.42, Rf(2) = 0.48] as well as strong signals for flavonoids [Rf(1) = 0.04, Rf(2) = 0.39, Rf(3) = 0.49, Rf(4) = 0.61] were detected. Alkaloids were not detected by TLC which indicated generally minor amounts of PAs in the root of this plant.

3.11.1.3. Determination of Shikonin Presence or Absence in the Aqueous and Ethanolic *A. Euchroma* Extracts by Thin Layer Chromatography

TLC was performed to investigate the determination of ingredient shikonin in the aqueous and ethanolic AREs (sec. 3.11.1). The experiment was performed in accordance with the friendly provided specifications of Phytochem® Referenzsubstanzen GbRmbH. Here, 5 mg dried aqueous or ethanolic extract were dissolved in 1 ml methanol, assisted by an incubation in an ultrasonic bath for 2 min at A. T. Aqueous ARE was used from distribution source I and III. Ethanolic ARE was prepared from source I. Shikonin was freshly prepared as 17 µM stock solution in methanol and used in different concentrations. The solutions were centrifuged for 2 min (6,000 - 10,000 rpm) and the application procedure was performed as described in the previous chapters. The solutions were applied as follows: Extracts as drop of 10 µl or 20 µl (lane 1 - 6); 2 µl (17 µM; lane 7), 10 µl (1.7 µM; lane 8), 10 or 20 µl shikonin (0.17 µM; lane 9 - 10) and 10 µl commercial methanolic ARE (lane 11). Tuluol/Ethylacetat (93:7, v/v) was used as mobile phase. And the derivatization was conducted using anisaldehyde-sulfuric acid, which was sprayed on the TLC plate after the separation experiment. The derivatization reaction was performed under 10 min of heating to 100 °C with the help of an incubator. The visual documentation was performed under normal daylight and UV light (254 nm).

3.11.2. Chromatographic Profiling of the Aqueous and Ethanolic *A. Euchroma* Extract

Aqueous and ethanolic AREs were comparatively investigated by UHPLC-HRMS and UHPLC-ELSD analyses. The more sensitive UHPLC-HRMS and UHPLC-ELSD studies were carried out for detailed extract characterization in collaboration with Prof. Jean-Luc-Wolfender (Phytochemistry & Bioactive Natural Products laboratory, Geneva, CH) and they were performed by Joëlle Houriet (Ph.D. student). Here, the aqueous and ethanolic AREs were diluted in water/methanol (85:15, v/v) and filtered on SPE C18 (Finisterre) before chromatographic analyses. The resulting fractions were dried and dissolved at 1 mg/ml for HRMS analyses and 10 mg/ml for ELSD analyses. Shikonin (Shyuanye), used as a reference, was diluted in methanol to a final concentration of 20 µg/ml.

Ultra High-Performance Liquid Chromatography - High-Resolution Mass Spectrometry of the *A. Euchroma* Extracts

The chromatographic separation was conducted on a Thermo Dionex Ultimate 3,000 UHPLC system hyphenated to an orbitrap Q-Exactive Plus HRMS with heated electrospray ionization source (HESI-II, Thermo Fisher Scientific; used parameters were described in Tab. 3.11. The metabolic profiling was performed on an Acquity UPLC® BEH C18 column (Milford; 1.7 µm, 2.1 x 150 mm; temperature: 40 °C).

Table 3.11.: Electrospray ionization source HESI-II parameters (S-Lens RF Level 50)

HESI-II parameters	**positive ion mode**	**negative ion mode**
Source voltage	4.0 kV	2.5 kV
Sheath gas flow rate, N_2	51 units	48 units
Auxiliary gas flow rate	13 units	11 units
Spare gas flow rate	2.6	2.3
Capillary temperature	266.25 °C	256.25 °C

The autosampler temperature was fixed at 10 °C. The mobile phases consisted of water (A) and acetonitrile (B), both with 0.1 % formic acid. A linear gradient of 95 % (A) and 5 % (B) was used over 30 min, followed by an isocratic step of 95 % (B) for 10 min terminated by 10 min re-equilibration. The injection volume was set at 2 µL with a fixed flow rate of 0.46 ml/min. The HRMS analyses were performed in positive and negative ion mode (mass range: 150 - 1,300; resolution: 70,000 full width at half maximum; m/z 200; ion injection time 200 ms). In positive mode, diisooctyl phthalate $C_{24}H_{38}O_4$ $[M+H]^+$ ion (m/z 391.28429) was used as internal lock mass. Mass analyzer calibration was performed according to the manufacturer's directions.
The resulting ThermoRAW data were converted to a mzXML format (ProteoWizard software; Kessner *et al.*, 2008). Open-source software mzMine 2.20 was used to pre-process and dereplicate the data (Pluskal *et al.,* 2010). Peak detection was achieved using the GridMass algorithm (Treviño *et al.*, 2015). A database for dereplication with the entries of the *Boraginaceae* family was built by using the Dictionary of Natural Products (DNP; *http://dnp.chemnetbase.com*). Conformities were further analyzed with DNP to specify their relation to genus *Arnebia* or the family of *Boraginaceae*. Peaks without a database match were compared to all entries of dicots by their predicted molecular formula.

Ultra High-Performance Liquid Chromatography - Evaporative Light Scattering Detector

The chromatographic conditions were similar to those used for the UHPLC-HRMS. This detector system determined polar compounds. The measurements were performed using an Acquity UPLC system (Waters), which included a binary pumping system, an autosampler, a column manager with a pre-column heater and an ELSD Sedex 85. The system was controlled using Empower 3 Software.

3.11.3. Studies of the Aqueous Extracts Anti-oxidative Capacity

The radical scavenging impact of aqueous ARE was investigated on organic radicals (2,2-diphenyl-1-picrylhydrazyl; DPPH assay) and peroxyl radicals (oxygen radical absorbance capacity; ORAC assay). Both assays were conducted according to Friedemann *et al.* 2014 with minor modifications and the analyses were performed as three independent experiments in triplicates (Friedemann *et al.*, 2014).

Anti-oxidative Studies with Organic Radicals (DPPH Assay)

The extract was prepared as a solution in *A. bidest.* (50 - 500 µg/ml) and each 50 µl were placed in a 96 well plate (Greiner) together with 200 µl of 75 µM DPPH (dissolved in methanol). Afterwards, 5 min incubation on a plate shaker (AIP 4 plate shaker, 650 rpm, light protected) and 25 min incubation in the dark (without shaking) were conducted before the measurement was started. The DPPH scavenging was quantified by the photometrical determination at 531 nm (Thermo Multiskan SPECTRUM). Water was used as negative- or background control, instead of the extract. Trolox and NAC (each dissolved in 80 % ethanol) were used as positive controls.

Anti-oxidative Studies with Peroxyl Radicals (ORAC Assay)

Trolox was used as positive control to test the peroxyl radical scavenging capacity of ARE by ORAC assay. Here, 225 µl, pre-warmed to 55 °C, 10 mM fluorescein solution dissolved in 75 mM sodium phosphate buffer with pH 7.4 were transferred to a 96 well plate. Following, 37 µl sodium phosphate buffer (blank, negative control), 37 µl trolox (20 - 80 µM; reference substrate, positive control) or 37 µl of ARE (7.5 - 50 µg/ml) were pipetted into the wells. The plate was incubated for 15 min (55 °C, water bath) and ice-cooled 37 µl 240 mM 2,2´-Azobis (2-methylpropionamidine)-dihydrochloride (in sodium

phosphate buffer) were added per direct injection immediately before measurement by the plate reader. The subsequent kinetic measurement was performed every 120 min after 15 sec shaking (Berthold; excitation: 485 mm, emission: 528 mm).

3.12. Tissue Culture Methods

A patented *ex vivo* WHM on porcine skin was used (PCT/DE2004/000782) to investigate the wound healing capacity of different herbal extracts. Punch biopsies were taken from the porcine´s living ear tissue, which was transported to the laboratory directly after animal slaughter for consumption. Therefore, animal experiments were avoided. The WHM was further injured in the center area and transferred into air-liquid culture condition to enable physiologically comparable nutrition during the attempt (Brandner *et al.*, 2004 & 2006; Fig. 3.3).

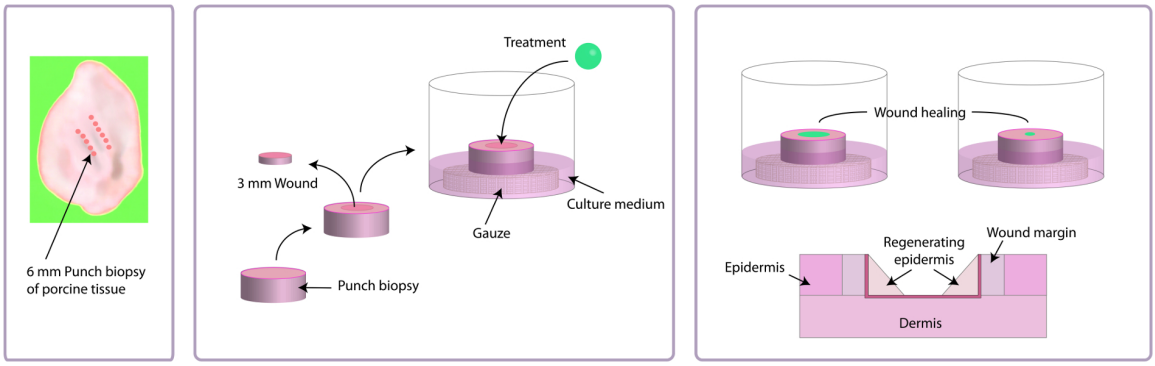

Figure 3.3.: *Ex vivo* wound healing model (WHM) to evaluate the healing capacity of different herbal extracts. Punch biopsies from the porcine ear skin were further wounded. The wounded WHM was transferred in medium containing culture plate on top of gauze to enable culturing under air-liquid interface. Extract therapy was applied on the center of the wound (refreshment every 24 h). Wound healing was terminated 48 h after start of treatment. The regenerating epidermis was measured in hematoxylin and eosin stained WHM slices [schema © S. Mirza, modified from (Brandner *et al.*, 2006)].

Different treatments can be applied. The wound healing impact of varying concentrations, as well as several application methods, can be investigated, while the WHMs were cultivated for the defined healing period. Afterwards, the WHMs were cut and the regenerating epidermis, influenced by different treatment conditions, was documented and evaluated (sec. 3.16). Two WHMs were prepared for each condition with each two wound margins, which could be evaluated. Wound margins or WHMs were excluded from the statistical evaluation in case of: present hair follicles or glands at the wound margin, experimental damages such as a broken wound margin, wounds were too deep or bacterial infections. Therefore, the final sample size varied.
This method can be adopted on human tissue as well.

3.12.1. Preparation and Culturing of *Ex-Vivo* Wound Healing Models

First of all, the vital pig ears were cleaned under tap water and the hairs were removed with the aid of scissors. The whole ear was disinfected with Sterilium and the inner part was incubated with sterilium saturated gauze for 10 min. Afterwards, the ear was washed with sodium chloride and brought under cell culture bench to obtain sterile conditions. The WHMs were generated by taking 6 mm punch biopsies from the plicae of the inner ear region (Fig. 3.3). Remaining hairs were cut as short as possible and subdermal fat tissue was removed, before the WHMs were transferred into DMEM medium containing culture plates (3 cm; Falcon).
The same procedure can be converted to human *ex vivo* WHMs. Here the sterile surgically removed fresh skin was delivered to the laboratory in culture medium directly after the operation. The 6 mm punch biopsies were taken from the skin on sterile gauze and fat tissue and the remaining hair was removed. Again, the biopsies were transferred into a medium containing culture dish.
The 6 mm biopsy was further injured by using a 3 mm punch biopsy out of the center area. Here, the epidermis and parts of the dermis were removed with the help of forceps and scalpel. These generated WHM can be placed in a 12 well plate (Falcon) which was previously prepared with a piece of sterile gauze and around 2 ml medium per well. Here, the medium surrounded the dermal part and the epidermis stayed in contact with air. These air-liquid-interface conditions mimic the physiological nutrient supply of the skin. The cultivation was carried out at 37 °C, 10 % CO_2 and 95 % relative humidity (Heraeus). Different concentrations of the herbal extracts were applied as 5 µl drop in the center area of the wound after injury (dermal/epidermal contact; refreshed after 24 h) before the wound regeneration was stopped after 48 h by snap freezing the WHMs in liquid nitrogen pre-cooled isopentane. The samples were stored in cryotubes at -80 °C until frozen sections (sec. 3.13.1) were prepared for evaluation and further analyses. Experiments were carried out in duplicates per tested condition.
The WHMs provided with nutrients were able to regenerate epidermal tissue within the duration of cultivation. This progress is influenced by the general healing capacity of the donor skin (monitored by an untreated control, w/o) and by the different treatments that could improve or delay the wound healing progress (sec. 3.12.4).
PBS was used as solvent control (NC) and untreated WHMs as an intrinsic healing control (w/o). The untreated control enabled a division in subgroups of intrinsic good and bad healing donor specimens. Wound regeneration of $\geq$ 638.9 µm was determined as good healing donor skin with respect to the mean wound tongue regeneration in all untreated porcine controls of the first experiment (w/o, 638.9 $\pm$ 64 µm). WHMs with

less regenerated epidermis were classified as bad healing specimens, with regeneration below average. Human skin samples showed an intrinsically slower healing capacity. Epidermal regeneration $\geq$ 216.7 µm was defined as good healer with respect to the mean of the untreated controls (216.7 $\pm$ 24.4 µm). Less wound recovery was defined as intrinsically bad healing specimen. For the experiments with ethanolic ARE and shikonin, which both had to be firstly dissolved in DMSO and further diluted in PBS, a DMSO control was added to the setup.

3.12.2. Application Time Point Analyses in *Ex Vivo* Wound Healing Models

The time point of extract application can influence the wound regeneration progress. This is why the AREs impact on later wounds was investigated, where we injured the WHMs and started the treatment 24 h after injury (refreshed after 48 h). The WHMs were cultured for 72 h after wounding before they were snap frozen.
Here, all samples with w/o $\geq$ 650.1 µm were defined as good healing specimens (mean of w/o = 650.1 $\pm$ 31.4 %). The general procedure and evaluation were conducted according to the 24 h cultured WHMs (sec. 3.12.1, sec. 3.13.1, sec. 3.13.2, sec. 3.12.4).

3.12.3. Application Method Studies in *Ex Vivo* Wound Healing Models

To analyze the impact of the application method, a direct wound application of 5 µl extract solution on top of the wound was compared with a wound margin application (epidermal and dermal versus only epidermal contact). An extract saturated sterile cotton bud was used to apply the treatment on the wound margin. The application was performed by surrounding the wound margin three times without contact to the wounded dermal area. The experiments were conducted and evaluated in all other parameters equally to the normal 24 h cultivated porcine WHMs.

3.12.4. Evaluation of the Wound Healing Models

Microscopic photos (light microscope DMLS and digital microscope camera EC 3; 100 x) of the WHMs were taken after hematoxylin & eosin (HE; 3.13.2) staining and aligned using Fiji software. Here, the regenerating epidermis was measured with help of the segmented line tool. The evaluation was performed under single blinded conditions, where the analyst was blinded to the used treatment of the WHMs till the calculations

were concluded. The measured regenerating epidermis was normalized to the NC control within one donor skin. This internal normalization allowed to consider the individuality of each donor and enabled the comparability between individuals.

3.13. Histological Methods

3.13.1. Preparation of Frozen Wound Healing Model Sections

The Cryomatrix (Leica) embedded WHMs were sliced vertically to the middle of the wound (Leica; -24 to -22 °C block- and chamber temperature; Fig. 3.3, on the right). The WHM sections (5 µm thick; 6 mm biopsy with 3 mm wound) were transferred onto microscopic slides (Thermo Fisher Scientific). These were dried at A. T. for at least 30 min. The samples were used for HE staining (sec. 3.13.2), ethanol fixed for IF staining (sec. 3.13.3) or stored until continuing (short-time: -20 °C, long-term: -80 °C). The cutting of the WHMs enabled the inclusion of blinding of the samples due to randomized numeration labeling of the slides.

3.13.2. Haematoxylin & Eosin Staining

Different cell structures can be stained with HE, where cell nuclei and the endoplasmatic reticulum are colored blue by hematoxylin and eosin dyes cytoplasm and ECM red.
The whole staining process is conducted at A. T. The slides, with dried WHMs, were put into filtered hematoxylin for 10 min and further washed, rinsing with cold tap water until all excessive color was removed and the water turned clear again (10 min). Afterwards, the slides were briefly washed in *A. dest.* and further stained in eosin for 30 sec before the coloring reaction was stopped by washing in *A. dest.* The tissue dehydration was enabled by dipping the slides compendiously in an ascending ethanolic series (70 %, 80 %, 95 % and absolute ethanol). A further step for 5 min in fresh absolute ethanol was enclosed. Thereafter, the samples were incubated 2 x 10 min in Xylol before they were covered with the help of cover slides, Eukitt embedding medium and dried at A. T. overnight.

3.13.3. Immunofluorescence Staining of the Porcine Wound Healing Models

Cellular proteins can be visualized and localized by IF staining with antibodies suitable to the antigens *in situ* (Tab. 3.6) that were further linked to fluorescent marked secondary antibodies (Tab. 3.7).
The tissue slides were previously fixed in ethanol at 4 °C for 30 min and 1 min in Aceton at -20 °C and completely dried before they were used for IF. The staining - process took place in a humid dark chamber at A. T. The used primary and secondary antibodies were diluted in solvent as mentioned in Tab. 3.6 and Tab. 3.7, mixed gently and centrifuged shortly up to 13,000 rpm. 40 µl antibody solution or isotype control were applied at the WHMs and incubated for 1 h (3.1.6). Afterwards, the slides were washed 1 x 5 min and 2 x 10 min in PBS (Tab. 3.4) before the species-specific secondary antibody was added and incubated for 30 min. Additionally, after 5 min of washing in PBS, a DAPI staining was performed for 1 min in the dark to enable monitoring of the cell nuclei. Again, the slides were washed 2 x 5 min with PBS and 2 x 3 min in *A. dest.*, covered with Fluoromont-G^{TM} and a cover slide before they were placed in the dark to dry overnight.
The stained samples were evaluated under a fluorescent microscope with 400 x magnification and exposure time and gain were kept constant. Photos were taken of control areas which were not affected by the center wound nor by the biopsy edge (unwounded area), the wound margins and the complete regenerating epidermis (Fig. 3.4). Digital RGB photos were analyzed using the Fiji software. The investigated proteins were evaluated due to their localization in the tissue of the WHM under different treatments.

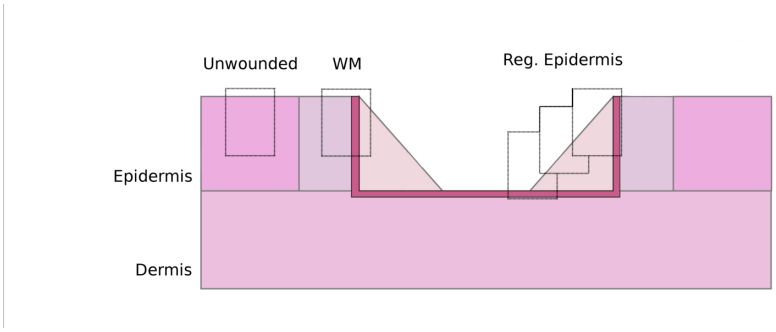

Figure 3.4.: Immunofluorescence stained and evaluated areas of the schematic wound healing model. Rectangles mark representatively the evaluated areas: control area (unwounded; independent of central wound area and biopsy margin), wound margin (WM) and regenerating (reg.) epidermis. Usually, the evaluation was conducted on three independent unwounded areas, two wound margins (left and right) and several pictures of the regenerating epidermis, depending on their lengths.

3.14. Cell Culture

All cell culture studies were conducted under sterile conditions using a cell culture bench with appropriate safety clothing. The culture solutions were pre-warmed to 37 °C if not mentioned differently.
Cells were checked regularly for mycoplasma contamination after isolation from donor skin and after thawing. Here, the My Taq DNA Polymerase Kit with specific primer sequences was used: Tuffw414 (sense) TCC AGG WCA YGC TGA CTA and Tufrev541 (antisense) ATT TTW GGA ACK CCW ACT TG. The analyses were performed by a technical assistant. Cell culture supernatant was centrifuged at 13,000 rpm for 5 min and removed from resulting pellet. The pellet was afterwards resolved in 100 µl *A. dest.* and denaturized at 95 °C for 5 min. Samples were kept on ice until the polymerase chain reaction (PCR) was prepared. For each sample 5 µl sample DNA were mixed with 5 x MyTaq PCR Buffer, 1.5 µl of each primer, 12.85 µl *A. dest.* and 0.15 µl My taq polymerase. The PCR was conducted including contaminated cell supernatant as positive control, a negative non-contaminated sample and a DNA-free water control [program: initial denaturation 2 min at 95 °C, 39 x (denaturation 30 sec at 95 °C, primer annealing 30 sec 55 °C, elongation 30 sec 72 °C), cooling at constant 4 °C]. Visualization of the elongated DNA fragments was performed by electrophoresis with a 2 % agarose gel and the samples were compared to controls (resulting target DNA fragment size: 150 kDa).

3.14.1. Preparation of Human Primary Cells

Human Keratinocytes

The foreskins were delivered in cell culture medium containing penicillin and streptomycin and were further incubated overnight at 4 °C to allow deeper disinfection. After identification of the outer dense skin, this part was separated from the muscular inner skin and connective tissue by help of a scalpel and scissors. The tissue was transferred into a 6 cm culture dish with PBS. Subsequently, the skin was moved on a slide with a PBS drop and cut into 1 - 2 mm^2 pieces. The skin samples were transferred to a 3.5 cm culture dish containing 2 ml 0.25 % trypsin (Tab. 3.5). The tissue digestion was conducted at either 4 °C overnight or 37 °C for 2 h and was stopped by transferring the cell trypsin solution into a centrifuge tube containing 4 - 6 ml 10 % FBS, which inactivates the enzyme. During digestion, the intercellular connections were broken, which was amplified by mechanical pipetting. This increased the number of single cells in suspension. After a centrifugation at 808 g for 5 min, the supernatant was

removed, the cells were resuspended in the appropriate culture medium (Tab. 3.5) and the cell number per milliliter was determined (cell counter, Thermo Fisher Scientific). Cells were seeded 100,000 cells/ml in 10 cm culture dishes and incubated for at least seven days at 37 °C and 5 % CO_2. Microscopic visualization was used to estimate the cell growth and division. In the case of cell colony formation, the medium was replaced by a fresh one, and the cells were further cultivated. Keratinocytes cultivation was stopped at a confluence of 70 - 80 % by removing the medium and adding with 2 ml sub-culturing trypsin (Tab. 3.5) for 5 min. The cells loosened their attachment to the culture surface and were transferred into a centrifuge tube with 5 ml 10 % FBS and centrifuged at 800 g for 5 min. The supernatant was removed from the cell pellet. The keratinocytes (passage zero) were resuspended in fresh culture medium for further cultivation and transferred into a new dish or they were frozen for experiments at later time points (sec. 3.14.3 or sec. 3.14.2).

Human Fibroblasts

Fibroblasts were isolated from the outer side of the foreskin as well. Here the skin was removed from the inner part and the remaining connected tissue with scissors. Afterwards, the tissue was cut on a slide as described for keratinocytes. The resulting tissue pieces were transferred into a T25 culture flask with 2.5 ml culture medium (Tab. 3.5) and cultivated at 37 °C and 5 % CO_2 untouched for at least seven days. The first medium change was conducted after optical monitoring of the growth rate. It was changed every three days from then on to final achieved confluence of 70 - 80 %. In the case of appropriate confluence the supernatant was removed and 4 ml PBS were added and incubated for 5 min to wash the remaining FBS from the cells. PBS was removed and 2 ml fibroblast trypsin (0.05 %/0.02 %, trypsin/EDTA) were added for 1.5 min. The trypsin digestion was stopped by adding 4 ml 10 % FBS. The cells were seeded into a new culture flask or frozen for later studies.

3.14.2. Cultivation and Sub-culturing

Primary keratinocytes and fibroblast were cultured to 70 - 80 % confluence as mentioned before. Therefore, they were subcultured by trypsinization (Tab. 3.5) every three days to obtain optimal culturing conditions and fresh nutrients to the cells. The second to fourth passage were used for the performed experiments to facilitate studies on cells with primary characteristics and without long-term culture influences.

3.14.3. Cryoconservation of Primary Cells and Re-culturing of Frozen Cells

To enable storage of the cells freezing conservation was performed. Here around 70 - 80 % of the confluent grown cells were resolved from culture surface and after centrifugation resolved in freezing medium (Tab. 3.5). Each culture vessel offered three vials with 1 ml cell-cryomedium-suspension. The cryovials were transferred in a cryoreservoir that contained isopropyl alcohol to enable a 1 °C per minute decrease in temperature in a -80 °C freezer overnight. On next day, the frozen cell vials were converted in liquid nitrogen to obtain long-term storage.
Cell thawing was performed as follows: The freezing medium contained DMSO that can harm the viability of the cells under longer exposure. Therefore, the frozen vials were thawed in a pre-warmed water bath at 37 °C. Afterwards, the cell suspension was transferred into a centrifuge tube with 5 ml PBS for DMSO dilution. After centrifugation at 800 g for 5 min, the supernatant was removed and the cell pellet was resolved in appropriate medium and the cell suspension could be seeded into a new culture vessel.

3.14.4. Cell Viability Studies

Wound healing promotion by ARE can be caused by an increased cellular viability of affected cells. Viability analyses were performed in two-dimensional cultured keratinocytes and fibroblast under different culture conditions. These studies enabled the evaluation of the AREs effect on these cell types, excluding interactions to other cells and molecules and without diffusion effects as they are present in the WHMs.
MTT method was used to determine changes in cellular viability by ARE treatments. Here, the interrelation between proliferation, apoptosis and senescence are measured as cell viability. This method enables the determination of the reduction equivalents of the MTT reagent named formazan that is generated in viable metabolically active cells. The culture medium and treatment were refreshed every 24 h if not mentioned differently. Moreover, the incubation was carried out at 37 °C, 5 % CO_2 and 95 % humidity.
ATP molecule determination, derived from the respiratory chain and glycolysis metabolism, as further viability analysis was conducted additionally for fibroblast. Petty *et al.* demonstrated more sensitive information about cellular metabolic activity by ATP measurement compared to MTT assay (Petty *et al.*, 1995). Both determine the cellular metabolic activity by biochemical redox reactions of members of the mitochondrial respiratory chain. The MTT assay is based on the enzymatic reduction of MTT reagent by a reductase which normally processes mitochondrial nicotinamide adenine

dinucleotide. This process enables proton transfer through the membrane for energy retrieval. Different enzymes complexes of the respiratory chain are able to increase the proton level of the mitochondrial inter-membrane space. And the ATP synthase phosphorylates ADP to ATP, which is an energy depending process and enabled by the reflow of the inter-membrane generated proton gradient. In contrast, the ATP measurement determines all produced ATP molecules by the mitochondrial system and additionally the ATP molecules originated from glycolysis (Im, 1979). Therefore, ATP determination results in a more complex and sensitive measured metabolic signal compared to MTT. The ATP determined the number of energy molecules under ARE treatments in this cell type. Here, free ATP was measured as a proportional increasing enzymatic luminescent signal, which was detected with the help of an appropriate plate reader.
All experiments were performed with cells from four donors for MTT and three donors for ATP assay in triplicates.

3.14.4.1. Viability analyses with Primary Keratinocytes (MTT Assay)

To investigate various differentiation stages of keratinocytes, as they occur in the wounded area, undifferentiated and differentiated cells were analyzed under AREs treatment. The primary keratinocytes were seeded in 96 well plates (in 100 µl medium per well), with 5,000 or 10,000 cells for subconfluent or confluent conditions. After achieving confluence, the undifferentiated cells were treated with the extracts as follows: aqueous ARE 1 - 500 µg/ml and ethanolic ARE 0.1 - 50 µg/ml or with the medium as negative control (NC) or DMSO as solvent control for the ethanolic extract over 48 h.
Stimulation of cell differentiation was another condition: Additionally, 10,000 cells were seeded to investigate different differentiation grades. After reaching confluence, the culture medium (0.06 mM calcium chloride) was shifted to high calcium (1.8 mM) for either three or five days before the extracts treatment was started. The differentiated keratinocytes were treated as described above for undifferentiated conditions.
Following the treatment period, the supernatant was removed from the cells, replaced by 100 µl 0.5 mg/ml MTT in culture medium and incubated for 3 h at 37 °C. After removal of the MTT reagent 100 µl isopropanol were added and the plate incubated for 30 min in the dark, A. T. The following photometrical measurement was performed, after 10 sec orbital shaking, with a Magellan Sunrise plate reader at 570 nm with 690 nm subtraction. The values were measured three times, the mean was calculated and the background subtracted (cell-free medium wells) before the different conditions were normalized to the medium control (100 %).

3.14.4.2. Viability analyses with Primary Fibroblasts (MTT Assay)

The extracts impact on fibroblast viability was analyzed in the presence or absence of FBS in the culture medium. The same extract concentrations were used as mentioned for keratinocytes (sec. 3.14.4.1). 5,000 cells per well were seeded in 100 µl in 96 well plate and incubated overnight to allow settling and accumulation. The medium was replaced with a fresh one, treatment was added and the cells were incubated for 24 or 48 h (with treatment refreshment after 24 h). For serum-free conditions, the medium was changed 2 h before treatment start. MTT viability measurement was performed according to the procedure with keratinocytes (sec. 3.14.4.1).

3.14.4.3. ATP Measurement in Cultured Fibroblasts

A further method to estimate cell viability was investigated, by determining the energy balance of the fibroblast. Here, the CellTiter-Glo Luminescent Cell Viability Assay (Tab. 3.3) was used to measure ATP content as a sensitive luminescent signal. Fibroblasts were seeded in white 96 well plates (NUNC) and pre-conditioned with or without FBS as described for MTT assay in 3.2.5.4.2. The cells were treated with 5, 10 or 50 µg/ml aqueous ARE; 1, 5 or 10 µg/ml ethanolic ARE; medium or DMSO for 24 or 48 h. The CellTiter-Glo assay solution was prepared and the analysis performed according to manufactures recommendation. An ATP standard (10 - 10,000 nM) was prepared on each plate and measurement in triplicates. The treatment was removed from the cells and 50 µl medium and 50 µl CellTiter-Glo-Reaction solvent were added and incubated for 2 min with orbital shaking to induce cell lysis. The plates were incubated at A. T. for a further 10 min and the luminescent detection was performed with a Mithras LB plate reader. First, the background subtraction was applied. The sample values were converted to ATP equivalent by linear regression with respect to the ATP standard. The resulting data were further normalized to the medium control.

3.14.5. Cell Proliferation Analyses

Cell proliferation analyses were performed by using the Cell Proliferation ELISA, BrdU labeling Kit (Tab. 3.3) according to the manufacturer's instructions with minor modifications for the individual cell type. The experiments were carried out with keratinocytes from four donors and fibroblast from three to four donors with appropriate culture medium. The experiments were performed in triplicates with medium and DMSO control at A. T. if not mentioned differently. Proliferation studies were performed over 24 or 48 h with treatment refreshment after 24 h. The resulting values were normalized to the medium control after background subtraction.

3.14.5.1. Proliferation Studies with Primary Keratinocytes (BrdU Assay)

Keratinocytes (10,000 or 5,000 cells in 100 µl medium) were seeded into a 96 well plate and they were cultivated to confluence achievement of the 10,000 cell containing wells. Again confluent and non-confluent undifferentiated cells were compared with keratinocytes pretreated with 1.8 mM calcium chloride for three or five days to induce confluence according to the MTT assay. Extracts treatment was started using: 1 - 500 µg/ml aqueous ARE; 0.1 - 50 µg/ml ethanolic ARE; medium or DMSO. At the appropriate time, the supernatant was removed and 100 µl BrdU-labeling-solution (1:1,000 in medium) were added and incubated 2 h at 37 °C. Afterwards, the labeling solution was removed and 200 µl fix-denat-solution transferred into each well, which fixed and denaturized the cells within 15 min in the dark. Then the fixation solution was removed and replaced by 100 µl anti-BrdU-POD antibody (1:100) and the samples were incubated for another 60 min. During the further washing periods of 3 x 200 µl washing buffer all unbounded antibody was removed. Finally, 100 µl substrate solution was transferred into the wells and incubated for 5 min. The reaction was stopped by addition 20 µl of 1 M sulfuric acid. The plate was measured within the next 5 min after 20 sec orbital shaking in a plate reader (Magellan Sunrise) at 450/690 nm.

3.14.5.2. Proliferation Studies with Primary Fibroblasts (BrdU Assay)

To investigate the extracts impact on fibroblasts cell division 5,000 cells were seeded into 96 well plates in 10 % FBS containing medium and incubated overnight to enable settling and acclimatization of the cells. 2 h before stimulation start, the medium was shifted to a serum-free one or refreshed for serum-containing conditions. Then, treatments (1 - 50 µg/ml aqueous ARE; 0.1 - 25 µl/ml ethanolic ARE; medium or DMSO) were added. After 24 h or 48 h the supernatant was removed. The BrdU assay was performed as described for keratinocytes with the following modifications: BrdU-labeling-solution for 4 h; fix-denat-solution for 30 min and substrate solution for 20 min to amplify the resulting signal.

3.14.6. Wound Closure and Adhesion Studies in Cultured Cells

Keratinocytes and fibroblasts wound closure capabilities were analyzed under AREs treatment, to evaluate the direct effects of the extracts on these cell types during wound healing. The *in vitro* two-dimensional wound closure experiments were conducted as scratch assays in 24 well plates at 37 °C, 5 % and 95 % humidity (Fig. 3.5). The confluent cell mono-layer was centrally injured. Here, the wound area decrease was

monitored every 12 h over 48 h (analogues to the *ex vivo* WHMs) and the experiment start was set as 0 h (100 %). All scratch assays were carried out as two technical replicates for each condition. The evaluation of the resulting digital data was performed with help of the TScratch-Software (Gebäck *et al.*, 2009). Here the wound area was marked and the area reduction over time was compared between different treatments. Finally, the software created percentages of wound areas that were further used to calculate real wound sizes in square millimeter. This was done using Microsoft Excel and evaluated for statistics with SPSS. Migration assay was conducted on keratinocytes of four and fibroblasts of five donors. Whereas the additional analysis on proliferation inhibited fibroblasts was performed on cells from three donor sources.

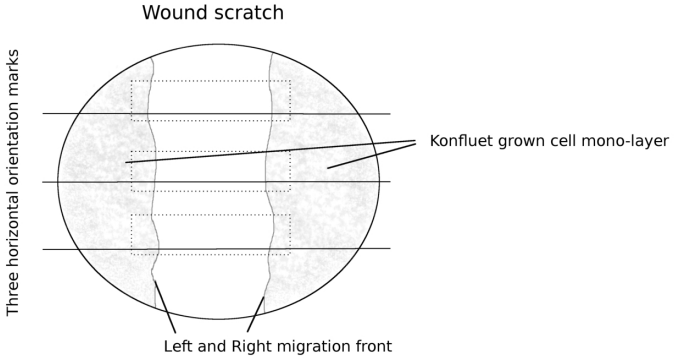

Figure 3.5.: Schematic wound scratch, representing one well with confluent and central injured cell mono-layer. The wound scratch was performed with help of a sterile pipette tip in the center of the well from top to bottom. Left and right wound margins were marked and documented every 12 h during the experiment. Three horizontal marks enabled orientation for the photo documentation. Three rectangles mark exemplary photo positions.

Changes in cell-matrix attachment are important for cell migration. Cells that want to move have to release the cell connections to surrounding cells and surfaces, migrate and rebuild new connections when they arrive at their new predestinated localization. To analyze the AREs impact on cell-matrix binding, a cell-matrix adhesion assay was performed. Therefore, keratinocytes were seeded into treatment containing well plates. The adhered living cells were determined by MTT assay after certain time points. These studies were performed with cells from three donors in triplicates.

3.14.6.1. Wound Closure Studies with Primary Keratinocytes (Scratch Assay)

Three marking lines were drawn on the bottom of each well of a 24 well plate to enable the same position for photo documentation of the wound closure (Fig. 3.5).
100,000 keratinocytes were seeded in 400 µl medium and cultivated till confluence was achieved. The confluent cell mono-layer was wounded with help of a sterile 200 µl pipette tip from one side to the other as a line through the well. Afterwards, the wells

were washed twice with PBS and 400 µl medium were added to the remaining cells. The treatment was started by adding 100 µl five-time concentrated reagents per well: 0.5, 5, 50 µg/ml aqueous ARE; 0.05, 0.5, 5 µg/ml ethanolic ARE; medium or DMSO control. Afterwards, time point zero photos were taken at three independent areas of the wound, using a light microscope and a camera (Leica; 50 x magnification). Then, the plates were transferred into the incubator and cultivated for two days. Every 12 h, photos of the same wound parts, were taken and medium, as well as treatment, were refreshed.

3.14.6.2. Cell-Matrix-Adhesion Assay with Primary Keratinocytes

To investigate the extracts impact on cell settling and adhesion a cell-matrix adhesion assay was performed. 50 µl aqueous or ethanolic ARE in different concentrations were pre-loaded in 96 well plate (1; 5; 10; 25; 50; 100; 200; 500 µg/ml aqueous or 0.5; 1; 2.5; 5; 10; 25; 50; 100 µg/ml ethanolic ARE, respectively). 50,000 keratinocytes were seeded into the treatment containing wells and incubated for 15, 30, 60, 120 or 180 min at 37 °C, 5 % CO_2 and 95 % humidity. Normal medium and DMSO were used as reference controls. Additionally, 50,000 cells were seeded in medium containing wells and they were incubated, untouched, within the experiment to achieve a maximum value as a positive control. During the experimental duration, the cells had the possibility to settle down and adhere to the plastic surface. After certain time points, the supernatant with possibly non-adhered cells was transferred into a new plate and the adhered cells were washed twice with medium. Finally, 100 µl fresh medium per well were added. The finished plates were further incubated until all time points were completed. Afterwards, 10 µl 0.5 µg/ml MTT reagent were added to the plates, containing adhered cells or the supernatant, and were incubated for a further 3 h at 37 °C. That followed, 100 µl Isopropanol were transferred into the wells and the parafilm sealed plates were incubated overnight at A. T. in the dark to enable proper formazan dissolving. After 20 sec orbital shaking, the preparations were measured three times at 570 nm with a plate reader (Magellan Sunrise). The mean ± SEM were calculated and the values normalized to medium control.

3.14.6.3. Wound Closure Studies with Primary Fibroblasts (Scratch Assay)

The scratch assays with primary fibroblasts were performed as described for keratinocytes (sec. 3.14.6.1; Fig. 3.5) with the following adjustments. 125,000 cells were seeded per well in medium containing 10 % FBS and incubated until 90 % confluence was reached overnight. 1 - 2 h before the experiment was started, the medium was

shifted to serum-free conditions. The cell mono-layer was scratched and documented as described before, but a medium change was only applied every 24 h to keep the treatment conditions as performed in the WHMs. 1; 10; 25 or 50 µg/ml aqueous ARE or 0.1; 1; 5 or 10 µg/ml ethanolic ARE, as well as medium or DMSO control were applied after the cell mono-layer was scratched and washed as described before (sec. 3.14.6.1). The wound healing process was evaluated as described in sec. 3.14.6 and sec. 3.16.

3.14.6.4. Migratory Studies with Proliferation Inhibited Fibroblasts (Scratch Assay)

The migratory behavior of proliferation inhibited fibroblasts under treatment with the extracts was further investigated. Here, one day after cell seeding in serum-containing medium, the cell mono-layer was irradiated with x-ray radiation (Gulmay; 200 kV, 15 mA, filter 5 mm copper and 0.8 mm beryllium, 13.20 min; dose rate 1.2 Gy/min). Afterwards, the medium was exchanged with fresh 10 % FBS-RPMI and the scratch assay was performed after one more day of accumulation according to the experiments with non-irradiated fibroblasts (sec. 3.14.6.3).

3.14.7. Barrier Formation Studies

To evaluate the impact of the extracts on barrier formation the transepidermal resistance (TER) of primary human keratinocytes was measured. 40,000 cells in 1.5 ml medium were seeded into transwell membrane filter inserts (Corning; placed in the cellZcope). The cells were cultured in the cellZcope device till hyper-confluence was achieved (37 °C, 5 % CO_2 and 95 % humidity). The medium was exchanged 72 h after seeding to high calcium medium (1.8 mM calcium chloride) to induce keratinocytes differentiation and barrier formation. Contemporaneously the treatment was added: 260 µl on filter membrane and 810 µl below the insert (1, 5 or 50 µg/ml aqueous ARE; 0.2, 2 or 20 µg/ml ethanolic ARE; medium or DMSO). The calcium switch and treatment addition was defined as the experimental start (0 h). The TER was monitored over five days every 2 h and medium/treatment was refreshed every 24 h. The experiment was carried out with cells from three (20 µg/ml ethanolic ARE), four (50 µg/ml aqueous ARE; 0.2 and 2 µg/ml ethanolic ARE) or five (NC, DMSO, 1 and 5 µg/ml aqueous ARE) different donors in duplicates. The resulting TER mean in resistance per area [Ω/cm^2] were normalized to medium or DMSO control.

3.15. Molecular Biological Protein Expression Studies in Cultured Fibroblasts

To determine the aqueous ARE influence on different molecules associated with apoptosis and the formation of an ECM by fibroblasts, protein level analyses were performed by WB. Total proteins were isolated from serum-free cultured, extract treated fibroblast (sec. 3.15.1). Here 437,500 cells were seeded in 5 ml 10 % FBS-RPMI in a 6 cm culture dish, analogous to the BrdU assay, and cultured at 37 °C, 5 % CO_2 and 95 % humidity. One day after seeding, the medium was changed to serum-free conditions and the treatment was started (5, 25, 50 µg/ml aqueous ARE). The cultivation with the extract was refreshed after 24 h and conducted over 48 h. Medium and DMSO were used as controls. Additionally, two apoptosis positive controls were gained by adding 1 µM staurosporine (kinase inhibitor) to fibroblasts or to Jurkat cells (Daubrawa, 2009). The separation of isolated proteins was performed by Sodium dodecyl sulfate-polyacrylamide gel electrophoresis (SDS-PAGE; sec. 3.15.3) and protein transfer by semi-dry or wet blot method (sec. 3.15.4). The experiments were conducted on fibroblasts of three donor sources.

3.15.1. Protein Extraction

Cell cultivation under extract treatment was terminated after 48 h by removing the supernatant. The cells were washed twice with 2.5 ml 4 °C PBS on ice. 200 µl RIPA-buffer (containing 1 % phosphatase inhibitor and 1 % protease inhibitor mix; Tab. 3.4) were added to each condition on ice under orbital shaking. The protein isolation was conducted with the help of a cell scraper (Sarstedt). Lysed cells were transferred into a 1.5 ml reaction tube, further incubated for 30 min on ice, and after strong mixing, centrifuged for 15 min at 13,000 rpm, 4 °C. The supernatants were transferred to new reaction tubes and stored at -80 °C or directly used for further analyses

3.15.2. Determination of Protein Concentration

Protein concentration analysis by Bradford (Bradford, 1976) was used to determine the amount of isolated total protein. Here, the colorant coomassie binds proteins to complexes what result in a conformation change with an absorption shift from 465 to 595 nm. This change can be measured as a colorimetrically shift with a photometric plate reader. A bovine serum albumin (BSA) standard curve was used to calculate the protein content of the samples.

The assay was performed in 96 well plates in triplicates. Protein samples were diluted in *A. dest.* (1:20; 1:19 µl). 1 µl *A. dest.*, instead of a protein sample, was used as negative control/blank. For the BSA standard, 1 µl RIPA buffer was mixed with 19 µl prepared a standard solution (0 - 0.45 mg/ml). Subsequent 180 µl Bradford reagent were added to each well and, after orbital shaking for 10 sec, the reaction was measured by a plate reader at 570 nm (Magellan Sunrise). The measured absorptions were referred to the BSA standard and the total protein content was calculated.

3.15.3. Electrophoreses Protein Separation

SDS-PAGE was used to separate the charged linear protein samples due to their molecular size, where small molecules migrate faster than bigger ones through the gel. As more compact the polyacrylamide network is, smaller molecules could be separated. According to Laemmli (Laemmli, 1970), the separation was conducted with a discontinuous polyacrylamide gel. Here, the denaturized and negatively charged proteins migrate concerning voltage to the anode.
Denaturation of the samples was obtained by adding 2 x SDS sample buffer (Tab. 3.4) to the isolated protein, which contained β-mercaptoethanol to solve hydrogen and disulfide bonds and disperse complex quaternary and tertiary structures. This was supported by 5 min heating to 93 °C with additional short centrifugation at 13,000 rpm and incubation on ice until the samples were loaded. Simultaneously, the discontinuous gels with low acrylamide amount, to collect the proteins on top, and smaller pored separation gel below were prepared using the Mini-PROTEAN®3 System (Bio-Rad). Here glass plates were cleaned carefully and put into the casting equipment. The gel solutions were prepared as described in Tab. 3.12, poured with 2 cm space to the upper end. Isopropanol was applied above to enable a plain surface. After 45 min the gel was polymerized, isopropanol was removed, the surface was washed with *A. dest* and the collection gel solution was added. Immediately a comb with ten pockets was placed in the gel chamber to enable protein loading. After a further 30 min, the whole SDS gel was ready to use and placed into the electrophoresis chamber with either a second gel or a placeholder dummy. The inner chamber and outer chamber were filled with 1 x running buffer (Tab. 3.4). The comb was removed, the pockets were flushed with running buffer and 5 or 10 µg protein solutions were loaded depending on the protein that should be determined. Protein marker was used as a size reference. All pockets were equally filled with (1 x SDS buffer adjusted) protein samples or sample buffer. (For investigating caspase 3/cleaved caspase 3 10 µg total protein was used. Collagen I, collagen IV and fibronectin were studied by separating 5 µg total proteins.) The lid of the running chamber was closed and the electrophoresis was performed for 10 min at

60 V and 75 min at 120 V. Electrophoresis with big proteins was conducted with ice surrounding the electrophoresis chamber, small molecules were separated at A. T. The run was terminated when the bromine phenol blue from the sample buffer reached the lower end of the gel. The collection part was removed from the gel before the separated proteins were transferred to nitrocellulose membrane by WB method (sec. 3.15.4).

Table 3.12.: Schematic overview of the acrylamide gel compositions used for SDS-PAGE

Gel preparation, 6x	**Collection gel**	**Separation gel**	
	4 %	6 %	14 %
Acrylamide solution	1.3 ml	6 ml	14 ml
Accumulation gel buffer	2.5 ml	7.5 ml	7.5 ml
Separation gel buffer		16.2 ml	8.2 ml
A. dest.	5.9 ml		
APS [10 %]	0.3 ml	0.3 ml	0.3 ml
TEMED	0.01 ml	0.01 ml	0.01 ml

3.15.4. Protein Transfer by Western Blot Method

The separated proteins were transferred onto the nitrocellulose membrane to achieve a stable analyze system for antigen-antibody detection. Here, the proteins were converted without localization changes by using an electrical field. Small molecules were transferred by semi-dry blot and big ones by wet blot method. The binding to the membrane was enabled by hydrophobic interactions due to hydrogen bonds.
The membrane´s bound proteins were stained with ponceau. This coloring solution contained tri-chlorine acetic acid that stained and fixed the protein-membrane-binding at the same time. Afterwards, the membrane was labeled by a soft pencil and if necessary, cut to separate the target proteins and loading controls (housekeeping proteins, which do not change their expression). The staining was bleached by incubating the membrane 3 x 5 min in TBS-T (Tab. 3.4).

Semi-dry Western Blot

The membrane and two filter papers were equilibrated in transfer buffer (Tab. 3.4). The blotting was prepared in the cassette of the Bio-Rad system. Here, the wet filter paper was placed on the bottom, the gel followed by the membrane and another filter paper were positioned above. Potential air bubbles were rolled away and the cassette was closed. The transfer cassette was placed in the blotting chamber and the proteins were transferred using 25 V, 1 A for 30 min at A. T.

Wet Western Blot

The gel and two filters were pre-incubated in transfer buffer with an additional two sponges. The transfer cassette was prepared as followed: black side down, sponge, filter, gel, nitrocellulose membrane, filter and sponge. Potential air bubbles were carefully rolled out. The cassette was folded together and placed into the wet blot chamber. An ice element, as well as a stirring magnet, was added and the chamber was placed on ice in a room with 4 °C. The blot chamber was filled with blot buffer. The chamber was closed and the transfer was conducted under continuous stirring at 100 V, 350 mA and 300 W overnight.

3.15.5. Evaluation of Western Blot Signals

The protein containing membranes were incubated under shaking in 5 % low-fat milk blocking solution (Tab. 3.4) over 60 min at A. T. after ponceau staining (sec. 3.15.4). Unspecific protein binding sites were blocked and the antigen binding resulted in higher specificity and resolution. Incubation with primary antibodies was performed overnight at 4 °C under continuous movement of the membranes that were previously laminated in a small bag with the antibody solution (Tab. 3.6). Afterwards, the unbound antibody was removed by washing the membrane 3 x in TBS-T buffer. Then, the species-specific secondary antibody (Tab. 3.7) was applied for 30 min at A. T. in a laminated bag under movement. Finally, the membranes were washed 3 x with TBS-T buffer and the development of the protein signals were conducted with a chemiluminescent kit (Tab. 3.3) for 5 min at A. T. under shaking in the dark. The reagent contained the substrate for the secondary antibody bound peroxidase (luminol) and hydrogen peroxide to enhance the reaction that emitted light. These signals can be transferred in seconds or minutes (depending on the protein signal intensity) onto x-ray film. Visualization was performed with help of a film developing machine (Agfa). After documentation, the membrane was washed again 3 x in TBS-T and completely dried before it was laminated for storage at A. T. protected from light.
The films were digitalized and the signal intensity evaluated with help of the Fiji software. The *rectangle tool* was used to mark the first band with the key combination ´strg + 1´. All other bands could be marked by shifting the new rectangle to the next bands and fixing them with ´strg + 2´. When all bands were marked, their plot was generated by pressing ´strg + 3´. Here, the *horizontal line tool* was used to mark the background threshold that was further applied to all plots. The *wand (tracing) tool* enables the selection of the area under the curve that represents the signal intensity. These data were plotted in an Excel table. The evaluation of collagen type I signals

was conducted divergently. All plotted bands (with the same size) were marked within one rectangle and the resulting plots were evaluated as described for single rectangles with background subtraction.
Further, the target protein signals were set in relation to the loading control proteins to gain relative protein amounts. They were further normalized to the untreated medium control (sec. 3.16).

3.16. Statistical Evaluation of Experimental Data

The evaluation of experimental data was conducted with the statistic software IBM SPSS version 21 or in Microsoft Excel 2007. Data were expressed as mean ± SEM. A p-value less than 0.05 or 0.01 was considered as statistically significant in ascending order.
The statistical evaluation for the *ex vivo* WHMs analyses was performed on two technical replicates with usually four single values per condition and donor skin (in cases without drop outs, see sec. 3.12). The results were normalized to the individual donor solvent control (NC). To evaluate the difference between the tested groups, a general linear model was used with additional independent paired t-test (ANOVA, Bonferroni correction).
All photometrically measured *in vitro* cell culture experiments were initially background subtracted. Afterwards, the mean of three technical replicates per donor was determined. In the case of more than 20 % deviation, the value was excluded from the experiment. The data were further normalized to the medium control. The statistical evaluation was conducted using ANOVA and Bonferroni correction on the mean ± SEM of the calculated single replicates from the different donors in.
Scratch assay studies were interpreted after using ANOVA with Bonferroni correction. Raw data from the Tscratch software were normalized to the wound size at the start of the experiment directly after injury (0 h). The wound closure was compared between the different treatments over time. The *in vitro* performed TER measurement with primary keratinocytes and the protein expression studies in cultured fibroblasts were evaluated with the student´s t-Test using Microsoft Excel.

4. Results

4.1. Hypothesis-driven Literature Search for Traditionally Used Wound Healing Promoting Chinese Herbs

Complementary medicines such as TCM represent a broad spectrum of therapeutic herbs. Herbal extracts showed good results on wound healing in the clinic (Budovsky *et al.*, 2015; Ho & Ong, 2015). However, the search for new products relied on high-throughput screening for single compounds. In contrast, hypothesis-driven screening is based on clinically used therapeutic strategies, their assessment with current practitioners and a complementation with scientific investigations (Friedemann *et al.*, 2015). It describes the evidence-based research approach from bedside-to-bench-to-bedside.
The passed on TCM knowledge and experience was used in this PhD thesis to identify medicinal herbs that were traditionally used for wound healing. The used traditional based written records were the "Pharmacopoeia of the People's Republic of China" (Chinese Pharmocopeia Comission, 2010) and the "Compendium of Materia Medica" (Compendium of Materia Medica, 2003), together with "Leitpfaden Chinesische Phytotherapie" (Hempen & Fischer, 2006) and "Checkliste Chinesische Phytotherapie" (Greten, 2009). The used search criteria were: (1) wound, (2) wound healing, (3) skin, (4) impaired and (5) chronic wounds, (6) diabetic and (7) ulcer. The herbs were selected if they met at least one of the search criteria (1 - 7). Here, 25 herbs were described to be used in phytotherapeutic, individual treatment combinations. This primary literature research was complemented by the knowledge of present TCM practitioners. They confirmed the current relevance and usage of the herbs and provided further information about the therapeutic frequency, possible health risks and the common method of application. Subsequently, plants which did not fulfill the requirements of the TCM practitioners were excluded. Twelve remaining herbs were further supplemented by scientific database research; due to the scientific plant name, genus and traditional names combined with search terms 1 - 7. Plants, which already have been studied in detail, were excluded at this point. All evaluations were performed

with respect to the improvement of re-epithelialization during wound healing.
Performing herbal selection based on expected mode of actions, resulted in gradually excluding plants comparable to a tightened bottleneck. The selected four herbal candidates were radix *A. propinquus*, radix *R. glutinosa*, rhizoma *C. chinensis* and radix *A. euchroma*. Their re-epithelialization capacities were further investigated in an *ex vivo* WHM, to screen the candidate for the most effective one.

4.2. Screening for Evidence of Traditional Described Wound Healing Improvement of Different Aqueous Chinese Herbal Extracts in a Porcine *Ex Vivo* Wound Healing Model

A. propinquus, *R. glutinosa*, *C. chinensis* and *A. euchroma* are traditionally used to treat wounds. The herbal extraction was performed by watery decoction, because most of the herbs are traditionally used as aqueous extracts. Their aqueous extracts were applied as wound dressings or given orally as an herbal tea (Chinese Pharmacopoeica Commission, 2010). The same extraction method offered a comparable evaluation of the observed wound healing impacts. The wound healing promotion effects of different aqueous Chinese herbal extracts derived from radix raw material were investigated on porcine WHMs. All skin samples were wounded, individually treated with different doses of the extracts and incubated under air-liquid interface condition for 48 h. Treatment was refreshed after 24 h. The HE-stained cryo-sections of the snap-frozen WHMs were evaluated by comparing the mean length of the regenerating epidermis to the solvent control (NC) that has been set up to 100 % for each tested individual donor skin.
The WHMs were not included in the statistical evaluation in case of wound margin present hair follicles or glands, experimental damages (*e.g.* broken wound margins), too deep wounds or bacterial infections. These WHMs were excluded, wherefore the sample size may be varied.

4.2.1. Wound Healing Analysis with an Aqueous *A. Propinquus* Extract

An aqueous extract of *A. propinquus* root material, as it is used in TCM, was investigated. A maximum of seven porcine skin donors was analyzed under treatment with

four different extract concentrations (250; 2,500; 12,500 and 25,000 µg/ml; n = 5 - 7). The concentrations were chosen with respect to the effective doses in cell culture experiments of Lau and coworkers (K. Lau *et al.*, 2012). They used concentrations up to 5,000 µg/ml extract. On the basis of our internal experiences with the *ex vivo* WHM, concentrations should be increased tenfold compared to maximum used *in vitro* dose. Additionally, the maximum solvent solubility of the extract was included and a maximum test dose of 25,000 µg/ml was chosen. The re-epithelization of the wounded area was evaluated compared to the controls. The extract of *A. propinquus* did not show a significant positive impact on wound healing in comparison to the controls (Fig. 4.1, A).

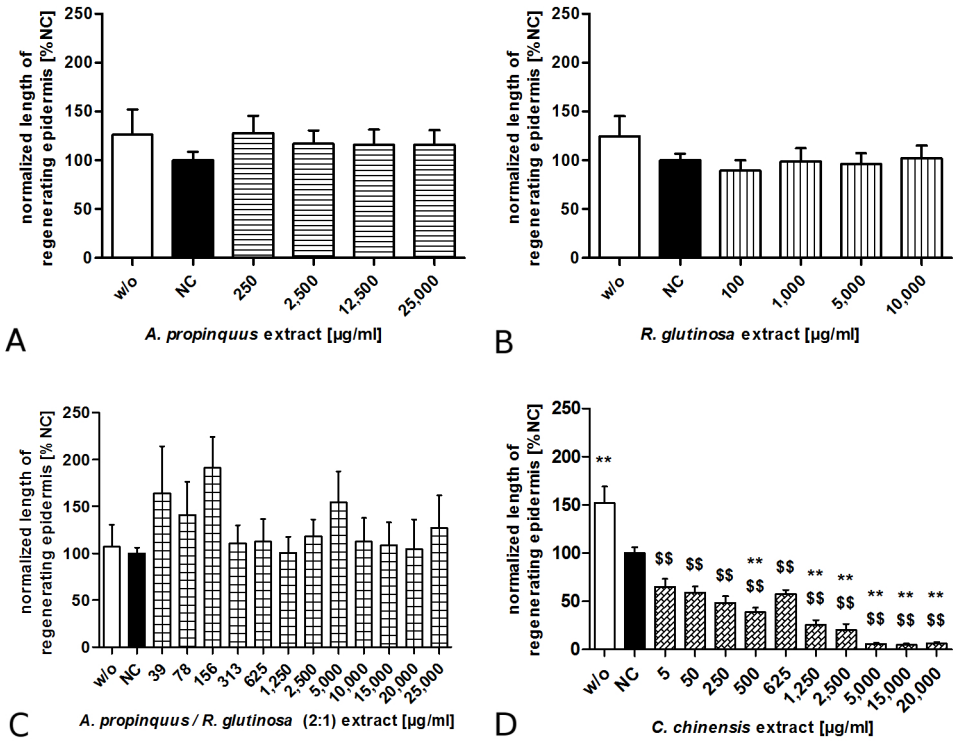

Figure 4.1.: Wound healing analysis of different aqueous herbal extracts on an *ex vivo* porcine skin model. Influence of various concentrations of (A) *A. propinquus* (n = 5 - 7), (B) *R. glutinosa* (n = 5), (C) their combined extract (ratio 2:1; n = 4 - 10) and (D) *C. chinensis* (n $\geq$ 5) on wound healing progress denoted as length of regenerated epidermis normalized to negative control (NC, solvent control). Results represent the mean ± SEM of n donor samples in duplicates with * $p < 0.05$ and ** $p < 0.01$ compared to NC and \$ $p < 0.05$ and \$\$ $p < 0.01$ compared to untreated control (w/o).

4.2.2. Wound Healing Analysis with an Aqueous *R. Glutinosa* Extract

To evaluate the traditional described wound healing promotion of an aqueous *R. glutinosa* extract five donor skin samples were treated with four different extract concentrations (100; 1,000; 5,000 and 10,000 µg/ml). The extract was prepared from dried radix raw material. Again, the concentrations were chosen with respect to the experiments of Lau *et al.*, our own *ex vivo* WHM experiences and the solubility of *R. glutinosa* extract in PBS (K. Lau *et al.,* 2012; sec. 4.2.1).
In comparison to the solvent control no wound healing improvement could be observed (Fig. 4.1, B).

4.2.3. Wound Healing Analysis With an Aqueous Extract Mixture of *A. Propinquus* and *R. Glutinosa*

The radix of *A. propinquus* and *R. glutinosa* are commonly used as aqueous herbal extract combination in a two to one ratio to treat wounds. The ground raw material of both was mixed and a combined extract prepared. The test concentrations orientated on the *in vitro* experiments of Lau et al., our own experience on *ex vivo* wound healing studies and the extracts maximum solubility (K. Lau *et al.*, 2012; sec. 4.2.1). A broad range of twelve concentrations (39 - 25,000 µg/ml) was investigated successively on their wound healing promotion in porcine WHMs. Not every concentration was tested on each donor skin, whereas the controls were conducted for each individual. Therefore, the sample size varied (n = 4 - 10).
A generally positive trend was observed within all tested concentrations (Fig. 4.1, C). However, there was no significant enhancement detectable within the tested specimens.

4.2.4. Wound Healing Analysis With an Aqueous *C. Chinensis* Extract

The re-epithelization impact of an aqueous *C. chinensis* extract, prepared from raw radix material, was investigated on porcine skin samples. In literature, different methods of extract application were mentioned as a direct application of the aqueous non-dried extract without naming a distinct maximum concentration (X.-J. Wang *et al.*, 2013). Friedemann et al. used up to 200 µg/ml aqueous extract *in vitro* without recognizing toxicity in cultured neuroblastoma cells (Friedemann *et al.*, 2014 & 2015). Kim and coworkers investigated concentrations up to 200 µg/ml in mouse

macrophages and 400 mg/kg bodyweight in inflammation studies in mice (H. Kim *et al.*, 2008). There was a lack of concentrations used for wound healing experiments. Therefore, a broad range of ten different concentrations (5 - 20,000 µg/ml) was tested with respect to the maximum solvent solubility of the *C. chinensis* extract. The investigation was started with high concentrations and minor ones were added later to the setup. The large concentration spectrum was investigated on five to ten different donor skin samples, whereas not all conditions were tested on the same donor specimen.
Fig. 4.1, D represents mostly high significant dose-dependent negative impact on wound regeneration due to the treatment with *C. chinensis* extract. The length of the regenerating epidermis was reduced by the extract treatment compared to NC. The measured lengths of the wound recovery were 65.1 ± 8.1 %; 58.9 ± 6.5 %; 48.4 ± 6.6 %; 38.6 ± 4.9 %; 57.2 ± 4.5 %; 25.6 ± 4.6 %; 20.3 ± 6.1 %; 5.9 ± 1 %; 4.6 ± 1.5 %; 6.4 ± 1.4 % with 5; 50; 250; 500; 625; 1,250; 2,500; 5,000; 15,000 and 20,000 µg/ml extract, respectively. Significances to NC were determined for 500 µg/ml and all concentrations bigger than 1,250 µg/ml with $p < 0.01$. Within this cohort, all tested conditions healed significantly less effective than the untreated control, which had a mean regenerated epidermis of 151.9 ± 17 % (all $p < 0.01$).

4.2.5. Wound Healing Analysis With an Aqueous *A. Euchroma* Extract

Different extracts of *A. euchroma* radix have been described to promote wound healing. Especially hydrophobic extracts contain naphthoquinone derivatives. Evidence-based data on topical used aqueous AREs´ wound healing capacity are missing. To enable comparability to the other aqueous extracts, watery decoction was used to prepare the extract. Kim and coworkers performed studies with aqueous extract of traditional synonymous used *L. erythrorhizon* on keratinocytes and fibroblast with non-toxic concentrations until 1,000 µg/ml. During this investigation, a maximum concentration of 1,000 µg/ml was used, with respect to the maximum solubility of the aqueous ARE. The wound healing progress of porcine skin WHMs ($n \geq 10$), treated with different concentrations (10 - 1,000 µg/ml) of the aqueous ARE, was studied. Again, not every concentration could be evaluated on each donor specimen. This is why, the sample size varied.
The analyses showed a significant positive dose-dependent impact on the epidermal regeneration after 48 h of cultivation with the extract (Fig. 4.2, A). The relative wound regeneration compared to NC was 86.8 ± 8.9 %; 128.2 ± 26.1 %; 168.2 ± 26.3 % [$p(NC) < 0.01$, $p(w/o) < 0.05$]; 161.8 ± 16.4 % [$p(NC) < 0.01$, $p(w/o) < 0.05$] and

99 ± 6.4 % with 10; 50; 100; 500 and 1,000 µg/ml ARE, respectively.

The WHMs were further differentiated due to the intrinsic wound healing capacity of the donor skin in good and bad healing specimens. This was performed concerning the mean wound regeneration of all tested untreated control samples 48 h after injury. Epidermal regeneration ≥ 638.9 µm was determined as a good healing specimen. In contrast, lower lengths were defined as below average healing sample, which is compact called a bad healer. Within the good healing group there was a significant epidermal regeneration improvement of 199.7 ± 32.6 % [p(NC) < 0.05] and 198.6 ± 27 % [p(NC) < 0.05] with 100 and 500 µg/ml ARE treatment (Fig. 4.2, B). A positive non-significant trend on bad healing samples was detected with 500 µg/ml ARE (118.5 ± 18.6 %). The other concentrations showed relatively similar regeneration means as the control (83.6 ± 13.2 %; 64 ± 7.8 %; 97.2 ± 34.9 % and 100.1 ± 8.3 % with 10; 50; 100 and 1,000 µg/ml ARE; Fig. 4.2, C).

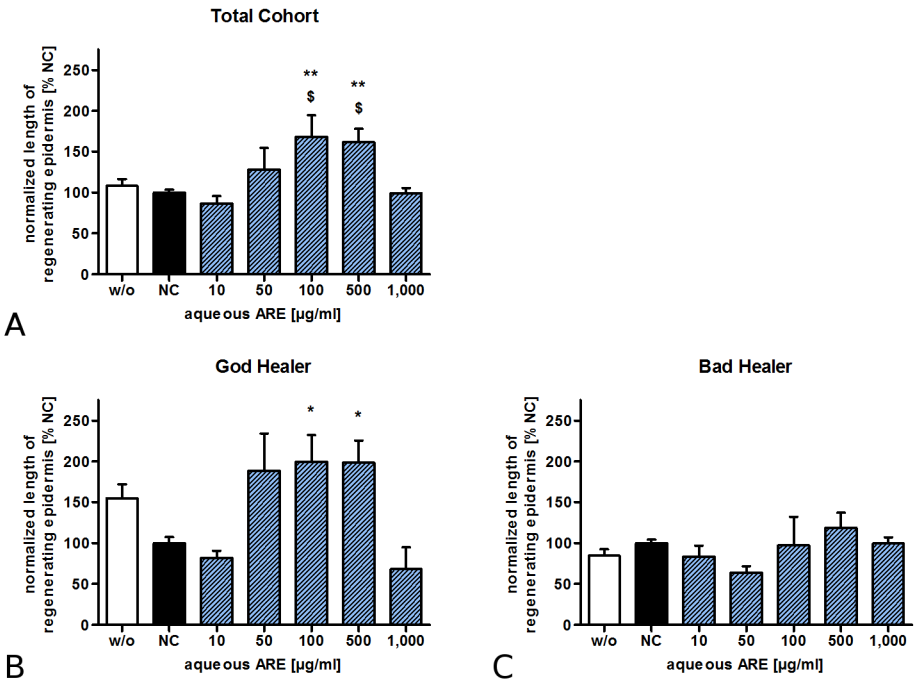

Figure 4.2.: Wound regeneration analyses with aqueous ARE in an *ex vivo* porcine skin model. (A) The impact of various concentrations of ARE on wound regenerating process measured as the length of regenerated epidermis normalized to negative control (NC, solvent control). Wound re-epithelialization impact of ARE was evaluated with respect to intrinsic (B) good healing and (C) bad healing donor specimens. The subdivision was performed with respect to the mean regenerated epidermis of all untreated controls within this cohort (≥ 638.93 µm). Results represent the mean ± SEM of n ≥ 10 donor skins in duplicates with * $p < 0.05$ and ** $p < 0.01$ compared to NC and \$ $p < 0.05$ compared to untreated control (w/o).

Continuing extract analyses with the aqueous ARE were performed because of the observed positive effect on epidermal regeneration. The concentration of 500 µg/ml ARE

showed significant wound healing improvement (161.8 ± 16.4 %) in the total cohort. The significant positive impact was also present in good healing specimens (198.6 ± 26.9 %) and a positive trend was detected in bad healing samples (118.5 ± 18.6 %). The results for WHMs tested with this concentration were more homogenous with less standard deviation compared to the 100 µg/ml treated samples. Therefore, further analyses were performed with 500 µg/ml and additionally 50 µg/ml as a tenfold minor concentration.

Since the aqueous ARE is used in further analyses, the extracted secondary metabolite composition was investigated chromatographically.

4.3. Characterization of different *A. Euchroma* Extracts

To address the underlying wound healing mechanism of aqueous ARE chromatographically and anti-oxidative analyses were performed. Traditionally ARE is prepared by decoction in water or boiled in oil (Chinese Pharmacopeia Commission, 2010). Laboratory studies often focus on hydrophobic extracts (Ashkani *et al.*, 2012; Nasiri *et al.*, 2016 & 2015). During our initial investigations, a wound regenerating promotion by the aqueous ARE was shown. The knowledge of the chemical composition of *A. euchroma* can be used to clarify the observed wound healing promotion effect of our studies compared to other research results. The analyses were conducted using the raw material extracted with water (decoct; sec. 3.10.1) or additionally ethanol (ultrasonic extract, 95 % ethanol in water; sec. 3.10.2) to allow a comprehensive conclusion concerning the herbal ingredient secondary metabolites.

4.3.1. Determination of Shikonin Presence or Absence in the Aqueous and Ethanolic *A. Euchroma* Extract by Thin Layer Chromatography

The question was addressed, whether the ethanolic or aqueous ARE contain shikonin that has been described as wound healing agent before (Papageorgiou *et al.*, 2008; Andújar *et al.*, 2013). Therefore, a TLC was performed to separate the extracts in comparison to pure shikonin (sec. 3.11.1.3, Fig. 4.3). The visualization was performed under daylight and UV light of 254 nm wavelength. The retention factor for HPLC-purified commercial shikonin was 0.32 to 0.34, depending on the loaded amount (Fig. 4.3; lane 7 - 10). There was a signal detectable at a comparable high

but with less intensity in the ethanolic ARE (lane 5 & 6) and in the methanolic ARE samples (lane 11; Rf = 0.32). No shikonin signal was visible in the aqueous ARE samples (lane 1 - 4).
A more sensitive chromatographic experiment was investigated, to proof shikonin presence in the ethanolic ARE (and the aqueous ARE).

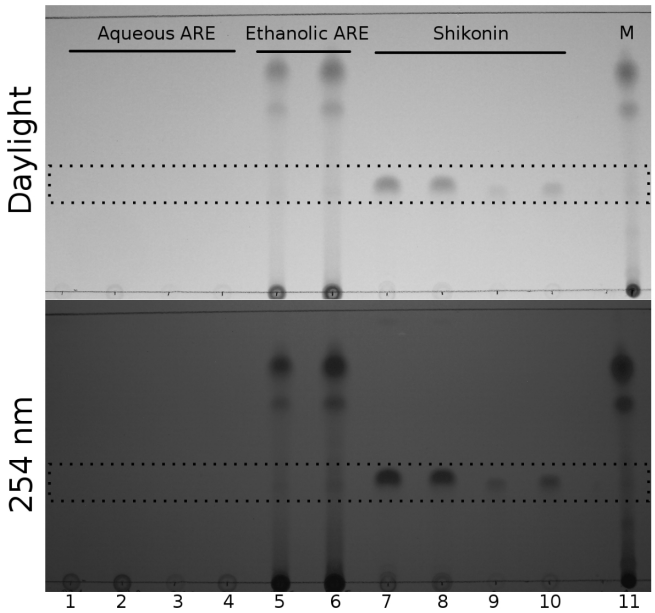

Figure 4.3.: Determination of shikonin presence in aqueous, ethanolic and methanolic ARE by TLC. Tuluol/Ethylacetat (93:7, v/v) was used as mobile phase and the derivatization was conducted using anisaldehyde-sulfuric acid under heating to 100 °C for 10 min. Visualization was performed using daylight (above) and 254 nm UV light (below). 5 mg aqueous ARE (distribution source I, lane 1 & 2; or source III, lane 3 & 4) or ethanolic ARE (source I, lane 5 & 6) were dissolved in 1 ml methanol. Applications were performed as follows: Extracts (lane 1 - 6) 10 µl or 20 µl (first and second lane); shikonin 2 µl (17 µM; lane 7), 10 µl (1.7 µM; lane 8), 10 or 20 µl (0.17 µM; lane 9 & 10); and 10 µl commercial methanolic ARE (lane 11). The dotted rectangles mark the level, were shikonin signal was detected (retention factor 0.32 to 0.34, depending on the loaded concentration).

4.3.2. UHPLC-HRMS Analyses of Naphthoquinones and Pyrrolizidine Alkaloids in Both *A. Euchroma* Extracts

To clarify the extracts´ presence of shikonin a more sensitive analysis, UHPLC-HRMS, was performed with pure shikonin as a reference. The UHPLC-HRMS analyses were conducted in positive (PI) and negative ion (NI) mode. Aqueous and ethanolic AREs (and shikonin) were compared by this sensitive analytical method. Secondary metabolites were putatively identified by dereplication against the DNP database which encompasses all natural products reported to date (sec. A.2, supplementary part).

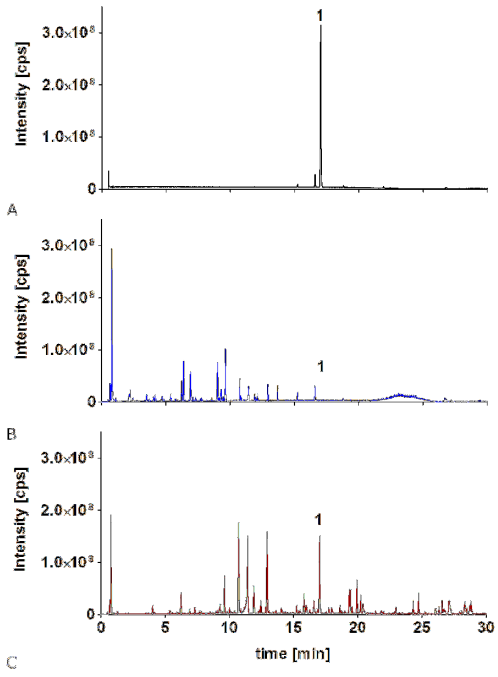

Figure 4.4.: UHPLC-HRMS analyses of aqueous and ethanolic ARE concerning the presence or absence of shikonin (negative ion mode). (A) The chromatogram of single shikonin standard (1; 20 µg/ml, methanol) showed a peak for the sum formula $C_{16}H_{16}O_5$ at 17 min (m/z 287.0927 $[M\text{-}H]^-$, 287.0927; 3.5 ppm) measured as intensity in counts per second (cps). (B) The Chromatogram of the aqueous ARE did not represent the main shikonin (1) peak at the retention time of 17 min. However, minor signals with the same mass and different retention times were observed. (C) The chromatogram of the ethanolic ARE showed the single peak of shikonin at 17 min and further peaks at different retention times with the same molecular mass; Both extracts 1 mg/ml, water/methanol, 85:15.

This method provided a high-resolution profiling of all ionized molecules and enabled a chromatographic comparison of the extracts. However, it did not offer a quantification of detected substances without analyzing known amounts of reference compounds under identical conditions.

A single shikonin peak in NI mode (m/z 287.0927 $[M\text{-}H]^-$, calculated for $C_{16}H_{16}O_5$, 287.0927; 3.5 ppm) at a retention time of 17 min was detected (Fig. 4.4, A). No signal for shikonin at the same retention time was observed in the aqueous ARE (Fig. 4.4, B). However, there were minor peaks with the same mass and different retention times that hint to isomeric or degraded molecules. The chromatogram (Fig. 4.4, C) of the ethanolic ARE represented the detected peak for shikonin at 17 min and further peaks, which indicated potential isomers and degraded molecules.

In the aqueous extract, respectively in the PI (Fig. 4.5, C), seven peaks were identified that are associated with naphthoquinones (*e.g.* anhydroalkannin, euchroquinol B and arnebin V) and ten peaks for PAs. In the NI (Fig. 4.5 A) 14 peaks for compounds belonging to naphthoquinones were detected. The anthracene compound eu-

chroquinol A and further rabdosiin, coumaric and rosmarinic acids, as well as peaks for polysaccharides, were identified exclusively in the aqueous ARE.
Fig. 4.5 shows the chromatograms of both AREs in NI (A & B) and PI (C & D) mode. Compound information concerning their putative identification by dereplication were listed in sec. A.2.

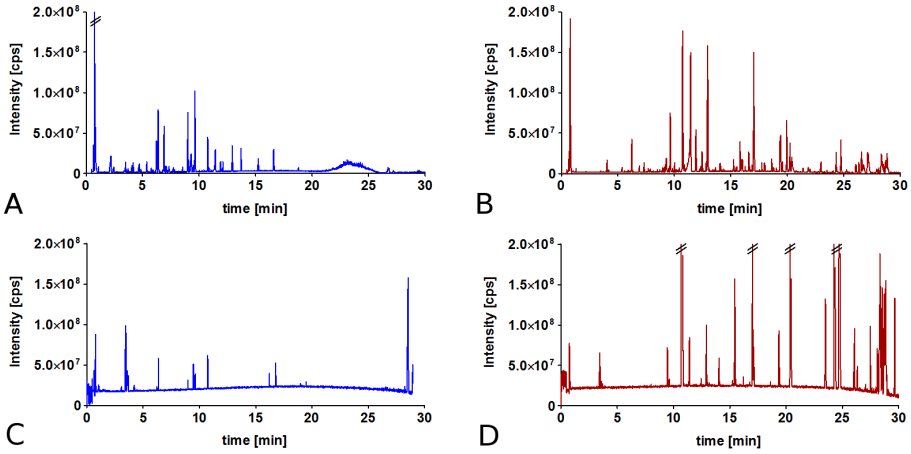

Figure 4.5.: Enlarged chromatograms from UHPLC-HRMS of (A & C) aqueous and (B & D) ethanolic ARE in NI (A - B) and PI mode (C - D). (B & D) The ethanolic ARE showed qualitatively more peaks with higher intensities compared to the aqueous ARE (A & C). The detailed putative information about the peaks at certain retention times were mentioned in the sec. A.2 in the supplementary part; double line marks peaks, which range out of the y-axis maximum.

The ethanolic extract showed in general more signals with higher intensity (Fig. 4.5, B & D). 21 (PI; Fig. 4.5, D) or 25 (NI; B) peaks were associated with naphthoquinones as mentioned for the aqueous ARE with additional peaks for potential isomers of alkannin/shikonin, α-methylbutyrylalkannin, shikonin acetate, arnebin I and II; meroterpenoids (as *e.g.* arnebifuranone and glaziovianol B). 12 peaks (PI) were associated with PAs.

4.3.3. UHPLC-ELSD Analyses of Polar Secondary Metabolites of the *A. Euchroma* Extracts

By UHPLC-ELSD investigation the test solution was inserted in the UHPLC-system and the evaporated secondary metabolite arrived at the laser detector. Here, the detection of reduced light intensity of the single compounds was determined (Douville *et al.*, 2006). This enabled detection of compounds, which are not able to absorb UV light as *e.g.* sugars, lipids, phospholipids and alcohols. The investigation showed a high amount of polar constituents, which were measured at the beginning of the detection at the detector, in the aqueous ARE compared to the ethanolic one (Fig. 4.6).

This strong polar peak represented the main ingredient group/groups of the aqueous ARE and may contain active compounds.

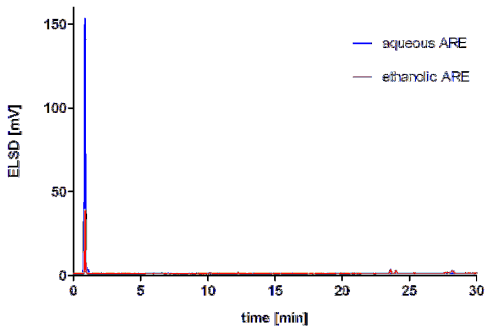

Figure 4.6.: Comparative UHPLC-ELSD analyses of aqueous and ethanolic ARE. Both extracts (1 mg/ml, water/methanol, 85/15) were analyzed, and the results were plotted as ELSD signal intensity [mV] per retention time [min]. The aqueous ARE (blue) showed a quantitative higher peak intensity compared to the ethanolic ARE (red).

4.3.4. Anti-oxidant Studies with the Aqueous Extract of *A. Euchroma*

Free radicals can cause delayed wound healing. Therefore, radical scavenging capacity is a biological characteristic with potential wound healing promotion (Guo & DiPietro, 2010). Wound regeneration can be supported by anti-oxidants due to the regulated redox homeostasis as described in detail in the review of Kurahashi & Fujii (Kurahashi & Fujii, 2015). The anti-oxidative capacity of different hydrophobic extracts of *Arnebia* species have been described in literature (Ganie *et al.*, 2012; Shameem *et al.*, 2015; Tiga *et al.*, 2016). Here, the anti-oxidant activities of aqueous ARE were determined by using the DPPH and ORAC assay, which measured the scavenging of free organic- (DPPH assay) or peroxyl radicals (ORAC assay; Friedemann *et al.*, 2014). Trolox and NAC were used as reference substances for the DPPH assay. The organic radical scavenging capacities of the different tested concentrations were 90.1 ± 0.6 %, 66.3 ± 0.7 %, 30.8 ± 0.9 %, 14.1 ± 0.2 %, 12.8 ± 0.3 % and 10.1 ± 0.9 % with 10, 20, 40, 60, 80 and 100 µg/ml ARE, respectively (Fig. 4.7, A). The calculated half-maximal inhibitory concentration of trolox (IC50 ± SEM; 4.3 ± 0.2 µg/ml), NAC (5.6 ± 0.1 µg/ml) and ARE (31.5 ± 1.6 µg/ml) were shown in Fig. 4.7, B. These results demonstrated that aqueous ARE had a radical scavenging capacity on organic radicals, although it was weaker than that of the reference substances.
The ORAC assay was performed with trolox as a reference substance. Here, 1 g aqueous ARE was determined to inhibit comparable amounts of peroxyl radicals as 1.9 ± 0.2 mM trolox.

In summary, aqueous ARE showed present moderate organic and peroxyl radical scavenging capacities.

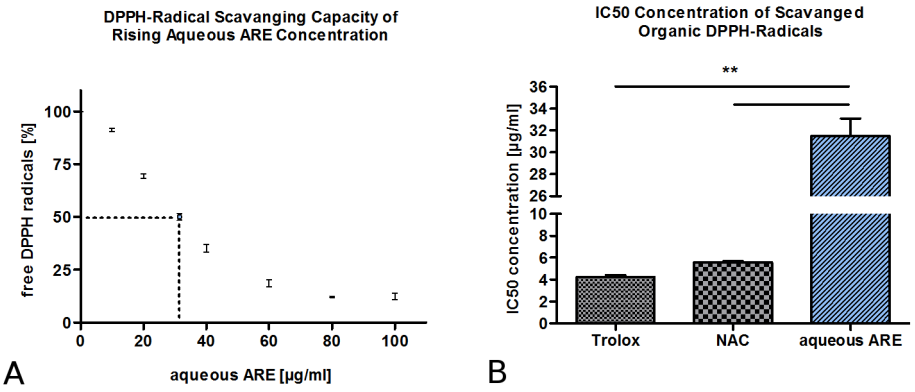

Figure 4.7.: Anti-oxidant activity of trolox, n-acetylcysteine (NAC) and aqueous ARE determined by DPPH-radical scavenging assay. (A) Measurement of the organic radical scavenging capacity of different ARE concentrations with the highlighted half-maximal inhibitory concentration (IC50). (B) The IC50 values of trolox and NAC were significantly lower than that one of the aqueous ARE. Results represent the mean ± SEM of three independent experiments in triplicates with ** $p < 0.01$.

4.4. Continuing Wound Healing Investigations With Aqueous *A. Euchroma* Extract, an Additional Ethanolic Extract and the Single Compound Shikonin

Investigations on human WHMs should confirm the observed wound healing promotion of the aqueous ARE, which was observed on porcine skin.
Furthermore, the re-epithelialization influences of the herbal origin were analyzed, with respect to the raw material compound composition. Additionally, the storage duration influences of the herbal raw materials were studied on the epidermal regenerating capacity.
As mentioned in chapter sec. 2.3.5 different extracts of the *A. euchroma* herb were investigated in wound healing research (S. Ashkani *et al.*, 2012; Nasiri *et al.*, 2015 & 2016). To investigate the complex wound healing capacity of the *A. euchroma* herb an ethanolic ARE was added to the experimental design. The re-epithelialization impact of both AREs was analyzed, to differentiate the observed positive wound healing impact of the aqueous ARE compared to another solvent extract. Therefore, porcine WHMs treated with the aqueous ARE were reproduced and an ethanolic one (sec. 3.10.2) and shikonin were added to the experimental setup. Shikonin has been used in wound

healing reagents and was described as a regeneration promoting agent (Andújar *et al.*, 2013). The re-epithelialization influences of the ethanolic ARE and shikonin were further investigated on human wound healing models treated analogue to the porcine specimens.

4.4.1. *Ex Vivo* Analyses in Human Skin Models

First of all, the aqueous ARE was tested on human WHMs analogous to the porcine WHMs over 48 h past injury (n = 9; Fig. 4.8, A - C). The wound regeneration was measured as 92.6 ± 7 % and 119 ± 8.7 % for 50 and 500 µg/ml ARE treatment. 500 µg/ml ARE significantly improved the wound healing capacity compared to the untreated control ($p < 0.01$).

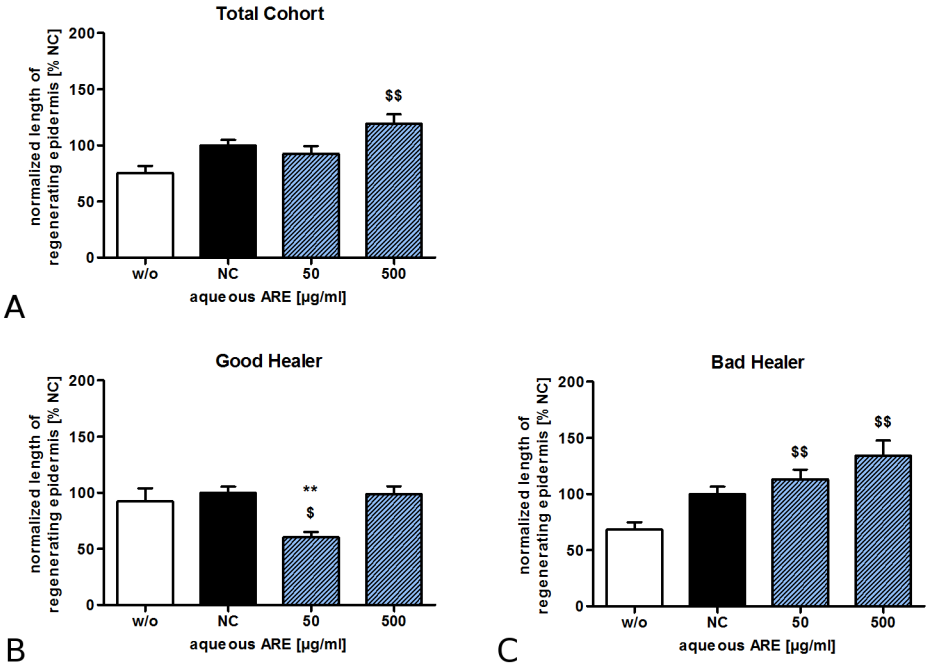

Figure 4.8.: Wound regeneration analyses in an *ex vivo* human WHM treated with aqueous ARE. (A) Wound healing influence on injured human skin samples treated with 50 or 500 µg/ml ARE (n = 9) evaluated as the normalized length of regenerating epidermis. Subdivision in intrinsic (B; n = 3) good and (C; n = 6) bad healing specimens with ≥ 216.7 µm defined as good epidermal regeneration; Results represent the mean ± SEM of n human donor skin samples in duplicates with ** $p < 0.01$ compared to the solvent (NC) and $ $p < 0.05$ and $$ $p < 0.01$ compared to untreated control (w/o).

The subdivision in good and bad healing specimens was determined with respect to the mean of all human untreated control samples with epidermal regeneration ≥ 216.7 µm set as good healer (Fig. 4.8, B; n = 3). Here, good healing specimens could not be further improved by the treatment [60.4 ± 4.9 %, p(w/o) < 0.05, p(NC) < 0.01 and

98.9 ± 6.9 % with 50 and 500 µg/ml]. In contrast, the positive influence on wound regeneration was prominent in intrinsic impaired healing specimens. Within this bad healing group significantly increased epidermal regeneration of 113.1 ± 8.6 % and 134.1 ± 13.6 % [p(NC) = 0.058] was observed for 50 and 500 µg/ml ARE compared to the untreated control [$p < 0.01$; Fig. 4.8, C; n = 6].

4.4.2. Wound Healing Capacity Analyses of Aqueous *A. Euchroma* Extracts of Different Raw Material Origins in Porcine and Human Skin Models

To evaluate potential differences between standardized extracts from diverse herbal origins, three independent sources of *A. euchroma* herbal material were compared. The tested radix raw materials were provided from different distribution sources: (I) Chinaturel, which was used for the initial *ex vivo* experiments and all further mechanism studies, (II) Rats Apotheke and (III) Mehler. Aqueous ARE of all sources was prepared and two concentrations were tested due to their wound healing capacity by WHM analyses in porcine and human skin. The treatments were conducted on the same donor specimens [50 and 500 µg/ml; n(porcine) ≥ 16, n(human) ≥ 4].

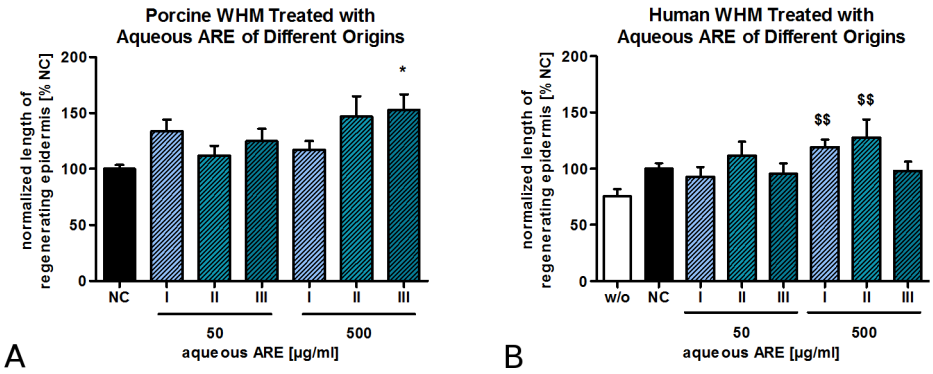

Figure 4.9.: Study of the *ex vivo* wound healing impact of aqueous ARE of different raw material origins. (A) The measured normalized length of regenerating epidermis in porcine skin models treated with aqueous AREs of different distribution sources over 48 h after injury (n ≥ 16; no w/o). (B) Evaluation of the wound regeneration impact of aqueous AREs of different sources in human skin samples (n ≥ 4). The herbal distribution sources were (I) Chinaturel; (II) Rats Apotheke and (III) Mehler. All comparative wound healing studies were performed within the same donor skin cohort; Results represent the mean ± SEM of n swine or human donor skins in duplicates with * $p < 0.05$ compared to the solvent (NC) and \$\$ $p < 0.01$ compared to untreated control (w/o).

Positive wound healing impact of all tested herbal extracts was observed in porcine and human *ex vivo* skin models. The effect intensity varied, measured as re-epithelialization promotion compared to NC (Fig. 4.9, A & B).

An untreated control was missing in the porcine experimental setup, which was caused by an increased number of treatments tested contemporaneously. The wound regenerating effect of source I showed a strong positive tendency in porcine WHMs of 133.7 ± 10.5 % and 117.2 ± 7.8 % with 50 and 500 µg/ml ARE (Fig. 4.9, A; n ≥ 17). However, the increased wound healing promotion of source I was not significant, when statistically evaluated together compared to the extracts of other sources. These findings were in contrast to expectations resulting from earlier experiments (see sec. 4.2.5). The epidermal regeneration with the extracts from origin II was enhanced to 112.3 ± 8.4 % and 147 ± 18.2 % with 50 and 500 µg/ml ARE (n ≥ 16). Source III showed a wound healing improvement of 125 ± 10.7 % and significant increase of 152.9 ± 13.9 % ($p < 0.05$) with 50 and 500 µg/ml ARE compared to NC, respectively (n = 18).

The extracts´ impact on human WHMs analogues to the porcine ones were further analyzed and compared to solvent and untreated controls (n ≥ 4; Fig. 4.9; B). The mean lengths of the regenerating epidermis were determined as following: source I had 92.6 ± 8.7 % and 119 ± 7 % [$p(w/o) < 0.01$; n = 9]; source II showed 111.8 ± 12.3 % and 127.8 ± 16 % [$p(w/o) < 0.01$; n = 4]; and source III had 95.4 ± 9.1 % and 98 ± 8.4 % (n = 4) when treated with 50 and 500 µg/ml aqueous ARE, respectively.

The herbal material from source I was obtained primarily. Therefore, the initial *ex vivo* investigations were performed with this raw material source. Because of the positive wound healing promotion impact of source I (sec. 4.2.5) all mechanism studies were performed with fresh extracts from the source I (Chinaturel Import Export B. V).

4.4.3. Wound Healing Capacities of Fresh Aqueous *A. Euchroma* Extracts of Different Radix Storage Duration Periods

When different herbal sources were compared due to their wound regenerating effects, a decrease in wound healing promotion of aqueous ARE from source I (sec. 4.2.5) compared to the first experiment was observed (see Fig. 4.9, A 1, 1. experiment, 128.2 ± 26.1 %, 161.8 ± 16.4 % $p(NC) < 0.01$, $p(w/o) < 0.05$; Fig. 4.9, A 2, 2. experiment: 133.7 ± 0.5 %, 117.2 ± 7.8 % with 50 and 500 µg/ml, respectively), even though there was still a strong positive trend. A third, later conducted experiment, resulted in promoted epidermal regeneration of 112.1 ± 9.3 % and 123.3 ± 5.8 %, $p(w/o) < 0.05$ with 50 and 500 µg/ml (sec. 4.4.7.1; Fig. 4.9, A 3, 3. experiment). The results of these three independent experiments were normalized to the mean of the solvent controls of each experimental cohort.

The experiments were always performed with fresh extracts of the same stored batch of *A. euchroma* herbal material, and therefore of different storage durations.
All wound healing analyses of aqueous AREs over the experimental duration of three years were additionally evaluated together compared to all solvent and untreated controls (Fig. 4.10, B). The results showed a clear significant wound healing improvement with a mean of 125.9 ± 8.6 % [p(NC) < 0.01, p(w/o) < 0.05] and 132.2 ± 6.2 % [p(NC,w/o) < 0.01; n ≥ 41] regenerated epidermis length with 50 and 500 µg/ml ARE.

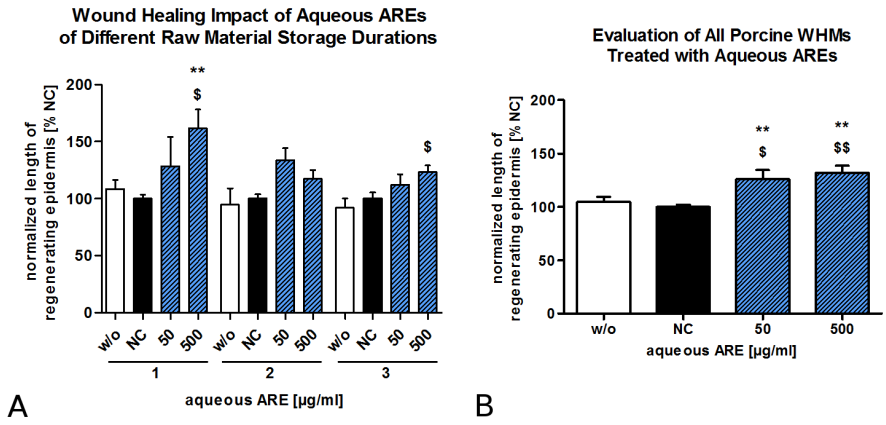

Figure 4.10.: Wound healing promotion investigation with aqueous ARE of different radix material storage durations on porcine WHMs. (A) The impact of aqueous ARE on the normalized length of regenerating epidermis measured in three independent experiments with freshly prepared extracts from the same herbal raw material. The first experiment (1; n ≥ 10; sec. 4.2.5) was compared to a second (2; n ≥ 16; sec. 4.4.2) and third (3; n = 11; 4.4.7.1) experiment. Treatment was performed with aqueous ARE of different raw material storage durations of the same raw material source I. (B) Additional, evaluation of all conducted experiments on *ex vivo* porcine skin models together (n ≥ 41); Results represent the mean ± SEM of n pig donor skins in duplicates with ** p < 0.01 compared to the solvent (NC), $ p < 0.05 and $$ p < 0.01 compared to untreated control (w/o).

4.4.4. Analyses of the Wound Healing Impact of an Ethanolic *A. Euchroma* Extract

Ethanolic ARE was investigated concerning its epidermal regeneration capacity analogous to the experiments with aqueous ARE on porcine and human WHMs over 48 h. The prepared ethanolic ARE was first resolved in DMSO and further diluted in PBS, wherefore another control (DMSO) was added to the experimental design. The investigations in porcine skin were conducted without an untreated control, because aqueous and ethanolic AREs as well as shikonin where tested in parallel. This is why a further subdivision into good and bad healing specimens of this cohort was not performed. Within the human specimens, an untreated control was conducted, wherefore intrinsic good and bad healing specimens were evaluated.

4.4.4.1. *Ex Vivo* Analyses of an Ethanolic *A. Euchroma* Extract in Porcine Skin Models

There were no transferable ethanolic ARE concentrations mentioned in previous published *in vitro* experiments. Therefore, the maximum concentration was chosen with respect to the solubility of the less hydrophilic ethanolic ARE in DMSO. This solution had to be further diluted in PBS, because DMSO on its own has an influence on wound recovery and can, as detergent, act cytotoxic in high concentrations (Capriotti & Capriotti, 2012). Therefore, the resulting DMSO concentration should be kept as low as possible. 200 µg/ml ethanolic ARE was chosen as the maximum concentration with additional tenfold minor 20 µg/ml. The measured re-epithelialization was normalized to the PBS (NC) control to enable comparison to the experiments with the aqueous ARE, which were performed in the same experimental cohort. There was no wound healing promotion detectable within the tested WHMs treated with the ethanolic ARE (Fig. 4.11; n $\geq$ 17).

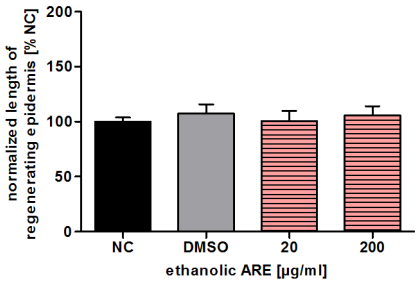

Figure 4.11.: Investigation of the impact of an ethanolic ARE on wound healing in an *ex vivo* porcine skin model. Analysis of the ethanolic extracts impact on re-epithelialization measured as the length of epidermal regeneration in the tested concentrations normalized to PBS control (NC); Results represent the mean ± SEM of n $\geq$ 17 pig donors in duplicates compared to NC and DMSO (solvent) control.

4.4.4.2. *Ex Vivo* Analyses of an Ethanolic *A. Euchroma* Extract in Human Skin Models

The wound healing analyses of ethanolic ARE on eight human WHMs also resulted in no detectable impact of the tested concentrations in the total cohort (Fig. 4.12, A). 95.3 ± 8 % and 96.5 ± 7.3 % epidermal regeneration were measured in the WHMs treated with 20 or 200 µg/ml ethanolic ARE compared to NC, DMSO and untreated control.

Here, an untreated control was conducted. Therefore, the results could be subdivided concerning their intrinsic good and bad healing capacities. Wound regeneration was decreased by the treatment in the intrinsically good healing skin group to 73.5 ± 6.5 %

and 78.8 ± 4.4 % (Fig. 4.12, B; n = 2). This diminished re-epithelialization was significant for DMSO with 65.3 ± 6.2 % [p(NC) < 0.05]. Epidermal regeneration was slightly increased in bad healing specimens by the treatments with the ethanolic ARE and DMSO (107.1 ± 11.2 %, 105.3 ± 10.3 % and 115.3 ± 10 %; with 20, 200 µg/ml and DMSO; Fig. 4.12, C; n = 6). The mean regenerating epidermis was significant for both concentrations of the ethanolic ARE with $p < 0.05$ and for DMSO with $p < 0.01$ compared to the untreated control.
The observed effects seem to be caused by the presence of DMSO.

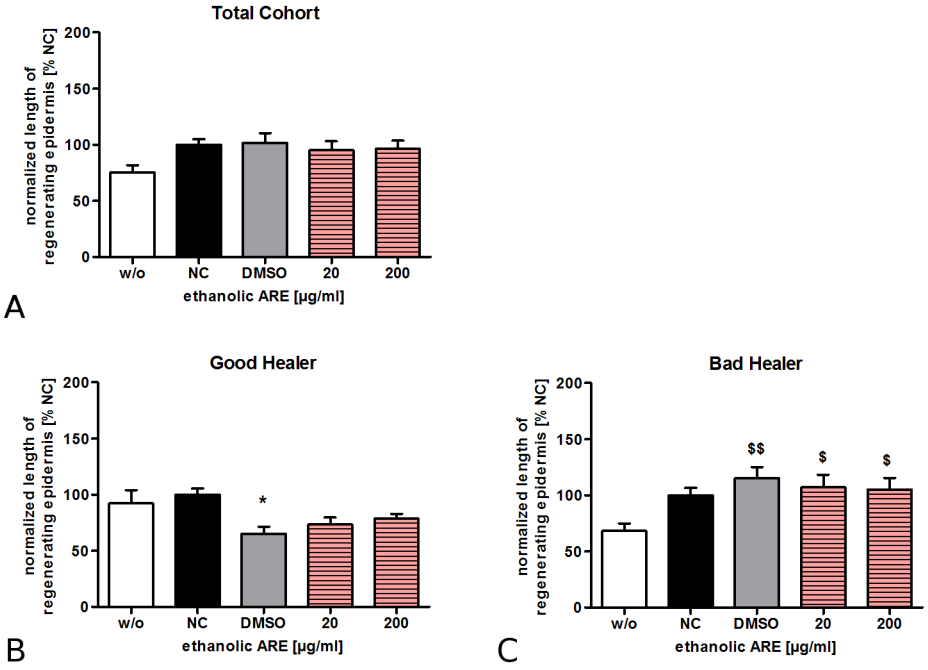

Figure 4.12.: Wound regeneration impact of an ethanolic ARE in an *ex vivo* human WHM. (A) Re-epithelialization influence of ethanolic ARE treatment of injured human skin models (total cohort; n = 8). Epidermal regeneration of intrinsic (B) good healing specimens (epidermal regeneration ≥ 216.7 µm; n = 2) or (C) impaired healing skin samples treated with ethanolic ARE (n = 6); Results represent the mean normalized regenerating epidermis ± SEM of n human donors in duplicates with * $p < 0.05$ compared to PBS (NC), DMSO, and \$ $p < 0.05$ and \$\$ $p < 0.01$ compared to untreated control (w/o).

4.4.5. Analyses of the Wound Healing Impact of Shikonin

The naphthoquinone shikonin is described as a secondary metabolite of the *A. eu-chroma* herb. Our UHPLC-HRMS investigations observed no presence of shikonin in the aqueous ARE compared to reference substance, but minor signals at early retention times that may indicate isomers or degradation products (sec. 4.3.2). Shikonin signal was detected in the ethanolic ARE. However, the chromatographic extracts investigations took a long time. During these wound healing investigations, it was still

questionable whether shikonin was contained in the aqueous or ethanolic ARE. Here, the question was addressed whether shikonin has an impact during re-epithelialization of the WHMs and if applicable, whether it was responsible for the previously detected wound healing improvement.
Several experimental studies showed cytotoxicity of shikonin when used in higher doses than 1 µM (Hou *et al.*, 2006; Fu *et al.*, 2013). Jing et al. demonstrated no effect on cell viability accompanied by a low apoptosis rate in HaCat keratinocytes treated with shikonin less than 1 µM (Jing *et al.*, 2016). Therefore, studies on WHMs treated with 0.5 or 0.05 µM of shikonin (dissolved in DMSO, further diluted in PBS) were investigated, with respect to its general solubility and a maximum low final DMSO concentration.
The resulting epidermal regeneration was normalized to the PBS control, to enable comparison between the experiments with different AREs, and evaluated compared to all controls.

4.4.5.1. *Ex Vivo* analyses of Shikonin in Porcine Skin Models

The analysis of 13 individuals (total cohort) showed a positive but non-significant tendency on wound healing by shikonin treatment. The normalized data represented epidermal regeneration of 113.2 ± 7.6 % and 119.6 ± 13.8 % with 0.05 and 0.5 µM shikonin in comparison to the PBS control (NC) and DMSO control (107.4 ± 8.6 %; Fig. 4.13).
Again, because of a lack of untreated controls within this cohort, the samples were not further divided into good and bad healing specimens.

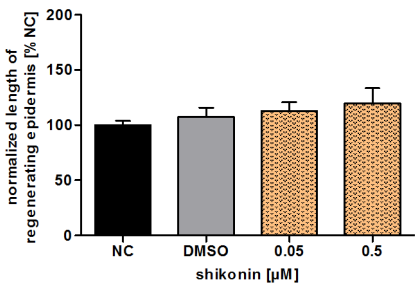

Figure 4.13.: Investigation of the impact of shikonin on wound healing in *ex vivo* porcine WHMs. Measurement of the length of regenerating epidermis in shikonin treated injured skin models; Results represent the mean ± SEM of n ≥ 13 swine donors in duplicates compared to PBS (NC) and DMSO control.

4.4.5.2. *Ex Vivo* Analyses of Shikonin in Human Skin Models

The wound healing impact of shikonin was analyzed on eight injured human skin samples, too. Within the total cohort, the treatment over 48 h after wounding resulted in 83.3 ± 7.9 % and 106.9 ± 11.3 % epidermal regeneration with 0.05 and 0.5 µM shikonin with no significant impact (Fig. 4.14, A).
Good healing specimens showed decreased wound regeneration by shikonin treatment [42.5 ± 3.8 %, p(NC, w/o) < 0.01; 72.9 ± 7.3 % with 0.05 and 0.5 µM shikonin]. DMSO reduced re-epithelialization itself [p(NC) < 0.05; Fig. 4.14, B; n = 2]. The observed significant wound healing improvement with 0.5 µM shikonin treated samples of bad healing WHMs (115.8 ± 13.6 %) was also present in the solvent control DMSO [both p(w/o) < 0.01; Fig. 4.14, C]. Shikonin impact on wound recovery was comparable to the WHMs treated with DMSO control. A direct influence of DMSO was assumed.

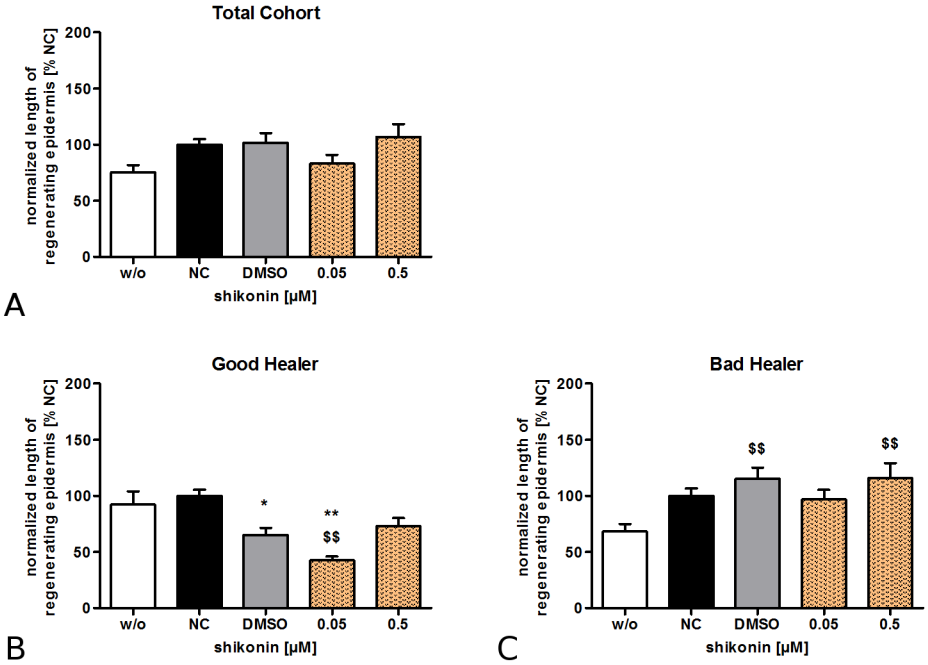

Figure 4.14.: Wound regeneration investigation in an *ex vivo* human WHM treated with shikonin. (A) Wound healing impact of shikonin treatment of injured human skin models (total cohort; n = 8). Epidermal regeneration of intrinsic (B; n = 2) good healing specimens (epidermal regeneration ≥ 216.7 µm) and (C; n = 6) impaired healing skin samples treated with shikonin; Results represent the mean ± SEM of n human donors in duplicates with * p < 0.05 and ** p < 0.01 compared to PBS (NC), DMSO and $$ p < 0.01 compared to untreated control (w/o).

4.4.6. Investigations of the Extracts Wound Healing Impact With Regard to an Alternative Application Time Point on Late Wounds

The application moment could be important for the wound regeneration progress. Usually treatment is applied on the wound with delay regarding the time of injury. Here, the question of the optimal wound healing treatments start was addressed. The impact of the aqueous and ethanolic AREs on later wounds, where the WHMs have been treated 24 h after injury for the first time and were cultivated for a further 48 h (72 h total experimental duration), was analyzed. Due to the previous missing positive impact of ethanolic ARE on epidermal wound recovery (sec. 4.4.4), the concentration spectrum was reduced. 2 and 20 µg/ml ethanolic ARE were investigated as used within the application method studies (sec. 4.4.7). The subdivision, due to intrinsic good and bad healing specimens, was performed with respect to the mean the untreated controls of this experimental cohort, with epidermal regeneration $\geq$ 650.1 µm defined as good healing specimens.

4.4.6.1. Late Wounds Treated With the Aqueous *A. Euchroma* Extract

Within the tested samples, there was a positive non-significant wound healing tendency to 110 ± 10.1 % and 119.1 ± 9.4 % with 50 and 500 µg/ml ARE detected (Fig. 4.15, A; n = 9).
The subdivision in good and bad healing specimens was performed with respect to the results of eight donors, because the untreated control of one specimen was not evaluable. No wound healing improvement could be observed in the subgroup of good healing skin samples (Fig. 4.15, B; 108.2 ± 17.4 % and 91.2 ± 9 % with 50 and 500 µg/ml ARE; n = 5). In contrast, the higher dose decreased epidermal regeneration. However, the bad healing skin specimens treated with 50 µg/ml (115.8 ± 12.9 %) or 500 µg/ml (136.6 ± 13.8 %) showed a strong positive trend on re-epithelization compared to the controls (Fig. 4.15, C; n = 3).
The aqueous ARE impact of treatment on later wounds, with advanced wound healing progress, was not significant and therefore lower than the application on fresh wounds (sec. 4.2.5 and 4.4.7.1).

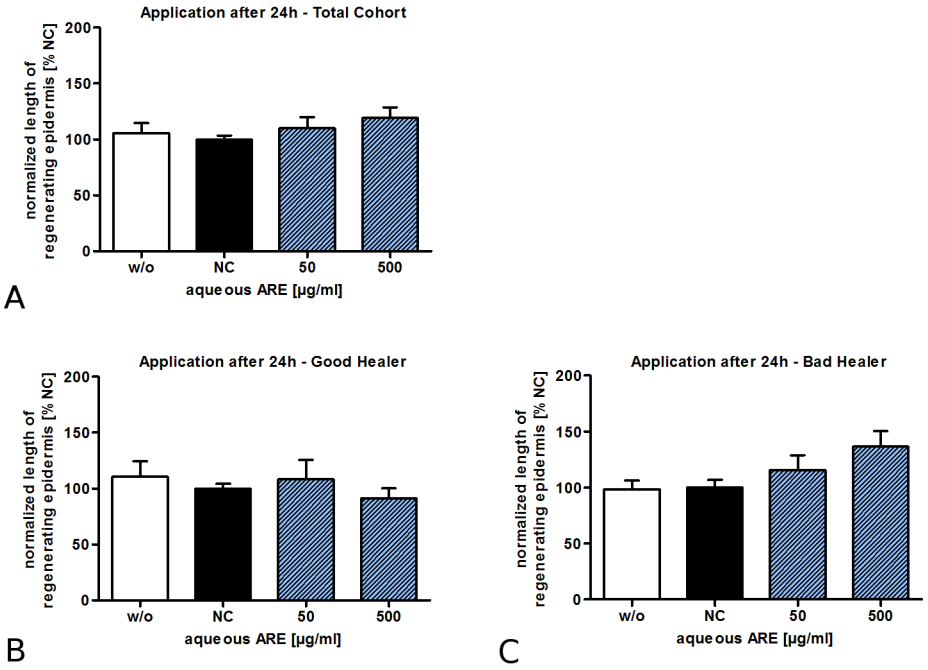

Figure 4.15.: Wound healing application studies on late wounds (24 h after injury) treated with aqueous ARE. (A) The normalized length of regenerating epidermis measured in the total cohort treated with aqueous ARE firstly 24 h past injury (n = 9). Subdivision in (B; n = 5) good healing and (C; n = 3) impaired healing skin specimens was performed for eight specimens with respect to the main of 650.1 µm wound recovery of all untreated controls (one drop out due to non-evaluable w/o); Results represent the mean ± SEM of n individuals in duplicates in comparison to solvent (NC) and untreated control (w/o).

4.4.6.2. Late Wounds Treated With the Ethanolic *A. Euchroma* Extract

The possible wound healing promotion effect of the ethanolic ARE on late wounds, that have been firstly treated 24 h past injury, was investigated. According to the experiments in chapter 4.4.7.2, the ethanolic ARE concentration spectrum was reduced to 2 and 20 µg/ml, because a wound healing promotion effect with 200 µg/ml was not determined previously (sec. 4.4.4). Here, nine to ten donor skin specimens treated with 2 or 20 µg/ml ethanolic ARE were investigated and evaluated compared to PBS (NC), DMSO (solvent) and untreated control (w/o).

The total cohort (Fig. 4.16, A), consisting of ten individuals, showed a positive impact on wound regeneration due to the treatment with the ethanolic ARE 24 h after injury. The mean of the regenerating epidermis were 120.5 ± 10.4 %, $p < 0.01$; 108.9 ± 13.6 %, $p < 0.05$ and 106.5 ± 10.2 %, $p = 0.066$ with 2 and 20 µg/ml ethanolic ARE or DMSO compared to the untreated control, respectively.

Good healing specimens (Fig. 4.16, B; n = 4) were not significantly affected by the treatment (111.2 ± 12.9 %, 91.1 ± 13 % with 2 and 20 µg/ml). A positive effect was observed within the impaired healing group (Fig. 4.16, C; n = 5). Here 2 µg/ml extract

showed significant enhanced epidermal regeneration (141.1 ± 19.3 %) in comparison to the untreated control (52.5 ± 6.8 %, $p < 0.01$). This result had no statistical significance compared to the NC and DMSO control [solvent; 110.5 ± 12.1 %, p(w/o) < 0.01]. The epidermal regeneration of the untreated control was nearly significant decreased compared to the NC control ($p = 0.05$).
The observed wound healing promoting impact of ethanolic ARE was not significant to the solvent control and therefore assumed to be in part caused by the present DMSO.

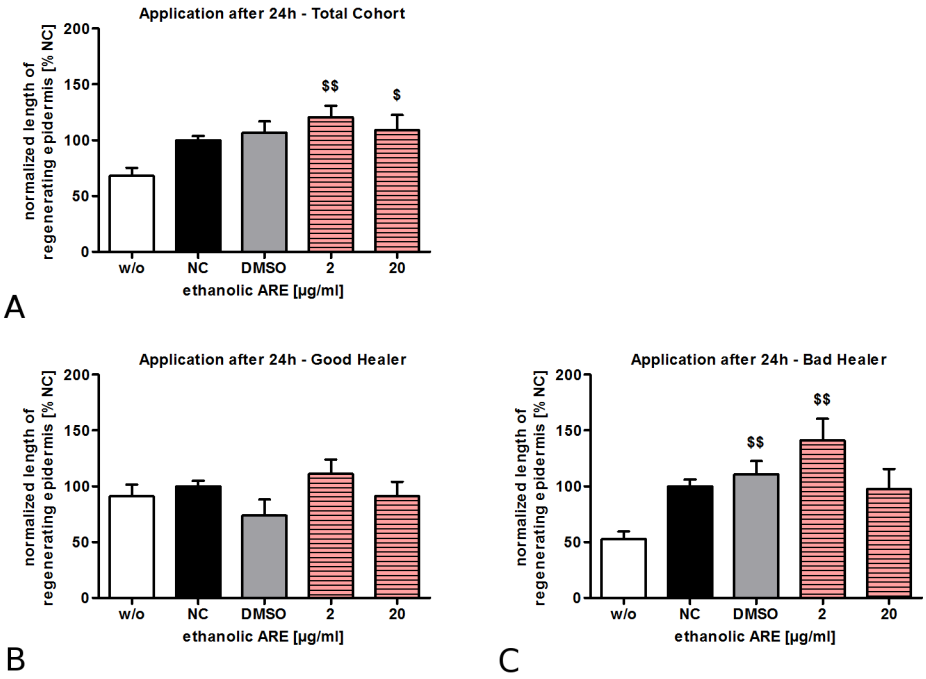

Figure 4.16.: Wound healing application investigations on late wounds (24 h past injury) treated with ethanolic ARE. (A) Regenerating epidermis measured in the total cohort treated with ethanolic ARE firstly 24 h past injury over 48 h (n = 10). Result subdivision in (B; n = 4) good healing and (C; n = 5) bad healing skin specimens was performed with respect to the main of 650.1 µm wound recovery of all untreated controls within this cohort; Results represent the mean length of normalized regenerating epidermis ± SEM of n porcine donor skins in duplicates with \$ $p < 0.05$ and \$\$ $p < 0.01$ in comparison to the untreated (w/o), PBS (NC) and DMSO (solvent) control.

4.4.7. Addressing the Influence of the Extracts Application Method on Wound Healing Improvement

Different methods of treatment application could also affect the wound regeneration. Therefore, the direct donation of 5 µl extract solution in the center area of the wound (as it was done before) was compared with the separate treatment of the wound margin by using an extract saturated cotton bud. The extracts wound healing impact with direct contact to the remaining dermis and epidermis (wound application) was compared with an epidermal application on the wound margin.

4.4.7.1. Application Studies With the Aqueous *A. Euchroma* Extract

Within the cohort of eleven individuals, a positive wound regenerating tendency was observed under direct stimulation of the wound compared to the untreated control (112.1 ± 9.3 %; 123.3 ± 5.8 %, $p < 0.05$, with 50 and 500 µg/ml aqueous ARE). The wound margin application, in contrast, showed no significant improvement on re-epithelialization (108.4 ± 6.1 %; 111.2 ± 10.3 % with 50 and 500 µg/ml ARE; Fig. 4.17, A).

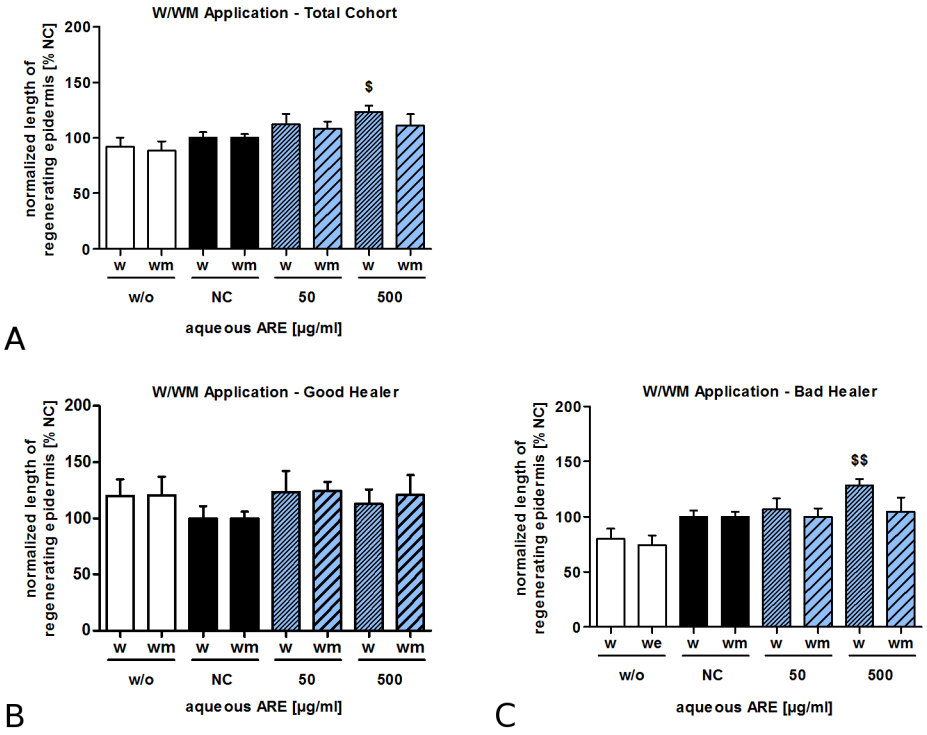

Figure 4.17.: Investigation on the application method impact on wound healing while using aqueous ARE as direct wound application (w) compared to wound margin (wm) treatment in porcine injured skin models. (A) Study of the extracts influence on epidermal regeneration comparing direct wound application method to wound margin application in the total cohort (n = 11). The results were further divided into subgroups of intrinsic (B; n = 4) good and (C; n = 7) bad healing specimens; Results represent the mean normalized length of regenerating epidermis ± SEM of n porcine donor skins in duplicates compared to the solvent (NC), \$ $p < 0.05$ and \$\$ $p < 0.01$ compared to untreated control (w/o).

Differentiated due to their intrinsic healing capacities, there was no significant impact on re-epithelialization detectable by both application methods on good healing samples (123.5 ± 19 %; 112.9 ± 12.9 % by wound; 124.4 ± 8.3 %; 120.8 ± 17.7 % by wound margin application with 50 or 500 µg/ml ARE; Fig. 4.17, B; n = 4). Within the bad healing group, there was a significantly higher therapy impact by direct wound application of 500 µg/ml ARE compared to the untreated control, that was not yet significant to the solvent control [128.1 ± 5.9 %, $p(w/o) < 0.01$, $p(NC) = 0.077$;

Fig. 4.17, C; n = 7]. However, the extract application on the wound margin did not show an impact on epidermal regeneration within the subgroup of bad healing specimens (99.7 ± 7.9 %; 104.5 ± 12.7 % with 50 or 500 µg/ml ARE).

4.4.7.2. Application Studies With the Ethanolic *A. Euchroma* Extract

To analyze whether the ethanolic extract shows a positive impact on wound regeneration by different application methods, direct wound application was investigated parallel to wound margin application on eleven porcine skin specimens. The ARE concentration spectrum was reduced to 2 and 20 µg/ml because a wound healing promotion effect with 200 µg/ml was not observed previously (sec. 4.4.4). Those lower concentrations were assumed to benefit the epidermal regeneration.

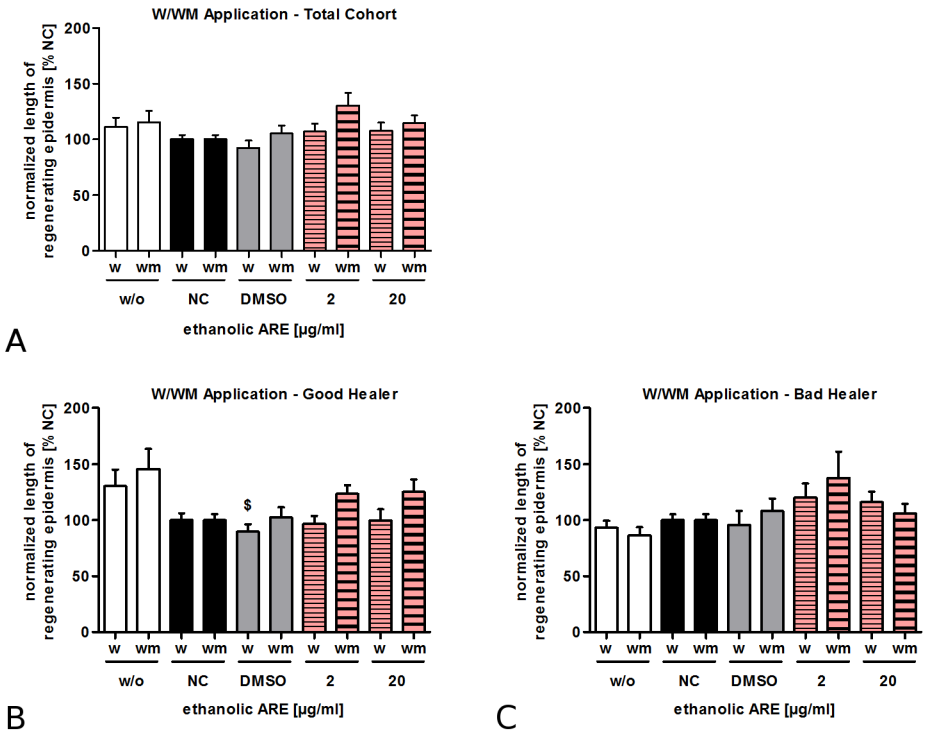

Figure 4.18.: Application studies with ethanolic ARE with direct treatment of the wound (w) or at the wound margin (wm) in porcine injured skin model. (A) Investigation of epidermal regeneration influenced by ethanolic ARE treatment, comparing direct wound application method to wound margin application in the total cohort (n = 11). The results were further divided into subgroups of intrinsic (B; n = 6) good and (C; n = 5) bad healing specimens; Results represent the mean normalized length of regenerating epidermis ± SEM of n swine donor skins in duplicates compared to the PBS (NC), DMSO and $ $p < 0.05$ compared to untreated control (w/o).

The ethanolic extract had no significant influence on epidermal regeneration in the total cohort (107.1 ± 7 %; 107.9 ± 7 % with 2; 20 µg/ml ethanolic ARE) by direct wound application. Whereas a strong positive trend on wound regeneration was

observed when the extract was applied on the wound margin compared to the control (130.2 ± 11.7 %; 114.6 ± 7 % with 2; 20 µg/ml; Fig. 4.18, A).
By result separation in subgroups, no wound healing impact was observed by direct wound application and a positive trend by wound margin treatment in good healing specimens. The mean regenerating epidermis were 96.6 ± 7.2 %; 99.8 ± 9.9 % by wound and 123.4 ± 7.7 %; 125.3 ± 11 % by wound margin application with 2 or 20 µg/ml ethanolic ARE (Fig. 4.18, B; n = 6). All treatments showed less wound regeneration than their belonging untreated control [wound: 130.2 ± 14.8 %, p(DMSO) < 0.05; wound margin: 145.7 ± 18 %, p(NC) = 0.055, p(DMSO) = 0.075].
The direct wound application, on bad healing specimens, showed a positive trend on regeneration to 120.1 ± 12.5 % and 116 ± 9.7 % treated with 2 and 20 µg/ml ethanolic ARE. Furthermore, bad healing specimens showed a strong positive wound healing trend when treated with 2 µg/ml ethanolic ARE applied on the wound edge (137.7 ± 23.4 %; Fig. 4.18, C; n = 5) in comparison to the controls. Again, DMSO control positively influenced wound regeneration itself (108.3 ± 10.7 %).
There were positive tendencies but no significant impacts on wound recovery by ethanolic ARE treatment detected, neither applied directly to the wound nor on the wound margin.

4.5. Investigations to Elucidate the Underlying Mechanism of the *Ex Vivo* Observed Wound Healing Promotion by Aqueous *A. Euchroma* Extract

Within this section, the mechanisms behind the observed improved *ex vivo* wound re-epithelialization by the aqueous ARE treatment were studied.

Molecular Analysis of the Aqueous *A. Euchroma* Extract Treated Wound Healing Models

The first porcine WHM cohort (sec. 4.2.5; Fig. 4.2) was stained with different IF protein markers, to evaluate the underlying mechanisms which were involved in the *ex vivo* detected wound healing promotion.

4.5.1. *In Situ* Proliferation Analysis

Cell proliferation is an important process in wound closure (Reinke & Sorg, 2012), this is why the therapeutic influence of the most effective concentration of 500 µg/ml aqueous ARE was investigated on proliferation *in situ*. Ki67 is used as a proliferation marker because it is expressed during G1-, S-, G2- and M-phase of the cell cycle (Scholzen & Gerdes, 2000). The influence on proliferation within the keratinocytes of the epidermis (Fig. 4.19, A) or fibroblasts of the dermis (Fig. 4.19, B) was performed by IF staining of Ki67. The Ki67 positive keratinocytes were counted within three areas of the WHMs: the regenerating epidermis, the wound margin (two per sample) and areas uninfluenced by the injury (as an internal control, three per sample; Fig. 3.4). The positive cells were normalized to all counted keratinocyte nuclei (DAPI) of the evaluated region.
The fibroblasts of the wounded area were counted in three independent representative microscopic fields of view and all Ki67 positive cells were normalized to the total cell number (DAPI).

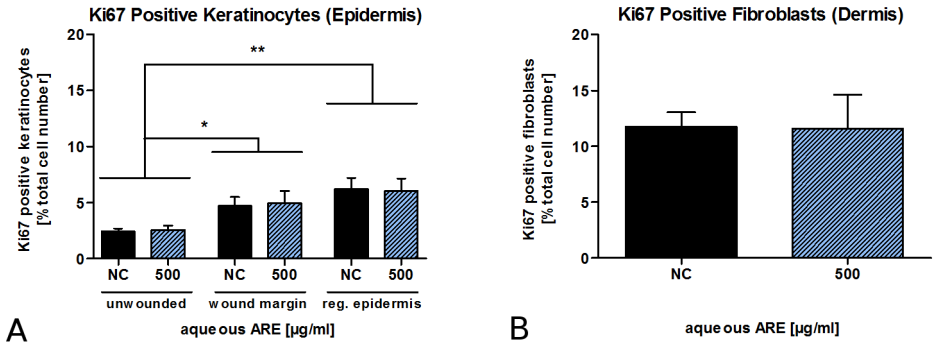

Figure 4.19.: Immunofluorescence staining of Ki67 to analyze the aqueous extracts impact on proliferation *in situ* in the *ex vivo* WHM of the first cohort (sec. 4.2.5). (A) The relative counted proliferation signal (Ki67) in keratinocytes of the epidermis was determined under different treatments. Here, different areas of the WHMs were evaluated: uninjured area (unwounded) was compared to wound margin and regenerating (reg.) epidermis (n = 10 - 12). (B) Examination of the aqueous ARE impact on dermal fibroblast proliferation, which were in direct contact with the wound area (n = 10); Results represent the mean of Ki67 positive cells (normalized to the total cell number, DAPI) ± SEM of n porcine WHMs in duplicates with * $p < 0.05$ and ** $p < 0.01$ between different evaluated tissue areas.

There was a significant increase in the number of proliferating keratinocytes when the wound margin and regenerating epidermis were compared with the unwounded area. The highest proliferation could be observed in the regenerating epidermis following the wound margin with low proliferating cell number in the unwounded area. In the PBS control group (NC) a mean of total Ki67 positive keratinocytes of 2.4 ± 0.3 %; 4.7 ± 0.4 % and 6.2 ± 1 % was found by counting the cells of the unwounded area,

wound margin and regenerating epidermis (Fig. 4.19, A). In samples incubated with 500 µg/ml ARE were 2.5 ± 0.4 %; 5.5 ± 1.1 % and 6 ± 1.1 % cells positive for Ki67 in the unwounded area, wound margin and regenerating wound tongue, respectively. The treatment with ARE compared to NC samples resulted in non-significant cell proliferation differences, with respect to one specific area of the wound model.
Fibroblasts of the wound underlying dermis did not show an influenced proliferation rate due to the different treatment conditions. The mean proliferating positive cell number was 11.8 ± 1.3 %; 11.6 ± 3.1 % with NC and 500 µg/ml aqueous ARE, respectively; Fig. 4.19, B).

4.5.2. *In Situ* Differentiation Analyses

Differentiation and dedifferentiation are important processes in wound healing (Safferling *et al.*, 2013). The question, whether the aqueous ARE has an influence on keratinocytes differentiation in the treated WHMs was addressed. Here, CK 14, as a marker for undifferentiated keratinocytes, was stained *in situ* in the WHMs from the first experiment (sec. 4.2.5). CK 14 is expressed in the basal layer of the healthy epidermis (Moll, 1982; Moll, 2008). This cell layer is still proliferating and the keratinocytes start their differentiation after leaving the basal membrane.
The analysis of CK 14 in the WHMs, with regard to its expression pattern and localization, showed clear signals in the cells of the basal layer (Fig. 4.20, upper lane). It was further detected at the wound margins. Cells of poly-layered regenerating epidermis showed CK 14 signals, which faded to the tip of the mono-layer wound tongues. There was no expression or localization difference between WHMs treated with aqueous ARE or the solvent control.
The signal of CK 10, marker for differentiated keratinocytes, was present in all suprabasal-layers of the healthy epidermis (Moll, 2008; Safferling, 2013; Fig. 4.20, lower lane). The CK 10 expression of the wound margin was analyzed compared to the regenerating epidermis and unwounded area under different treatment conditions (500 µg/ml ARE or NC). The protein was expressed in the suprabasal-layers of the wound margin and unwounded regions and was nearly absent in mono-layer areas like the tip of the wound tongue. There was no difference in intensity or localization due to the treatments.

A wound regenerating impact of aqueous ARE by inducing proliferation or affecting the differentiation of keratinocytes *in situ* was thus not observed.

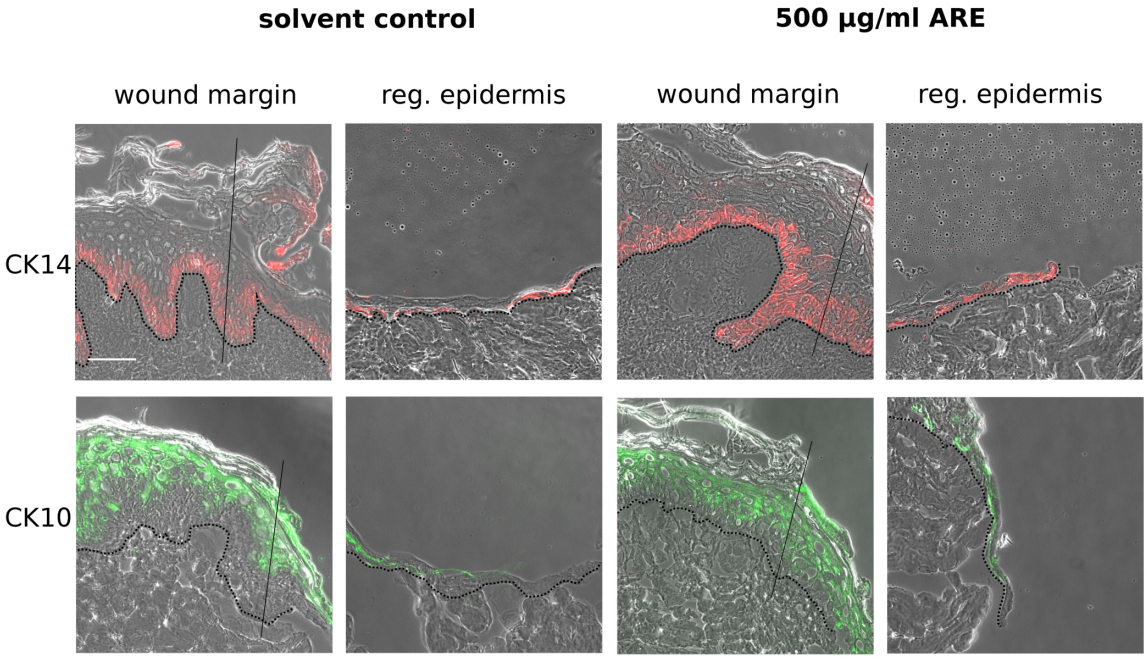

Figure 4.20.: Differentiation studies of the *ex vivo* WHMs (from the first experiment, sec. 4.2.5) by immunofluorescence staining of red CK 14 (upper panel) and green CK 10 (lower panel). The CK 14 and CK 10 staining were each overlaid with the related gray phase contrast picture. The *in situ* detection showed CK 14 protein distribution in the basal cell layer of unwounded areas and wound margin. The poly-layered regenerating (reg.) epidermis was positive whereas the protein signal in mono-layered wound tongue was weak or missing. CK 10 protein was expressed in all suprabasal layers of the unwounded areas and the wound margin. The multi-layer regenerating epidermis was positive for CK 10 with fading signal in mono-layered wound tongues. The localization and intensity were comparable between the ARE treatment and control; Representative CK protein expression of the porcine specimens treated with the 500 µh/ml aqueous ARE or PBS control. The experiment was performed in n $\geq$ 10 WHMs in duplicates; (first picture) gray scale bar represents 50 µm; WHMs are orientated from the margin, over the reg. epidermis, to the wound center (from left to right); dotted black line marks the basal membrane or the lower side of the wound tongue and the black thin line indicates the transition from the wound margin to the wound.

4.5.3. *In Vitro* Mechanism Studies in Cultivated Primary Human Keratinocytes

Keratinocytes, as dominant cell type of the epidermis, are the cells who primarily re-migrate into the wounded area. They refill the original epidermal gap and rebuild the barrier function (Brandner *et al.*, 2002 & 2006). A better epidermal regeneration was observed in the *ex vivo* model treated with aqueous ARE compared to the medium control. Hence, a direct influence on wound healing associated characteristics of keratinocytes was assumed. The extracts impact was investigated on cell viability, proliferation, migratory capacity and cell-matrix adhesion, as essential mechanisms that are involved in wound closure. Keratinocytes occur with varying differentiation

stages in the stratified epidermis as well as during wound healing. Furthermore, they can be detected as compact cell-cell arrangement (confluent) of the intact epidermis. Or they occur more isolated as detached cells (subconfluent) *e.g.* when they migrate into injured tissue. The question, of whether there are different extract influences, confluent (10,000 seeded cells) and subconfluent (5,000) cells was investigated. Additionally, the extracts impact on cells of variable differentiation level, as they occur in wounds without stratified epidermal layers, was analyzed. Here, after confluence achievement (10,000 cells), the keratinocytes were pretreated with high calcium medium to induce differentiation, for three or five days, before the treatment with the extracts was started. These conditions refer to early and later differentiation grades of the cells concerning shorter or longer cultivation with high calcium medium. Since ethanolic ARE was commonly used for experimental studies and showed wound healing promotion on later wounds together with a strong positive tendency by wound margin application, both extracts were investigated in the following experiments.

4.5.3.1. Viability Studies in Primary Keratinocytes treated with the AREs

The *ex vivo* observed wound healing can be caused by more present keratinocytes. This is why the extracts impact on cell viability was investigated by MTT method. Here, increased enhanced metabolic activity and cell proliferation or reduced apoptosis can result in increased MTT signal intensity. The investigation further enabled the determination of possible cytotoxic concentrations. The settled cells were cultivated with different extract concentrations for 48 h, analogous to the *ex vivo* WHMs. The observed viability changes were compared to NC (and DMSO) control. Here, metabolic active cells transformed MTT (yellow) to formazan (purple) by the mitochondrial reductase which can be measured photometrically by a change in optical density. The measurements were normalized to the untreated medium control.
The analyses were performed with respect to different cell differentiation grades (undifferentiated confluent and subconfluent cells compared to keratinocytes of early, three days high calcium, or later differentiation, five days).

Impact of the Aqueous *A. Euchroma* Extract on Cell Viability

There was no significant impact of aqueous ARE detectable on subconfluent (Fig. 4.21, A, left) and confluent (right) undifferentiated cells except for decreased viability with 500 µg/ml. The subconfluent cells showed viability mean ± SEM of 74.9 ± 4.6 %; 86.9 ± 1.7 %; 81.1 ± 2.6 %; 91.2 ± 1.7 %; 94.8 ± 2.1 % and 69.2 ± 8 % ($p < 0.01$) with 1; 5; 10; 25; 50 and 500 µg/ml ARE. A cellular viability of 87.1 ± 2.4 %; 89.2 ± 2.6 %;

92.6 ± 2.7 %; 94.8 ± 2.7 %; 92.3 ± 3.2 % and 79.5 ± 4.8 % ($p < 0.01$) with 1; 5; 10; 25; 50 and 500 µg/ml ARE was measured within the confluent grown group, respectively. Differentiated keratinocytes were expected, in addition to undifferentiated, in the wound area (Nickoloff *et al.*, 1988). To analyze the impact on differentiated cells, the culture medium was changed to high calcium level to induce differentiation. No effect was observed within the three days high calcium differentiated cells due to the treatment (Fig. 4.21, B, left; 99.1 ± 2.2 %; 93.1 ± 2.8 %; 93.8 ± 2.6 %; 87.2 ± 2.6 %; 88.7 ± 2.4 % and 101.9 ± 5.4 % with 1; 5; 10; 25; 50 and 500 µg/ml ARE). Within the differentiated treated keratinocytes, a positive tendency on cell viability was detected with 1 and 500 µg/ml aqueous ARE when the keratinocytes were on high calcium over five days (Fig. 4.21, B, right; 108.9 ± 6.2 %; 113.4 ± 7.3 % with 1 and 500 µg/ml ARE; other concentrations: 98.7 ± 4.8 %; 93.4 ± 4.2 %; 92.7 ± 3.9 %; 102.4 ± 5.2 % with 5; 10; 25; 50 µg/ml).

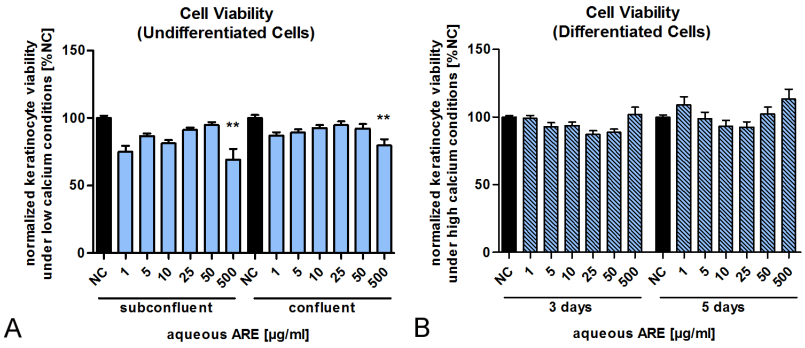

Figure 4.21.: Cell viability studies on cultured primary human keratinocytes treated with aqueous ARE. (A) Measurement of cell viability of (left) subconfluent and (right) confluent cultured, and extract treated undifferentiated keratinocytes. (B) Keratinocytes viability was further determined on early (left; three days after calcium shift) and later (right; five days) differentiated cells; Results represent the mean normalized cell viability ± SEM of keratinocytes from four donor sources in triplicates with ** $p < 0.01$ compared to medium control (NC).

Impact of the Ethanolic *A. Euchroma* Extract on Cell Viability

The investigation of the ethanolic ARE impact on keratinocytes viability was conducted with an adjusted concentration spectrum compared to the *ex vivo* investigations. Here, similar concentrations, as used with the aqueous extract, were studied to enable better comparability. The experiment was conducted analogously to the MTT above.
A negative tendency on cell viability was detected by the treatment of subconfluent grown keratinocytes with the ethanolic ARE (Fig. 4.22, A, left; 81.8 ± 3 %; 84.2 ± 3 %; 89.7 ± 2.3 %; 94.7 ± 2.4 %; 85.3 ± 5.7 % and 83.5 ± 11.9 % with 0.1; 1; 5; 10; 25 and 50 µg/ml). The ethanolic extract inhibited the viability of confluent keratinocytes

significantly to 78.5 ± 2.4 %; 80.9 ± 1.4 %; 79 ± 2.8 % [all three p(NC/DMSO < 0.01]; 87.3 ± 2.7 %; 89.1 ± 2.5 % and 89.4 ± 5.3 % with 0.1; 1; 5; 10; 25 and 50 µg/ml compared to medium and DMSO control (Fig. 4.22, A, right).

The ethanolic ARE also had a negative influence on the cellular viability of differentiated keratinocytes, which were preconditioned with high calcium for three days. The concentrations 5 - 25 µg/ml ethanolic ARE showed significant decreased viability compared to NC (86.9 ± 5.2 %; 81.9 ± 3.7 %, $p < 0.01$; 82.3 ± 2.3 %, $p < 0.01$; 82.9 ± 3 %, $p < 0.05$; 92.6 ± 2.7 % with 1; 5; 10; 25 and 50 µg/ml, respectively; Fig. 4.22, B, left]. Even the DMSO solvent control had negative impact on keratinocytes viability (92.8 ± 2.1 %). Furthermore, the ethanolic ARE partly impaired the cell viability of keratinocytes preconditioned over five days on high calcium compared to NC [97.8 ± 3.7 %; 90.5 ± 5.8 %; 83.8 ± 4 %; 72.5 ± 4.6 %; 77.5 ± 4.9 %, $p < 0.05$; 95.2 ± 6.6 % with 0.1; 1; 5; 10; 25 and 50 µg/ml, respectively; Fig. 4.22, B, right]. Here, the viability of the DMSO control was also reduced to 94.7 ± 3.9 %.

These results were not significant compared to the DMSO solvent control and may be partly caused by the impact of DMSO.

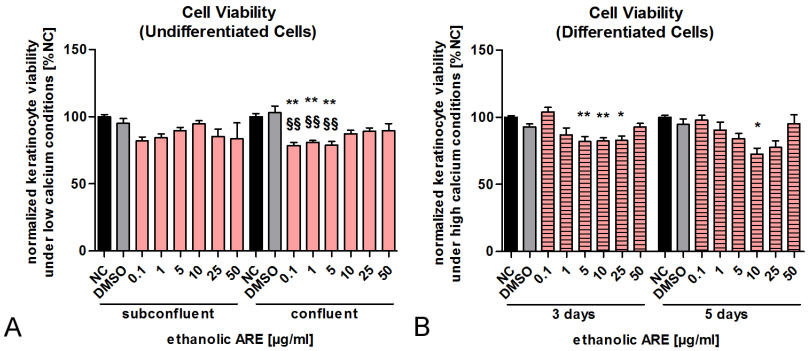

Figure 4.22.: Investigation on the ethanolic ARE impact on cell viability in cultured primary human keratinocytes. (A, left) Subconfluent grown cells were treated with the extract over two days before MTT assay was performed. The results were compared to (right) confluent extract treated grown keratinocytes. (B) Keratinocytes of (left; three days after calcium shift) early and (right; five days) later differentiation grades were treated with the ethanolic ARE and their viability was determined; Results represent the mean normalized cell proliferation ± SEM of keratinocytes from four donor sources in triplicates with * $p < 0.05$ and ** $p < 0.01$ compared to medium control (NC) and §§ $p < 0.01$ compared to DMSO (solvent) control.

4.5.3.2. Proliferation Analyses in Primary Keratinocytes treated with the *A. Euchroma* Extracts

Proliferation is important during wound healing (Falanga, 2005). Many cells and cell types are needed to close a skin injury.

There was a positive viability enhancing tendency observed by MTT assay on differentiated cells and a significant reduction on undifferentiated cells treated with 500 µg/ml

aqueous ARE. In general, MTT assay is influenced by cell proliferation, metabolic cell activity and apoptosis. No impact on cell proliferation was detectable *ex vivo*. The missing proliferation promotion *in situ* can be due to chemical diffusion as well as the extracts interactions with different cell types and molecules in the wound tissue (Singer *et al.*, 1999). However, these findings guided to the question of whether or not cell division is influenced by the direct extracts treatment in culture.
The impact of the aqueous and ethanolic AREs were investigated on the proliferation rate in cultured keratinocytes to discover the direct impact on this cell type compared to non-treated medium cells (NC). Therefore, the settled cells were treated with ARE in a broad concentration range for two days, according to the *ex vivo* WHMs treatment. Afterwards the BrdU labeling assay was performed for 2 h. Again, the experiments were performed on subconfluent and confluent undifferentiated cultured keratinocytes as well as on keratinocytes of early and later differentiation levels (sec. 4.5.3.1).

Effect of Aqueous *A. Euchroma* Extract on *in vitro* Proliferation

The cell division of subconfluent cells was negatively influenced by the extracts´ treatment [57.4 ± 12.3 %, $p < 0.05$; 57.9 ± 13.6 %; 57.7 ± 9.9 %, $p < 0.05$; 46 ± 9.8 %, $p < 0.01$; 39.7 ± 9.3 %, $p < 0.01$ and 23.8 ± 4.8 %, $p < 0.01$ with 1; 5; 10; 25; 50 and 500 µg/ml ARE, respectively; Fig. 4.23, A).

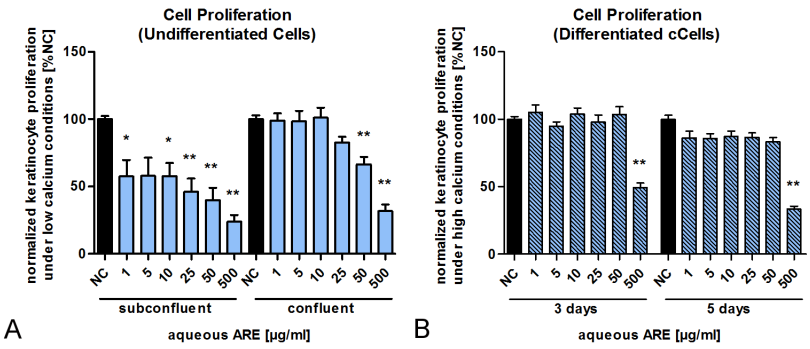

Figure 4.23.: Proliferation analysis in primary human keratinocytes treated with aqueous ARE. (A) Measurement of proliferating undifferentiated keratinocytes under (left) subconfluent and (right) confluent conditions treated with aqueous ARE. (B) Determination of aqueous ARE impact on proliferation of cultured (treatment start after three days past calcium shift) early or (five days) later differentiated cells; Results represent the mean normalized cell proliferation ± SEM of cells from four donors in triplicates with * $p < 0.05$ and ** $p < 0.01$ in comparison to medium control (NC).

The aqueous extract showed a dose-dependent proliferation decrease when confluent keratinocytes were treated with higher doses (66.5 ± 5.5 % and 31.7 ± 5 % with 50 and 500 µg/ml ARE, both $p < 0.01$; Fig. 4.23, A). There was no impact of lower concentrations (98.8 ± 5.3 %; 98.3 ± 7.9 %; 101.1 ± 7.5 %; for 1, 5, 10 µg/ml). The

ARE treatment showed no positive impact on cell division of differentiated keratinocytes, neither on cells differentiated for three days nor on cells that were five days on high calcium [except the highest dose of 500 µg/ml ARE with 49.4 ± 3.6 % (three days) and 33.4 ± 2.3 % (five days), both $p < 0.01$; Fig. 4.23, B].

Effect of Ethanolic *A. Euchroma* Extract on Proliferation

Subconfluent undifferentiated cells showed a dose-dependent decrease in cell proliferation [93.8 ± 5.3 %; 92.8 ± 7.5 %; 86.3 ± 6.3 %; 81.4 ± 10.8 %; 44 ± 8.7 % and 35.5 ± 9.7 % with 0.1; 1; 5; 10; 25 and 50 mg/ml ethanolic ARE, with significance of p(NC/DMSO) < 0.01 for 25 and 50 µg/ml; Fig. 4.24, A left]. The ethanolic ARE had a significant negative impact on the cellular proliferative activity in confluent grown keratinocytes compared to medium control (Fig. 4.24, A right). Here, the mean measured cell division rate were 76.4 ± 2.9 %; 73 ± 7.8 %, $p < 0.05$; 68.9 ± 2.9 %, $p < 0.01$; 73.3 ± 4.6 %, $p < 0.05$; 56.1 ± 4.9 %, $p < 0.01$ and 36.4 ± 7.8 %, $p < 0.01$ treated with 0.1; 1; 5; 10; 25 and 50 mg/ml ethanolic ARE, respectively. In contrast, the DMSO control significantly increased the proliferation in confluent (133.9 ± 4.6 %, $p < 0.01$) and still by strong trend in subconfluent grown cells (121.3 ± 5 %) compared to the treatments.

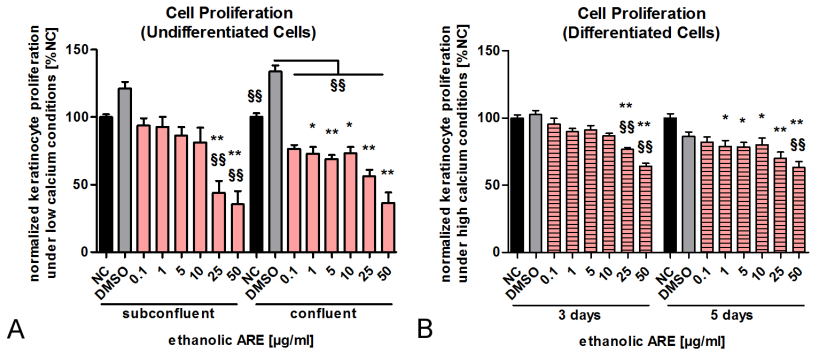

Figure 4.24.: Proliferation analysis in primary human keratinocytes treated with ethanolic ARE. (A) Analysis of the extracts impact on cellular proliferation in cultured (left) subconfluent and (right) confluent keratinocytes. (B; three days after calcium shift; left) Early and (five days; right) later differentiated cells were treated with the ethanolic ARE and investigated due to its influence on cellular proliferation levels; Results represent the mean normalized cell proliferation ± SEM of keratinocytes from four donor sources in triplicates with * $p < 0.05$ and ** $p < 0.01$ compared to medium (NC) and §§ $p < 0.01$ compared to DMSO (solvent) control.

The proliferation of differentiated keratinocytes was not positively affected by the treatment with ethanolic ARE whereas higher doses harmed the proliferation (Fig. 4.24, B). Cells that were pre-incubated with high calcium for a short period of three days showed dose-dependent decrease in cell division [95.4 ± 4.2 %; 89.6 ± 2.7 %; 91.2 ± 3.1 %;

86.5 ± 2.1 %; 76.5 ± 1.5 % and 64.2 ± 2% with 0.1; 1; 5; 10; 25 and 50 mg/ml, with p(NC/DMSO) < 0.01 for 25 and 50 µg/ml; Fig. 4.24, left]. This decrease was also detected in keratinocytes that were pre-cultured for a longer period on high calcium (five days; 82 ± 3.9 %; 78.8 ± 4.4 %, p(NC) < 0.05; 78.5 ± 3.2 %, p(NC) < 0.05; 80 ± 5 %, p(NC) < 0.05; 70 ± 4.5 %, p(NC) < 0.01 and 63.2 ± 4.3 %, p(NC/DMSO) < 0.01 with 0.1; 1; 5; 10; 25 and 50 mg/ml; Fig. 4.24, B, right). Here, DMSO had no positive influence on cell division.

4.5.3.3. *In Vitro* Wound Closure Analysis in Undifferentiated Primary Keratinocytes (Scratch Assay) treated with the *A. Euchroma* Extracts

Cell migration is one of the most important processes in wound regeneration (Singer *et al.*, 1999; Brandner *et al.*, 2006).This is why the extracts impact on wound closure in two-dimensional cell culture was investigated. Here, effects such as cell migration and proliferation were the present mechanisms to close the injury. Previous investigations on negatively influenced cell viability and proliferation suggested higher extract impact on undifferentiated keratinocytes. These cells were further expected to have higher migratory activity than differentiated cells. Therefore, the scratch assay analyses were performed on confluent grown undifferentiated keratinocytes that were injured by using a sterile pipet tip (sec. 3.14.6). The wound closure was documented every 12 h up to 48 h past injury and interpreted in relation to the untreated medium control (NC) and DMSO control. All primary wound sizes at 0 h were set to 100 %. The normalized evaluation was performed with respect to the decreasing wound size over the experimental duration in relation to the initial wound area. Additionally, the remaining wound area differences during the 12 h intervals were evaluated. Here, the actually closed wound area during the cultivation interval was expressed, measured in pixel. The more effectively the treatment influenced wound closure, the faster a reduced wound area was observed whereas the values for the 12 h intervals increased.

Effect of the Aqueous *A. Euchroma* Extract on *in Vitro* Wound Closure

Based on the observed reduced cellular viability by the treatment with 500 µg/ml aqueous ARE the investigated concentrations were decreased to non-toxic *in vitro* concentrations of 50 µg/ml with further tenfold serial dilution.
The wound closure in cultured primary keratinocytes was not positively affected by the treatment with the aqueous ARE (Fig. 4.25, A). The highest tested concentration of 50 µg/ml significantly inhibited the wound recovery of the cells [94 ± 1.7 %;

84.8 ± 1.8 %; 77.2 ± 2.3 % and 69.1 ± 2.2 % at the time points 12; 24; 36 and 48 h past injury; all $p < 0.01$ compared to NC]. 5 µg/ml ARE was observed to reduce wound closure after 36 h past injury, which was shown by a bigger remaining wound area (20.6 ± 3.3 %) compared to control (4.4 ± 1.4 %, $p < 0.01$).
The same significant result for cells treated with 50 µg/ml ARE was found, when the wound closure was evaluated with respect to the 12 h closing intervals (Fig. 4.25, B). This concentration showed minimal wound recovery during all intervals. Additionally, 5 µg/ml significantly reduced wound closure compared to the control within the second healing period (Fig. 4.25, B; 12 - 24 h). Treatment with 5 µg/ml ARE showed further positive wound regeneration within the last interval (36 - 48 h; $p < 0.05$). However, this observed significant positive effect was of no biological relevance. The control was nearly closed 36 h after injury (4.4 ± 1.4 %; Fig. 4.25, A) and the 5 µg/ml treated cells still had wound space left (20.6 ± 3.3 %) which could be closed. So, the difference in wound area that can possibly be closed, was already small in the control.
The treatment with the aqueous ARE had in high dose a negative impact on wound recovery in human keratinocytes *in vitro*.

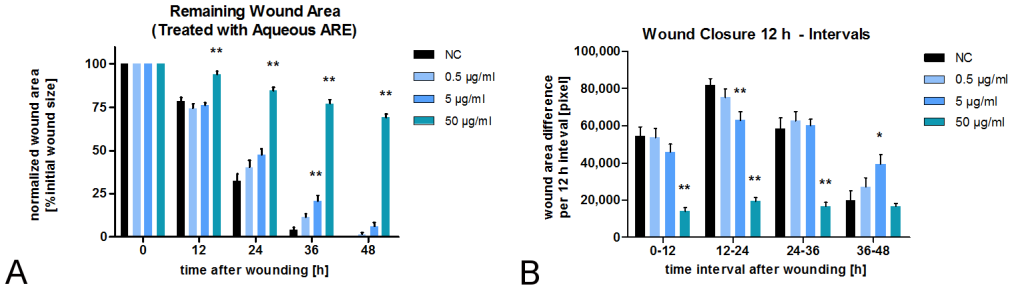

Figure 4.25.: Wound closure studies in primary human keratinocytes treated with the aqueous ARE. Scratch assay was performed on confluent grown keratinocytes. They were wounded, treated with the different extracts conditions and monitored every 12 h up to 48 h past injury. (A) Documentation of the decreasing wound area due to wound closure during the experiment. (B) Evaluation of the closed wound area of each 12 h interval influenced by different treatments; Results represent the mean (A) normalized remaining wound area [initial wound size] or (B) actual closed area per 12 h interval [pixel] with SEM. The injured keratinocytes derived from four donor sources and the experiments were conducted in duplicates with each three measurements with * $p < 0.05$ and ** $p < 0.01$ compared to medium control (NC).

Effect of the Ethanolic *A. Euchroma* Extract on *in Vitro* Wound Closure

Wound migration was not improved by the treatment with the ethanolic ARE *in vitro*. All treatments showed comparable wound area reduction as controls, except the highest concentration of 5 µg/ml ethanolic ARE, which significantly inhibits the wound closure compared to NC (24 - 48 h) and DMSO solvent control (36 - 48 h; Fig. 4.26, A).
With respect to the 12 h time intervals (Fig. 4.26, B) the negative delay on wound

closure by 5 µg/ml ethanolic ARE treatment was only detectable in the 12 - 24 h interval. All other intervals showed comparable wound closure to the controls. This indicated that the reduced wound recovery during the second interval (Fig. 4.26, B) resulted in a delayed wound closure by the 5 µg/ml treatment (A).

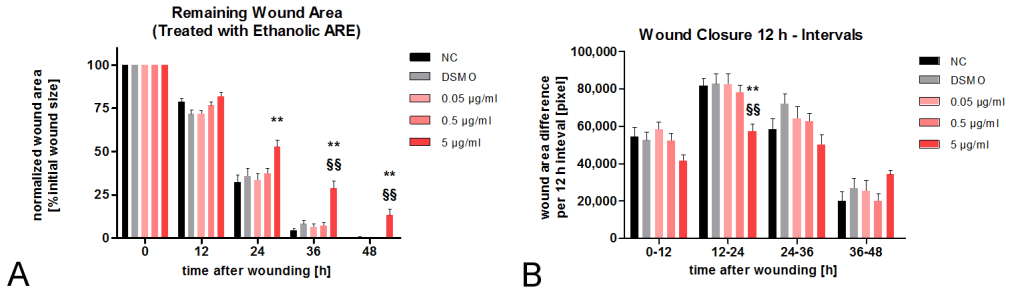

Figure 4.26.: *In vitro* wound healing studies in primary human keratinocytes treated with the ethanolic ARE. Confluent keratinocytes were wounded, treated with the different concentrations of the ethanolic ARE and monitored from injury every 12 h up to 48 h by scratch assay method. (A) Documentation of the decreasing wound area due to wound closure during the experiment. (B) Evaluation of the closed wound area of each 12 h interval influenced by different treatments; Results represent the mean (A) normalized remaining wound area [initial wound size] or (B) actual closed area per 12 h interval [pixel] with SEM. The injured keratinocytes derived from four donor sources and the experiments were conducted in duplicates with each three measurements with ** $p < 0.01$ compared to medium (NC) and §§ $p < 0.01$ compared DMSO control (solvent).

4.5.3.4. Influence of the Different Extract Treatments on Cell Adhesion of Primary Keratinocytes treated with the *A. Euchroma* Extracts

The process of cell migration was influenced by different processes as cell attachment, detachment, the number of present cells (proliferation) and the migration itself. Here, the question was addressed of whether the extracts influence the adhesion of cells that started to migrate into the wound area. Therefore, the cells were seeded in 96 well plates that already contained different treatment concentrations. At distinct time points after seeding the unattached cells contained in the supernatant were removed, medium renewed and the adhered cells measured by MTT method. The resulting data were evaluated normalized to the medium control that was set to 100 % for each time point.

Impact of the Aqueous *A. Euchroma* Extract on Cell-Matrix Adhesion

The aqueous AREs impact on the adherence of keratinocytes at certain time points after seeding was studied. Within the first 15 min all aqueous extract concentrations, except 0.5 µg/ml (90.1 ± 7.7 %), significantly inhibited the adherence of the seeded cells

to 51.8 ± 6 %; 43.7 ± 9.2 %; 31.6 ± 3.4 %; 29.7 ± 3 %; 26.4 ± 2.4 %; 30.1 ± 5.5 %; 30 ± 3.8 % and 43 ± 3.5 % with 1; 5; 10; 25; 50; 100; 200 and 500 µg/ml ARE, respectively ($p < 0.01$; Fig. 4.27, A). 30 min after seeding the concentration of 0.5 µg/ml ARE significantly enhanced the number of adhered keratinocytes to 130.2 ± 7.1 % ($p < 0.01$). Further, the higher concentrations of 50 and 500 µg/ml aqueous ARE significantly reduced the number of adhered cells 30 min after seeding ($p < 0.01$). The decrease of adhered cells was detectable up to 120 min after seeding into 500 µg/ml ARE containing wells ($p < 0.01$).

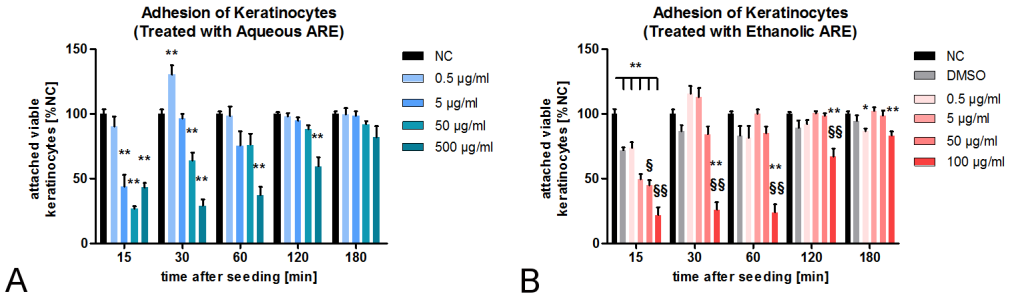

Figure 4.27.: Cell-matrix adhesion assay with primary human keratinocytes treated with the aqueous or ethanolic ARE. The cells were seeded in a 96 well plate. At certain time points, the settled viable ones were stained using the MTT method, after removing the supernatant. The measured values were normalized to the mean of the medium control (NC) at each time point; Results represent the mean normalized settled viable cell number ± SEM of cells from three donor sources in triplicates with * < 0.05 and ** $p < 0.01$ in comparison to medium (NC) and § $p < 0.05$ and §§ $p < 0.01$ compared to DMSO control.

Impact of the Ethanolic *A. Euchroma* Extract on Cell-Matrix Adhesion

Cell adhesion during the first 15 min after seeding was significantly reduced with all tested concentrations of the ethanolic ARE compared to NC ($p < 0.01$). The mean cell numbers were 73.6 ± 4.3 %; 60.3 ± 3.6 %; 59.4 ± 7.3 %; 49.4 ± 4.3 %; 56 ± 8.8 %; 48.2 ± 5.9 %; 44.6 ± 4.1 % [p(DMSO) < 0.05] and 21.7 ± 6.2 % [p(DMSO) < 0.01] with 0.5; 1; 2.5; 5; 10; 25; 50 and 100 µg/ml extract (Fig. 4.27, B). DMSO itself significantly decreased the amount of viable adhered cells compared to medium control to 71.6 ± 2.6 % ($p < 0.01$). The highest concentration of 100 µg/ml ethanolic ARE significantly diminished the cell adherence up to 120 min after seeding compared to DMSO and up to 180 min compared to medium control (all $p < 0.01$). 180 min after seeding, 0.5 g/ml ethanolic ARE treatment resulted in additional significant decreased cell number compared to NC ($p < 0.05$) but not significant to DMSO.

4.5.3.5. Analysis of the *A. Euchroma* Extracts Impact on Barrier Formation

The barrier formation is an important part of the wound healing rearranging phase that enables a new protection shield to the outer risks such as pathogens, microbes and several others (Bäsler *et al.*, 2016). Since we are interested in the impact of the ARE on the early barrier formation, both extracts were analyzed in different concentrations in an assay were the TER was measured (sec. 3.14.7). The TER was determined as the expression of barrier formation in cultured keratinocytes which were set on high calcium to induce differentiation. As the TER gets higher, the barrier gets stronger and tighter (Zorn-Kruppa *et al.*, 2016; Kirschner *et al.*, 2013). The extracts´ treatment was started together with the switch to high calcium and conducted for five days past the calcium switch. Medium or DMSO controls were defined as 100 % depending on the used extract and used to normalize the resulting data.

Effect of the Aqueous *A. Euchroma* Extract on Barrier Formation

Aqueous ARE was used in non-toxic concentrations without 500 µg/ml, based on the observed reduced cellular viability. The differentiated keratinocytes were treated with 1; 5 or 50 µg/ml aqueous ARE and the measured TER was normalized to medium control (Fig. 4.28, A - C; n = 4 - 5).
All tested concentrations showed positive impact up to 122 % increase of TER formation after day one that was only significant with 5 µg/ml ARE ($p < 0.05$; Fig. 4.28, B). Additionally, 1 µg/ml (Fig. 4.28, A) and 50 µg/ml ARE (C) treatment showed positive trend up to 135 % TER around day one after the calcium switch compared to control without significance. 50 µg/ml ARE increased TER level directly after calcium switch and after five days, again without significance.

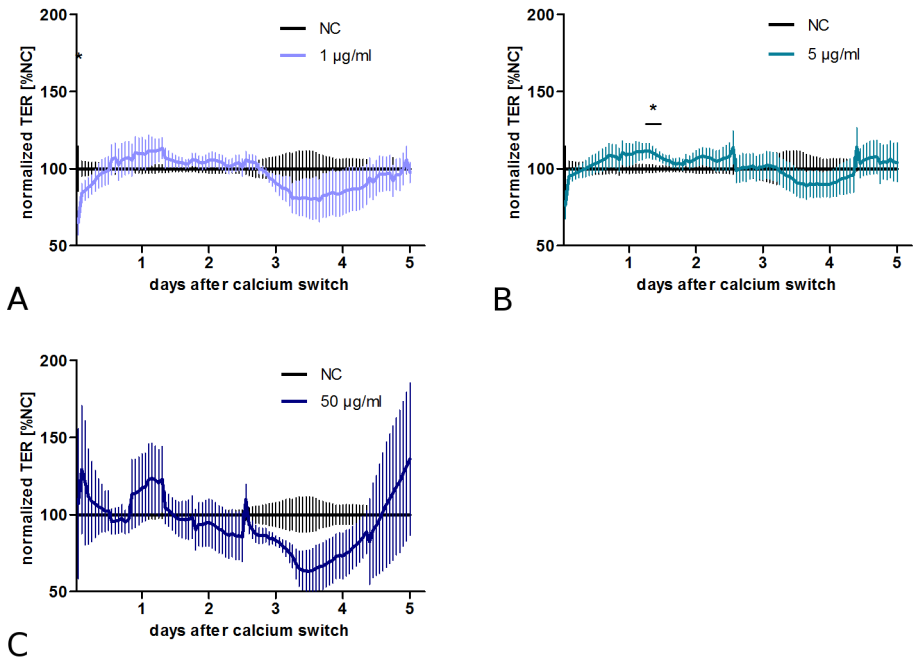

Figure 4.28.: Barrier formation investigation by measuring the TER [Ω x cm^2] influenced by aqueous ARE treatment. Cells were seeded on membrane filter inserts and cultured until poly-layered confluence was achieved. The medium was further shifted to high calcium condition in order to induce differentiation and barrier formation. Contemporaneously the extract treatment was started and the experiment conducted over five days past calcium switch. The resulting TER measurements were normalized to medium control (NC) and were shown for (A) 1 µg/ml, (B) 5 µg/ml and (C) 50 µg/ml aqueous ARE treated differentiated keratinocytes; Results represent the mean normalized TER ± SEM (dashed area) of n donor sources in duplicates with * $p < 0.05$ compared to medium control [n(NC, 1 µg/ml, 5 µg/ml) = 5, n(50 µg/ml) = 4].

Effect of the Ethanolic *A. Euchroma* Extract on Barrier Formation

The ethanolic ARE showed a significant negative impact on the TER with 0.2 µg/ml (89 ± 7.3 %; Fig. 4.29, A) and 2 µg/ml (88.7 ± 7 %; B) within the first day after the calcium shift compared to solvent (DMSO) and medium control. A strong positive trend with a peak around day three was further observed with both of these concentrations (TER increased to 228 ± 89 %, 213.1 ± 77.6 % with 0.2 and 2 µg/ml ethanolic ARE). 20 µg/ml ethanolic ARE treatment induced a significant increase in TER formation directly after the calcium switch (140.1 ± 8 %; Fig. 4.29, C). All later time points showed reduced TER signal compared to DMSO and medium control, with significance from day two to four.

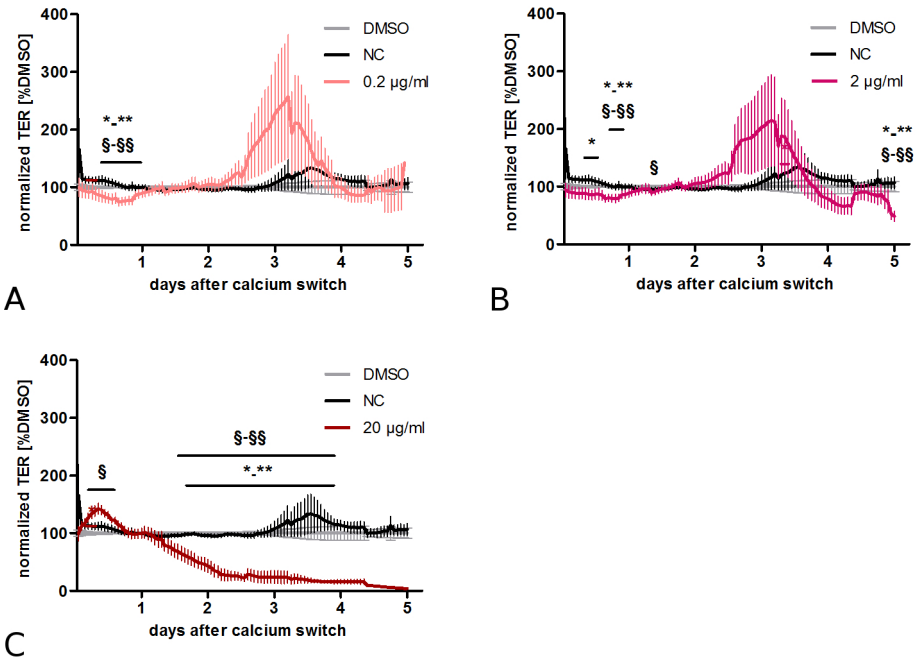

Figure 4.29.: Barrier formation analysis by measuring the TER [Ω x cm^2] influenced by ethanolic ARE treatment. Keratinocytes were seeded on filter inserts and cultured until confluence was achieved. Calcium content in the medium was shifted to induce differentiation and barrier formation. Contemporaneously the extract treatment was started and the experiment conducted over five days past calcium switch. The resulting TER measurements were normalized to DMSO solvent control and further compared to medium control (NC). TER measurements were shown for (A) 0.2 µg/ml, (B) 2 µg/ml and (C) 20 µg/ml ethanolic ARE treated differentiated keratinocytes; Results represent the mean normalized TER ± SEM (dashed area) of n keratinocyte donor sources in duplicates with * $p < 0.05$ and ** $p < 0.01$ in comparison to medium (NC), and § $p < 0.05$ and §§ $p < 0.01$ compared to DMSO solvent control [n(NC, DMSO) = 5, n(0.2 µg/ml, 2 µg/ml) = 4, n(20 µg/ml) = 3].

4.5.4. *In Vitro* Mechanism Studies in Cultivated Primary Human Fibroblasts

Fibroblasts, as dominant cell type of the dermis, are essentially involved in the wound closure process. They are for example responsible for the appropriation of a provisory ECM and the later building of a reorganized matrix. Fibroblasts express cytokines and chemokines, which attract other cell types to migrate into the wounded area and start to clean and rearrange the injured environment (Darby *et al.*, 2014).

Because of the missing positive impact on cultured primary keratinocytes, fibroblasts were supposed to be beneficially affected by the extract treatment. Here, the direct impact of both AREs should be analyzed on fibroblasts as well as fibroblast-mediated mechanisms, which are involved in the recovery of an injury. The investigations were performed under normal *in vitro* used culture conditions (10 % FBS containing RPMI medium) in comparison to serum free cultivation conditions. Here, potential

interactions between the extracts ingredients and the FBS can be excluded. All cells were basically cultured and plated under serum containing conditions. In the case of FBS-free analyses, the medium was changed 2 h before treatment was started.
Investigations of the AREs influence on cell viability, proliferation, energy balance, migration and protein level of ECM compounds, as essential wound healing mechanisms, were performed.

4.5.4.1. *A. Euchroma* Extract Impact on Cell Viability in Cultured Fibroblasts

MTT assay was used to analyze the AREs impact on cell viability of cultured human primary fibroblasts. The cells were either cultivated for 24 or 48 h with different concentrations of the extracts in serum-containing culture medium or under serum-free conditions. Following the mitochondrial activity was measured by MTT assay (sec. 3.14.4.2).

Influence of the Aqueous *A. Euchroma* Extract on Fibroblast Viability

The aqueous extract did not increase the viability of fibroblasts, whether within the first 24 h nor later (48 h) in FBS-containing culture conditions (Fig. 4.30, A). High concentrations inhibited the cell viability significantly (24 h: 0.7 ± 0.5 % with 500 µg/ml; 48 h: 57.3 ± 9.4 % and 5.1 ± 1.8 % with 50 and 500 µg/ml, all $p < 0.01$).

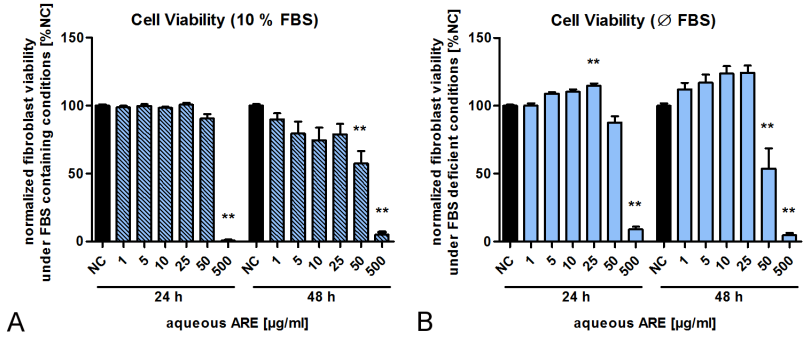

Figure 4.30.: Influence of aqueous ARE on human primary fibroblasts cell viability. (A) Viability was determined in fibroblasts cultured in the presence of 10 % FBS-RPMI (n = 4). Extract treatment was performed over (left) 24 h or (right) 48 h before MTT assay was performed. (B) MTT influenced by aqueous ARE treatment over 24 h or 48 h in the absence of serum in the culture medium (n = 3); Results represent the mean normalized cell viability ± SEM of cells from n donors in triplicates with ** $p < 0.01$ in comparison to medium control (NC).

Under serum free conditions a dose-dependent cell viability increase was detected by the treatment within the first 24 h [100.3 ± 1.5 %; 108.9 ± 1.2 %; 110.4 ± 1.9 %; 115 ± 1.7 % ($p < 0.01$); 87.9 ± 4.5 % with 1; 5; 10; 25; 50 µg/ml, respectively;

Fig. 4.30, B, left]. Whereas, 500 µg/ml significantly decreased the viability to 9 ± 2.1 % ($p < 0.01$). The viability promoting trend of the minor ARE concentrations was still detectable after 48 h treatment (112.3 ± 4.7 %; 117.2 ± 5.9 %; 123.8 ± 5.7 % and 124.4 ± 5.4 % with 1; 5; 10 and 25 µg/ml; Fig. 4.30, B, right). Again, the highest concentrations significantly harmed the cell viability (54 ± 14.8 %; 4.9 ± 1.6 % with 50 and 500 µg/ml, both $p < 0.01$).

Influence of the Ethanolic *A. Euchroma* Extract on Fibroblast Viability

The investigated ethanolic ARE concentrations were adjusted to the ones of the aqueous ARE, to obtain optimal comparability. The fibroblasts viability significantly decreased when treated with the ethanolic extract compared to the medium and DMSO control under serum containing conditions [Fig. 4.31, A; 24 h: 100.3 ± 1.4 %; 103.8 ± 1.2 %; 40.4 ± 4.4 %; 22 ± 1.6 %; 0 ± 0 % and 0.7 ± 0.4 % with 0.1; 1; 5; 10; 25 and 50 µg/ml; 5 - 50 µg/ml with p(NC) < 0.01 and 1 - 50 µg/ml p(DMSO) < 0.01]. This effect was even stronger after 48 h extract treatment [75.1 ± 11.7 %; 89.3 ± 8.4 %; 10.7 ± 5.8 %; 0.1 ± 0 %; 0 ± 0 % and 3.3 ± 1.7 % with 0.1; 1; 5; 10; 25 and 50 µg/ml, 5 - 50 µg/ml with p(NC, DMSO) < 0.01].

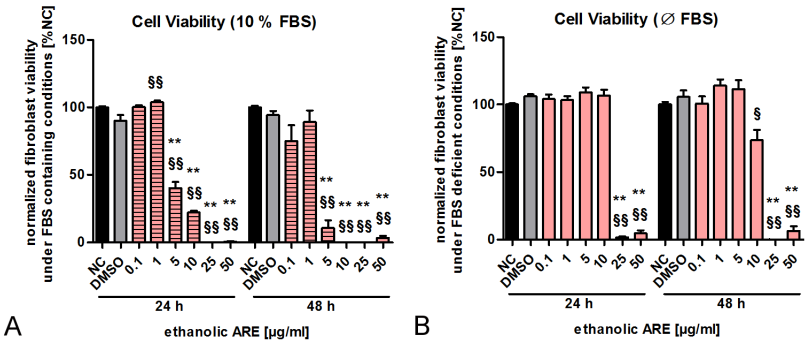

Figure 4.31.: Viability assay on human primary fibroblasts treated with the ethanolic ARE. (A) Determination of fibroblasts cellular viability cultured in the presence of 10 % FBS-RPMI (n = 4). Extract treatment was performed over (left) 24 h or (right) 48 h before MTT assay was conducted. (B) Viability influenced by ethanolic ARE treatment over 24 h or 48 h in the absence of serum in the culture medium (n = 3); Results represent the mean normalized cell viability ± SEM of fibroblasts from n donors in triplicates with ** $p < 0.01$ in comparison to medium (NC) or § $p < 0.05$ and §§ $p < 0.01$ in comparison to DMSO control.

Serum free cultured fibroblast had no negatively influenced viability within low concentrations (24 h: 0.1 - 10 µg/ml; 48 h: 0.1 - 5 µg/ml; Fig. 4.31, B). 1 and 5 µg/ml even showed an increased tendency after 48 h treatment. High concentrations of 25 and 50 µg/ml significantly decreased the cell viability compared to both controls [24 h: 1.7 ± 0.8 % and 4.8 ± 2.1 %; 48 h: 0.2 ± 0.1 % and 6.4 ± 3.4 %, all $p < 0.01$]. Additionally, 10 µg/ml ethanolic ARE significantly decreased cell viability after 48 h

compared to DMSO (73.9 ± 7.3 %, $p < 0.05$).
There was a partly significant negative influence on cell viability under culture with the ethanolic ARE detectable.

4.5.4.2. Influence of the *A. Euchroma* Extracts on Fibroblast Cell Proliferation

Because of the observed positive tendency by aqueous ARE treatment (MTT) under serum-free conditions an extract impact on cell proliferation in primary fibroblasts was supposed. To investigate the cell proliferation influence of both AREs in cultured cells, in the presence or absence of serum, a BrdU assay was performed as described for keratinocytes (sec. 4.5.3.1) after 24 or 48 h extract treatment and a 4 h BrdU incorporation period.

Effect of the Aqueous *A. Euchroma* Extract on Fibroblasts Cell Division

The proliferating analyses were conducted with 1 - 50 µg/ml aqueous ARE. 500 µg/ml aqueous ARE was not investigated, which is caused by the observed fibroblasts viability reducing impact of this concentration (sec. 4.5.4.1). The aqueous ARE did not show a positive proliferation impact on fibroblasts in serum containing culture conditions whereas high concentrations diminished the cell division after 48 h significantly [79 ± 4.8 %, $p < 0.05$; 54.7 ± 10.8 %, $p < 0.01$ with 25 and 50 µg/ml; Fig. 4.32, A).

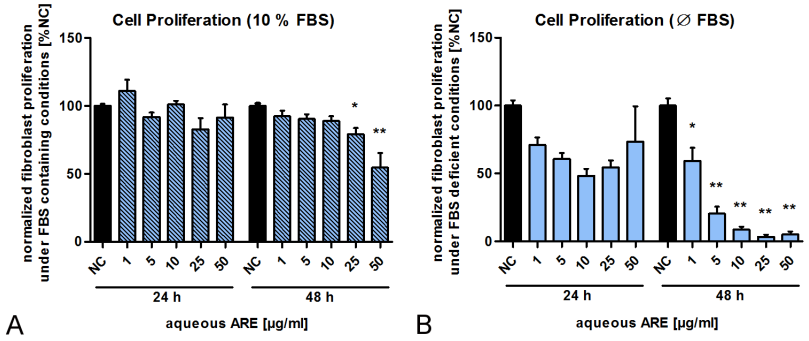

Figure 4.32.: Proliferation studies of aqueous ARE treated primary human fibroblasts using BrdU labeling method. The cells were treated over 24 or 48 h with the extract, under serum containing (A; FBS; n = 4) and serum free (B; n = 3) culture conditions and the BrdU labeling was performed afterwards; Results represent the mean normalized cell proliferation ± SEM of n fibroblast donors in triplicates with * $p < 0.05$ and ** $p < 0.01$ compared to medium control (NC).

Fibroblast treated with the extract in the absence of serum showed a decrease in cell proliferation, which was significant and dose-dependent after 48 h extract treatment (59.3 ± 9.7 %, $p < 0.05$; 20.4 ± 5.1 %; 8.7 ± 2.2 %; 3.4 ± 1.6 %; 5.3 ± 2.1 % with 1;

5; 10; 25 and 50 µg/ml; all, except 1 µg/ml, $p < 0.01$; Fig. 4.32, B).
Cultivation under extract treatment in the absence of serum diminished cell division, whereas the cells were still viable (Fig. 4.30).

Effect of the Ethanolic *A. Euchroma* Extract on Fibroblasts Cell Division

Compared to the controls, a negative effect of the ethanolic ARE on fibroblast proliferation was observed (Fig. 4.33, A & B).

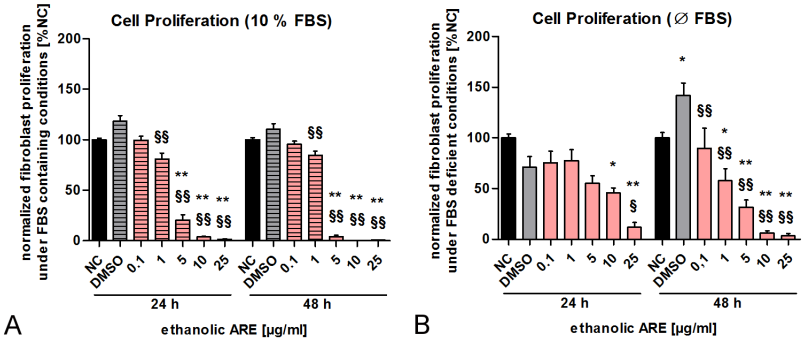

Figure 4.33.: BrdU proliferation assay in primary human fibroblasts treated with the ethanolic ARE. Fibroblasts were treated for (left) 24 or (right) 48 h with the ethanolic extract, under (A; 10 % FBS; n = 4) serum containing and (B; n = 3) serum-free conditions, before the BrdU labeling was performed; Results represent the mean normalized cell proliferation ± SEM of fibroblasts from n fibroblast donors in triplicates with * $p < 0.05$ and * $p < 0.01$ compared to medium control (NC), and § $p < 0.05$ and §§ $p < 0.01$ compared to DMSO (solvent) control.

The ethanolic ARE showed a dose-dependent significant decrease in cell proliferation, of fibroblast cultured in the presence of FBS, within the first 24 h [81 ± 5.8 %; 20.5 ± 5.3 %; 3.6 ± 0.7 % and 1.5 ± .4 % with 1; 5; 10; 25 and 50 µg/ml; Fig. 4.33, A]. This impact was still present after 48 h ethanolic ARE treatment in serum containing culture medium [84.7 ± 3.8 %; 3.9 ± 1.6 %; 0 ± 0 %; 0.6 ± 0.3 % with 1; 5; 10 and 25 µg/ml]. Significant proliferation reduction was observed with 1 - 25 µg/ml ethanolic ARE compared to DMSO, $p < 0.01$, and with 5 - 25 µg/ml compared to NC, $p < 0.01$, at both tested time points. A proliferation induction trend was detected by the DMSO control under serum containing condition (24 h: 118.4 ± 5.7 %; 48 h: 105.8 ± 5.1 %). The treatment under serum free culture conditions inhibited the cell proliferation as well [24 h: 75.5 ± 11.2 %; 77.6 ± 10.8 %; 55.1 ± 7.7 %; 45.8 ± 4.9 %, $p(NC) < 0.05$ and 11.8 ± 4.6 %, $p(NC) < 0.01$, $p(DMSO) < 0.05$; Fig. 4.33, B]. A dose-dependent proliferation decrease was determined after 48 h, too [89.5 ± 19.9 %; 57.8 ± 11.7 %, $p(NC) < 0.05$; 31.6 ± 7 %; 6.1 ± 2.3 % and 3.5 ± 2.3 % with 0.1; 1; 5; 10 and 25 µg/ml, with significance ($p < 0.01$) for 5 - 25 µg/ml compared to NC and 0.1 - 25 µg/ml to

DMSO]. The DMSO control showed a significant proliferation promoting effect after 48 h treatment in relation to NC (141.5 ± 12.5 %, $p < 0.05$).

4.5.4.3. Analysis of *A. Euchroma* Extracts Impact on Adenosine Triphosphate Level in Fibroblasts

Since a positive trend on cell viability but no positive impact on cell proliferation under aqueous ARE treatment and serum-free conditions was detected, the fibroblasts were expected to be more metabolically active. Therefore, a sensitive method was used to analyze the cellular ATP content by luminescent measurement. This method was able to detect small changes in the cellular energy level and is more sensitive than the MTT method (Friedemann *et al.*, 2016). The intracellular free ATP amount was detected after preconditioning with the extracts over 24 or 48 h compared to a standard curve of ATP and normalized the results to medium controls (sec. 3.14.4.3).

Energy Level under Aqueous *A. Euchroma* Extracts Impact

In fact, there was a significant increase of nearly 200 % free ATP detectable when the fibroblasts were treated with the aqueous ARE (24 h: 172.6 ± 11.4 %; 198.1 ± 9.7 %; 197.2 ± 12.7 % with 5; 10 and 50 µg/ml ARE, all $p < 0.01$; Fig. 4.34, A). The positive impact was still significantly present after 48 h of pre-treatment with the extract (172.7 ± 10.2 %; 182.7 ± 9.6 %, both $p < 0.01$ and 116.1 ± 8.8 % with 5; 10 and 50 µg/ml aqueous ARE).

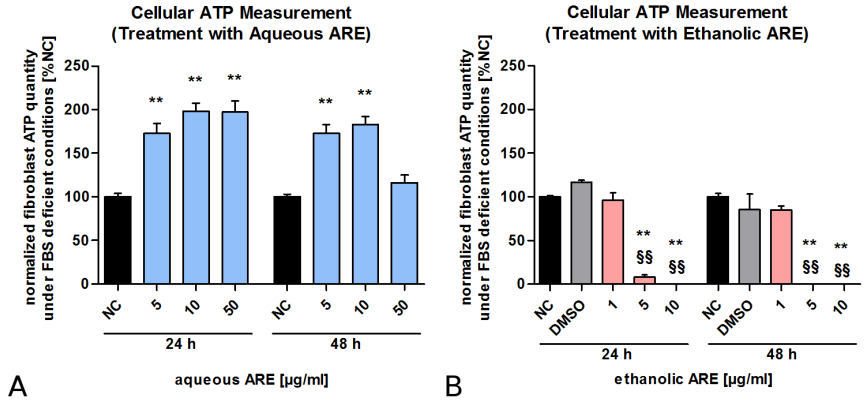

Figure 4.34.: Measurement of free ATP as an indicator of the cellular energy level of primary human fibroblasts that were cultivated in the presence of (A) aqueous or (B) ethanolic ARE. Cells were cultured in the absence of FBS and treated for (left) 24 h or (right) 48 h with the AREs; Results represent the mean measured ATP quantity ± SEM of cells from three donor sources in triplicates with ** $p < 0.01$ compared to medium (NC) and §§ $p < 0.01$ in comparison to the DMSO control.

Energy Level under Ethanolic *A. Euchroma* Extracts Impact

The ethanolic extract showed no positive impact on ATP level. A significant dose-dependent decrease of free ATP was detected due to the treatment with 5 and 10 µg/ml ethanolic ARE, time point independently [Fig. 4.34, B; 24 h: 96.4 ± 8.2 %; 8.3 ± 2.4 %; 0 ± 0 %; 48 h: 84.6 ± 5.1 %; 0 ± 0 % and 0 ± 0 % with 1; 5 and 10 µg/ml ethanolic ARE, with p(NC/DMSO) $<$ 0.01 for 5 and 10 µg/ml]. There was a positive ATP increasing trend in the DMSO control group to 117.1 ± 2.1 % measurable within the first 24 h.

4.5.4.4. *In Vitro* Wound Healing Analysis With Primary Fibroblasts (Scratch Assay)

Mobility and migration of fibroblasts are important for wound healing to establish granulation tissue formation and enable regeneration (Singer *et al.*, 1999). Here, effects such as cell migration and proliferation are the present mechanisms to close the injury. Fibroblasts proliferation was not positively affected, whereas cell viability was improved by trend and the ATP amount was significantly increased (Ø FBS). The hypothesis was addressed if the increased energy level was used to improve fibroblasts migratory abilities under the AREs treatments.
The experiment was conducted on serum-free cultured fibroblasts. Using this condition, the positive influence of the aqueous ARE on fibroblast viability and energy level was observed. We suppose that the serum interferes with the extracts ingredients and therefore influence the AREs impact in cell culture. Confluent grown human primary fibroblast, cultivated in serum containing medium, were switched to FBS-free conditions 2 h before the experiment was started. The cell mono-layer was scratched and the aqueous or ethanolic extracts were applied. The wound closure was documented every 12 h for 48 h, measured as increasing wound area and evaluated in relation to medium control and for the ethanolic extract additionally to DMSO control. Again, the open wound area at each time point was evaluated and the closed wound area of each 12 h interval (sec. 3.14.6.3).

Effect of the Aqueous *A. Euchroma* Extract on *In Vitro* Wound Recovery

The tested concentrations of the aqueous extract significantly inhibited the wound closure in a dose-dependent manner with 10 - 50 mg/ml ARE within all time points ($p < 0.01$; Fig. 4.35, A). 1 µg/ml aqueous ARE showed wound regeneration comparable to control.

The evaluation of the 12 h intervals showed significantly reduced wound regeneration in extract treated cells especially with 25 and 50 µg/ml compared to the medium control (Fig. 4.35, B).
The aqueous ARE significantly reduced the *in vitro* wound closure of primary fibroblasts.

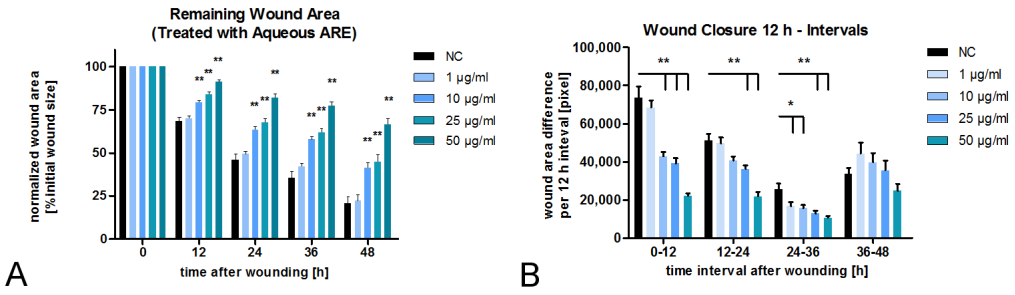

Figure 4.35.: Wound healing assay with cultured primary human fibroblasts treated with the aqueous ARE. Confluent cells were scratched two hours after the medium switch, to medium without FBS, and the wound closure was documented every 12 h for 48 h during incubation with different aqueous ARE concentrations. (A) Remaining normalized open wound area measured every 12 h past injury under different treatments. (B) Evaluation of the closed wound area per time interval of 12 h; Results represent the mean normalized (A) remaining wound area [% initial wound size] or (B) closed area per 12 h interval [pixel] ± SEM of cells from five donors in duplicates, each three independent measurements with * $p < 0.05$ and ** $p < 0.01$ compared to medium control (NC).

Effect of the Ethanolic *A. Euchroma* Extract on *In Vitro* Wound Recovery

None of the tested ethanolic concentrations showed an impact on the wound closure in cultured primary fibroblasts (Fig. 4.36).

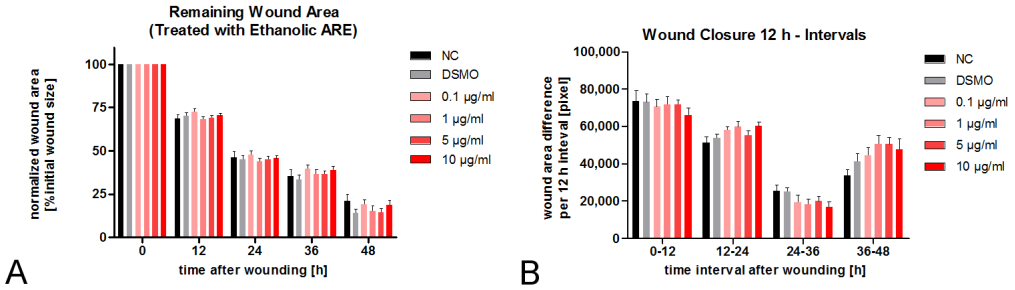

Figure 4.36.: Wound healing investigations with cultured primary fibroblasts treated with the ethanolic ARE. Two hours after medium switch, to medium without FBS, the confluent fibroblasts were scratched and the wound closure was documented every 12 h for 48 h. Cells were treated with different ethanolic ARE concentrations during wound recovery. (A) Remaining normalized open wound area measured every 12 h past injury. (B) Evaluation of the closed wound area per time interval of 12 h; Results represent the mean normalized (A) remaining wound area [% initial wound size] or (B) closed area per 12 h interval [pixel] ± SEM of cells from five donors in duplicates, each three independent measurements compared to medium (NC) and DMSO control.

The wound recovery showed no significant difference compared to the medium and DMSO control, neither with respect to the closing wound area (Fig. 4.36, A) nor to wound regeneration progress in 12 h interval (B).

Migratory Effect of the Ethanolic *A. Euchroma* Extract on Proliferation Inhibited Fibroblasts

There was no impact of the ethanolic ARE observed on cell migration, combined with negative impact on viability (sec. 4.5.4.1) and proliferation (sec. 4.5.4.2) in earlier experiments. Therefore, the question was addressed, of whether wound closure can be improved by the extract under proliferation inhibited conditions. Here, wound recovery was enabled by migrating cells whereas the proliferation influence was eliminated. X-ray radiation was used to keep the fibroblasts in the cell cycle arrest phase and prevent cell division. Fibroblast treated with the ethanolic ARE were supposed to migrate faster, compared to medium conditions, because of the lack of positive proliferation influence in medium control.
In fact, a generally positive impact due to the treatment with the ethanolic ARE on wound closure was not discovered (Fig. 4.37, A & B) in proliferation inhibited fibroblast compared to both controls. Fibroblast recovered the wound area in comparable manner as the controls did.

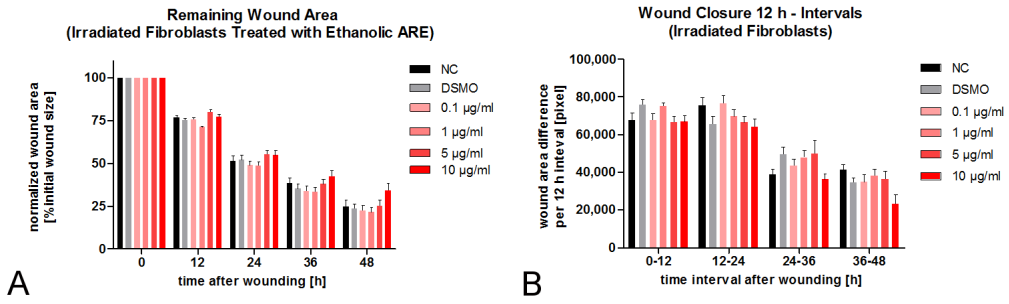

Figure 4.37.: Wound healing analysis in proliferation inhibited primary human fibroblasts. Confluent grown fibroblasts were proliferation inhibited by x-ray radiation and further investigated by scratch assay method. (A) Decreasing normalized wound size over the experimental duration under treatment with ethanolic ARE. (B) Evaluation of the closed wound area during 12 h intervals under ethanolic ARE treatment; Results represent the mean normalized (A) remaining wound area [% initial wound size] or (B) closed area per 12 h interval [pixel] ± SEM of fibroblasts from three donor sources in duplicates, with each three independent measurements in comparison to medium (NC) and DMSO control.

4.5.4.5. Western Blot Analysis of Apoptosis Induction by Aqueous *A. Euchroma* Extract Treatment

Within the prevoiusly described experiments, some direct influence of the aqueous ARE on cultured fibroblast were discovered. To address the question of whether the aqueous ARE having an impact on apoptosis, cultured cells were stimulated with different extract concentrations (5; 25 and 50 µg/ml; in the absence of FBS). After 48 h, the cellular expressed proteins were isolated and WB analyses were performed with 10 µg total protein (sec. 3.15.4). Apoptosis induction was determined by the detection of caspase 3 and cleaved caspase 3 protein level. In case of apoptosis induction, caspase 3 is decreasing whereas cleaved caspase 3 level is rising. Here, the results were compared to the medium control (NC) and to a positive control were apoptosis was induced in cultured untreated fibroblasts by staurosporine (+Stau; Fig. 4.38, A) as well as a positive control of apoptotic Jurkat cells (J). The experiments were performed with cells from three donor sources.

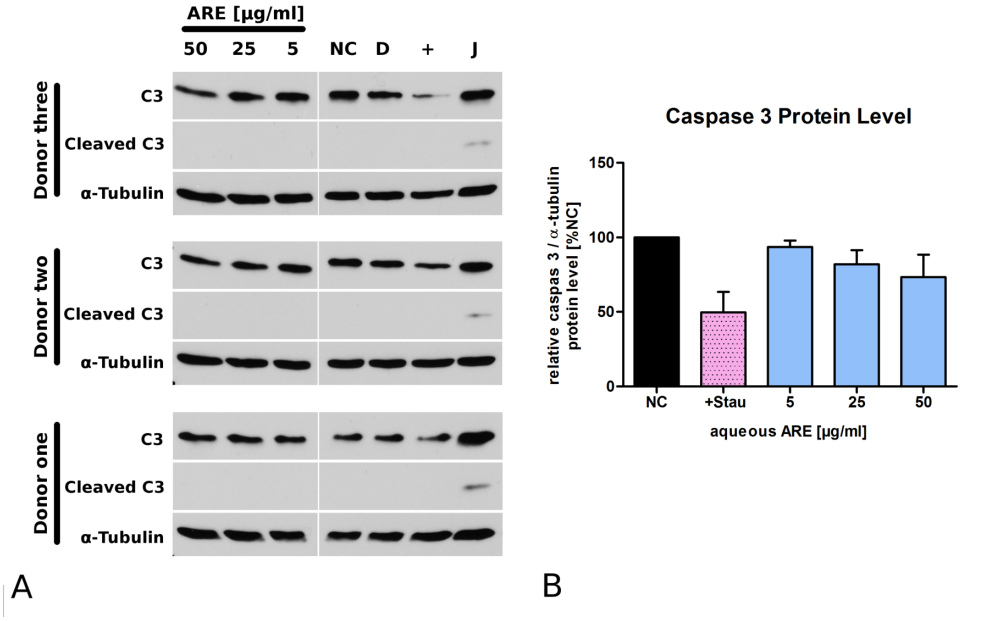

Figure 4.38.: Analysis of the influence of aqueous ARE on apoptosis measured by the caspase 3 (C3) and cleaved caspase 3 (cleaved C3) protein level in cultured primary human fibroblasts. Fibroblasts were serum-free cultured and treated over 48 h with the extract concentrations (5; 25; 50 µg/ml ARE). (A) Total protein was isolated and protein separation of 10 µg was conducted by a SDS-PAGE method for all conditions on the same gel. Proteins were further transferred onto a nitrocellulose membrane using western blot method. The membrane-bound proteins were incubated with anti-caspase 3 (35 kDa), anti-cleaved caspase 3 (17/19 kDa) and α-tubulin (50 kDa) antibodies. (B) The semi-quantitative mean of caspase 3 protein level ± SEM from fibroblasts of three donor sources in relation to the loading control α-tubulin and normalized to medium control; (J) Jurkat cells with staurosporine-induced apoptosis were used as positive control; (+) staurosporine treated fibroblasts; (D) DMSO control.

The investigations showed no increasing impact of the aqueous ARE on caspase 3 protein level (35 kDa; Fig. 4.38, B). A dose-dependent tendency of decreased caspase 3 protein level was observed when the results of three fibroblast donors were quantified (Fig. 4.38, B; 93.6 ± 4.3 %; 82 ± 16.4 %; 73.4 ± 26.1 % with 5; 25 and 50 µg/ml). Cleaved caspase 3 could not be detected in all samples except the positive control with extracted proteins of apoptotic Jurkat cells (J; Fig. 4.38, A; 17/19 kDa).

4.5.4.6. Western Blot Analysis of Extracellular Matrix Molecules Under Aqueous *A. Euchroma* Extract Treatment

Further, the question was investigated, of whether the treatment with the aqueous ARE induces or reduces the protein level of molecules from the ECM expressed by fibroblasts. Here, the protein extracts were used that we already analyzed due to their caspase 3 level (sec. 4.5.4.5). SDS-PAGE protein separation was performed using 5 µg total protein with following WB analyses to investigate the aqueous ARE impact on collagen type I and IV, and fibronectin protein level.

Collagen Type I Protein Level in Cultured Fibroblasts

Collagen I is the dominant collagen type in the connective tissue. It was present in healthy tissue and precursor proteins were increasingly expressed on day three after injury (Haukipuro *et al.*, 1991). During early granulation tissue formation collagen III was the dominant fiber molecule which was successively replaced by collagen I during the remodeling phase. The collagen I protein expression was increased with enhanced remodeling of the granulation tissue (Gay *et al.*, 1978). The hypothesis was addressed of whether the increased ATP amount (sec. 4.5.4.3) was accompanied with early increased collagen type I protein level. This could lead to an accelerated started remodeling of the ECM which indicates faster wound healing.
The influence of aqueous ARE on collagen type I protein level was investigated in primary human fibroblasts. The experiment was conducted as described in chapter sec. 3.15.4 following. The anti-collagen I antibody detected a broad range of protein bands, which represented the subunits α-I-chain (139 kDa; Fig. 4.39, A above), α-II-chain (129 kDa; Fig. 4.39, A below) as well as several collagen I isoforms and splice variants. The isoforms and splice variants were not further evaluated (data not shown). After normalization, a partly significant dose-dependent decrease of α-II-chain protein level was detected due to the treatment with ARE. The calculated mean ± SEM were 98 ± 33 %, 78.6 ± 32.2 % and 40.9 ± 15.2 % ($p < 0.05$) with 5, 25 and 50 µg/ml, respectively (Fig. 4.39, B). The α-I-chain level was not affected by the treatment

(95.7 ± 3.7 %, 98.9 ± 14.7 % and 99.2 ± 33.5 % with 5, 25 and 50 mg/ml). The collagen I subunits expression was semi-quantified shown in Fig. 4.39, B.

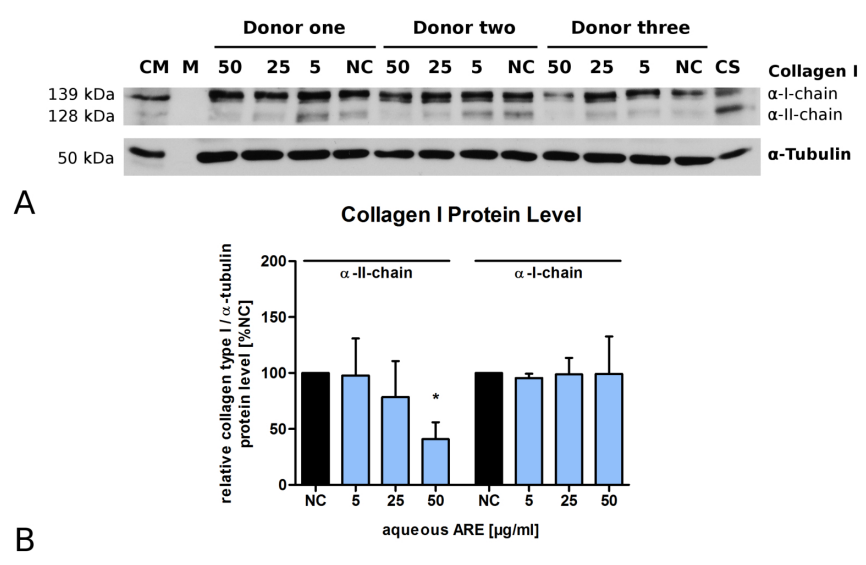

Figure 4.39.: Western blot analysis of collagen type I level on fibroblasts which were treated with the aqueous ARE over 48 h. (A) Western blot investigation on α-II-chain and alpha-I-chain of collagen type I protein level influenced by the treatment (128/139 kDa). The experiment was performed analogously to experiment sec. 4.5.4.5 with 5 µg protein isolated from fibroblasts from three independent donor sources. Results are represented as semi-quantitative mean collagen type I protein level ± SEM in relation to α-Tubulin (50 kDa; B) and normalized to the medium control (NC) with * $p < 0.05$ compared to NC; CM = control mouse vestibule, CS = control sheep ventricle, M = protein marker.

Collagen Type IV Protein Level in Cultured Fibroblasts

Collagen type IV is involved in proper tissue organization and is associated with structural tissue integrity. It is a main component of the basal membrane. MMPs secreted by keratinocytes degraded this collagen and laminins of the basal membrane to enable cell migration into the wound of previously bound cells (J. Li *et al.*, 2007). Collagen IV expression was increased when structures of the basal membrane were being rebuilt (Saarialho-Kere *et al.*, 1993). However, it is additionally an important component of the provisional ECM, which enables a network for all migrating cells (Grove, 1982).

The impact of ARE treatment on the expression of collagen type IV was analyzed in cultured primary human fibroblast, analogously to the previously shown western blot experiments. There was no significant impact of the treatment on the amount of collagen IV level detectable (Fig. 4.40). The calculated mean protein levels were 81.4 ± 12.5 %, 70.7 ± 15.1 % and 56.5 ± 30.3 % with 5, 25 and 50 µg/ml aqueous ARE, respectively (Fig. 4.40, B).

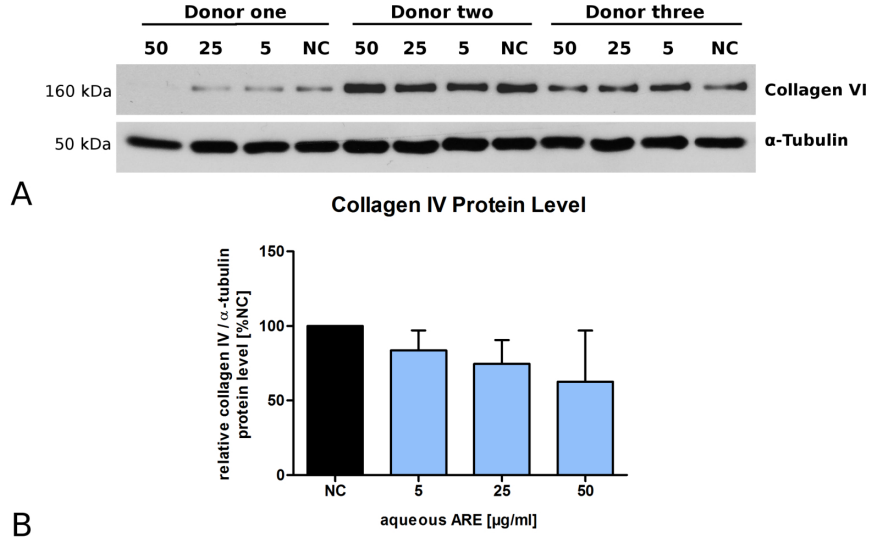

Figure 4.40.: Western blot analysis of human fibroblast treated with aqueous ARE and analyzed due to the extracts impact on collagen type IV protein level. (A) Protein separation and western blot were performed with 5 µg protein per test condition. Anti-collagen type VI (160 kDa) was used to stain the protein level. (B) Semi-quantitative evaluation of the western blot experiment. The investigation was performed with cells from three donors and the results were represented as semi-quantitative mean of collagen type IV protein level ± SEM in relation to α-tubulin, normalized to the medium control (NC).

Fibronectin Protein Level in Cultured Fibroblasts

Fibronectin, as a molecule of the extracellular matrix, represents a glycoprotein that is involved in wound healing especially due to its assistance in cell migration and adhesion (J. Li *et al.*, 2007). It is important during hemostasis due to its thrombocytes and platelets aggregating capacity. Fibronectin was further involved in the establishment of a provisory ECM and attracted fibroblasts and others to migrate into the wound area (Fallanga, 1993; Singer *et al.*, 1999; Reinke & Sorg, 2012).
The aqueous ARE influence on the protein level of fibronectin (262 kDa; Fig. 4.41) was studied. Here, a strong positive trend on protein level was found after semi-quantitative evaluation of the protein signals (Fig. 4.41, A) that is not yet significant (B). The calculated mean protein level under ARE treatment were 252 ± 157.2 %, 294 ± 145.2 % and 214.7 ± 168.3 % with 5, 25 and 50 µg/ml.

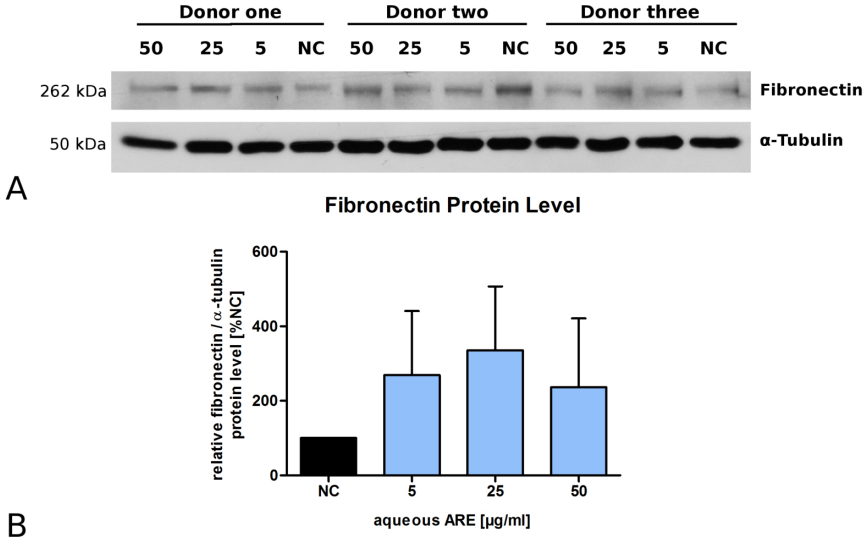

Figure 4.41.: Investigation on fibronectin protein level of cultured human fibroblast that were treated with aqueous ARE. (A) The protein level of fibronectin (262 kDa; 5 µg total protein loaded) was analyzed in aqueous ARE treated fibroblasts. (B) Semi-quantitative evaluation of fibronectin level of the western blot results. The experiment was performed with fibroblasts from three donors and the results are represented as semi-quantitative mean of fibronectin protein level ± SEM in relation to α-tubulin (50 kDa), normalized to the medium control (NC).

5. Discussion

Skin injuries of different severities occur consistently during lifetime and are regenerated by wound healing process in healthy human. In contrast, the cure of impaired wounds is long-term, may result in chronic wounds and dramatically increases health care costs. Especially in low-income countries, Medicare is not open to the public and particularly expensive drugs are not available for everyone. This socioeconomic burden enhances the necessity of new wound healing therapeutics. The current therapies contain mostly synthetically designed single compounds. These influence specific relevant target molecules and pathways. Herbal extracts, containing multiple compounds, may act in a more complex manner with potential synergistic and additive effects. The diverse ingredient chemical molecules can target specific, but different, signaling pathways and therefore greatly improve the wound healing process compared to a single compound. Furthermore, medicinal plants are a comparable low-cost therapy of widely grown herbs, which enables availability, especially for low-income countries. The request for complex wound healing therapeutics is still rising whereas the focus directs to natural resources of ethnopharmacological approaches (Budovsky *et al.*, 2015).

5.1. Hypothesis-Driven Herbal Selection, Extraction and Evaluation of Re-epithelialization in an *Ex Vivo* Wound Healing Model

5.1.1. Herbal Selection

These investigations were based on a hypothesis-driven literary search for traditionally used medicinal herbs. TCM phytotheraputic extracts showed good results on wound healing in the clinic (Budovsky *et al.*, 2015; Ho & Ong, 2015). However, evidence-based mechanisms studies were often missing or incomplete. Entire understanding of the promoted mechanisms enables optimized therapeutic usage, on the one hand, and is further important to identify possible side-effects by harmful or toxic ingredients

contained in the herbal material.
The selection of four herbal candidates was the result of traditionally predicted wound healing impacts, published evidence-based experiments, but not yet completely understood wound healing capacities of radix *A. propinquus*, radix *R. glutinosa*, rhizoma *C. chinensis* and radix *A. euchroma*. This hypothesis-based screening has advantages over single compound screening. Here, clinically used herbs were systematically analyzed due to their complex mode of actions including additive or synergistic effects. Single compound screening, in contrast, enables high-throughput investigations with partly missing effort due false negative and false positive results with comparable high costs (Friedemann *et al.*, 2015). Possible weaknesses of the here used complex method are the chosen search criteria for the primary herbal election. It might by thinkable to overlook further relevant candidates. Additionally, the specialized estimation of the TCM practitioners is based on their individual knowledge and may exclude herbs that are rarely used but would be highly effective. Furthermore, the laboratory screening systems are commonly restricted. Here, the wrong model may give false negative screening results. In summary, criteria for inclusion and exclusion must be chosen very carefully and they should be based on solid hypothesis. They directly govern the quality and success of the screening. In fact, hypothesis-driven screening is no quick and easy method. It is dependent on a collaboration of expert knowledge due to the complex mode of action by herbal therapeutics, but it enables the discovery of promising therapeutic strategies.

5.1.2. Standardized Herbal Extraction

The chemical composition of herbal material can vary depending on the soil where the plant was grown, possible herbicide treatments and plant-derived secondary metabolites, which protect them from herbivores (European Medicines Agency, 2014; Pinho *et al.*, 2012). Therefore, it is essential to verify the herbal material before use and appropriate trustful sources from which to purchases; in our case, certified TCM pharmacies. The pharmacies cooperate with external testing laboratories, which excluded possible intoxication by heavy metals or other chemical compounds. The herbal identities of the used materials and comparability composition, in the case of several herbal sources, were confirmed in our laboratory (sec. 3.11.1.1, Fig. 3.1) and additionally in an external reference laboratory. The herbal extraction was based on the traditional extraction method by decoction in water, which is either given orally or applied as a wound dressing. To stay close to the therapeutic approach, the ground-up herbal material was boiled, the extract concentrated, completely dried under constant conditions and stored at -20 °C. The extracts were used within a maximum of six

months after extraction. This standardized procedure enables extracts investigations with direct acquisition to the clinic. The extraction yields of *e.g. A. euchroma* were similar from extract to extract of the same raw material. They were further convenient to the extraction yield of 4.7 % reported by Kaith *et al.* (Kaith *et al.*, 1996). Minor deviations were possible due to the drying process, which used a rotation-evaporator, where remains in the glass flasks were not possible to prevent. The extraction yield varied with respect to these remains (sec. 3.10).
During later investigations, a more hydrophobic ultrasonic-based ethanolic ARE was used. According to other investigations on herbal material, reflux and ultrasonic extraction were mentioned as being traditionally used, rather than aqueous decoction (Meng *et al.*, 2013; Chinese Pharmacopoeia Commission, 2010). Again, the extraction method was completely standardized in order to enable reproducibility.

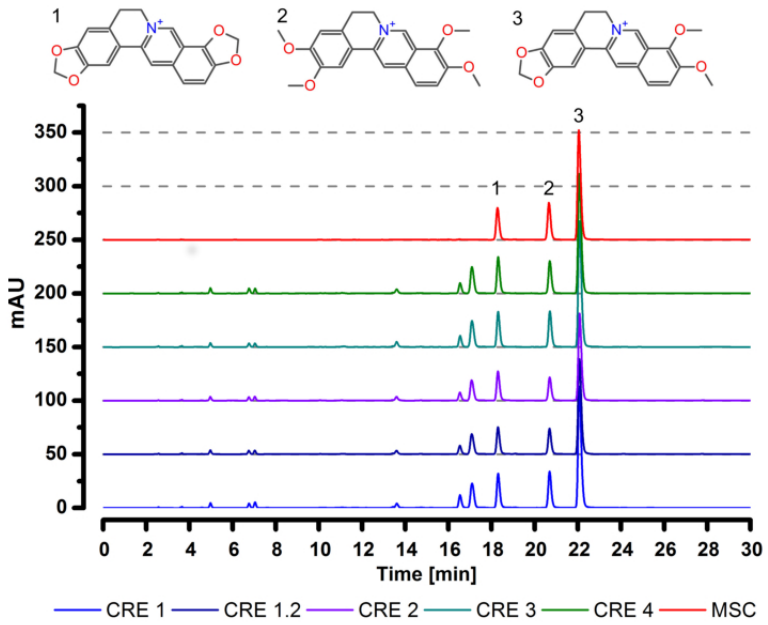

Figure 5.1.: Comparative HPLC-MS of five different aqueous extracts from *C. chinensis*. Red line (MSC): mixture of known main compounds (1) coptisine, (2) palmatine and (3) berberine. CRE (*Coptis chinensis* rhizoma extract) 1 and CRE 1.2 are independent extracts from the same raw material whereas CRE 1 - CRE 4 are extracts of *C. chinensis* obtained from four different origins. There was no significant difference in the composition of all tested extracts. Data and figure were provided by Friedemann *et al.*, 2015; ACD/ChemSketch (*http://www.acdlabs.com/resources/freeware/chemsketch/*) was used to design chemical structures; mAU = milli-absorbance-units.

To verify our standardized extraction method, exemplary HPLC-MS studies were investigated on two aqueous *C. chinensis* extracts of the same raw material and of extracts of different herbal origins. The results showed a high similarity between the extracts composition regarding their extracted main compounds (Fig. 5.1; Friedemann, 2015, Ph.D. thesis). These results confirmed the present extraction method of comparable efficiency with respect to the main compound signals.

These extracts were dissolved and investigated for the wound healing capacities in a patented *ex vivo* porcine WHM (Fig. 3.3; Brandner *et al.*, 2004 & 2006).

5.1.3. Initial Herbal Screening Using an *Ex Vivo* Porcine Wound Healing Model

During the initial screening, the aqueous herbal extracts impacts were addressed on early wound re-epithelialization in a porcine *ex vivo* WHM. Here, all tested conditions for *A. propinquus*, *R. glutinosa*, a combined extract of them both and *C. chinensis* extract did not significantly enhance wound recovery in *ex vivo* WHM (sec. 4.2). *C. chinensis* even showed significant negative impact on re-epithelialization (Fig. 4.1). In contrast, aqueous ARE treatment significantly improved epidermal regeneration (Fig. 4.2).

It was shown before that extracts from *C. chinensis*, *A. euchroma* and combinations of *A. propinquus* and *R. glutinosa* have a positive effect on epidermal regeneration (see introduction, chapter sec. 2.3.1 - sec. 2.3.5). It came as little surprise, that single *A. propinquus* and *R. glutinosa* extracts had no influence on epidermal regeneration in the WHM. Traditional wound dressings contain individually arranged combinations of herbs (Krishnan, 2006; X. Li *et al.*, 2015). Here, the effectiveness of herbal treatments can be based on synergistic or additive compound effects. This is what Lau *et al.* showed for the wound healing promotion by *A. propinquus* and *R. glutinosa* extracts treatment (K.-M. Lau *et al.*, 2012). On their own, neither promoted wound healing in diabetic foot ulcers in rats. However, the extracts' combination showed significantly improved epidermal wound recovery in the model (K. M. Lau *et al.*, 2012; T. W. Lau *et al.*, 2008). Lau *et al.* explained the increased wound regeneration with enhanced granulation tissue formation, reduced inflammation and improved angiogenesis. However, the combined extracts treatment in the WHMs did not significantly increase re-epithelialization either. *C. chinensis* extract even showed negative impact on re-epithelialization in our model, although it is used in wound healing formulations. Here, wound healing promotion of *C. chinensis* containing formulations was commonly interpreted by reduced inflammation (W. L. Li *et al.*, 2004; K. Kim *et al.*, 2008; Ma *et al.*, 2010; J. M. Kim *et al.*, 2010) accompanied with positive modulation of reduced oxidative stress (X.-J. Wang *et al.*, 2013). *R. glutinosa* was further shown to improve wound healing by its anti-inflammatory impact. This was demonstrated for extract treated wounds in rats, which resulted in reduced inflammation (T. W. Lau *et al.*, 2009). The analyzed herbal extracts may still improve wound healing, but within the WHMs the early epidermal regeneration process was focused. This model system is limited to investigations on wound re-epithelialization

and, with respect to present blood vessels, to some questions on early inflammation (Brandner *et al.*, 2006). There is no blood microcirculation due to the removed biopsy tissue. So, the question of microcirculation involved mechanism as the late macrophage-dominated inflammation phase and angiogenetic processes cannot be addressed. It is possible to keep the WHMs alive for up to seven days in culture within this system. This excludes granulation tissue remodeling and scar formation studies which occur much later after injury (Brandner *et al.*, 2006). If the extracts ingredient compounds address one of these mentioned mechanisms, it would not be detectable within this model. In contrast, animal studies allow the analysis of all wound healing phases in a living environment during long-term treatment (over days and weeks), which may further explain the differences of our results to previous findings. The wound healing animal experiments were mostly conducted in rodents. They are small, easy to handle with low cost for housing and feeding. However, rodent skin shows a number of differences to human wound healing, *e.g.* they have a comparable thin epidermis and a lower re-epithelialization due to contraction mediated wound closure (Sullivan *et al.*, 2001; Galiano *et al.*, 2004). In contrast, the swine has an anatomically and physiologically similar skin with comparable wound healing to humans. The epidermal-dermal ratio is comparable and the epidermis shows similar thickness to human epidermis with similar permeability (Meyer, 1996; Sullivan*et al.*, 2001). Epidermal turnover, keratin- and lipid composition, as well as similar *stratum corneum* properties, have been described (Weinstein, 1966 as cited in Sullivan *et al.*, 2001; Gray & Yardley, 1982; Sekkat *et al.*, 2002). Both species resemble similar collagen composition and wound healing associated collagen usage (Heinrich *et al.*, 1971). Furthermore, distribution, size, dermal location and orientation of blood capillaries are close to man (Forbes, 1969 as cited in Sullivan *et al.*, 2001). Present body hair of both species is reduced, follows hair cycle and takes action in re-epithelialization in wound healing. Therefore, wound healing studies on porcine skin may have fewer species differences to humans when compared with rodents. It further provides a more suitable animal model for testing dermatological hypothesis (Sullivan *et al.*, 2001; Sekkat *et al.*, 2002). Used as an *ex vivo* WHM, porcine skin offers investigations on animals slaughtered for consumption, and therefore avoids animal experiments. Their availability, together with their small size, enables an *in situ* test system of larger series with several treatments in multiple concentrations contemporaneously (Brandner *et al.*, 2006). Here, tissue present cells and structures are kept alive under defined air-liquid culture conditions. The interference of therapeutic treatments and epidermal regeneration can be directly examined.

Moreover, the extract preparations can uncontroversially influence the ingredient compound composition. Besides the usage of different solvents, the extraction method

varied between the described studies. In clinic, mainly decoction or ointments were used, whereas laboratory studies often focused on reflux-based soxleth and ultrasonic-based extraction methods (Yoo *et al.*, 2014; Meng *et al.*, 2013). Furthermore, the chosen applied extract concentrations may be responsible for non-beneficial results. It could be conceivable, that lower concentrations would have shown other results. Traditionally the herbs are used as herbal combinations and extracted together. Therefore, the final effective compound concentration of each herb may be smaller in a combined extraction, due to saturation effects, than compared to pure single extracts. The same is true for the application method. The reported investigations on animal models were conducted by wound dressings whereas our studies were conducted as liquid drop extract applications. Therefore, the final effective dose may vary.
However, for the first time an aqueous *A. euchroma* extract showed significant wound healing improvement in the porcine *ex vivo* WHM (Fig. 4.2, A). It was previously shown that AREs of different solvents other than water improved epidermal recovery in wound healing of acute and different burn wounds in animal models and in the clinic (X. Pei *et al.*, 2007; Pirbalout *et al.*, 2011; Nasiri *et al.*, 2015 & 2016). The mentioned studies showed generally improved epidermal regeneration accompanied by enhanced granulation tissue formation and angiogenesis promotion (sec. 2.3.5).
Aqueous extract of *A. euchroma* was selected by the initial wound healing screening out of 25 traditionally used herbs (sec. 5.1). It was further investigated to understand the underlying mechanisms in the affected cell types. The investigations were conducted with an additional ethanolic ARE and the single compound shikonin. Here their previously described wound healing impact was specifically addressed on early re-epithelialization. Phytochemical analyses, combined with time point- and wound application studies of the herbal extract on WHMs, should help to elucidate the mode of action of this herbal drug.

5.2. Investigation on *Ex Vivo* Wound Re-epithelialization Improvement of Aqueous and Ethanolic *A. Euchroma* Extracts and the Single Compound Shikonin

5.2.1. Wound Healing Impact of Aqueous ARE

The aqueous ARE significantly improved re-epithelialization in a dose-dependent manner within the initial investigations in *ex vivo* porcine WHMs (sec. 5.1.3). The

doses of 100 and 500 µg/ml significantly increased wound recovery to 168.2 ± 26.3 % and 161.8 ± 16.4 % compared to solvent and untreated control (Fig. 4.2, A). A subdivision of intrinsic good and bad healing donor skins showed significantly improved re-epithelialization on good healing and a positive tendency in impaired healing specimens. Additional, *ex vivo* investigations on human WHMs also showed a significant positive impact on epidermal regeneration with 500 µg/ml compared to untreated control (Fig. 4.8, A). There was no positive impact on intrinsic good healing specimens detected whereas bad healers were significantly improved compared to the untreated control (Fig. 4.8, C). Aqueous ARE enhanced wound re-epithelialization in both species with respect to the total cohort. The missing significance of the positive trend by the ARE treatment in human, compared to the solvent control, could be caused by the small sample size. Differences between the subgroups of intrinsic good and bad healing specimens between the donor species might be due to unlike group size and their sample's distribution. Three human WHMs donors were categorized as good healers and six as bad healing specimens. This factor (1:2) differs from that of the porcine donor samples (1:1.5) and might influence the results explanation power. Moreover, minor species differences could be responsible for the lower impact in porcine bad healing specimens. In fact, wound healing of porcine and human skin follows a comparable mechanism, with respect to the involved cells and molecules (Sullivan *et al.*, 2001; Brandner *et al.*, 2004). Species differences might result in varying outcomes concerning specific time points of the healing. This could be caused by slightly different activated pathways and may result in minor variations during the wound healing process. Additionally, the human donor specimens were derived from different thoracal origins, whereas the porcine samples were always taken from the ears. This different location may influence the wound healing progress. However, the general increase in epidermal regeneration, accompanied by positive impact on impaired healing skin, indicated a promising usage of aqueous ARE on early re-epithelialization in patients with disturbed wound recovery.

These investigations firstly described positive wound healing promotion by an aqueous ARE. The present extraction by aqueous decoction was used to obtain comparable conditions to the other initially screened herbal extracts, which are traditionally extracted by aqueous decoction. Additionally, the wound healing capacity of the aqueous extract of another Zicao species had been described before (H. Kim *et al.*, 2011). Kim *et al.* showed improved keratinocytes and fibroblasts migration *in vitro* by treatment with an aqueous extract of *L. erythrorhizon*. *L. erythrorhizon* is traditionally synonymously used, besides *A. euchroma*, as herbal drug Zicao (Chinese Pharmacopoeica Commission, 2010). It was described that the compositions of the plant's main compounds resemble each other (Zhou *et al.*, 2011; Hou *et al.*, 2006). This

enables the interchangeable usage of these Boraginaceae species for wound healing treatment in the clinic. Additionally, Kaith *et al.* demonstrated anti-inflammatory edema inhibition by an orally given aqueous ARE decoction (Kaith *et al.*, 1996). Certainly, the comparison of topical application and orally therapy has to be performed carefully. Those findings indicated wound healing capacity of aqueous ARE. The *in situ* re-epithelialization impact of an aqueous ARE has not been reported before and is, therefore, a new finding.

5.2.2. Wound Healing Impact of Ethanolic ARE

Additionally, the aqueous and an ethanolic ARE were comparatively studied. The hydrophilic and more hydrophobic extracts were investigated to comprehensively explore the wound healing potential of the complex chemical *A. euchroma* raw material composition. Further, it enabled the comparability of the obtained data with published reports about more hydrophobic AREs. Previous studies described wound healing promoting capacities of other ethanolic AREs (Kaith *et al.*, 1996, orally given; S. Ashkani-Esfahani *et al.*, 2012, topical; Ashkani-Esfahani *et al.*, 2012). Within the tested total cohort, there was no detectable effect on epidermal wound recovery, whether in porcine or in human skin specimens (Fig. 4.11 and Fig. 4.12, A). There was a significant positive influence on extract treated intrinsic bad healing human skin samples compared to the untreated control (Fig. 4.12, C). However, this wound healing impact was caused by the present DMSO which became obvious when comparing solvent, untreated and DMSO control. The last one improved wound re-epithelialization even stronger than the ethanolic extract did. Therefore, a direct impact on early re-epithelialization of the tested ethanolic ARE concentrations could be declined. The positive impact of the topical DMSO on wounds with severe impairment to their healing process was already discussed in the review by Duimel-Peeters (Duimel-Peeters *et al.*, 2003). They support our findings of the generally positive wound recovery impact of DMSO. The missing positive influence of the ethanolic ARE stays in contrast to previously published research with other ethanolic AREs. The here investigated ethanolic ARE was obtained by ultrasonication-based extraction. This enables a fast and highly efficient (Yoo *et al.*, 2014) completely dried extract as an advantage in comparison to other hydrophobic extraction solvents as *e.g.* petroleum ether and chloroform. The complete extract drying is obligatory for using defined extract amounts, without solvent influences in the following analytical studies. It further enables longer extract storage durations with reduced compound degradation compared to dissolved extracts. The present labor equipment did not enable the evaporation of more hydrophobic solvents as *e.g.* petrol ether and chloroform. Therefore, the extraction was performed using

ethanol to guarantee reproducible investigations; in contrast to analyses with non-dried extract. Ashkani-Esfahani *et al.* used the plant´s leaves and the radix as raw material and performed a soxhlet extraction 50 % ethanol in water with longer extraction duration (S. Ashkani-Esfahani, 2012). Therefore, the extract's composition is assumed to vary compared to our ethanolic ultrasonicated extraction. A further difference can be seen in the extract's application, which was performed in a 2 % carboxymethylcellulose (2 g in 98 ml distilled water) solution (S. Ashkani-Esfahan, 2012; Kaith *et al.*, 1996). During the present approach, the extract was dissolved in DMSO, further diluted in PBS and applied as a solution. The previously demonstrated improved healing of burn wounds treated with an ethanolic ARE in rats' was caused by increased granulation tissue formation and enhanced angiogenesis (S. Ashkani-Esfahani *et al.*, 2012 and 2012). Nasiri *et al.* showed improved collagen fiber formation and significantly enhanced wound contraction in rats burn wounds (ARE ointment; Nasiri *et al.*, 2015). The latter is obligatory for rodents' wound healing but plays a minor role in human skin and could be an explanation for the missing impact *ex vivo*. Such species differences can cause different results between the investigations which have been discussed earlier in chapter sec. 5.1.3. Burn wounds are a result of heat-induced tissue damage which goes along with protein degradation and function loss. The support of the re-establishment of an ECM and proper granulation tissue is important during wound recovery, but may have a minor impact in our re-epithelialization WHMs. The absent positive impact in our WHM may be further caused by a shorter treatment duration of only two days compared to treatment up to 28 days past injury. Animal studies and clinical trials are evaluated at certain time points of wound healing and often oblique to the complete healing. Therefore, longer treatment duration is favored. The previously investigated wound healing parameters as *e.g.* angiogenesis were not addressed in the present *ex vivo* WHM. In contrast, former investigations did not explicitly address it´s re-epithelialization capacity. Therefore, the new finding is that ethanolic ARE has no direct impact on re-epithelialization during early wound healing.

5.2.3. Wound Healing Impact of Shikonin

Due to the present literature, most evidence-based experiments were conducted with hydrophobic extracts of *A. euchroma* (sec. 2.3.5). It was shown that they contain high amounts of naphthoquinone derivatives, as *e.g.* shikonin, which have been described for their wound healing promotion capacities (Papageorgiou *et al.*, 1999 & 2008; Pinho *et al.*, 2012). Therefore, the question was addressed if shikonin has an impact on early re-epithelialization and if the discovered wound healing promotion by aqueous

ARE can be explained by the influence of the ingredient shikonin. Chromatographic investigations on the herbal extracts compound composition were performed in parallel to these investigations (5.4). They took longer than expected, whereas the proof of the shikonin presence in the extracts was missing while this analysis was performed. No significant wound recover was detected by the treatment with shikonin in the porcine skin (Fig. 4.13). Within the tested human specimens, there was also no positive effect of shikonin detectable (Fig. 4.14, C). The significant positive impact compared to untreated control on impaired healing samples, was caused by the DMSO influence. There was no increase in early re-epithelialization detectable by shikonin treatment in the performed *ex vivo* model, independent of the investigated donor species. The investigation on shikonin impact on short-term treated acute wounds was performed for the first time. The previously described wound healing impact of this naphthoquinone is not caused by early re-epithelialization with respect to the present results. Increased blood perfusion and epithelial thickness, decreased wound size, with improved collagen production and angiogenesis were prominent during the healing of acute wounds in dogs treated with a mixture of shikonin and its derivatives (HELIX-DERM®; Karayannopoulou *et al.*, 2011). Xie *et al.* demonstrated an improved scar formation mechanism by induced apoptosis accompanied by decreased collagen type I and III expressions *in vitro* in scar-derived and normal human fibroblasts (Y. Xie *et al.*, 2015). Further animal experiments described promoted neovascularization, granulation tissue formation with increased collagen synthesis and re-epithelialization during wound healing process (Ozaki *et al.*, 1998; P.J. Lu *et al.*, 2008; Papageorgiou *et al.*, 2008). The varying species and treatment durations may be further reasons for the missing impact on the *ex vivo* WHM. These findings were supplemented by the finished chromatographic analyses, which showed shikonin absence in the aqueous ARE (chapter sec. 5.4). The ethanolic ARE was observed to contain shikonin, but had no impact on the WHM studies as well. Neither supported the here investigated wound healing parameters concerning early re-epithelialization. Their described wound healing capacities must be explained by other wound healing mechanisms as discussed above. In contrast, aqueous ARE significantly enhanced early epidermal regeneration.

5.3. Investigation on Wound Healing Associated Mechanisms

5.3.1. The Extracts Influence on Related Wound Healing Mechanisms *In Situ* and *In Vitro* in Human Keratinocytes

Keratinocytes have an essential role in the healthy epidermis and during regeneration of skin trauma. To evaluate the underlying mechanism of the *ex vivo* observed wound healing promotion by aqueous ARE, *in situ* and *in vitro* studies were performed. *In vitro* investigations in human skin cells with an aqueous ARE have not yet been reported.
To evaluate the extracts´ influence on cell differentiation, two cytokeratins were stained in the *ex vivo* models, which showed enhanced wound healing by aqueous ARE treatment. Here, ARE treatment did not show an impact on keratinocytes differentiation *in situ*. In the WHMs, CK 10 and CK 14 were expressed in unwounded areas, at the wound margins, where stratified tissue was still present, and in the regenerating epidermis (Fig. 4.20). The expression of CK 14 in the regenerating epidermis was weak in mono-layered areas and basal present in multi-layers. CK 10 was expressed in cells of the wound tongue but with a fading signal to the regenerating tip. There was no difference in expression pattern detectable between ARE treatment and control. In healthy epithelium undifferentiated, CK 14 positive, keratinocytes are predominantly present in the basal cell layer and CK 10, as a late differentiation marker, is expressed in all suprabasal layers *in situ* (Moll *et al.*, 2008). The fading and partly weak CK 10 signal in the regenerating epidermis can be explained by a replacement of later differentiation markers as involucrin as Safferling *et al.* observed 48 h after injury (Safferling *et al.*, 2013). They further showed that CK 14 was present in cells behind the leading wound tip. The missing influence of aqueous ARE on these differentiation markers was described firstly within the present studies.

To analyze the AREs impact on keratinocytes *in vitro*, different culture conditions, imitating the cell characters as they may occur in the wound associated area, were investigated. Confluent and subconfluent grown keratinocytes were treated to mimic compact tissue and looser cell unions. These undifferentiated conditions were further compared to differentiated epidermal cells. Here, the normal culture medium was shifted to high calcium level which induces differentiation (Bikle *et al.*, 2012). This pre-conditioning was conducted over three or five days to enable different differen-

tiation levels. Keratinocytes were treated with the extracts and the impact on cell viability was evaluated after 48 h of cultivation, equivalent to the WHMs by MTT method. The cell viability of undifferentiated keratinocytes was not positively affected by the aqueous ARE treatment (Fig. 4.21). The *ex vivo* used concentration of 500 µg/ml aqueous ARE significantly reduced the cellular viability. Differentiated cells were not influenced by the treatment. However, an enhanced tendency of mitochondrial activity was observed in later differentiated cells treated with the highest dose. There was a partial negative impact detectable by ethanolic ARE treatment independent of the cellular differentiation (Fig. 4.22). Previous WHM experiments indicated a concentration transferability of one to ten when changing *in vitro* culture system to *ex vivo* models and back. With *ex vivo*, a positive influence of 500 µg/ml was determined. Differentiated keratinocytes showed a tendency to enhance cell viability, which support the *in situ* findings. However, there was a negative impact on undifferentiated cells *in vitro*. The question is whether the high concentration is able to reach undifferentiated keratinocytes in the WHM without being dissolved by diffusion through the stratified epidermis. In two-dimensional cultured cells, treatment directly affects the single cells because it is contained in the culture medium surrounding the cells. In tissue, with a united cell-cell structure, the treatment is supposed to influence the cells on top directly with decreasing impact on lower cell layers by diffusion and osmotic effects. It can further be presumed, that other elements and molecules, which are present in the tissue but not in single culture, may bind or interact with the extract compounds. The viability decrease in undifferentiated cultured cells could be explained by reduced metabolism, initiated cell cycle arrest or viability reduction effects due to the extracts treatment. The positive tendency of 500 µg/ml aqueous ARE on the viability of differentiated cells can be caused by increased metabolism or proliferation. A further explanation, is reduced cellular uptake of the ARE due to a modified membrane during formation of a cornified envelope by keratinization (Eckert & Rorke, 1989; Moll *et al.*, 2008). Neither aqueous nor the ethanolic ARE significantly promote keratinocytes viability in culture, which was described for the first time.

Nevertheless, the extracts treatment may affect the cell proliferation, which can improve re-epithelialization. Therefore, the question was addressed of whether the positive impact of aqueous ARE on *ex vivo* epidermal regeneration was caused by enhanced cell proliferation. *Ex vivo* cell division studies showed uninfluenced cell proliferation rates of keratinocytes by aqueous ARE treatment (Ki67 staining; Fig. 4.19, A). The proliferating activity was the highest in the regenerating epidermis, followed by the wound margin and unwounded area, independent of the treatment. Increased proliferation level at the wound margins and of the wound area invading cells has been

reported before to be essential for wound recovery (Singer *et al.*, 1999).
However, the AREs influence on proliferation in cultured keratinocytes was addressed. An influenced proliferation rate was assumed by the aqueous ARE treatment in cultured keratinocytes, which could be diminished in *ex vivo* due to diffusion effects. This investigation was performed analog to the MTT with BrdU labeling after extract treatment. A dose-dependent decrease on cell division of undifferentiated keratinocytes was discovered under aqueous ARE treatment. There was no positive influence detected on differentiated cells, independent of the differentiation duration (Fig. 4.23). The highest concentration also significantly reduced cell proliferation. These findings in differentiated keratinocytes were supported by reported uninfluenced proliferation rates of (1.2 mM) high calcium cultured keratinocytes, which were treated with aqueous extract of another Zicao species (*L. erythrorhizon*; H. Kim *et al.*, 2011). Ethanolic ARE treated keratinocytes showed a dose-dependent significant decrease in proliferation rate (Fig. 4.24). The DMSO control significantly improved the cell division rate of undifferentiated and, by a strong trend, in subconfluent keratinocytes; it had no influence on differentiated cells. Diffusion differences affect a regenerating tissue differently than a cell culture system as already discussed above. Therefore, the direct impact on cellular proliferation might be diminished in tissue, whereas the extract reduced cell proliferation *in vitro*. The inhibition of cell proliferation in the experiments can be caused by naphthoquinone derivatives contained in the AREs (see also chapter sec. 5.4). *E.g.* shikonin, contained in the ethanolic ARE, was described to decrease cell proliferation especially in cancer cell lines (Zhao, 2015) but also in cultured primary keratinocytes (Xie, 2015). Within our analysis, a final DMSO concentration minor 1 % was used, with respect to the experimentally used highest DMSO concentrations of the ethanolic ARE or shikonin. In contrast, Xie *et al.* described no DMSO impact on viability and proliferation of undifferentiated keratinocytes with doses less than 1 % (Y. Xie *et al.*, 2015). The difference in our findings with increased proliferation level might be explained by different culture conditions as a used medium and the supplementation of 10 % FBS by Xie *et al.* compared to present serum free conditions. The selection of an appropriate medium for *in vitro* studies has an enormous influence on the experimental outcome (Zorn-Kruppa *et al.*, 2016). Zorn-Kruppa and coworkers demonstrated expression and characteristic differences of primary human keratinocytes from the same donor source cultured comparatively under different conditions and in different media. The proliferation increase by DMSO might be an explanation for the observed positive tendency on wound healing in DMSO treated *ex vivo* WHMs. However, unaffected keratinocytes viability levels, together with reduced proliferation, indicated more metabolically active undifferentiated keratinocytes due to the aqueous ARE treatment.

Based on improved *ex vivo* epidermal regeneration, enhanced wound recovery of cultured undifferentiated keratinocytes *in vitro* was supposed by the aqueous ARE treatment. This might be caused by active migration with respect to the missing increased proliferation level. Undifferentiated keratinocytes have the possibility to migrate because of fewer and looser built cell-cell connections, compared to differentiated cells (Eckert & Rorke, 1989; Nickoloff *et al.*, 1988). They are generally more metabolically active and proliferative. These capabilities get lost with rising differentiation (Bikle *et al.*, 2012). Cell migration of cultured and wounded undifferentiated keratinocytes treated with the aqueous or ethanolic ARE was not improved compared to the controls measured by scratch assay method. There was a dose-dependent delay detectable on wound closure that was significant with the highest aqueous and ethanolic concentration compared to medium control (Fig. 4.25, A and Fig. 4.26, A). With respect to the recovered wound area every 12 h, the ethanolic ARE showed wound healing progress comparable to the controls (Fig. 4.26 B). Whereas 50 µg/ml aqueous ARE significantly reduced wound closure (Fig. 4.25, B). Interestingly, although the DMSO control itself tended to improve wound closure, the treatment with ethanolic ARE showed minor positive tendency 24 h past injury. Partially reduced *in vitro* wound recovery by cellular migration and proliferation was observed during these investigations. The present findings are in contrast to the observed increase in migration of keratinocytes treated with low dose of an aqueous Zicao extract of *L. erythrorhizon* (H. Kim*et al.*, 2011). Here, high doses did not affect the migration capacity. It should be mentioned, that the experiments were conducted under high calcium level and therefore on differentiated cells. Further, they used different culture medium conditions and reduced cell proliferation by mitomycin C pre-treating. In the end, the impact of varying extraction methods by longer performed decoction (3 h) and differing raw material solvent ratio (1:500) accompanied with non-dried used extract may affect the result as well. Wound recovery is dominated by cell migration and proliferation (Vellnar *et al.*, 2009). Our previous findings showed reduced proliferation of undifferentiated keratinocytes. These results supplement the missing positive impact on *in vitro* wound closure. It is assumed that the improved *ex vivo* observed improved epidermal regeneration is not directly caused by the aqueous ARE influence on the migrating keratinocytes. It seems to be an indirect effect, which might be induced by an interaction with other involved cells and secreted (not present here in culture) chemical metabolites (Nickoloff *et al.*, 1988; Ueck *et al.*, 2017). Therefore, a discrepancy between *ex vivo* and *in vitro* gained results may arise.

Another important aspect for proper cell migration and following wound closure is the capacity of controlled cell-cell and cell matrix detachment and newly formed attach-

ment (Velnar *et al.*, 2009; Chester & Brown, 2016). Because of the reduced wound recovery *in vitro*, increased cell-matrix attachment was supposed to be caused by the aqueous ARE treatment. Therefore, the impact of both AREs on cell-matrix adhesion after seeding in treatment containing culture dishes was analyzed. Interestingly, all test substances significantly diminished the cell adhesion within the first 15 min after seeding, compared to medium control (Fig. 4.27). An exception was the lowest concentration, which still showed a trend to reduced attachment. The highest concentrations of the aqueous ARE even decreased the number of attached keratinocytes until 30 min (50 µg/ml) and 120 min (500 µg/ml). Besides the initial 15 min, the highest concentration of the ethanolic ARE significantly decreased cell attachment up to 120 min (compared to DMSO and NC) and until 180 min (to NC). The reduced cell-matrix binding, especially by the aqueous ARE, may positively contribute to the wound regeneration. Bouzaiene *et al.* described reduced cellular attachment and migration of human tumor cells treated with coumarin acid (Bouzaiene *et al.*, 2015). This anti-oxidative substance was detected in the aqueous ARE by our previous investigations (sec. 5.4) and may contribute to the retarded cell attachment. Interestingly, the reduced initial cell attachment should promote wound closure *in vitro*, which was not detected. Here, a possible explanation can be the experimental setup with settled confluent grown cells for the scratch assay compared to non-acclimatized fresh seeded keratinocytes in the cell-matrix adhesion assay. The keratinocytes in the scratch cultures were able to adhere and fix the plastic surface without treatment influence. During the adhesion assay, the cell attachment was directly influenced by the AREs. Therefore, a cell-adhesion reducing impact could be an explanation for the *ex vivo* observed wound healing promotion, where the cells migrate under the direct influence of the ARE from the injury on. Another explanation for the missing improved wound closure in culture may be the absence of essential signals as *e.g.* growth factors expressed by fibroblasts amongst others, which are crucial for the cellular migration (Velnar *et al.*, 2009; Nickoloff *et al.*, 1988). Additionally, Ueck *et al.* demonstrated that simplified cell culture models may help to discover wound healing mechanism caused by fewer cell types and reduced cellular interplay when compared to *in situ* situations (Ueck *et al.*, 2017). However, this simplification may also have the disadvantage of reducing the comparability to more complex *in vivo* situation.

In summary, reduced cell adhesion accompanied with partly reduced cell migration, proliferation and viability of cultured undifferentiated keratinocytes treated with the aqueous ARE, together with missing impact on differentiated cells, were here firstly described. The observed influences of the ethanolic and aqueous ARE on cultured keratinocytes have not yet been reported. However, these findings do not explain the improved *ex vivo* re-epithelialization. Further studies of the extracts on fibroblast were

investigated.

5.3.2. The Extracts Influence on Related Wound Healing Mechanisms *In Situ* and *In Vitro* in Human Fibroblasts

Analyses on cultured fibroblasts, as another important cell type involved in the wound healing processes, were performed. Fibroblasts, as dominant cell type of the dermis, have an essential role in normal tissue and during regeneration of skin trauma, inflammation, angiogenesis and granulation tissue formation.
Fibroblasts are commonly cultured in the presence of FBS which provides a complex medium supplementation as *e.g.* minerals, vitamins and different growth factors (Keira *et al.*, 2004; Gstraunthaler, 2003). This serum supplementation is problematic during treatment studies because FBS ingredient compounds may possibly influence the wound healing mechanism. Further, it is difficult and complex to ensure that the serum does not interact with the extracts ingredients. In the *ex vivo* WHMs, the treatment had no contact with the culture medium, because of the direct wound application under air-liquid interface condition. Here, medium extract interaction was excluded. Thus, we decided to investigate studies on the serum-cultured AREs treated fibroblast compared to cells which were cultured in presence but treated and measured in the absence of serum to avoid possible interactions.

The improved epidermal regeneration *ex vivo* by aqueous ARE treatment was assumed to be caused by enhanced fibroblasts viability. This would further enable increased metabolic activity associated with wound healing promotion by intercellular interactions. The impact of aqueous and ethanolic ARE was investigated on the viability of primary human fibroblasts after 24 h or 48 h treatment by MTT method. The aqueous ARE showed no influence on fibroblasts viability in serum containing cultured cells. In contrast, fibroblasts under serum-free conditions showed a partially significant, dose-dependent increase in viability during the first 24 h treatment and a strong positive trend after 48 h (Fig. 4.30). High doses of 50 and 500 µg/ml in part, significantly reduced the cellular viability serum and cultivation duration independently. A dose-dependent viability decrease was observed in serum-cultured and ethanolic ARE treated fibroblasts (Fig. 4.31). Serum-free conditioned cells were not significantly affected, besides high doses that reduced viability. The missing positive impact on cellular viability in serum containing compared to serum-free conditions was assumed to be caused by interactions between the FBS ingredients and the aqueous extract. Here, viability-promoting molecules may be bound or inactivated.

The negative impact with ethanolic ARE treatment under FBS culture conditions may also be caused by the generation of toxic metabolites or binding and inactivation of extracts ingredients and the serum molecules (Gstraunthaler, 2003). These *in vitro* influences of both AREs on the viability of cultured primary fibroblasts have not been reported before.

Based on the observed increasing viability trend under aqueous ARE treatment, an enhanced proliferation was assumed. However, the *in situ* proliferation of fibroblasts was not affected by the aqueous ARE treatment (Ki67 staining; Fig. 4.19, B), which could be caused by molecular diffusion *in situ* as mentioned before. The experiment on cultured cells was conducted as described for the MTT, whereas the cell division was measured by BrdU assay. The proliferation was not influenced by aqueous ARE treatment under serum containing conditions, except high doses which significantly reduced cell proliferation (Fig. 4.32, A) as detected before within the viability studies. FBS-free treated fibroblasts showed reduced proliferation rate with significance after 48 h treatment (Fig. 4.32, B). Kim *et al.* showed non-affected cell proliferation by the treatment of serum-cultured and wounded fibroblasts after 24 and 48 h aqueous *L. erythrorhizon* extract (H. Kim *et al.*, 2011). Although this investigation was performed under different culture conditions and on injured cells, the non-influenced cell proliferation suits to the present findings. The ethanolic ARE significantly diminished fibroblasts proliferation in a dose-dependent manner independent of serum presence or absence (Fig. 4.33). In contrast, the DMSO control showed improved cell proliferation. The observed proliferation induction by DMSO may support the enhanced epidermal regeneration in *ex vivo* WHMs. The decreased cell division under serum-free conditions can be caused by a negative impact of the AREs treatment, which is not present under serum condition due to possible inactivation as discussed before. In fact, cell division is dependent on several chemical factors and the provided environment (Gstraunthaler, 2003). Therefore, the reduced proliferation can be in part a result of missing essential compounds, related to proliferation induction, contained in the serum. The results for ethanolic ARE treated fibroblast stays in contrast to the observed increased cell number by previous *in vivo* studies in different wound types (S. Ashkani-Esfahan *et al.*, 2012; Mohsenikia *et al.*, 2015; X. Pei *et al.*, 2007). However, as discussed above *in vivo* effects must not be detectable *in vitro* due to a simplified system with missing diverse interactions (Ueck *et al.*, 2017). Furthermore, species and systematic differences, as *e.g.* extraction method, culture condition and treatment duration, may influence the cellular proliferation as discussed before.

Interestingly, reduced cell division rate (BrdU) was observed and accompanied by with increased cell viability (MTT) under serum-free conditions and aqueous ARE treatment. The present increased viability can be caused by enhanced metabolic activity, which can be used for further wound healing related processes. Such processes as *e.g.* migration and synthesis of essential and wound healing associated molecules are energy-dependent processes (Im & Hoopes, 1970; Rodriguez *et al.*, 2008). ATP molecules, derived from the respiratory chain and glycolysis metabolism, can be determined, which gives more sensitive information about cellular metabolic activity compared to MTT assay (Petty *et al.*, 1995). To verify the hypothesis, the free ATP amount was determined under extracts treatment. The measured ATP level was significantly increased in fibroblasts cultured in the presence of aqueous ARE, whereas the impact was stronger during the first 24 h up to almost 200 % (Fig. 4.34, A). Ethanolic ARE treatment did not enhance the free ATP level in cultured cells. The metabolic activity of the aqueous ARE treated fibroblast was enormously enhanced, which was indicated by MTT before. Both methods determine the cellular metabolic activity by redox reactions of the mitochondrial respiratory chain. The MTT assay is based on the enzymatic reduction of MTT reagent by a reductase. In contrast, the ATP measurement determines all produced ATP molecules by the mitochondrial ATP synthase and ATP originated from glycolysis (Im, 1979). Therefore, the resulting signal is more sensitive than MTT. Previous studies showed increased amounts of ATP and enzymes, associated with the energy-generating metabolism, during wound healing (Im, 1970). ATP treatment increased the regeneration of acute and even ischemic wounds in rabbits (J. Wang *et al.*, 2009). An explanation for the increased ATP amount by aqueous ARE treatment could be the chromatographically detected high number of polar compounds (sec. 4.3.2 - sec. 4.3.3). It is in all probability that these secondary metabolites contain polysaccharides. Former studies showed improved wound healing by crude sugar application due to pH reduction with various anti-bacterial capacities and local osmotic influences (Biswas *et al.*, 2010; Chirife *et al.*, 1983). In the last one increased granulation tissue formation was observed. If the detected polar compounds should be mainly polysaccharides, what must be investigated in the future, the enhanced ATP amount could be additionally caused by increased glycolysis (Im & Hoopes, 1979). Here, elevated polysaccharide compounds in the wound bed may increase this metabolic pathway resulting in enhanced ATP amounts. However, enhanced ATP level may also indicate reduced ATP consumption. Or, the other way around, the reduced ATP level in ethanolic ARE treated cells may be caused by ATP consumption of fewer cells due to decreased proliferation (BrdU). In fact, the actual energy metabolism should be determined by investigating the cellular oxygen consumption. This can be determined by different methods as *e.g* molecular oxygen sensing by

photoluminescence detection, which was described in detail in a review by Dmitriev *et. al.* (Dmitriev & Papkovsky, 2012). However, the present findings support the hypothesis that accelerated wound healing is caused by increased energy level of fibroblasts, discovered under aqueous ARE treatment.

The increased amount of energy of the fibroblasts was expected to be used to enhance migration into the wound (Im & Hoopes, 1970). This would explain the obtained wound healing promotion *ex vivo*. Enhanced migration into the wound bed could accelerate the establishment of an improvised ECM and granulation tissue, which is obligatory for migration of keratinocytes and others and therefore for wound recovery (Nickoloff *et al.*, 1988; Singer *et al.*, 1999). Here, the different AREs impacts on fibroblasts wound closure were analyzed in two-dimensional mono-culture by scratch assay method. Surprisingly, a significant dose-dependent delay in wound recovery was discovered with the aqueous ARE treatment (Fig. 4.35). Fibroblasts treated with the ethanolic ARE were not affected and migrated comparable to the controls (Fig. 4.36). These findings are contradictory to the assumed enhanced migration. *In vitro* wound healing investigations under AREs treatment in fibroblasts have not been reported, yet. Hsiao *et al.* documented a dose-dependent cell migration inhibition by an ethanolic Zicao species extract of *L. erythrorhizon*, in wound closure assay. This was measured by scratch (24 h) and Boyden-chamber assay (6 h), where the fibroblasts had to migrate additionally through a membrane (Hsiao *et al.*, 2012). The discrepancy between our findings may be caused by the use of a different Zicao species and a varying extraction method. However, under the current culture and experimental conditions, the cellular movement was not improved. Although this method is standardized and commonly used for investigating fibroblast's movement (Hulkower & Herber, 2011), the attachment on a plastic surface may be inadequate for proper cell migration by myosin-actin stretching. The insufficient attachment with respect to the missing ECM network could reduce the general cellular movement. Usually, fibroblasts migrate with the help of receptors as integrins and laminins (Chester & Brown, 2016; Grinnel & Petroll, 2010). They bind with these specific ligands to cell surfaces or preferred ECM molecules such as fibrin, fibronectin and collagens. Therefore, other experimental conditions such as collagen pre-coated culture plates may change the outcome of this investigation (Liang *et al.*, 2007).

During migration cellular movement (detachment, attachment) is combined with cell proliferation. Because of the missing migratory impact of ethanolic ARE, accompanied by observed reduced proliferation, an increased migration of proliferation inhibited fibroblasts was expected, compared to control cells. Though, fibroblasts with x-ray radiation inhibited cell division also migrated comparably fast as control

cells (Fig. 4.37). A possible explanation for the uninfluenced migration can be the shown significantly reduced cell viability.
Although it is possible that the aqueous ARE increased the fibroblasts migration *in situ* due to the combined stimulation of the whole surrounding environment of cells and chemical mediators. However, this impact was not detected under the chosen culture conditions *in vitro*.

An enhanced energy level accompanied with a positive trend on cell viability may indicate reduced apoptosis by aqueous ARE extract. Here, the influence on apoptosis-related proteins was studied. Within this investigation there was no detectable induction of apoptotic pathways related to caspase 3 protein by the aqueous ARE treatment (Fig. 4.38). Investigations on AREs, with respect to apoptosis induction, have not been reported. Previous studies with shikonin, as an active component of *A. euchroma*, have shown increased numbers of apoptotic fibroblasts after 96 h treatment, detected by Terminal deoxynucleotidyl Transferase dUTP nick end labeling (TUNEL) assay (Y. Xie *et al.*, 2015). They further performed protein and gene level analyses and observed enhanced apoptosis by caspase 3 activation with increased cleaved caspase 3 level due to shikonin treatment. Aqueous ARE did not induce caspase 3 related apoptosis, which could be caused by missing shikonin in this extract. The missing apoptosis induction matches the increased viability and energy level due to the presence of aqueous ARE during cultivation.

The enhanced energy level of cultured fibroblasts by the aqueous ARE treatment seemed not to be used for cell proliferation or migration *in vitro*. Therefore, the enlarged ATP amount was supposed to increase the syntheses of molecules concerning granulation tissue formation. Protein level studies of different important ECM molecules were conducted only on aqueous ARE treated unwounded fibroblasts, because of the missing positive impact with the ethanolic ARE treatment. The establishment of an improvised ECM after injury is an important wound healing associated mechanism, which enables cell migration into the injured area (Singer *et al.*, 1999; Velnar *et al.*, 2009; Mouw *et al.*, 2014).
The question was addressed, whether the enlarged energy level of fibroblasts was used to increase the synthesis of collagen type I, which would enable a faster rearrangement of the improvised ECM. Here, a reduced protein level of collagen type I α-II-chain was observed in fibroblasts treated over two days with ARE together with non-affected α-I-chain level (Fig. 4.39). Haukipuro *et al.* observed that procollagen type I and III were increased in the wound fluid during the first days after injury in human, whereas

type I was more prominent than the others (Haukipuro *et al.*, 1991). Another study demonstrated elevated amounts of collagen type III in early wound healing in human, whereas collagen type I protein was absent and its level increased three days after injury (Gay *et al.*, 1978). As collagen type I is normally the dominant type present in unwounded skin (Smith, 1975), the measured reduced protein level of the sub-unit could be caused by decreased protein expression or post-translational degradation. Additionally, the occurrence of other fiber structured collagen molecules, such as collagen type III, would be presumable, and should be investigated in further studies. Moreover, it is possible that the treatment increased the expression of collagenases, which degrade collagen proteins and therefore reduce the level of intact collagen fibers. This could be beneficial during scar formation, where disorganized collagen I bundles, and therefore keloid formation, can be prevented (Gauglitz *et al.*, 2011) if the ARE treatment reduces the protein level. The extracts´ impact on the expression and activity of proteases must be investigated in following studies to clarify the question of reduced protein expression or increased degradation. However, the experiment was conducted without wounding of the cell mono-layer. Therefore, the protein level may be differing from that influenced by secreted chemical wound healing mediators.

Increased collagen type IV level was assumed due to the new formation of a basal membrane during wound recovery. This network-forming collagen type forms the basis of the basal membrane structure (Lodish *et al.*, 2000) and is additionally an important structural protein of the provisional ECM (Grove, 1982). During our investigations, collagen type IV protein level was not significantly affected by the ARE treatment (Fig. 4.40). These findings indicated specified regulation of collagen I protein level without affecting collagen IV by the treatment. In the case of generally increased collagenase activities, both collagen levels would have been reduced by degradation. This hints to a reduced collagen I expression. On the other hand, two days of treatment might be too early of a time point in which to detect elevated amounts of collagen IV. The investigations further focused another central ECM molecule, fibronectin. This protein is essential for the proper ECM formation (Chester & Brown, 2016). Moreover, fibronectin is an active component of the early generated fibrin clot which enables the initial wound closure and hemostasis. The investigations on fibronectin showed a strong tendency of increased protein level, which was three-fold up-regulated compared to medium control (Fig. 4.41). This impact was not yet significant, caused by the differing fibroblast donor influences on the protein level. The finding of elevated fibronectin level strongly hints to increased formation of an improvisational ECM, which can be an explanation for the *ex vivo* observed improved wound re-epithelialization. Again, this experiment was performed on unwounded cells. The effect is assumed to be

increased due to injury mediated released cell signals, which should be investigated in further studies. Additionally, fibronectin is essential for cellular migration, which was demonstrated by Cheng and coworkers (Cheng *et al.*, 1988). Here, improved wound healing by fibronectin application was detected in rats. It was further shown that fibronectin application improved the healing of lesions in rats with the biggest impact on day two and three after wounding (Jo *et al.*, 1991). These findings support the present assumption of accelerated *ex vivo* re-epithelialization by enhanced fibronectin level. Further studies on fibronectin gene and protein expression must be performed in order to verify increased synthesis or decreased protein degradation by proteinases as MMPs. The aqueous ARE treatment seems to support the formation of the provisional ECM, which was shown by elevated fibronectin level as well as by reduced collagen I progenitor. They provide a network for migrating cells, which can accelerate epidermal wound recovery as well as neovascularization (Grove, 1982).

The positive wound healing effect of the aqueous ARE detected in *ex vivo* cannot be completely explained by these *in vitro* investigations. It could be caused by the aqueous ARE effect on fibroblast energy balance and activity. This elevated energy level increased production of ECM-related molecules, which improved the granulation phase. Moreover, an amplified migratory ECM network accelerates re-epithelialization. Further studies should evaluate the effects of fibroblasts mediator secretion, which can influence keratinocytes, under aqueous ARE treatment (*e.g.* by enzyme-linked immunosorbent assay method).

Cultured human skin cells are commonly used, simplified test systems to address specific questions in preliminary investigations. However, mono-cultures are limited to one cell type and miss inter-cellular interactions and complex chemical influences (Ueck *et al.*, 2017). Therefore, discrepancies between *in vitro* data and *in vivo* situation occur frequently. However, they help to understand complex mechanisms in simplified systems, but their informative value is limited. *In vitro* investigations on co-culture systems and skin-equivalents are recommended. In fact, these culture systems are much more complex in handling and cost intensive. Furthermore, the findings in cell culture systems are dependent on the chosen medium and supplements (Zorn-Kruppa *et al.*, 2016). The medium can influence protein level and expression pattern and therefore may influence the transferability from cell culture results to *ex vivo* WHMs. Moreover, the used cells were derived from infant, male, healthy donors of the same age (under five years of age). This enables a comparable homogeneity of the donor sources compared to the differing sex of porcine and human *ex vivo* WHMs. Infant cells were described

to show faster wound healing in comparison to adult-derived cells (Mateu *et al.*, 2016).

The validation of these *in vitro* findings should be supplemented by appropriate animal investigations or transferred back to clinic approaches of different treatment durations.

5.3.3. Anti-oxidative Capacities of Aqueous *A. Euchroma* Extract

The initial inflammation phase during wound healing was shown to be accompanied by the elevated formation of free radicals (Hasio *et al.*, 2012; Blakytny & Jude, 2006). Radicals detoxified wounds from foreign particles and pathogens and acted as a second messenger to recruit immune active and epithelial cells (Dunnill *et al.*, 2017; Singer *et al.*, 1999). Here, modulated by increased expression of pro-angiogenic factors, angiogenesis and therefore proper wound bed supply were improved (Kurahashi & Fujii, 2015). Healthy tissue hemostasis was kept up by balanced radical presence. Low levels resulted in cell cycle arrest with cytostatic effects (Dunnill *et al.*, 2017). Increased ROS, in contrast, degraded membrane structures and induced the transcription of genes associated with cell death activation or cause direct DNA, protein or lipid damage (R. Thakur *et al.*, 2011). These processes are summarized as oxidative stress. The amount of ROS was shown to be frequently increased in impaired healing wounds (Schäfer & Werner, 2008). Oxidative stress is normally prevented and regulated by molecules with radical scavenging capacities. These molecules can be oxidized and transfer electrons to radicals which are thereby reduced and re-establish a non-active condition. Anti-oxidative effects of herbal compounds were demonstrated to promote wound healing by reducing amounts of free radicals that can otherwise damage intact tissue cells and negatively influence pH. Further, oxidative stress was observed to degrade ECM molecules, as collagens, resulting in amplified skin aging and delayed wound healing (Yoo *et al.*, 2014). The equilibrium between reactive radicals and radical scavengers determine the wound healing outcome.
Parts of the observed improved *ex vivo* re-epithelialization by aqueous ARE treatment were assumed to be caused by anti-oxidative impacts. The ethanolic ARE showed no impact on early re-epithelialization, therefore we only investigated the aqueous ARE to identify its anti-oxidative characteristics. Studies of the fresh aqueous decoction of *A. euchroma* were performed on peroxyl- and organic radical scavenging capacity by DPPH and ORAC assay. The hydrophilic extract reduced available radicals in a dose-dependent manner (Fig. 4.7). 31.5 ± 1.6 µg/ml aqueous ARE inhibited the half of the present peroxyl radicals. Therefore, the effective extract doses used in *ex vivo*

were able to scavenge even more peroxyl radicals in the wound, which may contribute to the improved wound healing. The effectiveness was moderate compared to trolox and NAC, which were used as anti-oxidant reference substances with high scavenging capacities. *Arnebia* species were described for their anti-oxidative impacts, which were documented investigating hydrophobic extracts in cell-free assays (Shameem *et al.*, 2015; Tiga *et al.*, 2016; Assimopoulou *et al.*, 2004). Ganie *et al.* studied soxhlet extracts on their radical scavenging capacity, with ethyl acetate, ethanol, methanol and water as consecutive solvents (Ganie *et al.*, 2014). The anti-oxidant capacity was demonstrated with the same hierarchy from high scavenging to lower capacity. The aqueous extract showed moderate DPPH scavenging capacity with a lower impact than the other solvents. A quantitative comparison of the present results was not possible due to unequally used reference compounds. Hsiao *et al.* documented reduced ROS production in fibroblasts cultured in the presence of an ethanolic *L. erythrorhizon* extract (Hsiao *et al.*, 2012). Additionally, some chromatographically detected molecules were described for their radical scavenging capacities, which supported these findings. During the chromatographic investigations, high amounts of polar compounds were detected, which are experience-based assumed to be mainly polysaccharides (sec. 4.3.2 - sec. 4.3.3). Ou *et al.* have previously shown that a crude polysaccharide extract of *A. euchroma* reduced oxidative stress and infection accompanied by activation of the complement system in rat lung infection models (Ou *et al.*, 2016) and therefore may positively contribute to wound recovery. The present moderate effect may protect the cells *in situ* from oxidative stress and damage by preventing increased radical levels (Velnar *et al.*, 2009; Falanga, 2005). However, due to sterile culture conditions in the *ex vivo* WHM, non-infected wounds were investigated with expected moderate radical levels. The determined radical scavenging capacity might be a beneficial side effect, which promoted the wound healing.

5.3.4. *A. Euchroma* Extracts Application Studies: Impact of Time Point and Application Method

Enhanced re-epithelialization was observed by treatment with the aqueous ARE within the first two days after injury. To optimize the therapeutic approach of AREs as skin injury treatment, *ex vivo* wound healing studies were investigated to clarify the ideal application time and method after wounding. Usually, an injury occurs and the adequate treatment is not directly available. Therefore, we wanted to address the question of whether the AREs have a positive impact on early advanced wound healing processes, 24 h past wounding. The extracts were applied one day after injury and the WHMs cultured for a further 48 h. Here, no significant influence was de-

tected on wound regeneration with the aqueous ARE (Fig. 4.15). In contrast, the ethanolic ARE showed a strong tendency to improved re-epithelialization in the general cohort and in the impaired healing sample group compared to untreated control (Fig. 4.16). However, this was not significant compared to the solvent control. DMSO control also improved wound healing whereas the ethanolic ARE impact may be in part explained by the DMSO influence. As mentioned in the material and methods section (sec. 3.12) inflammation and hemostasis are reduced in the *ex vivo* WHM due to the lack of microcirculation. The model primarily addressed questions of the epidermal regeneration, which starts within hours after injury. One day after the injury, the re-epithelialization progress is already advanced. Hence, processes as *e.g.* cell proliferation and the establishment of a provisional ECM are taking place. The application effort of aqueous ARE was more beneficial in the first hours directly after wounding (sec. 4.2.5) whereas the ethanolic extract showed a positive trend on wound healing in later wounds. The present investigation showed wound healing promotion during granulation tissue formation and the ECM arrangement, which improved epidermal recovery. This was supported by the findings that hydrophobic AREs enhanced the subsequent granulation and angiogenesis-related processes in animal experiments over long-term durations for weeks after injury, which has been discussed in the previous chapters. Ethanolic ARE was further observed to improve collagen bundle density in burn wounds after 18 days of therapy in rats (Ashkani-Esfahani *et al.*, 2012) which indicates improved ECM formation and supports our results. Both AREs have clearly different impacts on other wound healing phases, whereas they should be used consecutively.

Moreover, the question of whether the application method changes the outcome of the therapeutic approach was addressed. The comparison of aqueous ARE as a central wound application after wounding with wound margin conditioning (only epidermal contact) showed higher wound healing improvement by direct wound application (Fig. 4.17). Here, the treatment stayed in contact with the present dermal and epidermal cells. This leads to the assumption that the aqueous extract affected the tissue present cell types in a complex and interactive manner. These findings were supported by our *in vitro* data, where fewer treatment impacts were observed in keratinocytes mono-culture compared to cultured fibroblasts. High energy levels of fibroblasts were discovered together with enhanced fibronectin expression, which can help to promote keratinocytes migration from the wound margins.
Interestingly, there was a strong positive trend of ethanolic ARE by wound margin application (Fig. 4.18; sec. 4.4.7). These findings indicate interactive stimulation of the tissue ingredient cells with respect to no detected positive impact on

cultured keratinocytes. Cultured fibroblasts were not affected by the ethanolic ARE *in vitro* regarding their migration or they were even negatively influenced as detected by the measured decreased viability, proliferation, and ATP level. These support the assumption of interacting cell types and chemical mediators during re-epithelialization *ex vivo*, which could not have been confirmed under the chosen *in vitro* conditions. Explanations for the discrepancy of *in vivo*, *in situ* and *in vitro* observed effects were discussed before in detail. In contrast to our previous findings, DMSO control applied on the wound, tended to decrease wound healing. The here missing positive impact can be caused by the prominent intrinsic good healing capacity of this cohort (w/o). A wound healing promotion effect in specimens with proper intrinsic healing is less visible than in donor skin with reduced intrinsic healing, which could be improved by external treatments. These samples were not as effectively addressed as previous ones (sec. 4.2.5).

5.3.5. Barrier Formation under *A. Euchroma* Extracts Influence as Important Aspect of Later Wound Healing Phases After Successful Re-epithelialization

A subsequent, important wound healing process is the re-establishment of a functional barrier. The observed dose-dependent positive tendency on cell viability of differentiated keratinocytes treated with the aqueous ARE, brought about the hypothesis of positive AREs impact on barrier formation. This analysis was investigated in differentiation induced and with both AREs treated keratinocytes (TER, sec. 4.5.3.5). The aqueous ARE showed a partly significant positive impact on early barrier formation around day one after calcium shift (Fig. 4.28). Here, the very initial barrier induction was improved and later ones were not or even negatively affected by the treatment. The concentrations of 0.2 and 2 µg/ml ethanolic ARE, on the other hand, showed a strong improvement on TER formation around day three after calcium shift (Fig. 4.29). The missing significance was caused by a high variation between the different tested cell donors as discussed before. The highest concentration improved the TER around day one as aqueous ARE did and showed, from then on, a significant reduction. The recent investigations showed improved barrier establishment by the aqueous and ethanolic AREs which were not documented before. Chang *et al.* documented improved skin barrier function due to the treatment with an emulsion of an ethanolic extract of *L. erythrorhizon* over 28 days on the healthy human skin (M.-J. Chang *et al.*, 2008). Here, transepidermal water loss was decreased by the treatment in a dose- and time-dependent manner. An effect on barrier establishment and its retention by ethanolic

ARE is therefore indicated and could be used in advanced wound healing therapy.

5.4. Phytochemical Analyses of Different *A. Euchroma* Extracts

A chromatographic investigation of the used extracts is essential to explain the chemical compound composition, get indications of the mode of actions as well as to publish the gained data. First of all, we investigated a TLC to detect the raw material ingredient, main chemical groups and thereby give hints to possible active compounds. This method was further used to clarify the herbal identity compared to reference extracts and to establish a fingerprint of the raw material of *A. euchroma*. A fingerprint enables the comparison to plants obtained in the future, for continued investigations with the successful wound healing promoting *A. euchroma* material of these analyses. A methanolic ARE was used to extract the main herbal ingredient compounds of *A. euchroma*. Signals belonging to anthracene, essential oils, saponins as well as strong signals for flavonoids were detected (Fig. 3.2, sec. 3.11.1.2). Previously, some representatives of flavonoids, saponins and essential oils/terpenes and conjugates of sugars have been described for their wound healing supporting capabilities (Tsuchiya *et al.*, 1996; Budovsky *et al.*, 2015). The molecular identification of the observed chemical signal spots has to be investigated in prospective studies to estimate their individual wound healing potentials.

Re-epithelialization was improved by aqueous ARE, whereas both the ethanolic ARE and shikonin showed no significant impact in the *ex vivo* model. It was supposed that the aqueous ARE contains active secondary metabolites, which are not present in the ethanolic one. Therefore, the AREs were compared regarding their ingredient compound classes and in particular their naphthoquinones content. The root of *A. euchroma* was described to contain shikonin and its derivatives (Sharma *et al.*, 2008; Zhou *et al.*, 2011; H.-M. Li *et al.*, 2011). Here, the question arose if shikonin, as a previously described wound healing promoting compound (Papageorgiou *et al.*, 2008), was contained in the effective aqueous ARE. TLC was performed to separate both AREs compared to commercial shikonin. There was a shikonin signal present in the ethanolic ARE samples and absent in the aqueous ones (Fig. 4.3). Depending on the applied amount of shikonin, the retention factor varied. Lower concentrated shikonin (lane 9 & 10) had the same retention factor than the signal in the ethanolic ARE. Additional signals in the lanes of ethanolic and methanolic extract indicated isomers and shikonin derivatives.

These findings were supplemented by a more sensitively comparative investigation using UHPLC-HRMS, following continuous evaluation of the resulting signals by dereplication process with herbal databases. Here, the characteristics of the detected peak were compared to present herbal specific information with described ingredient chemical compounds. This investigation verified the TLC results of the missing shikonin signal in aqueous and the present signal in the ethanolic ARE (Fig. 4.4). The discovered wound healing capacity of the aqueous ARE cannot be explained by the impact of this single compound. Continuative UHPLC-HRMS analyses were conducted with subsequent dereplication of both AREs. This method is very sensitive and traces of secondary metabolites can be detected. In general, fewer peaks with minor intensities were observed in the aqueous extract compared to the ethanolic ARE (Fig. 4.5, sec. A.2). In both extracts, there were peaks that could be identified as other naphthoquinones. This was in good agreement with studies that described the presence of naphthoquinones *e.g.* shikonin, acetyl shikonin, β-β-dimethylacryl-shikonin, β-acetoxyisovalerylshikonin in the herbal material of *A. euchroma* (Xiao *et al.*, 2011; Sharma *et al.*, 2008). Moreover, rosmarinic acid was identified exclusively in the aqueous ARE. This flavonoid was already described for its wound healing promotion by its anti-oxidative capacity (Soni & Singhai, 2012). It supported the wound recovery by positively influencing the redox balance in the wound. The described anti-oxidative capacities may explain (at least in part) the observed radical scavenging and can contribute to the *ex vivo* re-epithelialization by the aqueous ARE. Rosmarinic acid was previously isolated from another *Arnebia* species and is therefore known to be a potential ingredient in this genus (Yuzbasioglu *et al.*, 2015).

Due to different extraction methods of watery decoction on the one hand and ethanolic ultrasonic extraction on the other hand, different polar chemical compounds were expected in the AREs. Aqueous ARE was supposed to contain mainly sugars and amino acids and some alcohols, whereas lipids should not be present with respect to their polarity. Ethanol may extract a comparable composition whereas lipids and more alcohols may be present in the extract. UHPLC-ELSD revealed high amounts of polar non-UV light-absorbing constituents in the aqueous ARE compared to the ethanolic one (Fig. 4.6). Such compounds are mainly sugars, amino acids, lipids and alcohols (Douville *et al.*, 2006). It has been described that an orally given aqueous crude polysaccharide extract from *A. euchroma* reduced oxidative stress and activated the immune complement system in rat models (gradual extraction with water, precipitated with trichloroacetic and ethanol to remove proteins; Ou *et al.*, 2016). The polysaccharide compounds significantly reduced lipid peroxidation and increased levels of superoxide dismutase, which is one of the most important endogenous anti-oxidative enzymes. All these supported the healing of acute lung infections and may indicate

wound healing potential of *A. euchroma* polysaccharides. However, it is critical to mention, that orally given polysaccharides are going to be processed by digestion whereas resulting secondary metabolites may be responsible for the observed effect. Local wound application may a have different impact. The main sugar representatives from both AREs need to be identified in further studies and their individual and combined wound healing capacities have to be evaluated. Further topical studies showed improved wound healing by application of crude sugar due to pH reduction with various anti-bacterial capacities and local osmotic influences (Chirife *et al.*, 1983; Biswas *et al.*, 2010). The former of these, increased granulation tissue formation (Chirife *et al.*, 1982). The detection of a huge amount of polysaccharides in the aqueous ARE may indicate an explanation for the observed accelerated epidermal regeneration. Furthermore, the ethanolic extract showed additional exclusive peaks for arnebin I and II. Arnebin I was shown to enhance wound healing in acute and impaired wounds in rats by promoting cell migration, proliferation and neovascularization (Sidhu *et al.*, 1999). Furthermore, it improved the recovery of wounds in diabetic rats (Zeng & Zhu, 2014). Zeng *et al.* demonstrated promotion of angiogenesis-related pathways by arnebin I in HUVEC (Zeng *et al.*, 2015). These reports described improved wound healing promotion, which was explained by accelerated neovascularization that could not be addressed in our *ex vivo* WHM.
The findings support the expectations concerning the extract differences by the solvents, water and ethanol and their resulting hydrophilic (aqueous) and more organic extract (ethanolic ARE). Those data support the different observed wound healing impact of aqueous ARE with respect to differing ingredient chemical compounds. The complete identification of the extracts ingredients is complex and depends on the existing incorporated chemical information of the used database and the effectiveness of the performed molecule separation. A complete determination and conclusions about quantities are only possible if the expected chemical substance is used as a direct reference in a defined amount.

A. euchroma and other Zicao species were described to contain PAs (P. P. Fu *et al.*, 2002; Röder & Rengel-Mayer, 1992). These secondary metabolites of plants were synthesized to protect them from herbivores. Unsaturated representatives are under suspicion to cause hepatic damage and, in high and long-term doses, cancer development. Therefore, the oral uptake was recommended to be reduced or avoided. Hydrophilic aqueous ARE was expected to contain fewer naphthoquinones and PAs than extracts of more hydrophobic solvents. During our TLC investigations, no alkaloid molecules were detected, which indicates general minor amounts of possible toxic PAs in the *A. euchroma* root. The present UHPLC-HRMS data of the AREs were analyzed with

respect to the presence of PAs. In both extracts signals of PAs were detected. In total six, possibly toxic, unsaturated PA compounds were isolated from *A. euchroma* roots by Smyrska-Wieleba *et al.* (Smyrska-Wieleba *et al.*, 2016). Traces of three PAs, discovered by Smyrska-Wieleba *et al.*, were observed in both extracts and one additional in the ethanolic ARE with comparable peak intensities (sec. A.2). The detected UHPLC-HRMS intensities were comparable. Since traces of alkaloids can be very sensitively detected by this method, further quantifications of these compounds need to be performed. The final identification and quantity of the specific PAs cannot be predicted and has to be quantitatively investigated in future studies. The consequences of these findings will be discussed in the next chapter sec. 5.5.
The findings are initial steps towards gaining a complete knowledge of the chemical composition contained in the root material of *A. euchroma* and its different, active wound healing extracts. The comparative chromatographic investigations should be expanded. This will determine the main compounds qualitatively and quantitatively within the analysis of partly fractionated extracts in accordance to reference substances.

5.5. Responsible Usage of Phytotherapeutics

Phytotherapeutics contain multi-component formulations (R. Thakur *et al.*, 2011). The ingredient compounds may react with each other and this can result in inactivated secondary metabolites or new compounds with possible toxicity. Additionally, there is the risk of containing toxic substances depending on the soil where the plant was grown, possible herbicide treatments and plant-derived secondary metabolites, which protect them from herbivores (European Medicines Agency, 2014; Pinho *et al.*, 2012). Therefore, it is essential to use the herbal material of trustful sources. Herbal specialized pharmacies cooperate with external testing laboratories, which exclude possible intoxication by heavy metals amongst others. The herbal identities of the used material and comparability compositions, in the case of several herbal sources, were confirmed by our laboratory and additionally by an external laboratory.
Wound healing promotions of varying intensities were detected by aqueous ARE of different raw material origins within the porcine and human *ex vivo* WHMs (Fig. 4.9). All showed positive wound healing impact and were identified as *A. euchroma* derived. However, the observed variation could be due to differing amounts of herbal secondary metabolites caused by different nutrition, due to the used soil, water content or plant treatment. Plant harvesting, drying and storage conditions may further affect the herbal ingredient chemical composition. These small differences were observed by varying TLC intensities of the detected chemical subgroups (Fig. 3.1). The

primary investigated herbal raw material (source I) was the same over the whole duration of the study. Therefore, it is comprehensible that the ingredient´s compounds stayed in contact with air, light and potential microbes during the project at every time point when the storage reservoir was opened for fresh extractions. It is further possible that the root material composition may vary concerning the radix area, central or outer sheet of the root. This is why small variations of extraction charges cannot be completely excluded. However, the present investigated extracts were standardized in preparation, completely dried, frozen, stored and used within a maximum of six months after extraction. The exact extract composition of different extracts can only be determined by complex and expensive investigations such as HPLC measurements. However, all tested concentrations and herbal sources tended to support epidermal wound regeneration *ex vivo*. When different sources were compared and application methods and time points were analyzed, reduced wound healing promotion was discovered by the aqueous extract, compared to the initial investigations (Fig. 4.10, A). The following evaluation during this project of all the performed aqueous ARE treated WHMs, resulted in significantly accelerated wound regenerating (132.2 ± 6.2 % with 500 µg/ml; Fig. 4.10, B). The weaker extract impact at later time points during this project can be caused by extended herbal storage duration. It can be a further effect caused by donor specimen heterogeneity (Ueck *et al.*, 2017).

The performed chromatographic investigations indicated the presence of PAs in the ethanolic and aqueous ARE. The high sensitivity analysis gives no conclusion about the amount and actual toxicity of the cutaneously applied molecules. Previous reports described small amounts of total PAs in *Arnebia* compared to other Zicao species (Röder, 1995 & 2000; Röder & Rengel-Mayer, 1993). With respect to the report of Dharmananda the total yield of PAs in *A. euchroma* is 0.0006 % (compared to *L. erythrorhizon* 0.02 %; Tang, 1995 as cited in Dharmananda, 2001). According to the European Medicines Agency report, the oral uptake of PAs is not to exceed 0.007 µg per kg body weight per day with a maximum of two weeks treatment (0.35 µg/day at 50 kg body weight). Their recommendation for topical short-term usage of unsaturated PAs should be less than 0.35 µg (adult, related to intact skin; Brauchli *et al.*, 1982 as cited in European Medicines Agency, 2014). We theoretically used less than 0.15 µg total PAs as an effective dose, (500 µg/ml) per day in the *ex vivo* WHMs with respect to the 0.0006 % assumed total amount in *A. euchroma* raw material. The controlled temporary usage should keep possible intoxication of PAs as small as comparable during normal food consumption. For example, honey and milk were proven to contain varying amounts of toxic alkaloids depending on the origin of the collected nectar and fodder plants (Röder, 1995; P. P. Fu *et al.*, 2002; Neuman *et al.*, 2015). However, Braucchli

et. al demonstrated 20 - 50 times increased PAs uptake by oral therapy compared to the application on injured skin (Brauchli *et al.*, 1982). To guarantee the safety of the herbal AREs, further phytochemical studies should be performed to ensure all extracted molecular identities and their total quantities. Here, the extracts would stay in direct contact with the blood stream, when applied on open wounds, and therefore the number of incorporated chemical molecules has to be judged differently than compared with intestinal uptake or application on intact skin. Previous studies support the safe usage of different AREs as wound healing agents with respect to non-documented harmful or toxic side-effects by the treatment, even during long-term usage over weeks (2.3.5).

5.6. Perspectives on Wound Healing Support by *A. Euchroma* Treatment

During the hypothesis-driven screening of this Ph.D. project wound healing promotion was observed by aqueous ARE short-term treatment in *ex vivo* human and porcine WHMs. This impact was more prominent by direct wound application, with dermal and epidermal treatment contact, compared to wound margin application. Aqueous ARE was initially shown to have moderate anti-oxidative capacities, which is supported by the finding of rosmarinic acid and high amounts of polysaccharides in the extract. The anti-oxidative capacity is expected to be involved in the wound recovery process. In the *ex vivo* study, standardized acute epidermal-dermal wounds were created under sterile, non-contaminated conditions. Hence, the described anti-microbial impact of different AREs (Kaith *et al.*, 1996; H.-M. Li *et al.*, 2011; Damianakos *et al.*, 2012; Haghbeen *et al.*, 2011) cannot be the complete explanation for the observed regeneration increase. These findings were supported by *in vitro* investigations. Here, aqueous ARE reduced cell attachment of undifferentiated keratinocytes which possibly enable improved mobility *ex vivo*. Additional to the re-epithelialization improvement aqueous ARE showed positive influence on early barrier formation of differentiating keratinocytes. Fibroblasts, treated with aqueous ARE, showed increased viability and generated higher amounts of ATP. The increased energy level can be, on the one, hand secreted and provide a general energy supply for all wound healing associated mechanisms in the tissue. It can, on the other hand, increase synthesis of keratinocytes migration improving molecules such as EGF, TGF-α and KGF (J. Li *et al.*, 2007), which would explain the improved re-epithelialization. Moreover, the formation of a provisional ECM was increased, determined by enhanced fibronectin level accompanied with reduced collagen type I. This accelerated improvisational ECM provides an excellent network for migrating keratinocytes to re-epithelialize the wounded area. In

previous studies, further molecular key players of the process as *e.g.* TGFs and other growth factors, MMPs and collagenases should be investigated to discover the complete mechanism behind the improved epidermal regeneration.
In contrast, ethanolic ARE tended to positively affect subsequent wound healing phases, which was shown in wounds that were treated 24 h after injury for the first time. Additionally, the wound healing improvement was enhanced by wound margin application. However, both effects were partly caused by ingredient DMSO. Again, barrier formation was improved in cultured differentiated keratinocytes where the ethanolic extract showed strong TER enhancing tendency around day three. Furthermore, this extract did not positively affect cultured keratinocytes and fibroblasts.
Different extracts of *A. euchroma* accelerated varying processes of wound healing and can be used with respect to their individual or additive effects. The present data suggest a combined utilization of firstly utilizing aqueous extract on fresh wounds with a shift to ethanolic ARE during the subsequent wound healing phases.
Aqueous ARE showed a great impact on early epidermal regeneration of acute wounds and ethanolic ARE can be used in a second instance to promote granulation tissue re-arrangement and angiogenesis. Further studies are needed to figure out the detailed molecular underlying mechanisms to enable optimized ARE treatment. Especially the detailed knowledge about the identity and quantity of the extracts chemical compounds will enable optimized ARE wound healing concepts. This project revealed indication for the effective usage of specific aqueous *A. euchroma* derived extract for external wound healing, which has to be verified in future clinical studies. The different extract studies should be investigated with regards to potential side effects and ensures their safe usage. These investigations enabled *ex vivo* and *in vitro* analyses of previously traditional described wound healing impacts that have to be re-transferred to the clinic in the future.

6. References

Abercrombie, M, Flint, M H, & James, D W (1956). Wound Contraction in Relation to Collagen Formation in Scorbutic Guinea-pigs. Development, 4(2), 167-175.

Aliasl, J, Khoshzaban, F, Barikbin, B, Naseri, M, Kamalinejad, M, Emadi, F, Razzaghi, Z, Talei, D, Yousefi, M, Aliasl, F, Barati, M, Mohseni-Moghaddam, P Hasheminejad, S A & Esmailzad Nami, H (2014). Comparing the Healing Effects of *Arnebia euchroma* Ointment With Petrolatum on the Ulcers Caused by Fractional CO2 Laser: A Single-Blinded Clinical Trial. Iranian Red Crescent Medical Journal, 16(10), e16239.

Andújar, I, Recio, M C, Bacelli, T, Giner, R M, & Ríos, J L (2010). Shikonin reduces oedema induced by phorbol ester by interfering with IkappaBalpha degradation thus inhibiting translocation of NF-kappaB to the nucleus. British Journal of Pharmacology, 160(2), 376-88.

Andújar, I, Ríos, J L, Giner, R M, & Recio, M C (2013). Pharmacological properties of shikonin - a review of literature since 2002. Planta Medica, 79(18), 1685–97.

Ashkani-Esfahani, S, Imanieh, M H, Khoshneviszadeh, M, Meshksar, A, Noorafshan, A, Geramizadeh, B, Ebrahimi, S, Handjani, F, Tanideh, N (2012). The healing effect of *arnebia euchroma* in second degree burn wounds in rat as an animal model. Iranian Red Crescent Medical Journal, 14(2), 70-4.

Ashkani-Esfahani, S, Imanieh, M H, Meshksar, A, Khoshneviszadeh, M, Noorafshan, A, Geramizadeh, B, Ebrahimi, S, Handjani, F, Nadimi, E & Jafari, S M S (2012). Enhancement of Fibroblast Proliferation, Vascularization and Collagen Synthesis in the Healing Process of Third-Degree Burn Wounds by Topical *Arnebia euchroma*, a Herbal Medicine. Galen Medical Journal, 1(2), 53-59.

Assimopoulou, A, Boskou, D, & Papageorgiou, V P (2004). Antioxidant activities of alkannin, shikonin and Alkanna tinctoria root extracts in oil substrates. Food Chemistry, 87(3), 433-438.

Assimopoulou, A N, & Papageorgiou, V P (2005). Radical scavenging activity of Alkanna tinctoria root extracts and their main constituents, hydroxynaphthoquinones. Phytotherapy Research, 19(2), 141-147.

Auyeung, K K, Han, Q-B, & Ko, J K (2016). *Astragalus membranaceus*: A Review of its Protection Against Inflammation and Gastrointestinal Cancers. The American Journal of Chinese Medicine, 44(1), 1-22.

Bäsler, K, Bergmann, S, Heisig, M, Naegel, A, Zorn-Kruppa, M, & Brandner, J M (2016). The role of tight junctions in skin barrier function and dermal absorption. Journal of Controlled Release, 424, 105-118.

Bikle, D D, Xie, Z, & Tu, C-L (2012). Calcium regulation of keratinocyte differentiation. Expert Rev Endocrinol Metab, 7(4), 461-472.

Biswas, A, Bharara, M, Hurst, C, Gruessner, R, Armstrong, D, & Rilo, H (2010). Use of sugar on the healing of diabetic ulcers: a review. Journal of Diabetes Science and Technology, 4(5), 1139-45.

Blakytny, R, & Jude, E (2006). The molecular biology of chronic wounds and delayed healing in diabetes. Diabetic Medicine, 23(6), 594-608.

Booth, B A, Polak, K L, & Uitto, J (1980). Collagen biosynthesis by human skin fibroblasts. I. Optimization of the culture conditions for synthesis of type I and type III procollagens. Biochimica et Biophysica Acta, 607(1), 145-60.

Bouzaiene, N N, Jaziri, S K, Kovacic, H, Chekir-Ghedira, L, Ghedira, K, & Luis, J (2015). The effects of caffeic, coumaric and ferulic acids on proliferation, superoxide production, adhesion and migration of human tumor cells *in vitro*. European Journal of Pharmacology, 766, 99-105.

Bradford, M M (1976). A rapid and sensitive method for the quantitation of microgram quantities of protein utilizing the principle of protein-dye binding. Analytical Biochemistry, 72(1), 248-254.

Brandner, J M, Houdek, P, Quitschau, T, Siemann-Harms, U, Ohnemus, U, Willhardt, I, & Moll, I (2006). An Ex-vivo Model To Evaluate Dressings & Drugs For Wound Healing Example: Influence of lucilia sericata extracts on wound healing progress. EWMA, 6(2), 11–15.

Brandner, J M, Kief, S, Grund, C, Rendl, M, Houdek, P, Kuhn, C, Tschachler, E, Franke, W W & Moll, I. (2002). Organization and formation of the tight junction system in human epidermis and cultured keratinocytes. European Journal of Cell Biology, 81(5), 253-63.

Brandner, J M, Moll, I, Siemann-Harms, U, & Houdek, P (2004). *Ex vivo* Skin Organ Model Made Of Pig Skin. Patent PCT/DE2004/000782.

Brandner, J M, Zorn-Kruppa, M, Yoshida, T, Moll, I, Beck, L A, & Benedetto, A D (2015). Epidermal tight junctions in health and disease. Tissue Barriers, 3(1-2).

Brauchli, J, Lüthy, J, Zweifel, U, & Schlatter, C (1982). Pyrrolizidine alkaloids from Symphytum officinale L. and their percutaneous absorption in rats. Experientia, 38(9), 1085-7.

Budovsky, A, Yarmolinsky, L, & Ben-Shabat, S (2015). Effect of medicinal plants on wound healing. Wound Repair and Regeneration: Official Publication of the Wound Healing Society [and] the European Tissue Repair Society, 23(2), 171-83.

Capriotti, K, & Capriotti, J A (2012). Dimethyl sulfoxide: history, chemistry, and clinical utility in dermatology. The Journal of Clinical and Aesthetic Dermatology, 5(9), 24-6.

Chang, I-C, Huang, Y-J, Chiang, T-I, Yeh, C-W, & Hsu, L-S (2010). Shikonin induces apoptosis through reactive oxygen species/extracellular signal-regulated kinase pathway in osteosarcoma cells. Biological & Pharmaceutical Bulletin, 33(5), 816-24.

Chang, M-J, Huang, H-C, Chang, H-C, & Chang, T-M (2008). Cosmetic formulations containing *Lithospermum erythrorhizon* root extract show moisturizing effects on human skin. Archives of Dermatological Research, 300(6), 317-23.

Chen, X, Yang, L, Zhang, N, Turpin, J J A J, Buckheit, R W, Osterling, C, Oppenheim, J J & Howard, O M Z (2003). Shikonin, a component of chinese herbal medicine, inhibits chemokine receptor function and suppresses human immunodeficiency virus type 1. Antimicrobial Agents and Chemotherapy, 47(9), 2810-2816.

Cheng, C Y, Martin, D E, Leggett, C G, Reece, M C, & Reese, A C (1988). Fibronectin enhances healing of excised wounds in rats. Archives of Dermatology, 124(2), 221-5.

Chester, D, & Brown, A C (2016). The role of biophysical properties of provisional matrix proteins in wound repair. Matrix Biology, (in press), 17.

Chinese Pharmacopeia Commission. (2010). Pharmacopoeia of the People's Republic of China, englisch Edition (Vol. I). Beijing: Chemical Industry Press, China.

Chirife, J, Herszage, L, Joseph, A, & Kohn, E S (1983). *In vitro* study of bacterial growth inhibition in concentrated sugar solutions: microbiological basis for the use of sugar in treating infected wounds. Antimicrobial Agents and Chemotherapy, 23(5), 766-73.

Chirife, J, Scarmato, G, & Herszage, L (1982). Scientific basis for use of granulated sugar in treatment of infected wounds. Lancet (London, England), 1(8271), 560-1.

Cho, H R, Cho, Y, Kim, J, Seo, D B, Kim, S H, Lee, S J, & Kim, N I (2008). The Effect of Gromwell (*Lithospermum erythrorhizon*) Extract on the *Stratum Corneum* Hydration and Ceramides Content in Atopic Dermatitis Patients. Annals of Dermatology, 20(2), 56-66.

Clark, R A (1993). Basics of cutaneous wound repair. The Journal of Dermatologic Surgery and Oncology, 19(8), 693-706.

Coldren, C D, Hashim, P, Ali, J M, Oh, S-K, Sinskey, A J, & Rha, C (2003). Gene Expression Changes in the Human Fibroblast Induced by Centella asiatica Triterpenoids. Planta Medica, 69(8), 725-732.

Czemplik, M, Kulma, A, Bazela, K, & Szopa, J (2012). The biomedical potential of genetically modified flax seeds overexpressing the glucosyltransferase gene. BMC Complementary and Alternative Medicine, 12, 251.

Damianakos, H, Kretschmer, N., Syklowska-Baranek, K, Pietrosiuk, A, Bauer, R, Chinou, I, Syklowska-Baranek, K & Chinou, I (2012). Antimicrobial and cytotoxic isohexenylnaphthazarins from *arnebia euchroma* (royle) jonst. (boraginaceae) callus and cell suspension culture. Molecules, 17(12), 14310-14322.

Darby, I A, Laverdet, B, Bonté, F & Desmoulière, A (2014). Fibroblasts and myofibroblasts in wound healing. Clinical, Cosmetic and Investigational Dermatology, 7, 301-11.

Daubrawa, M (2009). Aktivierung eines neuartigen Apoptose-Signalweges durch den Proteinkinaseinhibitor Staurosporin. Ph.D. Thesis. University Hohenheim, Germany.

Dharmananda, S (2001). Safety Issues Affecting Herbs: Pyrrolizidine Alkaloids. Retrieved April 29, 2017, from http://www.itmonline.org/arts/pas.htm

DiPietro, L A, & Polverini, P J (1993). Role of the macrophage in the positive and negative regulation of wound neovascularization. Behring Institute Mitteilungen, 92, 238-47.

Dmitriev, R I & Papkovsky, D B (2012). Optical probes and techniques for O2 measurement in live cells and tissue. Cellular and Molecular Life Sciences : CMLS, 69(12), 2025-39.

Dong, Y, He, L & Chen, F (2005). Enhancement of wound healing by taspine and its effect on fibroblast. Zhong Yao Cai = Zhongyaocai = Journal of Chinese Medicinal Materials, 28(7), 579-82.

Douville, V, Lodi, A, Miller, J, Nicolas, A, Clarot, I, Prilleux, B, Megoulas, N & Koupparis, M (2006). Evaporative light scattering detection (ELSD): a tool for improved quality control of drug substances. Pharmeuropa Scientific Notes, 2006(1), 9-15.

Dreifke, M B, Jayasuriya, A A, & Jayasuriya, A C (2015). Current wound healing procedures and potential care. Materials Science & Engineering. C, Materials for Biological Applications, 48, 651-62.

Duimel-Peeters, I G P, Houwing, R H, Teunissen, C P, Berger, M P F, Snoeckx, L H E H & Halfens, R J G (2003). A Systematic Review of the Efficacy of Topical Skin Application of Dimethyl Sulfoxide on Wound Healing and as an Anti-Inflammatory Drug. Wounds, 15(11), 361-370.

Dunnill, C, Patton, T, Brennan, J, Barrett, J, Dryden, M, Cooke, J, Leaper, D & Georgopoulos, N T (2017). Reactive oxygen species (ROS) and wound healing: the functional role of ROS and emerging ROS-modulating technologies for augmentation of the healing process. International Wound Journal, 14(1), 89-96.

Eckert, R L, & Rorke, E A (1989). Molecular biology of keratinocyte differentiation. Environmental Health Perspectives, 80, 109-16.

Efferth, T, Li, P C H, Konkimalla, V S B, & Kaina, B. (2007). From traditional Chinese medicine to rational cancer therapy. Trends in Molecular Medicine, 13(8), 353-361.

Eming, S A, Krieg, T & Davidson, J M (2007). Inflammation in wound repair: Molecular and cellular mechanisms. Journal of Investigative Dermatology, 127(3), 514-525.

European Medicines Agency (2014). Public Statement on the Use of Herbal Medicinal Products Containing Toxic, Unsaturated Pyrrolizidine Alkaloids (PAs).

Falanga, V (1993). Growth Factors and Wound Healing. The Journal of Dermatologic Surgery and Oncology, 19(8), 711-714. Falanga, V (2005). Wound healing and its impairment in the diabetic foot. The Lancet, 366(9498), 1736-1743.

Feng, Y, Siu, K-Y, Ye, X, Wang, N, Yuen, M-F, Leung, C-H, Tong, Y & Kobayashi, S (2010). Hepatoprotective effects of berberine on carbon tetrachloride-induced acute hepatotoxicity in rats. Chinese Medicine, 5, 33.

Friedemann, T (2015). Neuroprotective effect of Coptis chinensis. Ph.D. Thesis, University Hamburg, Germany.

Friedemann, T, Li, M, Fei, J, Schumacher, U, Song, J, & Schröder, S (2015). Hypothesis-driven screening of Chinese herbs for compounds that promote neuroprotection. Science, 350(6262), 569-571.

Friedemann, T, Otto, B, Klätschke, K, Schumacher, U, Tao, Y, Leung, A K-M, Efferth, T & Schröder, S. (2014). Coptis chinensis Franch. exhibits neuroprotective properties against oxidative stress in human neuroblastoma cells. Journal of Ethnopharmacology, 155(1), 607-15.

Friedemann, T, Schumacher, U, Tao, Y., Leung, A K-M, & Schröder, S (2015). Neuroprotective Activity of Coptisine from Coptis chinensis (Franch). Evidence-Based Complementary and Alternative Medicine, 2015(Article ID 827308), 9.

Friedemann, T, Ying, Y, Wang, W, Kramer, E R, Schumacher, U, Fei, J & Schröder, S (2016). Neuroprotective Effect of Coptis chinensis in MPP+ and MPTP-Induced Parkinson's Disease Models. The American Journal of Chinese Medicine, 44(5), 907-925.

Fritsch, P (2004). Dermatologie Venerologie: Grundlagen. Klinik. Atlas, 2. Auflage. Berlin Heidelberg: Springer-Verlag Berlin Heidelberg.

Fu, Z, Deng, B, Liao, Y, Shan, L, Yin, F, Wang, Z, Zeng, H, Zuo, D, Hua, Y & Cai, Z (2013). The anti-tumor effect of shikonin on osteosarcoma by inducing RIP1 and RIP3 dependent necroptosis. BMC Cancer, 13, 580.

Fu P P, Yang Y-C, Xia, Q, Chou, M W & Lin G (2002). Pyrrolizidine Alkaloids - Tumorigenic Components in Chinese Herbal Medicines and Diatary Supplements. Journal of Food and Drug Analysis, 10(4), 198-211.

Fujita, N, Sakaguchi, I, Kobayashi, H, Ikeda, N, Kato, Y, Minamino, M & Ishii, M (2003). An extract of the root of *Lithospermun erythrorhizon* accelerates wound healing in diabetic mice. Biological & Pharmaceutical Bulletin, 26(3), 329-35.

Gaddipati, J P, Mani, H, Shefali, R K, Mathad, V T, Bhaduri, A P, & Maheshwari, R K (2000). Inhibition of growth and regulation of IGFs and VEGF in human prostate cancer cell lines by shikonin analogue 93/637 (SA). Anticancer Research, 20(4), 2547-52.

Gailit, J, Xu, J, Bueller, H, & Clark, R A F (1996). Platelet-derived growth factor and inflammatory cytokines have differential effects on the expression of integrins α1β1 and α5β1 by human dermal fibroblasts *in vitro*. Journal of Cellular Physiology, 169(2), 281-289.

Galiano, R D, Michaels, V J, Dobryansky, M, Levine, J P, & Gurtner, G C (2004). Quantitative and reproducible murine model of excisional wound healing. Wound Repair and Regeneration, 12(4), 485-492.

Ganie, S A, Dar, T A, Hamid, R, Zargar, O, Ul Abeer, S, Masood, A, Amin, S & Zargar, M A (2014). *In Vitro* Antioxidant and Cytotoxic Activities of Arnebia benthamii (Wall ex. G. Don): A Critically Endangered Medicinal Plant of Kashmir Valley. Oxidative Medicine and Cellular Longevity, 2014, 1-8.

Ganie, S A, Jan, A, Muzaffar, S, Zargar, B A, Hamid, R & Zargar, M A (2012). Radical scavenging and antibacterial activity of Arnebia benthamii methanol extract. Asian Pacific Journal of Tropical Medicine, 5(10), 766-72.

Gauglitz, G G, Korting, H C, Pavicic, T, Ruzicka, T & Jeschke, M G (2011). Hypertrophic scarring and keloids: pathomechanisms and current and emerging treatment strategies. Molecular Medicine (Cambridge, Mass.), 17(1-2), 113-25.

Gay, S, Vijanto, J, Raekallio, J & Penttinen, R (1978). Collagen types in early phases of wound healing in children. Acta Chirurgica Scandinavica, 144(4), 205-11.

Gebäck, T, Schulz, M M P, Koumoutsakos, P & Detmar, M (2009). TScratch: A Novel and Simple Software Tool for Automated Analyses of Monolayer Wound Healing Assays. BioTechniques, 46(4), 265-74.

Gerber, H P, Dixit, V & Ferrara, N (1998). Vascular endothelial growth factor induces expression of the antiapoptotic proteins Bcl-2 and A1 in vascular endothelial cells. The Journal of Biological Chemistry, 273(21), 13313-6.

Gray, G M & Yardley, H J (1975). Lipid compositions of cells isolated from pig, human, and rat epidermis. Journal of Lipid Research, 16(6), 434-40.

Greten, J H (2009). Checkliste Chinesische Phytotherapie. Stuttgart: Hippocrates Verlag in MVS Medizinverlage Stuttgart GmbH &Co. KG.

Grinnell, F & Petroll, W M (2010). Cell Motility and Mechanics in Three-Dimensional Collagen Matrices. Annual Review of Cell and Developmental Biology, 26, 335-361.

Grove, G L (1982). Age-related differences in healing of superficial skin wounds in humans. Archives of Dermatological Research, 272(3-4), 381-5.

Gstraunthaler, G (2003). Alternatives to the use of fetal bovine serum: serum-free cell culture. ALTEX, 20(4), 275-81.

Guo, S & Dipietro, L A (2010). Factors affecting wound healing. Journal of Dental Research, 89(3), 219-29.

Guo, X P, Zhang, X Y & Zhang, S D (1991). Clinical trial on the effects of shikonin mixture on later stage lung cancer. Zhong Xi Yi Jie He Za Zhi = Chinese Journal of Modern Developments in Traditional Medicine, 11(10), 598-9, 580.

Gurtner, G C, Werner, S, Barrandon, Y & Longaker, M T (2008). Wound repair and regeneration. Nature, 453(7193), 314-321.

Haghbeen, K, Pourmolaei, S, Mareftjo, M J, Mousavi, A, Akbari Noghabi, K, Hosseini Shirazi, F & Meshkat, A (2011). Detailed investigations on the solid cell culture and antimicrobial activities of the Iranian *Arnebia euchroma*. Journal of Biomedicine & Biotechnology, 2011(165852).

Han, Y, Jung, H W, Lee, J Y, Kim, J S, Kang, S S, Kim, Y S & Park, Y-K (2012). 2,5-Dihydroxyacetophenone Isolated from Rehmanniae Radix Preparata Inhibits Inflammatory Responses in Lipopolysaccharide-Stimulated RAW264.7 Macrophages. Journal of Medicinal Food, 15(6), 505-510.

Haukipuro, K, Melkko, J, Risteli, L, Kairaluoma, M & Risteli, J (1991). Synthesis of type I collagen in healing wounds in humans. Annals of Surgery, 213(1), 75-80.

Heinrich, W, Lange, P M, Stirtz, T, Iancu, C & Heidemann, E (1971). Isolation and characterization of the large cyanogen bromide peptides from the alpha1- and alpha2-chains of pig skin collagen. FEBS Letters, 16(1), 63-67.

Hempen, C-H, & Fischer, T (2006). Leitpfaden Chinesische Phytotherapie (2. Auflage). Urban & Fischer Verlag/Elsevier GmbH.

Ho, J & Ong, P H (2015). Traditional Chinese Medicine in Dermatology. In Pediatric Skin of Color (pp. 427-437). New York, NY: Springer New York.

Hoo, R L, Wong, J Y, Qiao, C, Xu, A, Xu, H & Lam, K S (2010). The effective fraction isolated from Radix Astragali alleviates glucose intolerance, insulin resistance and hypertriglyceridemia in db/db diabetic mice through its anti-inflammatory activity. Nutrition & Metabolism, 7(1), 67.

Hou, Y, Guo, T, Wu, C, He, X & Zhao, M (2006). Effect of Shikonin on Human Breast Cancer Cells Proliferation and Apoptosis *In Vitro*. The Pharmaceutical Society of Japan, 126(12), 1383-86.

Hsiao, C-Y, Tsai, T-H & Chak, K-F (2012). The molecular basis of wound healing processes induced by *lithospermi* radix: a proteomics and biochemical analysis. Evidence-Based Complementary and Alternative Medicine, 2012, 508972.

Huang, K C (1999). The Pharmacology of Chinese Herbs. CRC Press Inc., Boca Raton, FL. Huang, Z-S, Wu, H-Q, Duan, Z-F, Xie, B-F, Liu, Z-C, Feng, G-K, Gu, L-Q, Chan, A S C & Li, Y-M (2004). Synthesis and cytotoxicity study of alkannin derivatives. European Journal of Medicinal Chemistry, 39(9), 755-64.

Huh, J-E, Nam, D-W, Baek, Y-H, Kang, J W, Park, D-, Choi, D-Y & Lee, J-D (2011). Formononetin accelerates wound repair by the regulation of early growth response factor-1 transcription factor through the phosphorylation of the ERK and p38 MAPK pathways. International Immunopharmacology, 11(1), 46-54.

Hulkower, K I & Herber, R L (2011). Cell migration and invasion assays as tools for drug discovery. Pharmaceutics, 3(1), 107-24. Im, M J C & Hoopes, J E (1970). Energy metabolism in healing skin wounds. Journal of Surgical Research, 10(10), 459-464.

Ishida, T & Sakaguchi, I (2007). Protection of human keratinocytes from UVB-induced inflammation using root extract of *Lithospermum erythrorhizon*. Biological & Pharmaceutical Bulletin, 30(5), 928-34.

Jin, S E, Lim, H-S, Kim, Y, Seo, C-S, Yoo, S-R, Shin, H-K & Jeong, S-J (2015). Traditional Herbal Formula Banhasasim-tang Exerts Anti-Inflammatory Effects in RAW 264.7 Macrophages and HaCaT Keratinocytes. Evidence-Based Complementary and Alternative Medicine, 2015, 728380.

Jing, H, Sun, W, Fan, J, Zhang, Y, Yang, J, Jia, J, Li, J, Guo, J, Luo, S & Zheng, Y (2016). Shikonin induces apoptosis of HaCaT cells via the mitochondrial, Erk and Akt pathways. Molecular Medicine Reports, 13(4), 3009-16.

Jo, J S, Hong, S B, Shin, H I & Choi, J J (1991). Homologous fibronectin enhances healing of excised wounds in rats. Journal of Korean Medical Science, 6(3), 197-205.

Jung, H A, Min, B-S, Yokozawa, T, Lee, J-H, Kim, Y S & Choi, J S (2009). Anti-Alzheimer and antioxidant activities of *Coptidis* Rhizoma alkaloids. Biological & Pharmaceutical Bulletin, 32(8), 1433-8.

Kaith, B S, Kaith, N S & Chauhan, N S (1996). Anti-inflammatory effect of *Arnebia euchroma* root extracts in rats. Journal of Ethnopharmacology, 55(1), 77-80.

Karayannopoulou, M, Tsioli, V, Loukopoulos, P, Anagnostou, T L, Giannakas, N, Savvas, I, Papazoglou, L G & Kaldrymidou, E (2011). Evaluation of the effectiveness of an ointment based on Alkannins/Shikonins on second intention wound healing in the dog. Canadian Journal of Veterinary Research = Revue Canadienne de Recherche Vétérinaire, 75(1), 42-8.

Keira, S M, Ferreira, L M, Gragnani, A, Duarte, I D S & Santos, I A N Dos (2004). Experimental model for fibroblast culture. Acta Cirurgica Brasileira, 19, 11-16.

Kessner, D, Chambers, M, Burke, R, Agus, D & Mallick, P (2008). ProteoWizard: open source software for rapid proteomics tools development. Bioinformatics, 24(21), 2534-2536.

Kim, H, Kim, J, Park, J, Kim, S H, Uchida, Y, Holleran, W M & Cho, Y (2011). Water extract of gromwell (*Lithospermum erythrorhizon*) enhances migration of human keratinocytes and dermal fibroblasts with increased lipid synthesis in an *in vitro* wound scratch model. Skin Pharmacology and Physiology, 25(2), 57-64.

Kim, J M, Jung, H A, Choi, J S & Lee, N G (2010). Identification of anti-inflammatory target genes of Rhizoma *coptidis* extract in lipopolysaccharide-stimulated RAW264.7 murine macrophage-like cells. Journal of Ethnopharmacology, 130(2), 354-362.

Kim, K, Rhee, H, Park, E, Jung, K & Jeon, H (2008). Anti-inflammatory effects of Radix *Gentianae Macrophyllae* (Qinjiao), Rhizoma *Coptidis* (Huanglian) and *Citri Unshiu* Pericarpium (Wenzhou migan) in animal. Chinese, 7, 3-9.

Kim, Y S, Cho, I-H, Jeong, M-J, Jeong, S-J, Nah, S Y, Cho, Y-S, Kim, S H, Go, A, Kim, S E, Kang, S S, Moon, C J, Kim, J C, Kim, S H & Bae, C S (2011). Therapeutic effect of total ginseng saponin on skin wound healing. Journal of Ginseng Research, 35(3), 360-7.

Kirschner, N, Rosenthal, R, Furuse, M, Moll, I, Fromm, M & Brandner, J M (2013). Contribution of tight junction proteins to ion, macromolecule, and water barrier in keratinocytes. The Journal of Investigative Dermatology, 133(5), 1161-9.

Klaus, V, Hartmann, T, Gambini, J, Graf, P, Stahl, W, Hartwig, A & Klotz, L-O (2010). 1,4-Naphthoquinones as inducers of oxidative damage and stress signaling in HaCaT human keratinocytes. Archives of Biochemistry and Biophysics, 496(2), 93-100.

Kong, W-J, Zhao, Y-L, Xiao, X-H, Jin, C & Li, Z-L (2009). Quantitative and chemical fingerprint analysis for quality control of rhizoma *Coptidis chinensis* based on UPLC-PAD combined with chemometrics methods. Phytomedicine : International Journal of Phytotherapy and Phytopharmacology, 16(10), 950-9.

Krishnan, P (2006). The scientific study of herbal wound healing therapies: Current state of play. Current Anaesthesia and Critical Care, 17(1-2), 21-27. Kunkel, S L, Standiford, T, Kasahara, K & Strieter, R M (1991). Stimulus specific induction of monocyte chemotactic protein-1 (MCP-1) gene expression. Advances in Experimental Medicine and Biology, 305, 65-71.

Kuonen, R, Weissenstein, U, Urech, K, Kunz, M, Hostanska, K, Estko, M, Heusser, P & Baumgartner, S (2013). Effects of Lipophilic Extract of Viscum album L. and Oleanolic Acid on Migratory Activity of NIH/3T3 Fibroblasts and on HaCat Keratinocytes. Evidence-Based Complementary and Alternative Medicine, 2013, 1-7.

Kurahashi, T & Fujii, J (2015). Roles of Antioxidative Enzymes in Wound Healing. Journal of Developmental Biology, 3, 57-70. Laemmli, U K (1970). Cleavage of structural proteins during the assembly of the head of bacteriophage T4. Nature, 227(5259), 680-5.

Laplante, A F, Germain, L, Auger, F A & Moulin, V (2001). Mechanisms of wound reepithelialization: hints from a tissue-engineered reconstructed skin to long-standing questions. FASEB Journal : Official Publication of the Federation of American Societies for Experimental Biology, 15(13), 2377-89.

Lau, K-M, Lai, K-K, Liu, C-L, Tam, J C-W, To, M-H, Kwok, H-F, Lau, C-P, Ko, C-H, Leung, P-C, Fung, K-P, Poon, S K-S & Lau, C B-S (2012). Synergistic interaction between Astragali Radix and Rehmanniae Radix in a Chinese herbal formula to promote diabetic wound healing. Journal of Ethnopharmacology, 141(1), 250-6.

Lau, T, Chan, Y, Lau, C & Chan, C (2007). Investigation of the effects of Chinese medicine on fibroblast viability: implications in wound healing. Phytotherapy, 947(March), 938-947.

Lau, T, Chan, Y, Lau, C & Lau, K (2009). Radix Astragali and Radix Rehmanniae, the principal components of two antidiabetic foot ulcer herbal formulae, elicit viability-promoting effects on primary fibroblasts. Phytotherapy, 23, 809-815.

Lau, T W, Lam, F F Y, Lau, K M, Chan, Y W, Lee, K M, Sahota, D S, Ho, Y Y, Fung, K P, Leung, P C & Lau, C B S (2009). Pharmacological investigation on the wound healing effects of Radix Rehmanniae in an animal model of diabetic foot ulcer. Journal of Ethnopharmacology, 123(1), 155-162.

Lau, T W, Sahota, D S, Lau, C H, Chan, C M, Lam, F C, Ho, Y Y, Fung, K P, Lau, C B S & Leung, P C (2008). An *in vivo* investigation on the wound-healing effect of two medicinal herbs using an animal model with foot ulcer. European Surgical Research. Europäische Chirurgische Forschung. Recherches Chirurgicales Européennes, 41(1), 15-23.

Lee, J H, Jung, K-M, Bae, I-H, Cho, S, Seo, D-B, Lee, S-J, Park, Y-H & Lim, K-M (2009). Anti-inflammatory and barrier protecting effect of *Lithospermum erythrorhizon* extracts in chronic oxazolone-induced murine atopic dermatitis. Journal of Dermatological Science, 56(1), 64-6.

Li, H-M, Tang, Y-L, Zhang, Z-H, Liu, C-J, Li, H-Z, Li, R-T & Xia, X-S (2011). Compounds from *Arnebia euchroma* and their related anti-HCV and antibacterial activities. Planta Medica, 78(1), 39-45.

Li, J, Chen, J & Kirsner, R (2007). Pathophysiology of acute wound healing. Clinics in Dermatology, 25(1), 9-18.

Li, W L, Zheng, H C, Bukuru, J & De Kimpe, N (2004). Natural medicines used in the traditional Chinese medical system for therapy of diabetes mellitus. Journal of Ethnopharmacology, 92(1), 1-21.

Li, X, Xiao, Q, Ze, K, Li, S, Wang, Y, Zhou, M, Yang, Q-T, Li, F-l & Li, B (2015). External Application of Traditional Chinese Medicine for Venous Ulcers: A Systematic Review and Meta-Analysis. Evidence-Based Complementary and Alternative Medicine, 2015(ID 831474).

Liang, C-C, Park, A Y & Guan, J-L (2007). *In vitro* scratch assay: a convenient and inexpensive method for analysis of cell migration *in vitro*. Nature Protocols, 2(2), 329-33.

Compendium of Materia Medica (2003). Li Shizhen; Compendium of Materia Medica (Bencao Gangmu), Book II. (Xiaoming, X, Zhengou, L, Kaimin, L & Yousheng, C Eds.) (1. Edition). Beijing, China: Foreign Languages Press.

Lobmann, R, Ambrosch, A, Schultz, G, Waldmann, K, Schiweck, S & Lehnert, H (2002). Expression of matrix-metalloproteinases and their inhibitors in the wounds of diabetic and non-diabetic patients. Diabetologia, 45(7), 1011-6.

Lodish, H, Berk, A, Zipursky, S L, Matsudaira, P, Baltimore, D & Darnell, J (2000). Collagen: The Fibrous Proteins of the Matrix. In Molecular Cell Biology. 4th edition.

Freeman, W H. Lu, L, Qin, A, Huang, H, Zhou, P, Zhang, C C, Liu, N, Li, S, Wen, G, Zhang, C C, Dong, W, Wang, X, Dou, Q P & Liu, J. (2011). Shikonin extracted from medici-

nal Chinese herbs exerts anti-inflammatory effect via proteasome inhibition. European Journal of Pharmacology, 658(2-3), 242-247.

Lu, P-J, Yang, C, Lin, C-N, Li, C-F, Chu, C-C, Wang, J-J & Chen, J-Y (2008). Shiunko and acetylshikonin promote reepithelialization, angiogenesis, and granulation tissue formation in wounded skin. The American Journal of Chinese Medicine, 36(1), 115-23.

Luo, X, Huang, P, Yuan, B, Liu, T, Lan, F, Lu, X, Dai, L, Liu, Y & Yin, H (2016). Astragaloside IV enhances diabetic wound healing involving upregulation of alternatively activated macrophages. International Immunopharmacology, 35, 22-28.

Ma, F, Chen, Y, Li, J, Qing, H-P, Wang, J-D, Zhang, Y-L, Long, B-G & Bai, Y (2010). Screening test for anti-Helicobacter pylori activity of traditional Chinese herbal medicines. World Journal of Gastroenterology : WJG, 16(44), 5629-34.

Mateu, R, Živicová, V, Krejčí, E D, Grim, M, Strnad, H, Vlček, Č, Kolář, M, Lacina, L, Gál, P, Borský, J, Smetana, K & Dvořánková, B (2016). Functional differences between neonatal and adult fibroblasts and keratinocytes: Donor age affects epithelial-mesenchymal crosstalk *in vitro*. International Journal of Molecular Medicine, 38(4), 1063-74.

Meng, Q-J, Yi, H, Yang, H, Zhu, L-W, Feng, J & Liu, X-Q (2013). Studies on flash extraction methods of *Arnebia euchroma*. Zhongguo Zhong Yao Za Zhi = Zhongguo Zhongyao Zazhi = China Journal of Chinese Materia Medica, 38(14), 2302-5.

Meyer, W (1996). Comments on the suitability of swine skin as a biological model for human skin. Der Hautarzt; Zeitschrift Für Dermatologie, Venerologie, Und Verwandte Gebiete, 47(3), 178-82.

Mohsenikia, M, Nuraei, H, Karimi, F, Jamalnia, N, Ashkani-Esfahani, S, Rafiee, S, Azizian, Z & Moradi, A (2015). Comparing Effects of *Arnebia euchroma* and Alpha Ointment on Wound Healing Process. Thrita, 4(1), e25781.

Moll, R, Divo, M & Langbein, L (2008). The human keratins: biology and pathology. Histochemistry and Cell Biology, 129(6), 705-33.

Morimoto, N, Takemoto, S, Kawazoe, T & Suzuki, S (2008). Nicotine at a Low Concentration Promotes Wound Healing. Journal of Surgical Research, 145(2), 199-204.

Moseley, R, Stewart, J E, Stephens, P, Waddington, R J, & Thomas, D W (2004). Extracellular matrix metabolites as potential biomarkers of disease activity in wound fluid: lessons learned from other inflammatory diseases? British Journal of Dermatology, 150(3), 401-413.

Mouw, J K, Ou, G & Weaver, V M (2014). Extracellular matrix assembly: a multiscale deconstruction. Nature Reviews Molecular Cell Biology, 15(12), 771-785.

Muhammad, A A, Pauzi, N A S, Arulselvan, P, Abas, F & Fakurazi, S (2013). *In vitro* wound healing potential and identification of bioactive compounds from Moringa oleifera Lam. BioMed Research International, 2013, 974580.

Nasiri, E, Hosseinimehr, S J, Azadbakht, M, Akbari, J, Enayati-Fard, R, Azizi, S & Azadbakht, M (2015). The Healing Effect of *Arnebia Euchroma* Ointment versus Silver Sulfadiazine on Burn Wounds in Rat. World Journal of Plastic Surgery, 4(2), 134-44.

Nasiria, E, Hosseinimehra, S J, Hosseinzadehd, A Z, Azadbakhta, M, Akbaria, J & Azadbakht, M (2016). The effects of *Arnebia euchroma* ointment on second-degree burn wounds: A randomized clinical trial. Journal of Ethnopharmacology, 189, 107-116.

Natarajan, S, Williamson, D, Stiltz, A J & Harding, K (2000). Advances in wound care and healing technology. American Journal of Clinical Dermatology, 1(5), 269-75.

Neuman, M G, Cohen, L B, Opris, M, Nanau, R & Jeong, H (2015). Hepatotoxicity of Pyrrolizidine Alkaloids. Suchergebnisse Journal of Pharmacy & Pharmaceutical Sciences, 18(4), 825-843.

Nickoloff, B J, Mitra, R S, Riser, B L, Dixit, V M & Varani, J (1988). Modulation of keratinocyte motility. Correlation with production of extracellular matrix molecules in response to growth promoting and antiproliferative factors. The American Journal of Pathology, 132(3), 543-51.

Noli, C & Miolo, A (2001). The mast cell in wound healing. Veterinary Dermatology, 12(6), 303-13.

Oeztuerk, N, Korkmaz, S, Oeztuerk, Y, & Baser, K (2006). Effects of Gentiopicroside, Sweroside and Swertiamarine, Secoiridoids from Gentian (Gentiana lutea ssp. s ymphyandra), on Cultured Chicken Embryonic Fibroblasts. Planta Medica, 72(4), 289-294.

Ou, Y, Jiang, Y, Li, H, Zhang, Y, Lu, Y & Chen, D (2016). Polysaccharides from *Arnebia euchroma* Ameliorated Endotoxic Fever and Acute Lung Injury in Rats Through Inhibiting Complement System. Inflammation, 40(1), 1-10.

Ozaki, Y, Sakaguchi, I, Tujimura, M, Ikeda, N, Nakayama, M, Kato, Y, Suzuki, H & Satake, M (1998). Study of the accelerating effect of shikonin and alkannin on the proliferation of granulation tissue in rats. Biological & Pharmaceutical Bulletin, 21(4), 366-70.

Ozgen, U, Ikbal, M, Hacimuftuoglu, A, Houghton, P J, Gocer, F, Dogan, H & Coskun, M (2006). Fibroblast growth stimulation by extracts and compounds of *Onosma argentatum* roots. Journal of Ethnopharmacology, 104(1-2), 100-103.

Papageorgiou, V P (1981). Patent US4282250 - Remedy for skin injuries and diseases. United States of America.

Papageorgiou, V P, Assimopoulou, A N & Ballis, A C (2008). Alkannins and shikonins: a new class of wound healing agents. Current Medicinal Chemistry, 15(30), 3248-67.

Papageorgiou, V P, Assimopoulou, A N, Couladouros, E A, Hepworth, D & Nicolaou, K C (1999). The Chemistry and Biology of Alkannin, Shikonin, and Related Naphthazarin Natural Products. Angewandte Chemie International Edition, 38(3), 270-301.

Park, T-J, Park, Y-S, Lee, T-G, Ha, H & Kim, K-T (2003). Inhibition of acetylcholine-mediated effects by borneol. Biochemical Pharmacology, 65(1), 83-90.

Pei, X-W, Wang, K-Z, Dang, X-Q, Song, J-H, Shi, Z-B & Gao, D-F (2006). Arnebia root oil promotes wound healing and expression of basic fibroblast growth factor on the wound surface in rabbits. Zhong Xi Yi Jie He Xue Bao = Journal of Chinese Integrative Medicine, 4(1), 52-5.

Pei, X, Liu, F, Wang, L, Li, Y, Zhang, Y, Song, J & Wang, K (2007). Clinical experimental study of Arnebia Root oil in increasing FGF expression and promoting wound surface healing. Journal of Nanjing Medical University, 21(5), 317-320.

Pei, X, Wang, K, Chen, J, Dang, X, Shi, Z & Gao, D (2005). Effect of arnebia root oil in promoting the tissue recovery of surface of wound and basic fibroblast growth factor (bFGF) mRNA expression. Zhongguo Zhong Xi Yi Jie He Za Zhi Zhongguo Zhongxiyi Jiehe Zazhi = Chinese Journal of Integrated Traditional and Western Medicine, 25(10), 892-4.

Petty, R D, Sutherland, L A, Hunter, E M & Cree, I A (1995). Comparison of MTT and ATP-based assays for the measurement of viable cell number. Journal of Bioluminescence and Chemiluminescence, 10(1), 29-34.

Pinho, B R, Sousa, C, Oliveira, J M A, Valentão, P & Andrade, P B (2012). Naphthoquinones' biological activities and toxicological effects. In Bioactive Compounds: Types, Biological Activities and Health Effects, 181-218.

Pirbalouti, A G, Azizi, S, Koohpayeh, A & Golparvar, A (2011). Evaluation of the Burn Healing Properties of *Arnebia Euchroma* Rolye (Johnst) in Diabetic Rats, 144-146.

Pirbalouti, A, Yousefi, M, Nazari Khanamiri, H, Karimi-Keisami, I, Koohpayeh, A & Karimi, F A (2009). Evaluation of burn healing properties of *Arnebia euchroma* and Malva sylvestris. Electronic Journal of Biology, 5(3), 62-66.

Pluskal, T, Castillo, S, Villar-Briones, A & Orešič, M (2010). MZmine 2: Modular framework for processing, visualizing, and analyzing mass spectrometry-based molecular profile data. BMC Bioinformatics, 11(1), 395.

Reinke, J M & Sorg, H (2012). Wound repair and regeneration. European Surgical Research. Europäische Chirurgische Forschung. Recherches Chirurgicales Européennes, 49(1), 35-43.

Remppis, A, Bea, F, Greten, J H, Buttler, A, Wang, H, Zhou, Q, Preusch, M R, Enk, R, Ehehalt, R, Katus, H & Blessing, E (2010). Rhizoma *Coptidis* Inhibits LPS-Induced MCP-1/CCL2 Production inMurineMacrophages via an AP-1 andNFκB-Dependent Pathway. Hindawi Publishing Corporation Mediators of Inflammatio, 2010.

Ren, J W, Chan, K M, Lai, P K K, Lau, C B S, Yu, H, Leung, P C, Fung, K P, Yu, W F X & Cho, C H (2012). Extracts from Radix Astragali and Radix Rehmanniae Promote Keratinocyte Proliferation by Regulating Expression of Growth Factor Receptors. Phytotherapy Research, (January).

Roberts, A B & Sporn, M B (1987). Transforming growth factor-beta: potential common mechanisms mediating its effects on embryogenesis, inflammation-repair, and carcinogenesis. International Journal of Radiation Applications and Instrumentation. Part B, Nuclear Medicine and Biology, 14(4), 435-9.

Robson, M C, Steed, D L & Franz, M G (2001). Wound healing: biologic features and approaches to maximize healing trajectories. Current Problems in Surgery, 38(2), 72-140.

Röder, E (1995). Medicinal plants in Europe containing pyrrolizidine alkaloids. Die Pharmazie, 50(2), 83-98.

Röder, E (2000). Medicinal plants in China containing pyrrolizidine alkaloids. Die Pharmazie, 55(10), 711-26.

Röder, E & Rengel-Mayer, B (1993). Pyrrolizidine Alkaloids from *Arnebia euchroma**. Planta Medica, 59(2), 192.

Rodriguez, P G, Felix, F N, Woodley, D T & Shim, E K (2008). The Role of Oxygen in Wound Healing: A Review of the Literature. Dermatologic Surgery, 34(9), 1159-1169.

Roosterman, D, Goerge, T, Schneider, S W, Bunnett, N W & Steinhoff, M (2006). Neuronal Control of Skin Function: The Skin as a Neuroimmunoendocrine Organ. Physiological Reviews, 86(4), 1309-1379.

Ross, R, Bowen-Pope, D F & Raines, E W (1985). Platelet-derived growth factor: its potential roles in wound healing, atherosclerosis, neoplasia, and growth and development. Ciba Foundation Symposium, 116, 98-112.

Saarialho-Kere, U K, Kovacs, S O, Pentland, A P, Olerud, J E, Welgus, H G & Parks, W C (1993). Cell-matrix interactions modulate interstitial collagenase expression by human keratinocytes actively involved in wound healing. The Journal of Clinical Investigation, 92(6), 2858-66.

Safferling, K, Sütterlin, T, Westphal, K, Ernst, C, Breuhahn, K, James, M, Jäger, D, Halama, N & Grabe, N (2013). Wound healing revised: a novel reepithelialization mechanism revealed by *in vitro* and in silico models. The Journal of Cell Biology, 203(4), 691-709.

Sasaki, K, Yoshizaki, F & Abe, H (2000). The anti-Candida activity of shikon. Yakugaku Zasshi : Journal of the Pharmaceutical Society of Japan, 120(6), 587-9.

Schäfer, M & Werner, S (2008). Oxidative stress in normal and impaired wound repair. Pharmacological Research, 58(2), 165-171.

Scholzen, T & Gerdes, J (2000). The Ki-67 protein: from the known and the unknown. Journal of Cellular Physiology, 182(3), 311-22.

Sekkat, N, Kalia, Y N & Guy, R H (2002). Biophysical study of porcine ear skin *in vitro* and its comparison to human skin *in vivo*. Journal of Pharmaceutical Sciences, 91(11), 2376-81.

Senger, D R, Claffey, K. P, Benes, J E, Perruzzi, C A, Sergiou, A P & Detmar, M (1997). Angiogenesis promoted by vascular endothelial growth factor: regulation through alpha1beta1 and alpha2beta1 integrins. Proceedings of the National Academy of Sciences of the United States of America, 94(25), 13612-7.

Sethi, K K, Yannas, I V, Mudera, V, Eastwood, M, McFarland, C & Brown, R A (2002). Evidence for sequential utilization of fibronectin, vitronectin, and collagen during fibroblast-mediated collagen contraction. Wound Repair and Regeneration, 10(6), 397-408.

Shameem, N, Kamili, A N, Parray, J A, Hamid, R & Bandh, S A (2015). Antimicrobial and antioxidant activity of methanol extracts of Arnebia benthamii (Wall ex. G. Don) Johnston—a critically endangered medicinal plant of North western Himalaya. Journal of Analytical Science and Technology, 6(1), 36.

Sharma, N, Sharma, U K, Malik, S, Bhushan, S, Kumar, V, Verma, S C, Sharma, N, Sharma, M & Sinha, A K (2008). Isolation and purification of acetylshikonin and beta-acetoxyisovalerylshikonin from cell suspension cultures of *Arnebia euchroma* (Royle) Johnston using rapid preparative HPLC. Journal of Separation Science, 31(4), 629-35.

Sherry, B, Tekamp-Olson, P, Gallegos, C, Bauer, D, Davatelis, G, Wolpe, S D, Masiarz, F, Coit, D & Cerami, A (1988). Resolution of the two components of macrophage inflammatory protein 1, and cloning and characterization of one of those components, macrophage inflammatory protein 1 beta. The Journal of Experimental Medicine, 168(6), 2251-9.

Sidhu, G S, Singh, A K, Banaudha, K K, Gaddipati, J P, Patnaik, G K & Maheshwari, R K (1999). Arnebin-1 accelerates normal and hydrocortisone-induced impaired wound healing. The Journal of Investigative Dermatology, 113(5), 773-81.

Simpson, D M & Ross, R (1972). The neutrophilic leukocyte in wound repair. Journal of Clinical Investigation, 51(8), 2009-2023.

Singer, A J, Richard, A. F & Clark, R A (1999). Cutaneous wound healing. The New England Journal of Medicine, 341(10), 738-46. Smith, Q T (1975). Collagen Metabolism in Wound Healing. In Trauma, 31-45. Boston, MA: Springer US.

Smyrska-Wieleba, N, Wojtanowski, K K & Mroczek, T (2016). Comparative HILIC/ESI-QTOF-MS and HPTLC studies of pyrrolizidine alkaloids in flowers of Tussilago farfara and roots of *Arnebia euchroma*. Phytochemistry Letters, in press.

Soni, H & Singhai, A K (2012). A recent update of botanicals for wound healing activity. International Research Journal of Pharmacy, 3(7), 1-7.

Sullivan, T P, Eaglstein, W H, Davis, S C & Mertz, P (2001). The pig as a model for human wound healing. Wound Repair and Regeneration, 9(2), 66-76.

Sun, T T, Cotsarelis, G & Lavker, R M (1991). Hair follicular stem cells: the bulge-activation hypothesis. The Journal of Investigative Dermatology, 96(5), 77S-78S.

Süntar, I P, Akkol, E K, Yalcın, F N, Koca, U, Keles, H & Yesilada, E (2010). Wound healing potential of Sambucus ebulus L. leaves and isolation of an active component, quercetin 3-O-glucoside. Journal of Ethnopharmacology, 129(1), 106-114.

Tam, J C W, Lau, K M, Liu, C L, To, M H., Kwok, H F, Lai, K K, Lau, C P, Ko, C H, Leung, P C, Fung, K P & Lau, C B S (2011). The *in vivo* and *in vitro* diabetic wound healing effects of a 2-herb formula and its mechanisms of action. Journal of Ethnopharmacology, 134(3), 831-8.

Thakur, L, Ghodasra, U, Patel, N & Dabhi, M (2011). Novel approaches for stability improvement in natural medicines. Pharmacognosy Reviews, 5(9), 48-54.

Thakur, R, Jain, N, Pathak, R & Sandhu, S S (2011). Practices in wound healing studies of plants. Evidence-Based Complementary and Alternative Medicine, 2011, 438056.

Tiga, S, Sarangi, P P, Chaurasia, O P & Kumar, B (2016). Antioxidant Potential of Selected Medicinal Plants of Trans-Himalayan Region. International Journal of Science and Research, 5(5), 2319-7064.

Treviño, V, Yañez-Garza, I-L, Rodriguez-López, C. E., Urrea-López, R., Garza-Rodriguez, M.-L., Barrera-Saldaña, H-A, Tamez-Peña, J G, Winkler, R & Díaz de-la-Garza, R-I (2015). GridMass: a fast two-dimensional feature detection method for LC/MS. Journal of Mass Spectrometry, 50(1), 165-174.

Tsuchiya, H, Sato, M, Miyazaki, T, Fujiwara, S, Tanigaki, S, Ohyama, M, Tanaka, T & Iinuma, M (1996). Comparative study on the antibacterial activity of phytochemical flavanones against methicillin-resistant Staphylococcus aureus. Journal of Ethnopharmacology, 50(1), 27-34.

Ueck, C, Volksdorf, T, Houdek, P, Vidal-y-Sy, S, Sehner, S, Ellinger, B, Lobmann, R, Larena-Avellaneda, A, Reinshagen, K, Ridderbusch, I, Kohrmeyer, K, Moll, I, Daniels, R,

Werner, P, Merfort, I &Brandner, J M (2017). Comparison of In-Vitro and Ex-Vivo Wound Healing Assays for the Investigation of Diabetic Wound Healing and Demonstration of a Beneficial Effect of a Triterpene Extract. PLOS ONE, 12(1), e0169028.

Usui, M L, Mansbridge, J G, Fujita, M & Olerud, J E (2008). Keratinocyte migration, proliferation, and differentiation in chronic ulcers from patients with diabetes and normal wounds. The Journal of Histochemistry and Cytochemistry : Official Journal of the Histochemistry Society, 56(7), 687-96.

Velnar, T, Bailey, T & Smrkolj, V (2009). The wound healing process: an overview of the cellular and molecular mechanisms. The Journal of International Medical Research, 37(5), 1528-42.

Visscher, M O (2009). Update on the Use of Topical Agents in Neonates. Newborn and Infant Nursing Reviews, 9(1), 31-47.

Visse, R & Nagase, H (2003). Matrix Metalloproteinases and Tissue Inhibitors of Metalloproteinases: Structure, Function, and Biochemistry. Circulation Research, 92(8), 827-839.

Wang, J, Zhang, Q, Wan, R, Mo, Y, Li, M, Tseng, M T & Chien, S (2009). Intracellular Adenosine Triphosphate Delivery Enhanced Skin Wound Healing in Rabbits. Annals of Plastic Surgery, 62(2), 180-186.

Wang, W J, Bai, J Y, Liu, D P, Xue, L M & Zhu, X Y (1994). The antiinflammatory activity of shikonin and its inhibitory effect on leukotriene B4 biosynthesis. Yao Xue Xue Bao = Acta Pharmaceutica Sinica, 29(3), 161-5.

Wang, X-J, Lin, S, Kang, H-F, Dai, Z-J, Bai, M-H, Ma, X-L, Ma, X-B, Liu, M-J, Liu, X-X & Wang, B-F (2013). The effect of Rhizoma *Coptidis* and *Coptis Chinensis* Aqueous Extract on Radiation-Induced Skin Injury in a Rat Model. BMC Complementary and Alternative Medicine, 13, 105.

Weinstein, G D (1966). Comparison of turnover time and of keratinous protein fractions in swine and human epidermis. Proceedings of a Symposium on Swine in Biomedical Research. Welch, M P, Odland, G F & Clark, R A (1990). Temporal relationships of F-actin bundle formation, collagen and fibronectin matrix assembly, and fibronectin receptor expression to wound contraction. The Journal of Cell Biology, 110(1), 133-45.

Werner, S & Grose, R (2003). Regulation of wound healing by growth factors and cytokines. Physiological Reviews, 83(3), 835-70.

WHO (1999). World Health Organization monographs on selected medicinal plants. WHO Library Cataloguing in Publication Data (Vol. 1). Geneva.

WHO (2007). World Health Organization monographs on selected medicinal plants. World Health Organization (Vol. 3).

Wong, M W N, Leung, P C & Wong, W C (2001). Limb salvage in extensive diabetic foot ulceration-a preliminary clinical study using simple debridement and herbal drinks. Hong Kong Medical Journal = Xianggang Yi Xue Za Zhi / Hong Kong Academy of Medicine, 7(4), 403-7.

Xiao, Y, Wang, Y, Gao, S, Zhang, R, Ren, R, Li, N & Zhang, H (2011). Determination of the active constituents in *Arnebia euchroma* (Royle) Johnst. by ionic liquid-based

ultrasonic-assisted extraction high-performance liquid chromatography. Journal of Chromatography. B, Analytical Technologies in the Biomedical and Life Sciences, 879(20), 1833-8.

Xie, W & Du, L (2011). Diabetes is an inflammatory disease: evidence from traditional Chinese medicines. Diabetes, Obesity & Metabolism, 13, 289-301.

Xie, Y, Fan, C, Dong, Y, Lynam, E, Leavesley, D I, Li, K, Su, Y, Yang, Y & Upton, Z (2015). Functional and mechanistic investigation of Shikonin in scarring. Chemico-Biological Interactions, 228, 18-27.

Xiong, W, Luo, G, Zhou, L, Zeng, Y & Yang, W (2009). *In vitro* and *in vivo* antitumor effects of acetylshikonin isolated from *Arnebia euchroma* (Royle) Johnst (Ruanzicao) cell suspension cultures. Chinese Medicine, 4(14).

Xu, L, Liu, Y & He, X (2005). Inhibitory effects of berberine on the activation and cell cycle progression of human peripheral lymphocytes. Cellular & Molecular Immunology, 2(4), 295-300. Yang, B, Ji, C, Chen, X, Cui, L, Bi, Z, Wan, Y & Xu, J (2011).

Protective effect of astragaloside IV against matrix metalloproteinase-1 expression in ultraviolet-irradiated human dermal fibroblasts. Archives of Pharmacal Research, 34(9), 1553-1560.

Yoo, H G, Lee, B H, Kim, W, Lee, J S, Kim, G H, Chun, O K, Koo, S I & Kim, D-O (2014). *Lithospermum erythrorhizon* extract protects keratinocytes and fibroblasts against oxidative stress. Journal of Medicinal Food, 17(11), 1189-96.

Yuzbasioglu, M, Kuruuzum-Uz, A, Guvenalp, Z, Simon, A, Tóth, G, Harput, U S, Kazaz, C, Bilgili, B, Duman, H, Saracoglu, I & Demirezer, L O (2015). Cytotoxic compounds from endemic Arnebia purpurea. Natural Product Communications, 10(4), 595-6.

Zeng, Z, Huang, W-D, Gao, Q, Su, M-L, Yang, Y-F, Liu, Z-C & Zhu, B-H (2015). Arnebin-1 promotes angiogenesis by inducing eNOS, VEGF and HIF-1α expression through the PI3K-dependent pathway. International Journal of Molecular Medicine, 36(3), 685-97.

Zeng, Z & Zhu, B.H (2014). Arnebin-1 promotes the angiogenesis of human umbilical vein endothelial cells and accelerates the wound healing process in diabetic rats. Journal of Ethnopharmacology, 154(3), 653-62.

Zhang, Q, Wei, F, Fong, C C, Yu, W K, Chen, Y, Koon, C M, Lau, K M, Leung, P C, Lau, C B S, Fung, K P & Yang, M (2011). Transcriptional profiling of human skin fibroblast cell line Hs27 induced by herbal formula Astragali Radix and Rehmanniae Radix. Journal of Ethnopharmacology, 138(3), 668-675.

Zhang, R-X, Li, M-X & Jia, Z-P (2008). *Rehmannia glutinosa*: review of botany, chemistry and pharmacology. Journal of Ethnopharmacology, 117(2), 199-214.

Zhang, W-J & Frei, B (2015). Astragaloside IV inhibits NF- ϰ B activation and inflammatory gene expression in LPS-treated mice. Mediators of Inflammation, 2015, 274314.

Zhao, Q (2015). Molecular mechanisms of shikonin and its derivatives in cancer therapy. Ph.D. Thesis. Johannes Gutenberg University Mainz.

Zhou, W, Jiang, H D G L, Peng, Y & Li, S S (2011). Comparative study on enantiomeric excess of main akannin/shikonin derivatives isolated from the roots of three endemic Boraginaceae plants in China. Biomedical Chromatography : BMC, 25(10), 1067-75.

Zorn-Kruppa, M, Volksdorf, T, Ueck, C, Zöller, E, Reinshagen, K, Ridderbusch, I, Bruning, G, Houdek, P, Moll, I & Brandner, J M (2016). Major cell biological parameters of keratinocytes are predetermined by culture medium and donor source. Experimental Dermatology, 25(3), 242-244.

A. Appendix

A.1. Abbreviations

Abbreviation	Description/Explanation
A. bidest.	*Aqua bidestillata*
ad	to final volume
A. dest.	*Aqua destillata*
A. euchroma	*Arnebia euchroma* (Royle) I. M. Johnst.
A. propinquus	*Astragalus propinquus* Schischkin.
APS	ammoniumpersulfat
ARE	*Arnebia euchroma* Radix Extract
AT	Austria
A. T.	ambient temperature
ATP	adenosine 5´-triphosphate
AUC	area under the curve
BrdU	bromdesoxyuridin
BSA	bovine serum albumin
Ca^{2+}	calcium ion
C. chinensis	*Coptis chinensis* Franch.
Chinaturel	Chinaturel Import Export B.V.; *A. euchroma* source I
CK	cytokeratin
Cl^-	chloride ion
cm	centimeter, distance unit
cm^2	square centimeter, area unit
CO_2	carbon dioxide
CRC	identification number
DAPI	4',6-diamidino-2-phenylindol
DE	Germany
DermaLab	laboratory of the dermatology and venerology, UKE
DNA	deoxyribonucleic acid
DNP	Dictionary of Natural Products

DMEM	Dulbecco's Modified Eagle Medium
DMSO	dimethylsulfoxid
DPPH	diphenyl-pikryl-hydrazyl; organic radical
ECM	extracellular matrix
EDTA	ethylendiamintetra acid
e.g.	exempli gratia, for example
EGF	epidermal growth factor
ELSD	evaporative light scattering detector
et al.	*et alii*
etc.	*et cetera*
F(ab')2	fragment antigen binding
FBS	fetal bovine serum
FGF	fibroblast growth factor
Fig.	figure
g	gram, mass unit
g	acceleration of gravity
h	hora; hour, time unit
HE	haematoxylin and eosin
HMEC1	human dermal microvascular endothelial cells 1
HMZ for TCM	HanseMerkur Center for Traditional Chinese Medicine
HRMS	high-resolution mass spectrometer
H_2SO_4	sulfuric acid
HUVEC	human umbilical vein endothelial cells
IF	immunofluorescence
IGF	insulin-like growth factors
Il	interleukin
JP	Japan
kDa	kilodalton, mass unit
KGF	keratinocytes growth factor
Ki67	Ki67 antigen, proliferation marker
M	molar, amount unit
MAPK	mitogen-activated protein kinase
µg	microgram, mass unit
µl	microliter, volume unit
µm	micrometer, distance unit
min	minute, time unit
mm	millimeter, distance unit
mm^2	square millimeter, area unit

mM	milimolar, amount unit
MMPs	matrix-metalloproteinases
MS	mass spectrometry
MTT	3-(4,5-Dimethylthiazol-2-yl)-2,5-diphenyltetrazoliumbromid
m/z	mass over time
n	number of independent experiments
NAC	n-Acetylcysteine
NC	non-stimulated (solvent/media/negative) control
NI	negative ionization
neg	negative
NFκB	nuclear factor kappa-light-chain-enhancer of activated B-cells
NGS	normal goat serum
NL	Netherlands
Ω	ohm; impedance unit
ORAC	oxygen radical absorbance capacity; peroxyl radical
p	(statistically) probability
PAs	pyrrolizidine alkaloid
PAGE	polyacrylamid gelelectrophoresis
PBS	phosphate-buffered saline
PDGF	platelet-derived growth factor
PI	positive ionization
PMSF	phenylmethylsulfonyl fluoride
PCR	polymerase chain reaction
pos	positive
ppm	parts per million
Rats pharmacy	Rats pharmacy Stralsund; *A. euchroma* source II
Rf	retention factor for TLC evaluation; signal/separation end front
RIPA	radioimmunoprecipitation assay
R. glutinosa	*Rehmannia glutinosa* (Gaertn.) DC.
ROS	reactive oxygen species
rpm	rounds per minute
s	second, time unit
SDS	sodium dodecyl sulfate
SEM	standard error of the mean
TER	transepidermal resistance [Ω/cm2]
Tab.	table
TCM	Traditional Chinese Medicine
TEMED	tetramethylethylendiamin

TER	transepidermal resistance [Ω/cm^2]
TGF	transforming growth factor
TIMPs	tissue inhibitor of metalloproteinases
TLC	thin layer chromatography
TNF-α	tumor necrosis factor alpha
TUNEL	terminal deoxynucleotidyl transferase dUTP nick end labeling
UHPLC	ultra high-performance liquid chromatography
UKE	University Clinic Hamburg-Eppendorf
US	United States (of America)
UV	ultraviolet
V	voltage, electrical tension unit
VEGF	vascular endothelial growth factor
WB	western blot
WHM	wound healing model
WHO	World Health Organization
w/o	without; also untreated control
XIC	extracted ion chromatogram

A.2. Supplementary Data

Table A.1.: Dereplication table of the UHPLC-HRMS data of the aqueous *A. Euchroma* Extract in positive ionization mode. The common name was added only if the identification number (CRC) was described for the genus *Arnebia*. The Type of Compounds referred to the classification done with the Dictionary of Natural Products (DNP; mass over time (m/z); parts per million (ppm); CRC, identification number).

Retention time [min]	**m/z $[M+H]^+$**	**Molecular formula**	**Mass accuracy [ppm]**	**Identification Number (CRC)**	**Type of Compound**	**Common Name**	**Taxonomy**
0.86	332.1703	C15H25NO7	-0.3	QVK05; QVJ96; RBR34	simple pyrrolizidine alkaloids	lepthanthine-N-oxide	Family
1.98	332.1703	C15H25NO7	-0.3	QVK05; QVJ96; RBR34	simple pyrrolizidine alkaloids	lepthanthine-N-oxide	Family
3.07	300.1806	C15H25NO5	0.1	LXQ07; GNN63	simple pyrrolizidine alkaloids	intermedine	Family
3.47	245.1861	C12H24N2O3	0.4	OTL82-B	amino acids		DNP-dicots
3.61	316.1756	C15H25NO6	0.4	GNP27; GNN58; MSX24; QVF89; QVD26; QVK04	simple pyrrolizidine alkaloids	intermedine-N-oxide	Family
3.87	318.1912	C15H27NO6	0.2	QVF95	simple pyrrolizidine alkaloids		Family

Retention time [min]	**m/z $[M+H]^+$**	**Molecular formula**	**Mass accuracy [ppm]**	**Identification Number (CRC)**	**Type of Compound**	**Common Name**	**Taxonomy**
4.06	286.2013	C15H27NO4	0	GNN86; LMB34; GNN92; GNN84; GNN94; GNN81; GNN75; GNN97; GNN93; OJL05	simple pyrrolizidine alkaloids		Family
4.21	302.1962	C15H27NO5	-0.1	GNN98; FYG99; QVF93; GNN82; GNN79; GNN87; MVL00	simple pyrrolizidine alkaloids		Family
4.43	300.1806	C15H25NO5	0.4	LXQ07; GNN63	simple pyrrolizidine alkaloids	intermedine	Family
5.43	358.1860	C17H27NO7	-0.1	DLY63; QVF92; QVF90; QVF94; QVJ97	simple pyrrolizidine alkaloids		Family
6.11	344.2068	C17H29NO6	0	FYH04	simple pyrrolizidine alkaloids		Family
6.24	271.0965	C16H14O4	0	QGD07	naphtho-quinones	anhydro-shikonin	Family
6.38	257.0808	C15H12O4	-0.2	JZR10-V	anthracene		DNP-dicots
6.90	313.0707	C17H12O6	0	LOK19; LOF32	norlignans		Family

Retention time [min]	**m/z $[M+H]^+$**	**Molecular formula**	**Mass accuracy [ppm]**	**Identification Number (CRC)**	**Type of Compound**	**Common Name**	**Taxonomy**
8.98	257.0808	C15H12O4	-0.2	JZR10-V	anthracenes		DNP-dicots
9.46	273.1121	C16H16O4	-0.2	CMW55; QVX08	naphtho-quinones	deoxy-shikonin; euchro-quinol B	Genus
9.62	289.1070	C16H16O5	-0.3	CLZ55; HDC64; HJB97	naphtho-quinones	shikonin and isomers	Genus
10.74	321.1334	C17H20O6	0.3	GCX11; OWC42	anthracenes		Family
10.87	319.1177	C17H18O6	0.2	GCV45; OKR45	anthracenes		Family
11.42	273.1121	C16H16O4	-0.2	CMW55; QVX08	naphtho-quinones	deoxy-shikonin; euchro-quinol B	Genus
11.53	321.1333	C17H20O6	0	GCX11; OWC42	anthracenes		Family
12.93	259.1329	C16H18O3	0	QVV93; QVX07	anthracenes	epoxyarnebinol; euchro-quinol A	Genus
12.93	291.1227	C16H18O5	-0.1	HFR69	naphtho quinones	arnebin V	Genus
13.63	273.1121	C16H16O4	-0.2	CMW55; QVX08	naphtho quinones	deoxy-shikonin; euchro-quinol B	Genus
14.60	285.1122	C17H16O4	0.1	QGD08	naphtho quinones		Family
16.22	288.2897	C17H37NO2	-0.1	RGN01-G	saturated unbranched alcohols		DNP-dicots

Retention time [min]	**m/z $[M+H]^+$**	**Molecular formula**	**Mass accuracy [ppm]**	**Identification Number (CRC)**	**Type of Compound**	**Common Name**	**Taxonomy**
16.78	288.2897	C17H37NO2	-0.1	RGN01-G	saturated unbranched alcohols		DNP
18.97	316.3210	C19H41NO2	-0.1	MTO65-R; OGZ46-Y	sphingolipids		DNP-dicots
19.48	316.3210	C19H41NO2	-0.1	MTO65-R; OGZ46-Y	sphingolipids		DNP-dicots

Table A.2.: Dereplication table of the UHPLC-HRMS data of the aqueous *A. Euchroma* Extract in negative ionization mode. The common name was added only if the identification number (CRC) was described for the Genus *Arnebia*. The Type of Compounds referred to the classification done with the DNP.

Retention time [min]	**m/z $[M+H]^+$**	**Molecular formula**	**Mass accuracy [ppm]**	**Identification Number (CRC)**	**Type of Compound**	**Common Name**	**Taxonomy**
2.16	167.0343	C8H8O4	-3.9	16 hits			DNP-dicot
2.22	197.0452	C9H10O5	-1.6	HZY36	simple benzoic acids and esters		Family
2.47	153.0185	C7H6O4	-5.3	6 hits	simple benzoic acids and esters		DNP-dicot
3.50	161.0812	C7H14O4	-4.4	BVJ76-T	2,6-Dideoxy sugars		DNP-dicot
3.70	323.1352	C13H24O9	1.4	PYW94-D; BVL95-I	disaccharides		DNP-dicot
3.72	161.0812	C7H14O4	-4.4	BVJ76-T	2,6-dideoxy sugars		DNP-dicot
4.05	335.1142	C17H20O7	1.8	JOW54	anthracenes		Family
4.71	355.0468	C18H12O8	2.5	11 hits			DNP-dicot
4.86	215.0923	C10H16O5	-0.8	4 hits	iridoid monoter-penoids		DNP-dicot
5.39	287.0930	C16H16O5	1.8	CLZ55; HDC64; HJB97	naphtho-quinones	shikonin and isomers	Genus
5.76	179.0344	C9H8O4	-3.1	10 hits	-		DNP-dicot
5.76	213.0766	C10H14O5	-1.0	28 hits	-		DNP-dicot

Retention time [min]	**m/z $[M+H]^+$**	**Molecular formula**	**Mass accuracy [ppm]**	**Identification Number (CRC)**	**Type of Compound**	**Common Name**	**Taxonomy**
6.24	287.0929	C16H16O5	1.5	CLZ55; HDC64; HJB97	naphtho-quinones	shikonin and isomers	Genus
6.40	417.1197	C21H22O9	1.5	74 hits		-	DNP-dicot
6.91	311.0566	C17H12O6	1.6	LOK19; LOF32	stilbenes		Family
7.10	717.1475	C36H30O16	2.0	HRD74; NMS01	cyclolignans	rabdosiin	Genus
7.26	287.0930	C16H16O5	1.8	CLZ55; HDC64; HJB97	naphtho-quinones	shikonin and isomers	Genus
7.33	163.0394	C9H8O3	-3.9	CMP74	simple phenyl-propanoids	coumaric acid	DNP-dicot
7.69	241.0871	C15H14O3	0.4	53 hits	-		DNP-dicot
7.84	359.0780	C18H16O8	2.2	CLS91	simple phenyl-propanoids	rosmarinic acid	Family
8.55	417.1199	C15H14O3	2.0	53 hits	-		DNP-dicot
8.99	287.0929	C16H16O5	1.5	CLZ55; HDC64; HJB97	naphtho-quinones	shikonin and isomers	Genus
9.01	255.0665	C15H12O4	0.9	62 hits			DNP-dicot
9.13	273.1137	C16H18O4	1.8	GMQ70	naphtho-quinones		Family
9.16	491.0992	C26H20O10	1.7	OHO73	cyclolignans		Family
9.30	275.0930	C15H16O5	1.9	105 hits			DNP-dicot

Retention time [min]	m/z $[M+H]^+$	Molecular formula	Mass accuracy [ppm]	Identification Number (CRC)	Type of Compound	Common Name	Taxonomy
9.45	287.0929	C16H16O5	1.5	CLZ55; HDC64; HJB97	naphtho-quinones	shikonin and isomers	Genus
9.47	255.0876	C12H16O6	0.8	6 hits			DNP-dicot
9.63	287.0929	C16H16O5	1.5	CLZ55; HDC64; HJB97	naphtho-quinones	shikonin and isomers	Genus
9.69	289.1087	C16H18O5	2.0	HFR69; GYV35	naphtho-quinones	arnebin V	Genus
10.04	273.1137	C16H18O4	1.8	GMQ70	naphtho-quinones		Family
10.30	315.0880	C17H16O6	1.9	CDO56	flavanones		Family
10.77	275.1293	C16H20O4	1.6	CMN87; PKV13	anthracenes		Family
10.87	287.0930	C16H16O5	1.8	CLZ55; HDC64; HJB97	naphtho-quinones	shikonin and isomers	Genus
11.05	287.0930	C16H16O5	1.8	CLZ55; HDC64; HJB97	naphtho-quinones	shikonin and isomers	Genus
11.43	271.0979	C16H16O4	1.3	CMW55; QVX08	naphtho-quinones	deoxy-shikonin; euchro-quinol B	Genus
11.47	239.0926	C12H16O5	0.5	NOY58	simple phenyl-propanoids		Family
11.92	243.1027	C15H16O3	0.2	85 hits			DNP-dicot
11.94	287.0927	C16H16O5	0.8	CLZ55; HDC64; HJB97	naphtho-quinones	shikonin and isomers	Genus

Retention time [min]	**m/z $[M+H]^+$**	**Molecular formula**	**Mass accuracy [ppm]**	**Identification Number (CRC)**	**Type of Compound**	**Common Name**	**Taxonomy**
12.06	255.0666	C15H12O4	1.3	62 hits	-		DNP-dicot
12.14	253.0872	C16H14O3	0.8	GYD43	benzoquinones		Family
12.95	289.1086	C16H18O5	1.6	HFR69; GYV35	naphtho-quinones	arnebin V	Genus

Table A.3.: Dereplication table of the UHPLC-HRMS data of the ethanolic *A. Euchroma* Extract in positive ionization mode. The common name was added only if the identification number (CRC) was described for the Genus *Arnebia*. The Type of Compounds referred to the classification done with the DNP.

Retention time [min]	**m/z $[M+H]^+$**	**Molecular formula**	**Mass accuracy [ppm]**	**Identification Number (CRC)**	**Type of Compound**	**Common Name**	**Taxonomy**
0.83	316.1756	C15H25NO6	0.4	GNP27; GNN58; MSX24; QVF89; QVD26; QVK04	simple pyrrolizidine alkaloids	intermedine-N-oxide	Family
0.85	332.1703	C15H25NO7	-0.3	QVK05; QVJ96; RBR34	simple pyrrolizidine alkaloids	lepthanthine-N-oxide	Family
1.98	332.1703	C15H25NO7	-0.3	QVK05; QVJ96; RBR34	simple pyrrolizidine alkaloids	lepthanthine-N-oxide	Family
3.07	300.1806	C15H25NO5	0.1	LXQ07; GNN63	simple pyrrolizidine alkaloids	intermedine	Family
3.46	245.1861	C12H24N2O3	0.4		naphtho-quinones		DND dicots
3.60	316.1756	C15H25NO6	0.4	GNP27; GNN58; MSX24; QVF89; QVD26; QVK04	simple pyrrolizidine alkaloids	intermedine-N-oxide	Family
4.22	302.1962	C15H27NO5	-0.1	GNN98; FYG99; QVF93; GNN82; GNN79; GNN87; MVL00	simple pyrrolizidine alkaloids		Family

Retention time [min]	**m/z $[M+H]^+$**	**Molecular formula**	**Mass accuracy [ppm]**	**Identification Number (CRC)**	**Type of Compound**	**Common Name**	**Taxonomy**
4.43	300.1806	C15H25NO5	0.1	LXQ07; GNN63	simple pyrrolizidine alkaloids	intermedine	Family
5.44	358.1860	C17H27NO7	-0.1	DLY63; QVF92; QVF90; QVF94; QVJ97	simple pyrrolizidine alkaloids		Family
6.10	344.2068	C17H29NO6	0	FYH04	simple pyrrolizidine alkaloids		Family
6.23	271.0965	C16H14O4	0	QGD07	naphtho-quinones	anhydro-shikonin	Genus
6.56	414.2122	C20H31NO8	-0.2	FYX29; GNP38; NMN64; QVJ99	simple pyrrolizidine alkaloids	echimidine-N-oxide	Family
6.66	398.2174	C20H31NO7	0.1	FYQ39; GNP36; LXG58; LHZ42; LCP26; QVD80; CGB79; FYH16; LDP35; QVJ98; GNP60	simple pyrrolizidine alkaloids		Family
8.04	257.1172	C16H16O3	-0.2	CMP10; GMR50; BFF44*	meroter-penoids; *Benzo-quinones		Family

Retention time [min]	m/z $[M+H]^+$	Molecular formula	Mass accuracy [ppm]	Identification Number (CRC)	Type of Compound	Common Name	Taxonomy
8.04	320.1857	C18H25NO4	0.1	CFF22	simple pyrrolizidine alkaloids		Family
8.99	273.1121	C16H16O4	-0.2	CMW55; QVX08	naphtho-quinones	deoxy-shikonin; euchro-quinol B	Genus
9.47	273.1121	C16H16O4	-0.2	CMW55; QVX08	naphtho-quinones	deoxy-shikonin; euchro-quinol B	Genus
9.62	271.0965	C16H14O4	0	QGD07	naphtho-quinones	anhydro-shikonin	Genus
9.62	289.1070	C16H16O5	-0.3	CLZ55; HDC64; HJB97	naphtho-quinones	shikonin and isomers	Genus
10.72	325.2275	C21H28N2O	0.1	4 hits	aspidosperma/ eburna alkaloids		DNP dicot
10.76	321.1338	C17H20O6	1.6	GCX11; OWC42	anthracenes		Family
10.87	319.1178	C17H18O6	0.5	GCV45; OKR45	anthracenes		Family
11.41	273.1121	C16H16O4	-0.2	CMW55; QVX08	naphtho-quinones	deoxy-shikonin; euchro-quinol B	Genus
11.90	289.1070	C16H16O5	-0.3	CLZ55; HDC64; HJB97	naphtho-quinones	shikonin and isomers	Genus
12.03	301.0707	C16H12O6	0	GMQ86; JOX41	naphtho-quinones		Family

Retention time [min]	**m/z $[M+H]^+$**	**Molecular formula**	**Mass accuracy [ppm]**	**Identification Number (CRC)**	**Type of Compound**	**Common Name**	**Taxonomy**
12.46	275.1277	C16H18O4	-0.4	GMQ70	naphtho-quinones		Family
12.93	259.1329	C16H18O3	0	QVV93; QVX07	anthracenes	epoxy-arnebinol; euchro-quinol A	Genus
12.93	273.1121	C16H16O4	-0.2	CMW55; QVX08	naphtho-quinones	deoxy-shikonin; euchro-quinol B	Genus
13.16	259.1329	C16H18O3	0	QVV93;QVX07	anthracenes	epoxy-arnebinol; euchro-quinol A	Genus
13.63	273.1121	C16H16O4	0.2	CMW55; QVX08	naphtho-quinones	deoxy-shikonin; euchro-quinol B	Genus
14.04	273.1121	C16H16O4	-0.2	CMW55; QVX08	naphtho-quinones	deoxy-shikonin; euchro-quinol B	Genus
14.05	271.1329	C17H18O3	0	MYH10; QBG81	phenanthrenes		Family
14.94	333.1332	C18H20O6	-0.3	QWN99	furo- naph-thalenes	euchroquinol C	Genus
15.24	319.1541	C18H22O5	0.2	KQO34	simple benzoic acids and esters		Family

Retention time [min]	**m/z $[M+H]^+$**	**Molecular formula**	**Mass accuracy [ppm]**	**Identification Number (CRC)**	**Type of Compound**	**Common Name**	**Taxonomy**
15.44	257.1172	C16H16O3	-0.2	CMP10; GMR50; BFF44*	meroter-penoids; *benzo-quinones		Family
15.53	287.1278	C17H18O4	0	QJH49; QJH50	naphtho-quinones		Family
15.81	389.1595	C21H24O7	0	JYM40; HFR68	naphtho-quinones	hydroxyl-isovaleryl-shikonin; arnebin II	Genus
16.22	288.2897	C17H37NO2	-0.1		saturated unbranched alcohols		DNP dicots
16.46	303.1227	C17H18O5	-0.1	MXL90; MXL91; MXM93*	anthracenes; *naphtho-quinones		Family
16.64	319.1541	C18H22O5	0.2	KQO34	simple benzoic acids and esters		Family
16.78	288.2897	C17H37NO2	-0.1		saturated unbranched alcohols		DNP dicots
17.01	271.0965	C16H14O4	0	QGD07	naphtho-quinones	anhydro-shikonin	Genus
17.01	289.1070	C16H16O5	-0.3	CLZ55; HDC64; HJB97	naphtho-quinones	shikonin and isomers	Genus
17.06	355.1541	C21H22O5	0.2	GMR51	benzo-quinones		Family
18.98	316.3211	C19H41NO2	0.2		sphingolipids		DNP-dicots
19.35	646.2650	C23H29NO10	0.5	KFV01-O	diterpene alkaloids		DNP dicot

Retention time [min]	**m/z $[M+H]^+$**	**Molecular formula**	**Mass accuracy [ppm]**	**Identification Number (CRC)**	**Type of Compound**	**Common Name**	**Taxonomy**
19.47	316.3210	C19H41NO2	-0.1		sphingolipids		DNP-dicots
19.94	295.2269	C18H30O3	0.4	DOM20	oxylipins		Family
19.95	277.2163	C18H28O2	0.3	FJC43; CPL82	oxylipins		Family
20.23	369.1333	C21H20O6	0	PLB53	flavones		Family
20.40	271.0965	C16H14O4	0	QGD07	naphtho-quinones	anhydro-shikonin	Genus
20.44	279.1591	C16H22O4	0	FKO94	resorcylic acid lactones	o-de-me-la-siodiplodin	Genus
22.32	271.0965	C16H14O4	0	QGD07	naphtho-quinones	anhydro-shikonin	Genus
23.48	271.0965	C16H14O4	0	QGD07	naphtho-quinones	anhydro-shikonin	Genus
24.73	271.0965	C16H14O4	0	QGD07	naphtho-quinones	anhydro-shikonin	Genus

Table A.4.: Dereplication table of the UHPLC-HRMS data of the ethanolic *A. Euchroma* Extract in negative ionization mode. The common name was added only if the identification number (CRC) was described for the Genus *Arnebia*. The Type of Compounds referred to the classification done with the DNP.

Retention time [min]	**m/z $[M+H]^+$**	**Molecular formula**	**Mass accuracy [ppm]**	**Identification Number (CRC)**	**Type of Compound**	**Common Name**	**Taxonomy**
5.38	287.0928	C16H16O5	1.1	CLZ55; HDC64; HJB97	naphtho-quinones	shikonin and isomers	Genus
6.25	287.0927	C16H16O5	0.8	CLZ55; HDC64; HJB97	naphtho-quinones	shikonin and isomers	Genus
6.90	311.0565	C17H12O6	1.3	LOK19; LOF32	stilbenes		Family
7.86	289.1084	C16H18O5	1	HFR69	naphtho-quinones	arnebin V	Genus
7.86	335.1140	C17H20O7	1.2	JOW54	anthracenes		Family
8.17	305.1034	C16H18O6	1.2	OWD16	meroter-penoids	glaziovianol B	Family
8.71	287.0929	C16H16O5	1.5	CLZ55; HDC64; HJB97	naphtho-quinones	shikonin and isomers	Genus
8.98	287.0927	C16H16O5	0.8	CLZ55; HDC64; HJB97	naphtho-quinones	shikonin and isomers	Genus
9.03	317.1033	C17H18O6	0.8	GCV45; OKR45	meroter-penoids		Family
9.12	273.1136	C16H18O4	1.4	GMQ70	naphtho-quinones		Family
9.25	287.0927	C16H16O5	0.8	CLZ55; HDC64; HJB97	naphtho-quinones	shikonin and isomers	Genus
9.45	287.0928	C16H16O5	1.1	CLZ55; HDC64; HJB97	naphtho-quinones	shikonin and isomers	Genus

Retention time [min]	**m/z $[M+H]^+$**	**Molecular formula**	**Mass accuracy [ppm]**	**Identification Number (CRC)**	**Type of Compound**	**Common Name**	**Taxonomy**
9.48	271.0977	C16H16O4	0.5	CMW55; QVX08	naphtho-quinones	deoxy-shikonin; euchro-quinol B	Genus
9.62	287.0927	C16H16O5	0.8	CLZ55; HDC64; HJB97	naphtho-quinones	shikonin and isomers	Genus
9.82	287.0928	C16H16O5	1.1	CLZ55; HDC64; HJB97	naphtho-quinones	shikonin and isomers	Genus
10.03	273.1135	C16H18O4	1.1	GMQ70	naphtho-quinones		Genus
10.17	287.0928	C16H16O5	1.1	CLZ55; HDC64; HJB97	naphtho-quinones	shikonin and isomers	Genus
10.29	315.0878	C17H16O6	1.3	CDO56	flavanones		Family
10.76	275.1291	C16H20O4	0.9	CMN87; PKV13	meroter-penoids		Family
10.76	319.1188	C17H20O6	0.3	GCX11; OWC42	meroter-penoids		Family
10.86	287.0928	C16H16O5	1.1	CLZ55; HDC64; HJB97	naphtho-quinones	deoxy-shikonin; euchro-quinol B	Genus
11.04	287.0928	C16H16O5	1.1	CLZ55; HDC64; HJB97	naphtho-quinones	shikonin and isomers	Genus
11.44	271.0977	C16H16O4	0.5	CMW55; QVX08	naphtho-quinones	deoxy-shikonin; euchro-quinol B	Genus
11.44	317.1031	C17H18O6	0.2	GCV45; OKR45	naphthalenes; meroter-penoids		Family

Retention time [min]	**m/z $[M+H]^+$**	**Molecular formula**	**Mass accuracy [ppm]**	**Identification Number (CRC)**	**Type of Compound**	**Common Name**	**Taxonomy**
11.46	239.0923	C12H16O5	-0.7	NOY58	Simple phenyl-propanoids		Family
11.92	243.1025	C15H16O3	-0.6	85 hits			DNP dicots
12.34	301.1084	C17H18O5	0.9	MXL90; MXL91; MXM93	polycyclic aromatic		Family
12.46	273.1134	C16H18O4	0.7	GMQ70	naphtho-quinones		Family
12.46	301.1083	C17H18O5	0.6	MXL90; MXL91; MXM93	polycyclic aromatic		Family
12.46	319.1188	C17H20O6	0.3	GCX11; OWC42	meroter-penoids		Family
12.94	271.0978	C16H16O4	0.9	CMW55; QVX08	naphtho-quinones	deoxy-shikonin; euchro-quinol B	Genus
12.94	289.1082	C16H18O5	0.3	HFR69; GYV35	naphtho-quinones	arnebin V	Genus
13.10	301.1084	C17H18O5	0.9	MXL90; MXL91; MXM93	polycyclic aromatic		Family
13.64	271.0978	C16H16O4	0.9	CMW55; QVX08	naphtho-quinones	deoxyshikonin; euchro-quinol B	Genus
14.06	271.0977	C16H16O4	0.5	CMW55; QVX08	naphtho-quinones	deoxy-shikonin; euchro-quinol B	Genus
14.38	269.0822	C16H14O4	1.1	QGD07	naphtho-quinones	anhydro-shikonin.	Family

Retention time [min]	m/z $[M+H]^+$	Molecular formula	Mass accuracy [ppm]	Identification Number (CRC)	Type of Compound	Common Name	Taxonomy
15.43	317.1397	C18H22O5	0.9	KQO34	meroterpenoids		Family
15.45	315.1240	C18H20O5	0.7	BZJ27	meroterpenoids	arnebifuranone	Genus
15.82	405.1558	C21H26O8	0.8	58 hits			DNP dicots
17.04	287.0927	C16H16O5	0.8	CLZ55; HDC64; HJB97	naphthoquinones	shikonin and isomers	Genus
17.09	353.1397	C21H22O5	0.8	GMR51	benzoquinones		Family
18.62	285.2073	C16H30O4	0.7	5 hits			DNP dicots
19.36	627.2240	C36H25O10	0.7	2 hits			DNP dicots
19.40	459.3695	C26H52O6	0.9	1 hits			DNP dicots
19.94	311.2231	C18H32O4	1.1	7 hits			DNP dicots
20.17	387.1454	C21H24O7	1.3	JYM40; HFR68;	naphthoquinones	hydroxyisovaleryl-shikonin; arnebin II	Genus
20.24	367.1189	C21H20O6	0.6	PLB53	flavones		Family
20.40	271.0978	C16H16O4	0.9	CMW55; QVX08	naphthoquinones	deoxyshikonin; euchroquinol B	Genus
20.42	329.1032	C18H18O6	0.5	CLZ56; CLZ54; OSH57	naphthoquinones	shikonin acetate	Genus
24.33	271.0977	C16H16O4	0.5	CMW55; QVX08	naphthoquinones	deoxyshikonin; euchroquinol B	Genus

Retention time [min]	m/z $[M+H]^+$	Molecular formula	Mass accuracy [ppm]	Identification Number (CRC)	Type of Compound	Common Name	Taxonomy
24.33	369.1345	C21H22O6	0.4	HJB95	naphtho-quinones	arnebin-1	Genus
24.73	371.1503	C21H24O6	0.8	JYM30; JYM35	naphtho-quinones	α-methyl-butyryl-shikonin; isovaleryl-shikonin	Genus
24.74	271.0977	C16H16O4	0.5	CMW55; QVX08	naphtho-quinones	deoxy-shikonin; euchro-quinol B	Genus
26.07	271.0977	C16H16O4	0.5	CMW55; QVX08	naphtho-quinones	deoxy-shikonin; euchro-quinol B	Genus
26.34	271.0977	C16H16O4	0.5	CMW55; QVX08	naphtho-quinones	deoxy-shikonin; euchro-quinol B	Genus
26.57	369.3013	C22H42O4	0.8	2 hits			DNP dicots
27.97	271.0977	C16H16O4	0.5	CMW55; QVX08	naphtho-quinones	deoxy-shikonin; euchro-quinol B	Genus
28.08	271.0977	C16H16O4	0.5	CMW55; QVX08	naphtho-quinones	deoxy-shikonin; euchro-quinol B	Genus
28.36	271.0977	C16H16O4	0.5	CMW55; QVX08	naphtho-quinones	deoxy-shikonin; euchro-quinol B	Genus

Retention time [min]	**m/z $[M+H]^+$**	**Molecular formula**	**Mass accuracy [ppm]**	**Identification Number (CRC)**	**Type of Compound**	**Common Name**	**Taxonomy**
28.52	271.0977	C16H16O4	0.5	CMW55; QVX08	naphtho-quinones	deoxy-shikonin; euchro-quinol B	Genus
28.82	271.0977	C16H16O4	0.5	CMW55; QVX08	naphtho-quinones	deoxy-shikonin; euchro-quinol B	Genus

A.3. Publications, Presentations and Awards

A.3.1. Publications

Houriet J, Buhlmann E, Rudigier C, Kiehlmann E, **Radtke J**, Heeren J, Friedemann T, Schröder S, Wolfrum C, Wolfender J-L . *Investigation of the anti-obesity effect of Pueraria montana var. lobata.* Planta Medica 2016; 82(S 01): S1-S381

Meyer-Hamme G, Beckmann K, **Radtke J**, Efferth T, Greten H J, Rostock M, Schröder M. *A Survey of Chinese Medicinal Herbal Treatment for Chemotherapy-Induced Oral Mucositis.* Evidence-based Complementary and Alternative Medicine 2013, 2013: 284959

Radtke J, Rezaie S G , Kugler C H, Zabel P, Schultz H, Vollmer E, Goldmann T, Lang D S. *Expression analysis of EML4 in normal lung tissue and non-small cell lung cancer (NSCLC) in the absence and presence of chemotherapeutics.* Romanian Journal of Morphology and Embryology 2010, 51(4): 647-653

Goldmann T, Drömann D, **Radtke J**, Marwitz S, Lang D S, Schultz H, Vollmer E. *CXCR7 transcription in human non-small cell lung cancer and tumor-free lung tissues; possible regulation upon chemotherapy.* Virchows Archiv 2008, 452: 347-348

A.3.2. Oral presentations

Radtke J, Friedemann T, Brandner JM, Schröder S

Wound healing improvement studies with Traditional Chinese Herbs in an Ex Vivo Porcin Skin Model.

Sino-German Symposium on Building Consensus out of Controversies in Transnational Chinese Medicine Research, 18.-21. October 2013, Shanghai, China

A.3.3. Poster

Radtke J, Friedemann T, Salchow R, Schröder S

Ex Vivo and In Vitro Wound Healing Progression Studies of Traditional Chinese Herb 22.

13th Meeting of Consortium for Globalization of Chinese Medicine (CGCM), 27-29 August 2014, Beijing, China

Radtke J, Friedemann T, Schröder S, Brandner JM

Wound Healing Studies with Traditional Chinese Herb 22 in an Ex Vivo Porcine Skin Model

41. ADF-Jahrestagung (Arbeitsgemeinschaft Dermatologische Forschung eV.), 13.-15. March 2014, Cologne, Germany

A.3.4. Awards

Travel Grant

13^{th} Meeting of Consortium for Globalization of Chinese Medicine (CGCM)

Beijing on August 27-29, 2014.

A.4. Affirmations

A.4.1. Language proof

Glenn E. Larkin
4021 Emerald Ln #F
Bowie MD 20716
USA

Doctoral Committee of Biology Biocentre Klein Flottbek
Studienbüro Biologie
Ohnhorststr. 18
22609 Hamburg
Germany

The 18th of April 2017

Certificate of language proof

To the chairman of the "Doctoral Committee of Biology" (Fach-Promotionsausschuss) of the Department Biology, MIN Faculty, at the University Hamburg.

The PhD thesis by Janine Radtke has been written in acceptable English.

Yours sincerely,

Glenn E. Larkin

A.4.2. Declaration of authorship

I hereby declare, on oath, that I have written the present dissertation by my own and have not used other than the acknowledged resources and aids.

Hiermit erkläre ich an Eides statt, dass ich die vorliegende Dissertationsschrift selbst verfasst und keine anderen als die angegebenen Quellen und Hilfsmittel benutzt habe.

Hamburg, 20/04/15

Janine Radtke

A.4.3. Acknowledgment

First of all, I would like to thank Prof. Johanna M. Brandner for taking supervision and guidance of my dissertation as well as for the critically scientific examinations of the produced data.

Special thanks go to M.D. Sven Schröder and Ph.D. Roland Salchow, who established the HanseMerkur Center for Traditional Chinese Medicine at the University Medical Center Hamburg-Eppendorf. I am thankful that I had the opportunity to work on such a fascinating topic within this team. It was a pleasure, to be part of the HMZ-for-TCM-at-the-UKE-Crew. Thanks to all the colleagues.

Prof. Thorsten Burmester always supported my projects, not only as a reviewer. I am thankful for the scientific and emotional support during the years.

Moreover, this project was enabled by the technical and mental support of Meike Riebe, Sarah Mirza, Sabine Vidal-y-Sy, Ewa Wladikowsky and Pia Houdek. I benefited from your laboratory know-how, friendly and helpful manners which were a big luck for me. Thanks to all the cooperating laboratories of the UKE e.g. the core facility for mass spectrometry of the UKE and all the laboratories which shared their instruments and knowledge with me.
A special thank goes to Jean-Luc Wolfender, Joëlle Houriet and their whole laboratory team. You supported my chromatographical investigations and we had a very nice, fruitful and informative time together in Genéva.
To my entire companions, as Ph.D. students and postdocs, thank you so much for sharing your experience and knowledge with me. Thank you for the whole time.

Furthermore, this project was enormously supported by my college and friend Thomas. It was definitely the right job interview, among compatible spirits at the right time. I already miss the pizza-happenings and your “wann machst du endlich Feierabend?” Thank you for everything.

Words cannot describe how deeply I feel loved by my family and friends. You all supported me with patience, confidence, sympathy, craziness and the right amount of motivation. I will always love you. Thank you mum, this all woud not have been possible without you.

Last but not least, I want to thank the former “Innovationsstiftung Hamburg” and “Bionorica” for the financial support of my studies.

This time of my life will never be forgotten. To say it in the words of a great music band: I followed. I failed. I repeated. In the end, everything is good. If not, this is not the end.

List of Figures

List of Tables